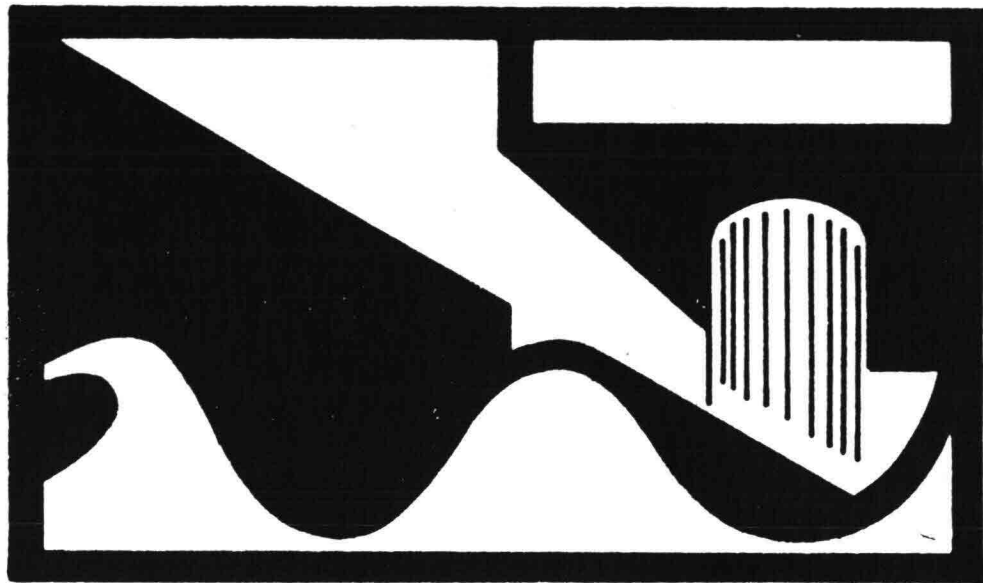


# Coastal Engineering

Volume I Introduction

Edited by W.W. Massie, P.E.

---



COASTAL ENGINEERING  
Volume I - Introduction

edited by

W.W. Massie, P.E.

Coastal Engineering Group  
Department of Civil Engineering  
Delft University of Technology  
DELFT  
The Netherlands

1976

Revised Edition 1982

Reprinted with some corrections, Winter 1985/86.

D.U.T. student-price:

		f11A - D2	600222					±f. 15.00
--	--	-----------	--------	--	--	--	--	-----------

"If you stay with a problem long enough you will get the answer. It may not be the one you expected, but the chances are it will be the truth."

Charles M. Allen

TABLE OF CONTENTS - VOLUME I  
INTRODUCTION TO COASTAL ENGINEERING

1. Introduction	1
1.1 Purpose	1
1.2 Subdivisions	1
1.3 Periodical Literature	2
1.4 Reference Books	3
1.5 Contributors	4
1.6 Miscellaneous Remarks	5
2. Overview of Coastal Engineering	6
2.1 Definition	6
2.2 Background Studies	6
2.3 Subdivisions	6
2.4 Harbors	6
2.5 Coastal Morphology	7
2.6 Offshore Engineering	8
3. Oceanography	9
3.1 Introduction	9
3.2 Description of The Oceans	10
3.3 Wind Driven Ocean Currents	11
3.4 Dynamics of Ocean Currents	11
3.5 Eckman Wind Drift	13
3.6 Physical Properties of Sea water	16
3.7 Density Currents	21
4. Beaufort Wind Scale	22
5. Short Wave Theory	24
5.1 Introduction	24
5.2 General Relationships	24
5.3 Simplifications	27
5.4 Approximations for Deep Water	27
5.5 Approximations for Shallow Water	29
5.6 Intermediate Water Depths	30
5.7 A Critical Reexamination	30
5.8 Examples	32
6. Wave Speed and Length Computations	33
6.1 Introduction	33
6.2 Iteration Method	33
6.3 Use of Tables	35
7. Effects of Shoaling Water	37
7.1 Introduction	37
7.2 Wave Height Changes	37
7.3 Example	39
7.4 Review of Example	41
7.5 Breaking Criteria	41

8. Types of Breakers	43
8.1 Introduction	43
8.2 Breaker Types	43
8.3 Quantitative Classifications	44
9. Wave Refraction and Diffraction	47
9.1 Introduction	47
9.2 Wave Refraction	47
9.3 Wave Diffraction	50
10. Wave Statistics Relationships	51
10.1 Introduction	51
10.2 The Phenomenon and its Characterizations	51
10.3 Determination of Frequency of Occurrence	55
10.4 Wave Periods	56a
11. Application of Wave Statistics	57
11.1 Introduction	57
11.2 Problem Statement and Assumptions	58
11.3 The Numerical Treatment	58
11.4 Example Problem	61
11.5 Further Development	62a
11.6 The Inverse Problem	62a
11.7 A Second Type of Problem	62a
12. Wave Data	63
12.1 Introduction	63
12.2 Existing Data	63
12.3 Measurement Program	63
12.4 Use of Substitute Data	64
12.5 SMB Prediction Method	64
13. Optimum Design	67
13.1 Introduction	67
13.2 Project Criteria	67
13.3 Optimization Procedure	67
13.4 Implicit Assumptions	68
14. History of Harbor Developments	69
14.1 Introduction	69
14.2 Early History	69
14.3 The Influence of Dredging	69
14.4 Modern Developments	70
15. Approach Channels	71
15.1 Introduction	71
15.2 Problems Encountered	71
15.3 The Optimization Problem	72

16. Dredging Equipment	73
16.1 Introduction	73
16.2 General Principles	73
16.3 Plain Suction Dredge	73
16.4 Cutter Suction Dredge	78
16.5 Trailing Suction Hopper Dredge	80
16.6 Bucket Dredge	80
16.7 Further Developments	83
17. Dredging Spoil Disposal	84
17.1 Introduction	84
17.2 Marine Disposal	84
17.3 Land Disposal	85
18. Breakwaters	86
18.1 Introduction	86
18.2 Morphological Function of Breakwaters	86
18.3 Other Considerations	87
19. Seiches	88
19.1 Definition	88
19.2 Simple Cases	88
19.3 Effects of Seiches	89
19.4 Seiche Prevention	89
20. Tidal Rivers	90
20.1 Introduction	90
20.2 River Mouths	90
20.3 River Channels	92a
20.4 Tidal Currents	92b
20.5 River Navigation	98
20.6 Example	98
20.7 Other Tidal Effects	103
21. River Tide Measurements	104
21.1 Introduction	104
21.2 Precise Problem Statement	104
21.3 A Simple Method of Solution	104
21.4 A Better Solution	107
21.5 Example	108
21.6 A Reexamination	111
22. Density Currents in Rivers	112
22.1 Introduction	112
22.2 Salinity Variations with Tide	112
22.3 Density-Salinity Relationship	116
22.4 Statics of Stratified Water Masses	116
22.5 Internal Waves	117
22.6 The "Static" Salt Wedge	119
22.7 Siltation Problems	121
22.8 Rotterdam Harbor Entrance	124
22.9 Pollution Problems	125
22.10 Methods to Combat Density Currents	125a

23.	Density Currents in Harbors	126
23.1	Tide Flow in Harbor	126
23.2	Density Current in Harbor	127
23.3	Superposition of Current Components	130
23.4	Currents in Finite Harbors	131
23.5	The Practical Problem	134
23.6	Other Current Influences	136
23.7	Harbor Siltation	137
23.8	Methods to Combat Density Currents in Harbors	143
23.9	Review	145
24.	Pollution	147
24.1	Definition	147
24.2	Polluting Materials	147
24.3	Control Measures	150
24.4	Proposed Disposal Systems	150
25.	Onshore-Offshore Sediment Transport	
25.1	Introduction	152
25.2	Basis Principles of Sediment Transport	152
25.3	Beach Profile Form	153
25.4	Dune Formations	156
25.5	Dune Erosion	156a
26.	Longshore Sediment Transport	157
26.1	Introduction	157
26.2	The CERC Formula	158
26.3	The Bijker Formula	159
26.4	Applications	160
27.	Mud Coasts	162
27.1	Physical Description	162
27.2	Properties and Transport Process	162
27.3	Influence of Rivers	166
27.4	Examples	166
27.5	The Coast of Suriname	166
28.	Coastal Formations	167
28.1	Introduction	167
28.2	Spit	167
28.3	Barrier	169
28.4	Tomolo	171
29.	Deltas	173
29.1	Introduction	173
29.2	Deltas on Quiet Coasts	173
29.3	Deltas with Moderate Distributing Influences	176
29.4	Deltas with Strong Distributing Influences	178
29.5	Influence of Longshore Transport	180

30. Shore Protection	182
30.1 Introduction	182
30.2 Eroding and Accreting Shores	182
30.3 Jetties	183
30.4 Groins	183
30.5 Dunes	185
30.6 Detached Breakwaters	186
30.7 Seawalls	186
30.8 Sand By-Passing	186
31. Coastal Morphologists' Ten Commandments	187
32. Offshore Engineering	188
32.1 Disciplines Involved	188
32.2 Types of Offshore Structures	188
32.3 Uses of Offshore Structures	193
32.4 Civil Engineering Aspects	196
32.5 Other Problems	199
 Symbols and Notation	 200
 References	 208

LIST OF TABLES

Table number	Title	Page
1.1	Contributing Staff	4
3.1	Polynomial Coefficients for $\sigma_t$ coefficients	18
3.2	Coefficients for $\sigma_t$ computation	18
3.3	$\sigma_t$ as function of temperature and salinity	20
4.1	Beaufort wind force scale	23
5.1	Deep and shallow water definitions	31
6.1	Wave length iteration	34
6.2	Functions of $h/\lambda_0$	36
7.1	Wave shoaling computation	40
8.1	Breaker classifications	46
9.1	Wave refraction computation	49
10.1	Rayleigh distribution data	54
11.1	Design Wave Height Probability Computations	62
12.1	Wave Generation Data	66a
16.1	Cutter suction dredge production	78
16.2	Bucket dredge production	83
20.1	Tide and current at Rotterdam	93
20.2	Tide and current for Western Schelde	96
20.3	Integration computation	101
21.1	Example tide data	105
21.2	Example tide data	108
22.1	Current and salinity at Rotterdam	112
22.2	River mixing criteria	114
22.3	Suspended load at Rotterdam	123

Table number	Title	Page
23.1	Harbor level and filling current	126
23.2	Density current at Rotterdam	129
23.3	Sedimentation summary	140
23.4	Sedimentation summary	143
23.5	Tide data for Hook of Holland	145
24.1	Concentrations of heavy metals	149
27.1	Properties of sling mud	163
31.1	Ten commandments	187
Symbols	Roman letters	200
	Greek letters	203
	Special symbols	204
	Subscripts	205
	Functions	205
	Dimensions and units	207

LIST OF FIGURES

Figure number	Title	Page
3.1	Depth distribution of Oceans	10
5.1	Hyperbolic functions	27
5.2	Orbital motion in deep water	28
5.3	Orbital motion in shallow water	30
8.1	Spilling breaker	43
8.2	Plunging breaker	44
8.3	Surging breaker	44
9.1	Wave refraction pattern	48
9.2	Wave diffraction pattern	50
10.1	Irregular wave profile	51
10.2	Rayleigh distribution graph	55
10.3	Long term wave height distribution	56b
12.1	Fetch - duration relationship	65
14.1	Ship camel	70
16.1	Suction dredge	74
16.2	Barge loading suction dredge	75
16.3	Dredge pump parameters	76
16.4	Barge unloading dredge	77
16.5	Cutter suction dredge	79
16.6	Trailing suction hopper dredge	81
16.7	Bucket dredge	82
16.8	Seagoing Suction Dredge	83a
16.9	Jack-Up Cutter Suction Dredge	83a
18.1	Columbia River entrance	87
19.1	Standing wave in closed basin	88
19.2	Seiche in harbor basin	88
19.3	Fifth harmonic seiche	89
20.a	Channel Velocity-Geometry Relationship	90
20.1	Schelde River at Antwerp	92a
20.2	Schelde River near Hansweert	92b
20.3	Current at Rotterdam	93
20.4	Idealized tide level and current curves	94
20.5	Tide data at Rotterdam	95
20.6	Tide levels in Western Schelde	97
20.7	Example river profile and tide	99
20.8	Ship position-time curves	102

Figure number	Title	Page
21.1	River plan	104
21.2	Uncorrected tide curves	105
21.3	Corrected tide curves	106
21.4	Example tide data	109
21.5	V-t curves	110
21.6	Graphical solution	110
22.1	Current and salinity at Rotterdam	113
22.2	Pressure on vertical interface	117
22.3	Internal wave	119
22.4	"Static" salt wedge	120
22.5	Suspended load at Rotterdam	123
22.6	Channel Bed Profiles	124
23.1	Harbor level and filling current	127
23.2	Dry bed curve	128
23.3	Harbor salinity and density current	129
23.4	Harbor entrance velocity profiles	130
23.5	Density current progress	131
23.6	Density current in harbor	133
23.7	Harbor example sketch	138
23.8	Schematized Salinity Curve	141
23.9	Summary of all tidal data for Rotterdam	146
24.1	Lead concentrations	149
25.1	Sediment Concentrations versus Time	153
25.2	Beach Profile	154
25.3	Flow in Breaker Zone	156
25.4	Dunes along Oregon Coast	156
25.5	Dune Erosion	156a
26.1	Longshore Transport Continuity	160
26.2	Sediment Transport Changes	161
27.1	Properties of sling mud	165
27.2	Features of mud shoals	166a
28.1	Beach near Budva, Yugoslavia	168
28.2	Block Island spit, U.S.A.	168
28.3	Wadden Islands, Netherlands	169
28.4	Barrier coast, U.S.A.	170
28.5	Barrier enclosing lake, U.S.A.	171
28.6	Natural tombolo, U.S.A.	171
28.7	Artificial tombolo, U.S.A.	172

Figure number	Title	Page
29.1	Delta development without waves	174
29.2	Lyéna delta, U.S.S.R.	175
29.3	Mississippi delta detail U.S.A.	175
29.4	Mississippi delta U.S.A.	175
29.5	Delta with moderate wave attack	176
29.6	Nile delta detail, Egypt	177
29.7	Niger delta, Nigeria	178
29.8	Amazon delta, Brazil	179
29.9	Coos Bay, U.S.A.	180
29.10	Netarts Bay, U.S.A.	181
30.1	Outer Cape Cod, U.S.A.	182
30.2	Accretion by Brouwersdam, Netherlands	183
30.3	Groins along coast	184
30.4	Groins along coast	184
30.5	Groin structure examples	185
32.1	Sketch of ANDOC gravity structure	189
32.2	Models of jacket constructions	190
32.3	Floating jack-up platform	191
32.4	Crane ship at work	192
32.5	Model of semi-submersible platform	192
32.6	Floating oil storage buoy	193
32.7	Light tower Goeree	194
32.8	Ekofisk oil storage tank	195
32.9	Production platform in storm	197

## 1. INTRODUCTION

W.W. Massie

### 1.1. Purpose

This set of lecture notes is written primarily to supplement the classes conducted by Prof. E.W. Bijker which are held in Delft, both at the University of Technology and at the International Course in Hydraulic Engineering. The lecture time will be used primarily to discuss and amplify these notes and answer questions.

Some can probably learn much from these books without having attended the classes at all. Questions are often posed within the text; all are intended to stimulate thought and verify understanding.

### 1.2. Subdivisions

The entire material of coastal engineering presented by Prof. Bijker at the Delft University of Technology is currently divided into four courses:

- a. Introduction to Coastal Engineering - a basis for the remaining volumes.
- b. Harbor and Beach Problems - a more advanced treatment of topics related to coasts, harbors and approach channels.
- c. Breakwater Design - treating both rubble mound and monolithic breakwaters.
- d. Pipelines and Offshore Moorings - discussing certain specific offshore topics.

This subdivision has been retained in the preparation of these books; the material is treated in separate volumes.

Another subdivision is also possible; it is often handy to subdivide the material of coastal engineering into three broad areas according to the types of problems which are treated. These three broad categories are Harbors, Morphology, and Offshore and are discussed further in chapter 2. This division has been retained in the first two volumes of this book. Within each of these volumes material has been grouped in each of these categories. This subdivision is not apparent in volume III since breakwaters fall almost exclusively into the harbor category.

A fourth category of information has been added in these notes to review necessary background theory normally presented in other courses; this is done for completeness. Many can skip over this category completely, others will find it useful. The understanding of this background is, however, of vital importance for the true coastal engineering topics which are

built upon this foundation.

### 1.3. Periodical literature.

Specific literature references have been included at the end of each of the volumes. These are indeed references; they provide background instead of highlighting the most recent developments. Periodical literature provides the best means of keeping up to date. Such literature can be grouped into five sorts, each is described a bit below.

#### General

Engineering periodical literature of this sort covers a broad spectrum of topics within engineering and, as such, occasionally contains something of direct interest to coastal engineers, even though such articles often lack specific technical detail. Examples of such periodicals are:

- a. Engineering New Record, published weekly by McGraw Hill Publications, New York, U.S.A.
- b. De Ingenieur, published weekly by the Royal Society of Engineers (Koninklijk Instituut van Ingenieurs), The Hague, The Netherlands
- c. Civil Engineering, published monthly by the American Society of Civil Engineers, New York, U.S.A.

#### General Specific

This group of journals provide general information about a specific topic area. These usually contain information of direct interest but specific technical details are usually still lacking. Examples of this sort of literature are:

- a. Ocean Industry, published monthly by the Gulf Publishing Co., Houston, Texas, U.S.A.
- b. The Dock and Harbor Authority, published monthly by Foxlow Publications, Ltd., London.

#### Technical Specific

This group of publications provide, in general, most of the specific technical details of a problem and its solution, and are often found in the references listed in articles found in the above sorts of periodicals. Examples of technical specific literature are:

- a. Journal of Waterway, Port, Coastal and Ocean Engineering, published quarterly by the American Society of Civil Engineers, New York, U.S.A.
- b. Shore and Beach, published semiannually by American Shore and Beach Preservation Association, Miami, Florida, U.S.A.
- c. Coastal Engineering in Japan, published annually by Japan Society of Civil Engineers, Tokyo, Japan.

### Strange Technical

These journals provide the same type of information as the previous sort of journals, but are intended for an entirely different specialty group. It takes a bit of ingenuity on the part of the investigator to discover related topic areas and patience to seek through its literature on the small chance that it contains something useful. Often this searching can be avoided by using an abstract index - see below. The examples listed below serve only to illustrate that useful information can be found in this sort of journal.

- a. An article on wave forces: Journal of the Engineering Mechanics Division, published by the American Society of Civil Engineers, New York, U.S.A.
- b. An article on wave action in harbors: Journal of the Acoustical Society of America, New York, U.S.A.

### Abstracts

Abstracts, indexed in some way, serve to provide easy access and quick reference to the vast domain of literature. Abstracts, of themselves, do not provide any new information; they simply condense and index existing articles. Among the excellent abstract and indexing services are:

- a. Documentation Data, published by the Delft Hydraulics Laboratory, Delft, The Netherlands
- b. Engineering Index, published by the Engineering Societies Library, New York, U.S.A.
- c. BHRA Fluid Engineering, an abstracting service of the British Hydraulics Research Association, Bedford, England.

There has been an explosive development of computer-based key word abstract searching systems within the past few years. All three of the above files - and many more - can currently be searched via a rather simple computer terminal and telephone line. Such a terminal is available - for a moderate hourly fee - in the Main Library of the Delft University of Technology.

### 1.4. Reference Books

A few general reference books of specific interest to coastal engineers are listed here. Each of these will tell something but usually not everything about a wide spectrum of coastal engineering topics.

- a. Per Bruun (1973): Port Engineering: Gulf Publishing Company, Houston, Texas, U.S.A.
- b. Arthur T. Ippen (1966): Estuary and Coastline Hydrodynamics: McGraw-Hill, New York.
- c. H. Lamb (1963): Hydrodynamics (6th edition): Cambridge Univ. Press.
- d. Muir Wood, A.M. (1963) Coastal Hydraulics: Macmillan and Co. Ltd., London, England.

- e. Robert L. Wiegel (1964): Oceanographical Engineering: Prentice-Hall, Inc., Englewood Cliffs N.J., U.S.A.

### 1.5. Contributors

These books are prepared by the entire staff of the Coastal Engineering Group of the Delft University of Technology. The primary authors of each section are listed at the beginning. Many others of the staff reviewed each section; final editing and assembly was the responsibility of W.W. Massie. Table 1.1. lists the entire contributing staff for this volume in alphabetical order.

#### Table 1.1. Contributors to this volume

Prof. Dr. Ir. E.W. Bijker, Professor of Coastal Engineering, Delft University of Technology, Delft.

Ir. C.J.P. van Boven, Offshore engineering consultant.

Ir. J.J. van Dijk, Senior Member of the Scientific Staff, Coastal Engineering Group, Delft University of Technology, Delft.

Ir. J. van de Graaff, Senior Member of the Scientific Staff, Coastal Engineering Group, Delft University of Technology, Delft.

Ir. L.E. van Loo, Senior Member of the Scientific Staff, Coastal Engineering Group, Delft University of Technology, Delft.

W.W. Massie, P.E., Senior Member of the Scientific Staff, Coastal Engineering Group, Delft University of Technology, Delft.

Ir. J. de Nekker, Chief Engineer for Harbors, Department of Public Works, Rotterdam.

Ir. A. Paape, Delft Hydraulics Laboratory, Delft.

### 1.6 Comparison to 1976 Edition

This revised version of volume I has undergone two major changes in addition many more minor changes and corrections. The first major change involves chapters 10 and 11. Section 10.3 has been revised and expanded; chapter 11 has been rewritten to include more modern insight on wave statistics.

The second major change involves the description of sand transport on beaches. Chapters 25 and 26 have been completely rewritten.

More minor changes have been made in chapters 8 - breaker types, 12 - wave generation, 16 - offshore dredging, 20 - stable channel dimensions, 22 - sedimentation, 30 - adapted to new chapters 25 and 26, and 32 - updated.

### 1.7 Miscellaneous Remarks

The spelling used in this set of books is American rather than English.

A sincere attempt has been made to use consistent, unambiguous notation. Symbols are defined when first introduced in each chapter and a comprehensive list of symbols is provided at the end of each volume.

Literature is cited in the text by author and year date. A complete list of references used is included at the end of each book.

Figures shown are drawn to scale whenever possible. Distorted figures will be specifically pointed out. Many figures in these books are reproduced at 80% of their original size. Their original dimensions can thus be reconstituted by measuring with a 1 : 1250 scale.

Many technical terms used in these notes are listed in a separate glossary giving definitions and Dutch translations.

Since the English system of units is still in common use in the marine industry several tables of units conversion factors are also available separately.

2.1. Definition

Coastal engineering is the collective term encompassing most of the engineering activities related to works along the coasts. In recent years, coastal engineers have often been involved in engineering of structures to be placed offshore as well. It is their primary task to apply technical knowledge to the construction of various works along coasts and offshore. Usually, designs are needed for works for which only incomplete theoretical models are available, thus a fundamental knowledge of the phenomena involved is required as well. Often, coastal engineers must extend the field of technical knowledge.

An additional complicating feature of coastal engineering is that many of the independent variables involved are of a stochastic nature. Statistical computations form the basis for the optimum design techniques applied to many coastal engineering problems.

2.2. Background studies

Among the fundamental problems facing the coastal engineer are the water movements along a coast, the interactions between moving water and loose beach and sea bed materials, and the hydrodynamic forces exerted by waves and currents on various constructions. These are simply examples for the fundamental phenomena; others will become apparent later. The investigation of these phenomena forms the basis for coastal engineering research.

2.3. Subdivisions

Coastal engineering has already been subdivided into main divisions in the general introduction. Here we shall summarize the technical content of each of these divisions.

2.4. Harbors

Harbors have developed along with man's desire to move goods by ship. It is important to develop harbors in such a way that they are both convenient and economical from all points of view. This must obviously result in a compromise. These aspects are treated primarily in volume II. The cooperation of naval architects and mariners is often very helpful when considering this optimization problem.

Many harbor entrances are protected by some form of breakwater; the design of these structures is the main topic of volume III of these notes.

Since many harbors are situated in river mouths or natural estuaries, the formation of shoals and channels in tidal rivers is often included in coastal engineering. Obviously, this aspect is also closely related to river engineering. Special attention is paid to the influence of density currents and time dependent salinity variations on the behavior of silt in harbors. Density currents are approached from a very practical viewpoint in these notes; fundamental theory is handled in other books and courses. The behavior of silt in harbors and river mouths can be of extreme importance since this mud can often dominate the dredging problems of the harbor and can occasionally even dominate the coastal morphology over a considerable distance as well. Harbor design problems are often closely linked to coastal morphological problems. Indeed, it is often impossible to separate these problems. Among the more significant morphological problems directly related to harbors are the siltation of approach channels and the influence of breakwaters on the coastal processes.

### 2.5. Coastal Morphology

Coastal morphology is the study of the interaction of waves and currents with the coast. Most often this coast will be formed from sandy material; this often responds the most rapidly to the influence of the waves and current. Rocky coasts usually respond very slowly to these influences and as such are more of concern to the geologist than to the coastal engineer. Why do coasts consisting of mud also respond relatively slowly to the action of waves and currents? This is answered in chapter 27 on Mud Coasts.

Luckily, the most common coastal material is sand. We are lucky because it can be moved rather easily by dredging and the changes which occur on sand coasts can be reasonably accurately predicted using mathematical models. These models are briefly described in this volume; more complete information is given in volume II.

It should be clear that one must first understand the motion of water (wave action and other currents) along a coast before he can predict morphological changes. Indeed, many concepts from hydraulics are needed; some of the more specialized topics are reviewed in the immediately following chapters.

The effect of waves and currents on beaches is still not completely understood. Longshore and on and offshore transport of sand is an important topic of coastal engineering research. Results of this research are continually being used to improve the mathematical models used to predict coastline changes.

Since not all natural coastal changes are desirable, coastal defense works can also be needed. Defense works are used to retard the natural coastal processes or, sometimes, simply to neutralize

their effects. For example, groins can be constructed perpendicular or parallel to a coast to retard erosion. Another alternative is to artificially move sand from areas of accretion to areas of erosion. Coastal defense works will be considered later in this volume.

Not only harbor breakwaters and approach channels disturb the coastal morphology; natural rivers and estuaries do this as well. This is also discussed in detail later in this volume.

## 2.6. Offshore Engineering

Until recently, harbors and coastal morphology formed the main topics associated with "conventional" coastal engineering. In recent times man's interest in working at sea has increased rapidly. The offshore branch is developing rapidly as coastal engineers who have worked along relatively shallow coastlines have been asked to solve completely new problems in the deep sea. Indeed, the following chapter on oceanography is included because of an increasing need to understand the processes which take place in the deeper ocean waters. The primary stimulus for offshore engineering has come from the petroleum companies.

The term "offshore engineering" is used, here, to refer to engineering for works which have no direct connection to the mainland. Some people also refer to this topic as "ocean engineering" but the whole study area is too young to have developed a uniform terminology. Confusion of terminology is bound to result; for example, some marine engineers design offshore works while others design power plants for ships!

Ships underway do not have a connection to the mainland, but are still excluded from offshore engineering; these are left for the naval architects. On the other hand, possible impact loads upon offshore structures caused by ships can be very important to us.

The offshore engineer draws on the specialized knowledge of other fields. Mining engineering, Mechanical engineering, and Naval architecture can all contribute to offshore engineering along with Civil engineering. Here in Delft, these departments are now cooperating closely on an interdisciplinary program of offshore engineering.

### 3. OCEANOGRAPHY

W.W. Massie

#### 3.1. Introduction

Oceanography is study of the oceans. Man has studied the oceans for centuries. Count L.F. Marsigli wrote one of the first books on the subject, published in 1725. A Dutch translation of this book was prepared in 1786 by Boerhaave; a copy exists in the Library of Leiden University.

M.F. Maury, a United States Naval Officer, wrote the first "modern" oceanography book in 1855 while he was Superintendent of the Naval Hydrographic Office. Many of his observations - compiled from ships logs - are excellent; all are interestingly explained, even though he had no knowledge of geophysics.

The first systematic, specific study of the oceans was carried out by the H.M.S. Challenger. The ship sailed from Portsmouth, England on 21 December 1872 and in 3½ years sailed more than 100,000 km producing a 50 volume report. This was also the first report to subdivide oceanography into its four modern major fields: biological, chemical, geological, and physical.

What is the importance of oceanography to the coastal engineer? This will be highlighted in the following more detailed descriptions of each field.

#### Biological Oceanography

Biological Oceanography concerns itself with living matter in the seas. Coastal engineers are seldom directly involved with biological problems, but biological factors can play important indirect roles. Marine fouling of structures and environmental impact studies can be important, for example.

#### Chemical Oceanography

The chemistry of sea water is obviously of great importance to the marine biologists but it is becoming more important to engineers concerning with structures in the sea as well. Materials used in construction in the oceans can behave in what seem like strange ways when exposed to sea water under a considerable pressure (depth); Concrete technologists worry about concrete in water depths of a few hundred meters. Special corrosion and fracture problems develop with steel at somewhat greater depths.

### Geological Oceanography

The geologists who find commercially valuable minerals on the bottom of and under the sea are indirectly responsible for providing jobs for many coastal engineers. While coastal engineers are not expected to be geologists, themselves, they can certainly get preliminary information about possible foundation problems for a proposed offshore structure from marine geologists.

### Physical Oceanography

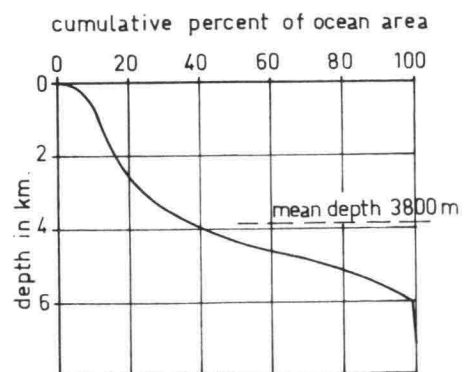
Physical oceanographers are most like the coastal engineers. Both worry about waves, tides and hydrodynamic problems in general. The concern with waves is interesting, if not serious. The oceanographers usually consider waves to be a necessary nuisance; coastal engineers, on the other hand, derive their most challenging problems from them. As offshore work progresses into still deeper water, coastal engineers must also begin to think about a topic which has, in the past, been restricted to physical oceanography: the location and strength of major ocean currents.

### 3.2. Description of the Oceans

A brief review of the physical features of the oceans will be helpful for our understanding of the dynamic processes which occur in the ocean.

Figure 3.1. shows the depth distribution of the oceans. The mean depth is about 3800 m. and the volume of the oceans is about  $1370 \times 10^{15} \text{ m}^3$ . By contrast, the North Sea has a mean depth of 94 m and a water volume of  $0.054 \times 10^{15} \text{ m}^3$  - pretty insignificant! The shallowest 200 m of the ocean (7.6% of the total area) is called the continental shelf. Only recently have coastal engineers been asked to venture beyond the shelf to the continental slopes; hence, the need to know a bit more about oceanography, now. Shelves border most of the continental coasts and range in width up to about 1200 km.

Figure 3.1  
DEPTH DISTRIBUTION  
OF THE OCEANS



data from :  
Sverdrup et al  
1942

The widest continental shelf is in the Arctic Ocean, north of Siberia; hardly any shelf is present along the west coast of the Americas (east coast of the Pacific Ocean).

The oceans are further divided into a series of interconnected basins in which most of the interesting physical oceanographic activity takes place. These basins are 3 to 5 km deep with occasional deeper or shallower spots.

Most of the interesting activity in the oceans takes place in the upper 1 to 2 km. Deeper than this, the oceans are of rather uniform salinity (35‰ - see section 3.6) and temperature ( $3^{\circ}$  -  $4^{\circ}$  C). Also, currents in this deep zone are very weak - often assumed to be zero. Currents in the upper layers are discussed in the next sections, while the physical properties of sea water are treated separately in section 3.6.

### 3.3. Wind-Driven Ocean Currents

The major driving force for ocean currents results from the wind forces on the ocean surface. The trade winds and the prevailing westerlies result in a generally westward ocean current at low latitudes and an eastward current at high latitudes. This manifests itself in the North Atlantic in the following current pattern:

The North Equatorial Current flows westward from the Cape Verde Islands to the Caribbean Sea. A portion enters this sea and a portion turns northwest east of the Caribbean Islands (Antilles Current) and joins the Florida Current. Water flows out of the Caribbean between Florida and Cuba in the Florida Current. The Florida Current (often called the Gulf Stream) continues north along North America to about  $45^{\circ}$  N. latitude where it turns eastward and spreads out forming the North Atlantic Current. A branch of this turns south, along Portugal to form the Canary Current and close the circuit.

Similar current patterns can be found in the South Atlantic and the other oceans. These major east-west currents correspond in latitude to the prevailing winds. The north-south currents guarantee continuity and conservation of mass.

How do the winds generate these major east-west currents? This is answered later in this chapter but first, the dynamic equilibrium of a flowing ocean current will be examined.

### 3.4. Dynamics of Ocean Currents

The familiar balance of gravity and friction forces which leads to the well-known Chézy Equation which is used to describe river flows does not work in the deep oceans. Since the oceans are so deep and the velocities are normally small (less than 1 m/s), friction forces become relatively unimportant. On the other hand, since the

ocean currents extend over great distances on the surface of a rotating earth, another influence, the Coriolis Force<sup>x</sup>, does become important.

Consider a current moving with constant speed along a "straight" path. ("Straight" means that it follows a great circle path.) The Coriolis acceleration acting on a unit mass of this water is:

$$a_c = 2 \Omega \sin \phi V$$

where:

$a_c$  = the Coriolis acceleration

$\Omega$  = the angular velocity of the earth =  $0.729 \times 10^{-4}/s$  †

$V$  = the current velocity, and

$\phi$  = the latitude

Further, this acceleration (or force per unit mass) acts toward the right facing in the flow direction in the northern hemisphere. (The direction is opposite south of the equator).

If this current is moving in a "straight" line, then the resultant acceleration perpendicular to the current direction must be zero. The Coriolis acceleration is balanced by a pressure gradient. This is a horizontal gradient also perpendicular to the current direction and counteracting the Coriolis acceleration. Equilibrium of these two components yields:

$$\frac{1}{\rho} \frac{\partial p}{\partial n} = 2 \Omega \sin \phi V \quad (3.02)$$

where:

$\rho$  is the water density, and

$\frac{\partial p}{\partial n}$  is the pressure gradient normal to the current.

Density differences are not sufficient to cause this pressure gradient, but a water surface slope can, and does provide the equilibrium. Thus, there are differences in mean sea level between points on the ocean surface.

This is demonstrated by computing the mean sea level difference across the Strait of Florida (across the Florida Current). This is located at latitude  $26^{\circ}$  N., the current is about 1.0 m/s., and the strait is about 80 km wide.

---

<sup>x</sup> A good review of Coriolis accelerations can be found in chapter 2 of Housner and Hudson (1959).

<sup>†</sup> This angular velocity is the absolute angular velocity based upon the sidereal day.

$$\begin{aligned}\frac{1}{\rho} \frac{\partial p}{\partial n} &= (2)(0.729 \times 10^{-4})(\sin 26^{\circ})(1.0) \\ &= 6.4 \times 10^{-5} \frac{\text{m}}{\text{sec}^2}\end{aligned}$$

In 80 km there is an elevation difference of:

$$\Delta z = \frac{6.4 \times 10^{-5}}{9.81} \times 80 \times 10^3 = 52. \times 10^{-2} \text{ m.}$$

This agrees reasonably well with an observed 45 cm value.

The currents just described are commonly called geostrophic currents.

Another interesting, (but less important from an oceanographic viewpoint) result can be obtained if we do allow our current to turn and let the horizontal pressure gradient be zero. In this case, the Coriolis acceleration is balanced by the centripetal acceleration.

$$\frac{v^2}{r} = 2 \Omega \sin \phi V \quad (3.03)$$

$$\frac{v}{r} = 2 \Omega \sin \phi \quad (3.04)$$

where  $r$  is the radius of curvature.

Currents of this sort cause little more than minor disturbances in oceanographic measurements; however, they can become a nuisance elsewhere. Such currents caused considerable problems in a sensitive hydraulic model at a lab in the U.S. some years ago. Perfectly quiet water without turbulence was required in a circular tank about 4 m in diameter. After filling the tank and letting it stand overnight, the investigator found a slow circulation current in the tank the next morning. Since the lab was located at latitude  $45^{\circ}$  N, this current was 0.2 mm/s.

These currents just described are independent of depth; they are constant over the entire depth, since friction has been ignored. This contradicts the earlier observation that there is little activity in the ocean deeper than 1 to 2 km. Actually, there is no real contradiction here, since we have not yet discussed the cause of the geostrophic currents, the wind, which, of course, acts over the surface of the oceans.

### 3.5. Eckman Wind Drift

Nansen (1902) reported observations of the drift of sea ice in the North Polar Sea. He found that the ice drifted not in the wind direction, but at an angle of  $20^{\circ}$  to  $40^{\circ}$  from the wind. He explained this as resulting from the Coriolis effect and further speculated that the current in successively deeper ocean layers, driven by shear stresses from layers above, must deviate even more to the right.

Eckman investigated this mathematically on the suggestion of Nansen. His results, published also in 1902, will not be derived here. We shall concern ourselves only with the basic starting point and the result. His work was done for an infinite ocean (also infinitely deep) with a wind of constant speed and direction over the entire surface. The ocean surface remains horizontal; the only driving force comes from the wind shear stress. In the steady state, (no acceleration) this results in:

$$\frac{\epsilon_z}{\rho} \frac{\partial^2 u}{\partial z^2} = + 2 \Omega \sin \phi v \quad (3.05)$$

$$\frac{\epsilon_z}{\rho} \frac{\partial^2 v}{\partial z^2} = - 2 \Omega \sin \phi u \quad (3.06)$$

where:

- u is the velocity component along a horizontal x axis
- v is the velocity component along a horizontal y axis
- z is the vertical coordinate measured from the ocean surface (+ up), and
- $\epsilon_z$  is the vertical eddy viscosity coefficient.

The further mathematics is given by Neumann and Pierson (1966). When they assume that the wind blows only in the y direction, the shear stress at the water surface is:

$$\tau_s = \epsilon_z \left. \frac{dv}{dz} \right|_{z=0} \quad (3.07)$$

and acts along the y axis.

This all results in the following:

$$u = V_s e^{\frac{\pi}{D} z} \cos \left( \frac{\pi}{4} + \frac{\pi}{D} z \right) \quad (3.08)$$

$$v = V_s e^{\frac{\pi}{D} z} \sin \left( \frac{\pi}{4} + \frac{\pi}{D} z \right) \quad (3.09)$$

which give the velocity components at any depth, once  $V_s$ , the velocity at the surface, and  $D$  are known.

$$D = \pi \sqrt{\frac{\epsilon_z}{\rho \Omega \sin \phi}} \quad (3.10)$$

$$V_s = \frac{\pi \tau}{\sqrt{2D\rho \Omega \sin \phi}} \quad (3.11)$$

Eckman calls  $D$  the "depth of frictional influence"; the depth over which the turbulent eddy viscosity is important. At this depth the velocity is about  $1/23$  of its value at the surface, and is directed in the opposite direction. This is in keeping with the hypothesis of Nansen mentioned earlier.  $D$  is normally about 50 meters, but increases very rapidly to  $\infty$  at the equator.

Substitution of  $z = 0$  into 3.08 and 3.09 yields a total velocity of magnitude  $V_s$  directed  $45^\circ$  to the right (in the northern hemisphere) of the wind direction.

The details of the current profile in three dimensions can be examined more conveniently by introducing polar coordinates.

$$|V| = V_s e^{-\frac{\pi}{D} z} \quad (3.12)$$

$$\theta = \frac{\pi}{4} + \frac{\pi}{D} z \quad ** \quad (3.13)$$

Indeed, the velocity,  $V$ , decreases exponentially with depth and the angle between the wind and current direction increases linearly with depth in a clockwise direction. The magnitude and direction of the resultant transport of ocean water is found by integrating 3.08 and 3.09 from  $z = -\infty$  to  $z = 0$ .

$$q_x = \frac{V_s D}{\pi \sqrt{2}} \quad (3.14)$$

$$q_y = 0 \quad (3.15)$$

where  $q_x$  and  $q_y$  are volume flow rates per unit of ocean width. The resultant transport is perpendicular in the wind direction!

This information does not seem too useful to us as coastal engineers. However, by allowing the ocean to have a coast, a surface slope, and a finite depth it is possible to begin\* to attack the problem of predicting storm surges near coasts. Such prediction can be very important especially in light of the devastation that such surges can cause.

Eckman (1905) considered the problem of an enclosed sea of finite, constant depth. An important result is:

$$\beta = \Lambda \frac{\tau_s}{\rho g h} \quad (3.16)$$

\* This is indeed still only a beginning. Influences of the barometric pressure changes and of complex bottom bathymetry are still being neglected.

\*\* Note that  $z < 0$  !

where:

$\beta$  = the water surface slope

$h$  = the depth, and

$\Lambda$  = a coefficient

Values of  $\Lambda$  vary between 1.0 for very deep water ( $h \gg \pi \sqrt{\frac{\epsilon z}{\rho \Omega \sin \phi}}$ ), and 1.5 for shallow water or where Coriolis influences are neglected. According to Neumann and Pierson (1966) Coriolis forces can be neglected in wind set-up problems and the direction of the maximum surface gradient does not deviate more than  $10^\circ$  from the wind direction.

If, however, the depth of the body of water varies (as it generally does) and the influence of the storm surge itself on the depth is included then we are forced to carry out a brute force integration of:

$$\frac{dz'}{dx} = \frac{\epsilon \tau}{\rho g z'} \quad (3.17)$$

where  $z'$  is now the depth measured from the actual water surface.

The solution to this is beyond the scope of these lecture notes. Hansen (1956) and Harris (1963) outline an approach to the problem.

### 3.6. Properties of Sea Water

The most important property of sea water from a coastal engineering point of view is its density. Its density is a function of three variables: salinity, temperature, and pressure. Of these, the pressure influence is least important and we can neglect it unless we are working at depths more than, say, 500 m.

In contrast to pure water, most sea water will continuously increase in density as it cools until it reaches its freezing temperature. Most sea water has a salinity varying between 34 and 36‰ (parts per thousand by weight). Some smaller isolated seas can have significant variations, however. The Baltic Sea, for example, sometimes has a salinity as low as 7‰. The Red Sea, on the other hand, has as much as 41‰ salinity.

Unfortunately, the dependence of density,  $\rho$ , on salinity,  $S$ , and temperature,  $T$ , is not simple. Fisher, Williams, and Dial (1970) published an empirically derived equation for the specific volume,  $v$ , of water as a function of salinity, temperature, and pressure. Their equation is:

$$v = v_\infty - K_1 S + \frac{K_3}{K_4 + K_2 S + p} \quad (3.18)$$

in which:

$K_1$  is a temperature dependent coefficient having units of

$$\frac{\text{cm}^3}{\text{g}\%},$$

$K_2$  is a temperature dependent coefficient with units  $\frac{\text{bars}^x}{\%}$

$K_3$  is a temperature dependent coefficient with units of

$$\frac{\text{bars cm}^3}{\text{g}},$$

$K_4$  is a temperature dependent coefficient with units of bars,

$p^1$  is the absolute pressure in bars,

$S$  is the salinity in ‰

$v$  is the specific volume in  $\frac{\text{cm}^3}{\text{g}}$ , and

$v_\infty$  is a temperature dependent coefficient having units of  $\frac{\text{cm}^3}{\text{g}}$

The five coefficients,  $K_1$ ,  $K_2$ ,  $K_3$ ,  $K_4$  and  $v_\infty$  are related to the temperature,  $T$  in degrees Celcius, by polynomial equations of form:

$$\sum_{i=0}^N a_i T^i \quad (3.19)$$

The coefficients,  $a_i$ , for these polynomials are given in table 3.1. Equation 3.18 is valid for the following ranges:

$$-2^0 < T < 100^0 \text{ C}; \quad 0 < p^1 < 1000 \text{ bars}; \quad 0 < S < 50\%$$

All of this makes equation 3.18 actually rather cumbersome in use. Therefore, Table 3.2 lists values of coefficients for equation 3.18 evaluated for various temperatures using table 3.1 and equation 3.19.

The water density in  $\frac{\text{kg}}{\text{m}^3}$  can be determined from the specific volume of equation 3.18 as follows:

$$\rho = \frac{1}{v} \times 10^3 \quad (3.20)$$

in which  $\rho$  is the density in  $\text{kg}/\text{m}^3$ .

---

\* 1 bar is  $10^6$  dynes/cm<sup>2</sup> or a pressure of  $10^5$  Pa =  $10^5$  N/m<sup>2</sup> or about 0.987 atmosphere.

TABLE 3.1 Polynomial Coefficients  $a_i$ , for  $K_1$ ,  $K_2$ ,  $K_3$ ,  $K_4$  and  $V_\infty$ 

## COEFFICIENT AND UNITS

i.	$K_1$	$K_2$	$K_3$	$K_4$	$V_\infty$
	$\frac{\text{cm}^3}{\text{g}\%}$	$(\frac{\text{bars}}{\%})$	$(\frac{\text{bars cm}^3}{\text{g}})$	(bars)	$\frac{\text{cm}^3}{\text{g}}$
0	$2.679 \times 10^{-4}$	10.874	1788.316	5918.499	0.6980547
1	$2.02 \times 10^{-4}$	$-4.1384 \times 10^{-2}$	21.55053	58.05267	$-7.435626 \times 10^{-4}$
2	$-6.0 \times 10^{-9}$		-0.4695911	-1.1253317	$3.704258 \times 10^{-5}$
3			$3.096363 \times 10^{-3}$	$6.6123869 \times 10^{-3}$	$6.315724 \times 10^{-7}$
4			$-7.341182 \times 10^{-6}$	$-1.4661625 \times 10^{-5}$	$9.829576 \times 10^{-9}$
5					$-1.197269 \times 10^{-10}$
6					$1.005461 \times 10^{-12}$
7					$5.437898 \times 10^{-15}$
8					$1.69946 \times 10^{-17}$
9					$-2.295063 \times 10^{-20}$

TABLE 3.2 Coefficients for

Eqn. 3.18 for various temperatures

## COEFFICIENT AND UNITS

T	$K_1$	$K_2$	$K_3$	$K_4$	$V_\infty$
( $^{\circ}\text{C}$ )	$(\frac{\text{cm}^3}{\text{g}\%})$	$(\frac{\text{bars}}{\%})$	$(\frac{\text{bars cm}^3}{\text{g}})$	(bars)	$(\frac{\text{cm}^3}{\text{g}})$
0	$2.6790 \times 10^{-4}$	10.87400	1788.316	5918.499	0.6980547
2	$2.7192 \times 10^{-4}$	10.79123	1829.563	6030.156	0.6967108
4	$2.7588 \times 10^{-4}$	10.70846	1867.201	6133.124	0.6956351
6	$2.7930 \times 10^{-4}$	10.62570	1901.373	6227.712	0.6948023
8	$2.8368 \times 10^{-4}$	10.54293	1932.222	6314.225	0.6941902
10	$2.8750 \times 10^{-4}$	10.46016	1959.885	6392.958	0.6937790
12	$2.9128 \times 10^{-4}$	10.37739	1984.500	6464.205	0.6935516
14	$2.9500 \times 10^{-4}$	10.29462	2006.198	6528.253	0.6934924
16	$2.9868 \times 10^{-4}$	10.21186	2025.111	6585.380	0.6935873
18	$3.0232 \times 10^{-4}$	10.12909	2041.365	6635.864	0.6938257
20	$3.0590 \times 10^{-4}$	10.04632	2055.086	6679.793	0.6941953
22	$3.0944 \times 10^{-4}$	9.96355	2066.396	6717.971	0.6946369
24	$3.1292 \times 10^{-4}$	9.88078	2075.413	6750.117	0.6952913
26	$3.1636 \times 10^{-4}$	9.79802	2082.253	6776.663	0.6960021
28	$3.1976 \times 10^{-4}$	9.71525	2087.030	6797.857	0.6968106
30	$3.2310 \times 10^{-4}$	9.63248	2099.855	6813.939	0.6977110
32	$3.2640 \times 10^{-4}$	9.54971	2090.836	6825.146	0.6986973
34	$3.2964 \times 10^{-4}$	9.46694	2090.076	6831.707	0.6997638
36	$3.3284 \times 10^{-4}$	9.38418	2087.679	6833.847	0.7009056
38	$3.3600 \times 10^{-4}$	9.30141	2083.743	6831.785	0.7021179
40	$3.3910 \times 10^{-4}$	9.21864	2078.365	6825.734	0.7033962

Since the density of salt water is usually a bit more than 1000 kg/m<sup>3</sup>, Oceanographers often subtract 1000 from the density values and denote the value by sigma. If this is done for atmospheric pressure, then a subscript t is usually added. Thus:

$$\sigma_t = \rho - 1000 \quad (3.21)$$

in which  $\rho$  is evaluated at atmospheric pressure.

Values of  $\sigma_t$  as a function of salinity and temperature are listed in table 3.3. These tables were computed using equation 3.18 with  $p' = 1.0133 \text{ bars} = 1 \text{ atmosphere}$ .

Since the equations (and their resulting tables) are a bit cumbersome in use, the Delft Hydraulics Laboratory uses a simpler relationship. In the notation already used,

$$\sigma_t = 0.75 S \quad (3.22)$$

Equation 3.22 neglects influences of temperature and pressure and is therefore more limited in use than equation 3.18. In practice, civil engineers will sometimes find equation 3.22 to be sufficient for problems in which density differences result exclusively from salinity differences and the water temperature is not extreme.

With this information on density we can return briefly to the description of the oceans, themselves. Usually, both salinity and temperature decrease with increasing depth in the ocean. Evaporation is responsible for the higher salinity of the surface layer; how can this float on less saline deeper water? The temperature differences are sufficient to maintain a density profile which increases with depth.

Density variations caused by differences in salinity and temperature can be used in ingenious ways such as to drive a salt fountain, made in the following way:

We take a long (1 km) pipe and extend it vertically down from the ocean surface. Next, we attach a pump and slowly draw up the deep water. We do this slowly so that the water rising in the pipe can be warmed by the surrounding ocean. After deep water reaches the surface we remove the pump and find that the water continues to flow. Why does it flow? No, it is not perpetual motion; the process stops as soon as the upper 1 km layer of the ocean has become mixed.

Currents caused by density differences are discussed in the next section and again, in detail, in chapter 22.

TEMPERATURE IN °C

S	0	2	4	6	8	10	12	14	16	18	20	22	24	26	28	30	32	34	36	38	40	S
0	-0.16	-0.06	-0.03	-0.06	-0.15	-0.30	-0.50	-0.75	-1.06	-1.40	-1.79	-2.23	-2.70	-3.21	-3.76	-4.35	-4.97	-5.62	-6.31	-7.03	-7.78	0
1	+0.66	+0.75	+0.78	+0.74	+0.64	+0.49	+0.28	+0.02	-0.28	-0.63	-1.03	-1.47	-1.94	-2.46	-3.01	-3.60	-4.22	-4.88	-5.57	-6.29	-7.04	1
2	1.48	1.57	1.58	1.54	1.44	1.28	1.06	0.80	+0.49	+0.14	-0.26	-0.70	-1.18	-1.70	-2.25	-2.85	-3.48	-4.13	-4.83	-5.55	-6.30	2
3	2.30	2.38	2.39	2.34	2.23	2.06	1.85	1.58	1.26	0.90	+0.50	+0.06	-0.43	-0.95	-1.51	-2.10	-2.73	-3.39	-4.08	-4.81	-5.56	3
4	3.12	3.19	3.19	3.14	3.02	2.85	2.63	2.36	2.04	1.67	1.27	0.82	+0.33	-0.19	-0.75	-1.35	-1.98	-2.64	-3.34	-4.07	-4.83	4
5	3.94	4.00	4.00	3.94	3.81	3.64	3.41	3.13	2.81	2.44	2.03	1.58	1.09	+0.56	0.00	-0.60	-1.23	-1.90	-2.60	-3.33	-4.09	5
6	4.76	4.81	4.80	4.73	4.61	4.42	4.19	3.91	3.58	3.21	2.80	2.34	1.85	1.32	+0.75	+0.15	-0.49	-1.15	-1.86	-2.59	-3.35	6
7	5.58	5.63	5.61	5.53	5.40	5.21	4.97	4.69	4.35	3.98	3.56	3.10	2.61	2.07	1.50	0.90	+0.26	-0.41	-1.11	-1.85	-2.61	7
8	6.40	6.44	6.41	6.33	6.19	6.00	5.75	5.46	5.13	4.75	4.32	3.86	3.36	2.83	2.25	1.65	1.01	+0.33	-0.37	-1.11	-1.87	8
9	7.22	7.24	7.21	7.12	6.98	6.78	6.53	6.24	5.90	5.51	5.09	4.62	4.12	3.58	3.01	2.40	1.75	1.08	+0.37	-0.36	-1.13	9
10	8.03	8.05	8.02	7.92	7.77	7.57	7.31	7.01	6.67	6.28	5.85	5.38	4.88	4.34	3.76	3.15	2.50	1.82	1.12	+0.38	-0.39	10
11	8.85	8.86	8.82	8.71	8.56	8.35	8.09	7.79	7.44	7.05	6.62	6.14	5.64	5.09	4.51	3.90	3.25	2.57	1.86	1.12	+0.35	11
12	9.66	9.67	9.62	9.51	9.35	9.13	8.87	8.56	8.21	7.82	7.38	6.90	6.39	5.84	5.26	4.64	4.00	3.31	2.60	1.86	1.08	12
13	10.48	10.48	10.42	10.30	10.14	9.92	9.65	9.34	8.98	8.58	8.14	7.66	7.15	6.60	6.01	5.33	4.74	4.06	3.34	2.60	1.82	13
14	11.29	11.28	11.22	11.10	10.93	10.70	10.43	10.11	9.75	9.35	8.91	8.42	7.91	7.35	6.76	6.14	5.49	4.80	4.09	3.34	2.56	14
15	12.10	12.09	12.02	11.89	11.71	11.48	11.21	10.89	10.52	10.11	9.67	9.18	8.66	8.11	7.52	6.89	6.24	5.55	4.83	4.08	3.30	15
16	12.92	12.90	12.82	12.69	12.50	12.27	11.99	11.66	11.29	10.88	10.43	9.94	9.42	8.86	8.27	7.64	6.98	6.29	5.57	4.82	4.04	16
17	13.73	13.70	13.62	13.48	13.29	13.05	12.76	12.43	12.06	11.65	11.19	10.70	10.18	9.61	9.02	8.39	7.73	7.04	6.31	5.56	4.78	17
18	14.54	14.50	14.41	14.27	14.08	13.83	13.54	13.21	12.83	12.41	11.96	11.46	10.93	10.37	9.77	9.14	8.48	7.78	7.06	6.30	5.52	18
19	15.35	15.31	15.21	15.06	14.86	14.61	14.32	13.98	13.60	13.18	12.72	12.22	11.69	11.12	10.52	9.89	9.22	8.53	7.80	7.04	6.26	19
20	16.16	16.11	16.01	15.85	15.65	15.39	15.10	14.75	14.37	13.94	13.48	12.98	12.45	11.88	11.27	10.64	9.97	9.27	8.54	7.78	7.00	20
21	16.97	16.91	16.81	16.64	16.43	16.18	15.87	15.53	15.14	14.71	14.24	13.74	13.20	12.63	12.02	11.38	10.71	10.01	9.28	8.52	7.74	21
22	17.78	17.72	17.60	17.44	17.22	16.96	16.65	16.30	15.91	15.47	15.00	14.50	13.96	13.38	12.77	12.13	11.46	10.76	10.03	9.26	8.47	22
23	18.59	18.52	18.40	18.23	18.00	17.74	17.42	17.07	16.67	16.24	15.77	15.26	14.71	14.14	13.52	12.88	12.21	11.50	10.77	10.01	9.21	23
24	19.40	19.32	19.19	19.02	18.79	18.52	18.20	17.84	17.44	17.00	16.53	16.02	15.47	14.89	14.28	13.63	12.95	12.25	11.51	10.75	9.95	24
25	20.20	20.12	19.99	19.80	19.57	19.30	18.98	18.61	18.21	17.77	17.29	16.77	16.22	15.64	15.03	14.38	13.70	12.99	12.25	11.49	10.69	25
26	21.01	20.92	20.78	20.59	20.36	20.08	19.75	19.38	18.98	18.53	18.05	17.53	16.98	16.39	15.78	15.13	14.45	13.74	13.00	12.23	11.43	26
27	21.81	21.72	21.58	21.38	21.14	20.86	20.53	20.15	19.74	19.30	18.81	18.29	17.74	17.15	16.53	15.88	15.19	14.48	13.74	12.97	12.17	27
28	22.62	22.52	22.37	22.17	21.92	21.63	21.30	20.93	20.51	20.06	19.57	19.05	18.49	17.90	17.28	16.62	15.94	15.23	14.48	13.71	12.91	28
29	23.43	23.32	23.16	22.96	22.71	22.41	22.07	21.70	21.28	20.82	20.33	19.81	19.25	18.65	18.03	17.37	16.69	15.97	15.23	14.45	13.65	29
30	24.23	24.12	23.95	23.75	23.49	23.19	22.85	22.47	22.05	21.59	21.09	20.56	20.00	19.41	18.78	18.12	17.43	16.72	15.97	15.19	14.39	30
31	25.03	24.91	24.75	24.53	24.27	23.97	23.62	23.24	22.81	22.35	21.85	21.32	20.76	20.16	19.53	18.87	18.18	17.46	16.71	15.93	15.13	31
32	25.84	25.71	25.54	25.32	25.05	24.75	24.40	24.01	23.58	23.11	22.61	22.08	21.51	20.91	20.28	19.62	18.93	18.20	17.45	16.68	15.87	32
33	26.64	26.51	26.33	26.11	25.84	25.52	25.17	24.78	24.34	23.88	23.37	22.84	22.27	21.66	21.03	20.37	19.67	18.95	18.20	17.42	16.61	33
34	27.44	27.30	27.12	26.89	26.62	26.30	25.94	25.54	25.11	24.64	24.13	23.59	23.02	22.42	21.78	21.11	20.42	19.69	18.94	18.16	17.35	34
35	28.24	28.10	27.91	27.68	27.40	27.08	26.72	26.31	25.88	25.40	24.89	24.35	23.78	23.17	22.53	21.86	21.17	20.44	19.68	18.90	18.09	35
36	29.04	28.90	28.70	28.46	28.18	27.85	27.49	27.08	26.64	26.16	25.65	25.11	24.53	23.92	23.28	22.61	21.91	21.18	20.43	19.64	18.83	36
37	29.84	29.69	29.49	29.25	28.96	28.63	28.26	27.85	27.41	26.93	26.41	25.87	25.28	24.67	24.03	23.36	22.66	21.93	21.17	20.38	19.57	37
38	30.64	30.48	30.28	30.03	29.74	29.41	29.03	28.62	28.17	27.69	27.17	26.62	26.04	25.43	24.78	24.11	23.40	22.67	21.91	21.12	20.31	38
39	31.44	31.28	31.07	30.81	30.52	30.18	29.80	29.39	28.94	28.45	27.93	27.38	26.79	26.18	25.53	24.86	24.15	23.42	22.66	21.87	21.05	39
40	32.24	32.07	31.86	31.60	31.30	30.96	30.58	30.16	29.70	29.21	28.69	28.14	27.55	26.93	26.28	25.60	24.90	24.16	23.40	22.61	21.79	40

TABLE 3.3  $\sigma_t$  as Function of T and S

20

### 3.7 Density Currents

Horizontal density gradients can also lead to unbalanced pressure forces which result in a current. The mechanics of such currents is the same in a harbor on a tidal river as in the oceans. In chapter 22 of this book, the mathematical details will be explained; here, we shall only describe a significant example which we find in the oceans.

The Mediterranean Sea is more saline, and hence more dense than the Atlantic Ocean. A permanent current in the order of  $\frac{1}{2}$  m/s flows outward through the deeper portions of the Strait of Gibraltar. At the the surface, an even stronger current flows inward. The density difference which drives this current is maintained by the evaporation from the Mediterranean Sea.

#### 4. Beaufort Wind Scale

E.W. Bijker

In 1806 Admiral Beaufort of the British Navy devised a wind speed scale which would be helpful to sailors on the large sailing ships of that time, especially the larger men-of-war. On this scale, zero denotes no wind and twelve is the maximum; the scale is shown more explicitly in figure 4.1.

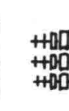
Captains of the large warships were often faced with a difficult choice: if they were cautious with the sails, they would preserve the ship, but might not catch their enemy or could be caught. If, on the other hand, they carried too much sail they had a better chance in battle, but ran a great risk of losing their masts and rigging (and possibly even their ship). Obviously, neither of these extremes is good for a career as navy officer. A bit of this controversy as commander is reflected in the racing sailor's description in the table.

This Beaufort Scale is still in common use, although slight variations in the wind speed limits of each scale division are possible.

Additional data relating this wind force scale to the sea state is provided in chapter 12. General wave theory is reviewed first in the next chapters.

WIND SPEEDS

TABLE 4.1 BEAUFORT WIND FORCE SCALE

Beaufort Number	knots	miles per hr. (U.S. Statute)	meters per sec.	km per hr.	Wind Press. N/m <sup>2</sup>	Beaufort description for square rigged ships 1806	Racing Sailor's description (C.A. Marchay, 1964)	U.S. Weather Service description	Dutch KNMI description	Beaufort Number
0	0	0	0	0				Calm	Windstil	0
1	1	3	0.5	2	0.14	Just Steerage Way	Boredom	Light air		1
2	4	6	2.1	7	2.4	1-3 knots close hauled	Mild pleasure	Light breeze	zwakke	2
3	7	10	3.6	13	7.7	4-5 knots close hauled	Pleasure	Gentle breeze		3
4	11	16	5.7	20	19	6-7 knots close hauled	Great Pleasure	Moderate breeze	matige	4
5	17	21	9	32	46	 Hull Speed Full Sail	Delight	Fresh breeze	vrij krachtige	5
6	22	27	11	41	77		Delight tinged with anxiety	Strong breeze	krachtige	6
7	28	33	14	52	125		Anxiety tinged with fear	Moderate Gale	harde	7
8	34	40	18	63	182		Fear tinged with terror	Gale	stormachtige	8
9	41	47	21	76	270		Great terror	Strong Gale	storm	9
10	48	55	25	89	360		Panic	Whole Gale	zware storm	10
11	56	63	29	104	500		I want my mummy!!	Storm	zeer zware storm	11
12	above 63	above 75	above 33	above 120	above 630	bare poles	Yes, Mr. Jones	Hurricane	orkaan	12

Storm warnings are usually issued for winds stronger than Beaufort force 6

5.1. Introduction

Some knowledge of the mechanics of short waves is essential for the good understanding of coastal engineering. Since the theory of short waves is not a prerequisite to this course, the more important wave relationships are given in this section. Derivations are not given; these may be found either in specialized courses in short wave theory or in the literature. Kinsman (1965) presents an excellent overview of short wave theory in a very readable fashion.

All of the results presented in this section have been derived using the Airy theory for a linear, sinusoidal wave form. "Ocean waves are not sinusoidal!" one will argue who has ever experienced the actual sea. This is true, but enough important properties of even irregular waves can be discovered by studying a single sinusoidal wave which does not break. This wave will be considered to be two dimensional: it will move along the horizontal x axis while the vertical z axis (positive upward) will have its origin at the still water surface.

5.2. General Relationships

Observation of a float on the surface of waves reveals that its position oscillates horizontally and vertically about a fixed position. This may seem strange since the wave profile moves forward past the float with a definite velocity. Obviously, the velocity of the float (water particle velocity) and the velocity with which the crest moves (phase velocity or wave celerity) are quite different. Let us first examine the motion of the float.

## Water Particle Velocities

The horizontal and vertical water particle velocity components are given by:

$$u = \frac{\omega H}{2} \frac{\cosh k(z+h)}{\sinh kh} \cos(kx - \omega t) \quad (5.01)$$

$$w = \frac{\omega H}{2} \frac{\sinh k(z+h)}{\sinh kh} \sin(kx - \omega t) \quad (5.02)$$

where: H is the wave height  
 h is the water depth  
 k is the wave number =  $\frac{2\pi}{\lambda}$   
 $\lambda$  is the wave length  
 t is the time  
 u is the instantaneous horizontal particle velocity  
 w is the instantaneous vertical particle velocity  
 x is the horizontal coordinate

- $z$  is the vertical coordinate measured from the still water surface (+ up)  
 $\omega$  is the circular frequency =  $\frac{2\pi}{T}$   
 $T$  is the wave period

Substitution of  $z = 0$  into equations 5.01 and 5.02, yields the instantaneous velocity components of the float.

#### Water particle displacements

The amplitude of the displacement of the float can be determined by integrating the velocity with respect to time. This yields:

$$\hat{\xi} = \frac{H}{2} \frac{\cosh k(z+h)}{\sinh kh} \quad (5.03)$$

$$\hat{\zeta} = \frac{H}{2} \frac{\sinh k(z+h)}{\sinh kh} \quad (5.04)$$

where:  $\hat{\xi}$  is the horizontal displacement amplitude,  
 $\hat{\zeta}$  is the vertical displacement amplitude, and  
 $\hat{\quad}$  denotes "amplitude of".

These define the semi-axes of ellipses. The water particles move along elliptical paths; the size of these ellipses is greatest at the water surface and decreases as the observer moves deeper.

#### Wave Speed

The speed at which a wave crest moves forward is given by:

$$c = \frac{\lambda}{T} = \frac{\omega}{k} = \sqrt{\frac{g}{k} \tanh kh} \quad (5.05)$$

where:  $g$  is the acceleration of gravity, and  
 $c$  is the wave celerity, or phase speed.

Equation 5.05 is a bit complicated to use in practice. Indeed, since both  $\lambda$  and  $k$  are dependent upon the answer,  $c$ , we cannot blindly substitute values into this equation for a simple solution. Therefore, the solution of this equation is taken up in section 6 again, where various tricks for its solution are explained.

If, for a moment, we examine a finite number (group) of waves propagating in otherwise still water, we will observe that waves seem to originate at the rear of the group, move forward through the group with speed  $c$ , and die out near the front of the group. Certainly this group moves forward as well, but with a smaller speed. The speed with which this group moves forward is given by:

$$c_g = \frac{c}{2} \left( 1 + \frac{2kh}{\sinh 2kh} \right) \quad (5.06)$$

or

$$\frac{c_g}{c} = \frac{1}{2} \left( 1 + \frac{2 kh}{\sinh 2 kh} \right) = n \quad (5.07)$$

As is indicated in equation 5.07, the ratio of group velocity to phase velocity is often denoted by  $n$ .

#### Wave energy

The energy contained in a wave of unit width (crest length) is:

$$E_T = \frac{1}{8} \rho g H^2 \lambda \quad (5.08)$$

where  $\rho$  is the mass density of water.

Often, it is more convenient to express energy in terms of energy per unit of water surface area.

$$E = \frac{1}{8} \rho g H^2 \quad * \quad (5.09)$$

This energy is propagated with the wave group speed,  $c_g$ .

#### Wave Power

Since power is energy per unit time one might attempt to find the power of waves by dividing equation 5.08 by the wave period. Unfortunately, this is incorrect since it was just pointed out that the energy moves forward with the group velocity. Thus, the correct relationship is:

$$U = E c_g = E n c \quad (5.10)$$

where  $U$  is the power per unit crest length.

#### Wave pressure

The presence of the waves shall influence the pressure within our body of water. The pressure under the waves is given by:

$$p = -\rho g z + \frac{\rho g H}{2} \frac{\cosh k(z+h)}{\cosh kh} \cos(kx - \omega t) \quad (5.11)$$

where  $p$  is the instantaneous pressure.

The first term on the right of equation 5.11 is the pressure which would be present in still water. The second term describes the variation in pressure caused by the waves. This pressure variation can be very important when designing a structure to be placed in the sea.

\* The reader should verify for himself that the dimensions of equation 5.09 are correct.

### 5.3. Simplifications

Equations 5.01 through 5.11 can be simplified when certain conditions are satisfied. This will be attempted via the hyperbolic functions. The behavior of the hyperbolic functions is shown in figure 5.1.

### 5.4. Approximations for Deep Water

For relatively, deep water ( $h > \frac{\lambda}{2}$ <sup>x</sup>; therefore,  $X > \pi$  in figure 5.1):

$$\sinh X \approx \cosh X \gg X \quad (5.12)$$

$$\tanh X \approx 1.0 \quad (5.13)$$

Now, substituting this and doing a bit of algebra with equations 5.01 through 5.11, we get:

$$u_0 = \frac{\omega H_0}{2} e^{k_0 z} \cos(k_0 x - \omega t) \quad (5.01a)$$

$$w_0 = \frac{\omega H_0}{2} e^{k_0 z} \sin(k_0 x - \omega t) \quad (5.02a)$$

$$\hat{\xi}_0 = \frac{H_0}{2} e^{k_0 z} \quad (5.03a)$$

$$\hat{\zeta}_0 = \frac{H_0}{2} e^{k_0 z} \quad (5.04a)$$

$$c_0 = \frac{\lambda_0}{T} = \frac{\omega}{k_0} = \frac{g}{2\pi} T \quad (5.05a)$$

$$c_{g_0} = \frac{c_0}{2} \quad (5.06a)$$

$$n_0 = \frac{1}{2} \quad (5.07a)$$

$$E_{T_0} = \frac{1}{8} \rho g H_0^2 \lambda_0 \quad (5.08a)$$

$$E_0 = \frac{1}{8} \rho g H_0^2 \quad (5.09a)$$

$$U_0 = E_0 n_0 c_0 \quad (5.10a)$$

$$p_0 = -\rho g z + \frac{\rho g H_0}{2} e^{k_0 z} \cos(k_0 x - \omega t) \quad (5.11a)$$

The subscript 0 has been added to denote deep water conditions; this is fairly common in the literature. This has not been done with T or  $\omega$  since these parameters remain constant.

<sup>x</sup> We shall re-examine this criteria in section 5.7.

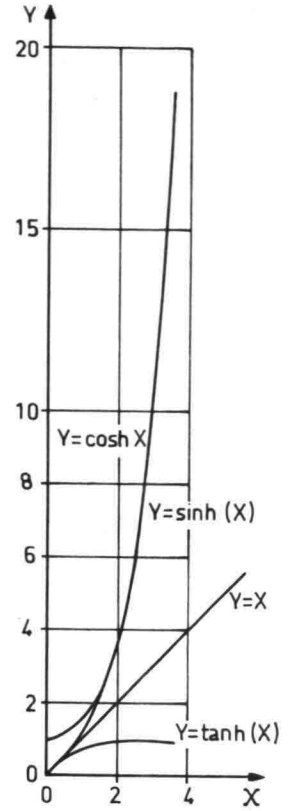


Figure 5.1  
BEHAVIOR OF  
HYPERBOLIC  
FUNCTIONS

Substituting values for  $g$  and  $\pi$  in equation 5.05a, we get:

$$\left. \begin{aligned} c_0 &= 1.56 T && \text{in m kg s units and} \\ c_0 &= 5.12 T && \text{in ft lb s units.} \end{aligned} \right\} \quad (5.14)$$

From the same equation, it follows that:

$$\left. \begin{aligned} \lambda_0 &= 1.56 T^2 && \text{in m kg s units and} \\ \lambda_0 &= 5.12 T^2 && \text{in ft lb s units.} \end{aligned} \right\} \quad (5.15)$$

Thus, in deep water, we avoid all the headaches of computing the wave speed using the full equation 5.05.

Note from equations 5.03a and 5.04a that the elliptical particle paths have reduced to circles which decrease in radius exponentially as one moves deeper in the water. Figure 5.2 shows this orbital motion in a deep water wave. In this figure, also, the water depth is equal to half the wave length; under these conditions, the ratio of particle displacement on the bottom to that at the water surface is  $e^{-\pi} = 0.043$ .

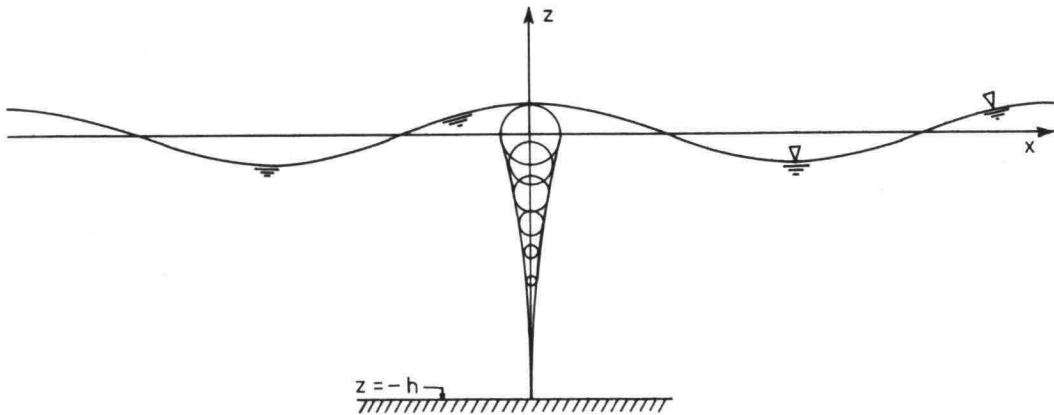


Figure 5.2  
ORBITAL MOTION UNDER  
A DEEP WATER WAVE

### 5.5. Approximations for Shallow Water

Another set of simplifying approximations can be substituted when the water is relatively shallow ( $h < \frac{\lambda}{25}$ ;  $X < 0.25$  in figure 5.1):\*

$$\sinh kh \approx \tanh kh \approx kh \quad (5.16)$$

$$\cosh kh \approx 1 \quad (5.17)$$

Again, using these and a bit of algebra in equations 5.01 through 5.11, we get:

$$u = \frac{\omega H}{2kh} \cos(kx - \omega t) \quad (5.01b)$$

$$w = \frac{\omega H}{2} \left(1 + \frac{z}{h}\right) \sin(kx - \omega t) \quad (5.02b)$$

$$\hat{\xi} = \frac{H}{2kh} \quad (5.03b)$$

$$\xi = \frac{H}{2} \left(1 + \frac{z}{h}\right) \quad (5.04b)$$

$$c = \frac{\lambda}{T} = \frac{\omega}{k} = \sqrt{gh} \quad (5.05b)$$

$$c_g = \frac{c}{2}(1 + 1) = c \quad (5.06b)$$

$$n = 1 \quad (5.07b)$$

$$E_T = \frac{1}{8} \rho g H^2 \lambda \quad (5.08b)$$

$$E = \frac{1}{8} \rho g H^2 \quad (5.09b)$$

$$U = Ec \quad (5.10b)$$

$$p = -\rho g z + \frac{\rho g H}{2} \cos(kx - \omega t) \quad (5.11b)$$

The wave phase velocity is now found to be independent of the wave period; it depends only upon the water depth. Further, the group velocity is equal to the phase velocity, and the horizontal particle velocity,  $u$ , is independent of the vertical position,  $z$ . Indeed, these equations are the same as those used for long waves.

The wave length can easily be computed using equation 5.05b:

$$\lambda = \sqrt{gh} T \quad (5.18)$$

\* We re-examine this limit, also, in section 5.7.

Once again, the simple form of equation 5.05b has eliminated the problems associated with the evaluation of equation 5.05.

Figure 5.3 shows the orbital motion under a shallow water wave. In this figure  $h = \lambda/25$ .

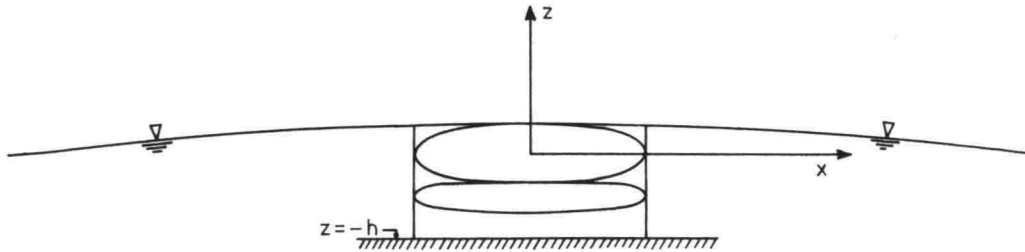


Figure 5.3  
ORBITAL MOTION UNDER  
A SHALLOW WATER WAVE

#### 5.6. Intermediate water depths

For water of all intermediate relative depths ( $\frac{\lambda}{25} < h < \frac{\lambda}{2}$ )\*

we are forced to work with the complete equations 5.01 through 5.11. Water particles move along elliptical paths which are nearly circles at the water surface and degenerate both horizontally and vertically to short horizontal lines at the bottom.

Since the use of equations 5.01 through 5.11 is impossible directly when only a water depth,  $h$ , wave period,  $T$ , and a wave height,  $H$ , are known (a very practical situation), special attention will be paid to this problem in chapter 6.

#### 5.7. A Critical Re-examination

Some important practical questions remain. The first is, "what wave length should be substituted into the ratio of  $h/\lambda$  to determine whether to use shallow, intermediate or deep water wave theory?" One answer is to say, "Use the actual wave length at that depth". This is not too bad, since the wave lengths in deep and shallow water can be computed quite easily using either equation 5.15 or 5.18 respectively. Another approach - which leads to quite different results! - is to always use the deep water wave length,  $\lambda_0$  from equation 5.15.

Another important related question is: "What is so sacred about the suggested values of  $h/\lambda$ ?"

Nothing!!!

\* subject to review in the next section.

There is certainly discussion and perhaps even disagreement about what these limits should be. Kinsman (1965) pp 129-133 points this out rather colorfully. As he indicates, there are two basic criteria for determining the acceptable accuracy for an approximation: a mathematician's, and an engineer's. The mathematician, worried about computational accuracy accepts an error of the approximation of about 0.5%. The engineer, on the other hand, is more aware of his other limitations and is happy with 5% accuracy. Now, perhaps, we can make a more intelligent appraisal of both our questions.

Table 5.1 lists the relative water depth limits for deep and shallow water according to various criteria.

TABLE 5.1. Comparison of  $\frac{h}{\lambda_0}$  and  $\frac{h}{\lambda}$  for various criteria

	$\frac{h}{\lambda_0}$	$\frac{h}{\lambda}$
<u>for deep water</u>		
section 5.4:	$\frac{1}{2.01}$	$\frac{1}{2}$
Mathematician's	$\frac{1}{2}$	1.99
Engineer's	$\frac{1}{4}$	$\frac{1}{3.73}$
<u>for shallow water</u>		
Mathematician's	$\frac{1}{200}$	$\frac{1}{35}$
section 5.5	$\frac{1}{102}$	$\frac{1}{25}$
	$\frac{1}{25}$	$\frac{1}{12}$
Engineer's	$\frac{1}{20}$	$\frac{1}{11}$

Thus, for deep water, the criteria as stated in section 5.4 is very conservative:  $h > \frac{\lambda_0}{4}$  would seem more appropriate. For shallow water, on the other hand, the limit criteria given in section 5.5 is not overly conservative, but could still be made a bit more flexible. In keeping with Kinsman's discussion,  $h < \frac{\lambda_0}{20}$  is suggested as a limit. Adoption of these suggested limits will greatly reduce the range of relative depths for which the full equations 5.01 through 5.11 must be used, while keeping our error usually less than about 5%.

### 5.8. Examples

First, let us examine some "typical" waves, and then, using some rather extreme examples, we shall observe that the relative depth  $\frac{h}{\lambda_0}$  is more important than the absolute depth.

1. North Sea,  $H = 0.8$  m,  $T = 8$  seconds, and  $h = 10$  m. (this is a very common wave on the North Sea). From 5.15,

$$\lambda_0 = (1.56)(8^2) = 100 \text{ m}; \quad \frac{h}{\lambda_0} = \frac{10}{100} = \frac{1}{10};$$

this is intermediate water depth, we are stuck until after chapter 6. Note, the wave height,  $H$ , was not used here at all.

2. Strait of Gibraltar,  $H = 25$  m,  $T = 15$  sec. and  $h = 1000$  m. (This is a severe storm wave in that area). From 5.15,

$$\lambda_0 = (1.56)(15^2) = 351 \text{ m}; \quad \frac{h}{\lambda_0} = \frac{1000}{351} > \frac{1}{4};$$

this is certainly deep water. We can determine the horizontal water particle velocity amplitude at a depth of 100 meters using equation 5.01a:

$$u_0 = \left(\frac{2\pi}{15}\right)\left(\frac{25}{2}\right) e^{-\left(\frac{2\pi}{351}\right)(100)}. \quad \text{The cosine term is dropped for determining the amplitude. Evaluating this, we get:}$$

$$u_0 = 5.24 e^{-1.79} = 0.87 \text{ m/s. The speed of this wave (from 5.14) is: } c_0 = (1.56)(15) = 23.4 \text{ m/s} = 84 \text{ km/hr} = 45.5 \text{ knots!}$$

3. North Sea (Dutch Coast),  $H = 1.5$  m,  $T = 8$  sec.,  $h = 4$  m.

$$\lambda_0 = (1.56)(8^2) = 100 \text{ m}; \quad \frac{h}{\lambda_0} = \frac{4}{100} = \frac{1}{25}, \text{ this is shallow water.}$$

Therefore, from 5.05b,  $c = \sqrt{(9.81)(4)} = 6.3$  m/s. The wave length is  $cT = (6.3)(8) = 50$  m. The energy in the wave per unit crest length is (eqn. 5.08b):

$$E_T = \left(\frac{1}{8}\right)(1030)(9.81)(1.5^2)(50) = 0.142 \times 10^6 \frac{\text{N} \cdot \text{m}}{\text{m}}$$

4. In a model we generate a wave with period 0.6 sec. in water 30 cm deep.

$$\lambda_0 = (1.56)(0.6^2) = 0.56 \text{ m}; \quad \frac{h}{\lambda_0} = \frac{30}{56} > \frac{1}{2}; \text{ this is deep}$$

water. The wave speed is  $c_0 = (1.56)(0.6) = 0.94$  m/sec.

6. WAVE SPEED AND LENGTH COMPUTATIONS

W.W. Massie

6.1. Introduction

For intermediate water depths ( $\frac{\lambda_0}{20} < h < \frac{\lambda_0}{4}$ ), there is no simple, direct means of determining the wave length or other related parameters given only the wave period. Two methods are presented here, both are derived from the non-linear equation for wave speed, equation 5.05.

6.2. Iteration Method

Recall equation 5.05,

$$c = \sqrt{\frac{g}{k} \tanh kh} = \frac{\lambda}{T} \quad (5.05) \quad (6.01)$$

in which  $c$  is the wave phase velocity

$g$  is the acceleration of gravity

$k$  is the wave number =  $\frac{2\pi}{\lambda}$

$h$  is the water depth

$\lambda$  is the wave length

$T$  is the wave period.

Substituting various definitions from chapter 5 into equation 6.01 yields:

$$\lambda = \lambda_0 \tanh \frac{2\pi h}{\lambda} \quad (6.02)$$

Since  $\lambda$ , the unknown, cannot be isolated on one side of this equation, a direct solution is impossible. Iterative solution schemes are possible. In fact most any iteration will eventually lead to the correct answer since the equation has only one solution for given values of  $\lambda_0$  and  $h$ .

One simple but rather inefficient iteration is to resubstitute successive answers from 6.02 (starting with  $\lambda = \lambda_0$ ) into the right hand side of the equation. Thus:

$$\lambda_{i+1} = \lambda_0 \tanh \frac{2\pi h}{\lambda_i} \quad (6.03)$$

where  $i = 0, 1, 2, \dots$

A much more efficient iteration is the following:

$$\lambda_{2i+1} = \lambda_0 \tanh \frac{2\pi h}{\lambda_{2i}}$$

$$\lambda_{2i+2} = \frac{2\lambda_{2i+1} + \lambda_{2i}}{3} \quad (6.04)$$

$$i = 0, 1, 2, \dots$$

While the algorithm is a bit more complex, it reduces the number of iterations considerably (three or four are usually more than sufficient) and can still be executed on many of the small pocket electronic calculators.

A direct technique attributed to Eckert (unpublished) which usually gives answers correct to within about 5 percent is simply:

$$\lambda = \lambda_0 \sqrt{\tanh \frac{2\pi h}{\lambda_0}} \quad (6.05)$$

Table 6.1 compares the results of these schemes.

Table 6.1. Wave length iterations

T = 19 seconds, h = 50 meters

	eqn. 6.03	eqn. 6.04
i	$\lambda_i$ (m)	$\lambda_{2i+2}$ (m)
0	563.8	378.1
1	285.2	382.0
2	451.6	381.6
3	339.2	381.6
4	410.9	
5	362.9	
6	394.2	
7	373.4	
8	387.0	
9	378.0	
10	384.0	
11	380.1	
12	382.6	
13	380.9	
14	382.0	
15	381.3	
16	381.8	
17	381.5	

The superiority of the second iteration scheme is obvious. For comparison purposes, equation 6.05 yields  $\lambda = 401.0$  which is off by 5.1%.

Obviously, now that the wave length has been determined all of the other related parameters can be easily evaluated.

### 6.3. Use of Tables

The computations outlined in the previous section were often cumbersome to carry out by hand. For this reason an alternative was developed in the form of a set of tables. By dividing both sides of equation 6.02 into  $h$  and doing a bit of algebra:

$$\frac{h}{\lambda_0} = \frac{h}{\lambda} \tanh \frac{2\pi h}{\lambda} \quad (6.06)$$

in which  $\frac{h}{\lambda_0}$  has been conveniently expressed in terms of  $\frac{h}{\lambda}$ . Thus,

by choosing various values of  $\frac{h}{\lambda}$ , corresponding values of  $\frac{h}{\lambda_0}$  can

be computed directly and tabulated. Interpolation in this table working either toward values of  $\frac{h}{\lambda_0}$  or toward values of  $\frac{h}{\lambda}$  is

all that is necessary to determine the wave length.

Wiegel (1954) worked out such a table. It is also published in his book *Oceanographical Engineering* (1964) and in the *Shore Protection Manual* (1973). An abbreviated version of this table is included here as table 6.2.

As an example, the previous iteration schemes can be checked.  $T = 19$  sec. and  $h = 50$  m yields  $\lambda_0 = 563.80$  m, and  $\frac{h}{\lambda_0} = 0.0887$ .

Interpolating in Wiegel (1964) yields  $\frac{h}{\lambda} = 0.1310$  and  $\lambda = 381.6$

which compares rather favorably to the earlier calculation.

TABLE 6.2. SINUSOIDAL WAVE FUNCTIONS

$\frac{h}{\lambda_0}$	$\tanh kh$	$\frac{h}{\lambda}$	$kh$	$\sinh kh$	$\cosh kh$	$\frac{H}{H_0}$
0.000	0.000	0.0000	0.000	0.000	1.00	$\infty$
0.002	112	0.179	112	113	01	2.12
0.004	158	0.253	159	160	01	1.79
0.006	193	0.311	195	197	02	62
0.008	222	0.360	226	228	03	51
0.010	0.248	0.0403	0.253	0.256	1.03	1.43
0.015	302	0.496	312	317	05	31
0.020	347	0.576	362	370	07	23
0.025	386	0.648	407	418	08	17
0.030	0.420	0.0713	0.448	0.463	1.10	1.13
0.035	452	0.775	487	506	12	09
0.040	480	0.833	523	548	14	06
0.045	507	0.888	559	598	16	04
0.050	0.531	0.0942	0.592	0.627	1.18	1.02
0.055	554	0.993	624	665	20	1.01
0.060	575	1.04	655	703	22	0.993
0.065	595	1.09	686	741	24	0.981
0.070	614	1.14	716	779	27	0.971
0.075	0.632	0.119	0.745	0.816	1.29	0.962
0.080	649	1.23	774	854	31	0.955
0.085	665	1.28	803	892	34	0.948
0.090	681	1.32	831	929	37	0.942
0.095	695	1.37	858	0.968	39	0.937
0.10	0.709	0.141	0.986	1.01	1.42	0.933
0.11	735	1.50	940	08	48	0.926
0.12	759	1.58	0.994	17	54	0.920
0.13	780	1.67	1.05	25	60	0.917
0.14	800	1.75	10	33	67	0.915
0.15	0.818	0.183	1.15	1.42	1.74	0.913
0.16	835	1.92	20	52	82	0.913
0.17	850	2.00	26	61	90	0.913
0.18	864	2.08	31	72	1.99	0.914
0.19	877	2.17	36	82	2.08	0.916
0.20	0.888	0.225	1.41	1.94	2.18	0.918

7.1. Introduction

Obviously, a wave breaks sometimes as it progresses from deep through intermediate depths to shallow water. Breaking will be considered later in this chapter and in chapter 8 as well. However, to begin with, consider a wave that is not yet broken, progressing into water which is gradually\* becoming shallower. In order to keep things from becoming too complicated, the discussion is still restricted to a two-dimensional case. In a practical sense, this means that the depth contours run parallel to the wave crests. This restriction will not be relaxed until chapter 9.

7.2. Wave Height Changes

Since so many of the relationships in chapter 5 were dependent upon the wave height, H, it seems logical to study how H varies as a wave progresses into shallower -- or back into deeper for that matter -- water. The relationship between H and h, the water depth, is exposed by applying conservation of energy. The energy transported through a vertical plane parallel to the wave crests is, in fact, the wave power per unit of crest length. This is sometimes called energy flux. Anyway, from equation 5.10:

$$U = E c_g = E n c \quad (5.10) \quad (7.01)$$

By assuming that this energy flux does not change as the wave progresses through water of varying depth, then:

$$U_2 = U_1 \quad (7.02)$$

or

$$E_2 n_2 c_2 = E_1 n_1 c_1 \quad (7.03)$$

where: c is the wave speed,

E is the wave energy per unit of surface area,

n is the ratio  $c_g/c$ ,

$c_g$  is the group velocity,

U is the power or energy flux, and

1,2 are subscripts indicating the location at which the parameters are evaluated.

Using equation 5.09 for E, and choosing location 2 to be deep water where the wave properties are easily evaluated, leads to:

$$\frac{1}{8} \rho g H_1^2 n_1 c_1 = \frac{1}{8} \rho g H_0^2 n_0 c_0 \quad (7.04)$$

---

\* "Gradually" means less than a few percent bottom slope.

Cancelling out a few unnecessary things and evaluating  $n_0$  from 5.07a:

$$H_1^2 n_1 c_1 = \frac{1}{2} H_0^2 c_0 \quad (7.05)$$

In another form, this is:

$$\frac{H_1}{H_0} = \sqrt{\frac{c_0}{c_1} \frac{1}{2n_1}} = K_{sh} \quad (7.06)$$

where:

$K_{sh}$  is the shoaling coefficient, and

$$n = \frac{1}{2} \left( 1 + \frac{2kh}{\sinh 2kh} \right) \quad (5.07)$$

This can be worked out a bit more by substituting for  $c_0$ , etc., and doing a lot of algebra; the final result is:

$$K_{sh} = \sqrt{\frac{1}{\tanh kh \left( 1 + \frac{2kh}{\sinh 2kh} \right)}} \quad (7.07)$$

Also, since  $k = \frac{2\pi}{\lambda}$ ,  $K_{sh}$  is purely a function of  $\frac{h}{\lambda}$  and, therefore, can be added to table 6.2; indeed,  $\frac{H_1}{H_0}$  is listed in the last column.

For completeness, we should check what the extreme values of  $K_{sh}$  can be in deep and shallow water. In deep water:

$$K_{sh_0} = 1 \quad (7.07a)$$

Mathematics confirm the result of physical reasoning in this case.

In shallow water, it is easiest to begin with equation 7.06. Using shallow water values of  $c_1$  and  $n_1$ :

$$K_{sh} = \sqrt{\frac{c_0}{\sqrt{gh}} \frac{1}{2}} \quad (7.08)$$

With a bit of algebra, this reduces to:

$$K_{sh} = \sqrt{\frac{1}{4\pi} \frac{\lambda}{h}} = 0.2821 \sqrt{\frac{\lambda}{h}} \quad (7.07b)$$

which approaches  $\infty$  as  $h$  approaches 0.

Expressed in another form, also for shallow water:

$$K_{sh} = \sqrt[4]{\frac{1}{8\pi} \frac{\lambda_0}{h}} = 0.4466 \left(\frac{\lambda_0}{h}\right)^{\frac{1}{4}} \quad (7.07b)$$

This gives  $K_{sh}$  purely as a function of  $h$  for a given wave condition.

### 7.3. Example

All the information is now available to compute the effect of depth changes on a two dimensional wave as long as the wave does not break. An example of how shoaling affects wave properties is shown in the following table.

In table 7.1. a very common sort of North Sea wave is followed as it progresses from deep water to shallow water. In deep water, equations 5.01a through 5.07a and 7.07a are used. In shallow water, equations 5.01b through 5.07b and 7.07b are used. The complete equations (actually the tables in Wiegel (1964)) are used for intermediate depths. Our wave has the following given properties:

$$H_0 = 2.0 \text{ m and } T = 7.0 \text{ seconds.}$$

From this follows that:

$$c_0 = 10.93 \text{ m/s and}$$

$$\lambda_0 = 76.53 \text{ m.}$$

TABLE 7.1. Wave Variations in Shoaling Water

$T = 7 \text{ s}$  ;  $H_0 = 2.0 \text{ m}$ ;  $c_0 = 10.93 \text{ m/s}$  ;  $\lambda_0 = 76.53 \text{ m}$

Water depth $h$ (m)	$\frac{h}{\lambda_0}$ (-)	Appli- cable Theory	$\frac{h}{\lambda}$ (-)	Wave Length $\lambda$ (m)	$n$ (-)	$c/c_0$ (-)	Phase velo- city $c$ (m/s.)	$\frac{H}{H_0} = K_s$ (-)	Wave height $H$ (m)	Wave steep- ness $H/\lambda$ (-)	$\frac{H}{h}$ (-)	Amplitude		Water depth (m)
												Surface velocity $u_s$ (m/s)	Bottom velocity $u_b$ (m/s)	
100	1.307	deep	1.307	76.53	0.500	1	10.93	1	2.0	0.02613	0.0200	0.90	0.00	100
75	0.980	deep	0.980	76.53	0.500	1	10.93	1	2.0	0.02613	0.0267	0.90	0.00	75
50	0.6533	deep	0.653	76.53	0.500	1	10.93	1	2.0	0.02613	0.0400	0.90	0.01	50
38.26	0.500	deep	0.500	76.53	0.500	1	10.93	1	2.0	0.02613	0.05227	0.90	0.04	38.26
28	0.366	deep	0.366	76.53	0.500	1	10.93	1	2.0	0.02597	0.0518	0.89	0.08	28
19.13	0.250	deep	0.250	76.53	0.500	1	10.93	1	2.0	0.02613	0.0714	0.90	0.09	19.13
15	0.196	inter.	0.2218	71.41	0.6164	0.9332	10.20	0.9323	1.86	0.0260	0.0972	0.89	0.32	15
10	0.131	inter.	0.1674	71.41	0.6724	0.8839	9.66	0.9172	1.83	0.0271	0.1220	0.93	0.43	10
5	0.0653	inter.	0.1094	59.74	0.7606	0.7824	8.55	0.9166	1.83	0.0306	0.1830	1.05	0.65	5
3.82	0.0500	inter.	0.09416	45.70	0.8713	0.5966	6.52	0.9808	1.96	0.0429	0.3920	1.48	1.18	3.82
3.00	0.0392	shallow	0.08913	40.57	0.8999	0.5310	5.80	1.023	2.05	0.0505	0.5366	1.73	1.47	3.00
2.00	0.0261	shallow	0.0790	42.86	1	0.5599	6.12	0.945	1.89	0.0441	0.4947	1.51	1.51	2.00
1.00	0.0131	inter.	0.0663	36.41	0.9207	0.4758	5.20	1.068	2.14	0.0588	0.7133	2.02	1.77	1.00
0.77	0.0100	inter.	0.0463	37.98	1	0.4968	5.43	1.004	2.01	0.0529	0.6700	1.82	1.82	0.77
		shallow	0.0645	30.17	0.9466	0.3939	4.43	1.158	2.32	0.0769	1.160	2.64	2.43	
		inter.	0.0456	31.01	1	0.4053	4.43	1.111	2.22	0.0716	1.110	2.47	2.47	
		shallow	0.0403	21.60	0.9729	0.2830	3.09	1.348	2.70	0.1250	2.70	4.28	4.11	
		inter.	0.0400	21.93	1	0.2864	3.13	1.321	2.64	0.1205	2.64	4.15	4.15	
		shallow		19.11	0.9792	0.2480	3.10	1.435	2.87	0.1502	3.73	5.20	5.03	
		inter.		19.24	1	0.2516	2.75	1.410	2.82	0.1466	3.66	5.04	5.04	

NOTE: NO CONSIDERATION OF BREAKING IS INCLUDED;

#### 7.4. Review of Example

A lot of useful conclusions can be drawn from table 7.1. For example, the results of the deep, intermediate, and shallow water wave equations can be compared for various values of  $h/\lambda_0$ . This might be helpful for reviewing the criteria for determining which, if any, approximation to use. With  $h/\lambda_0 = 0.5$ , the amplitude of the horizontal velocity at the bottom  $u_b$  varies by a factor of two depending upon the approximation used. This may or may not be serious, depending upon the character of the particular engineering problem involved. For a floating structure, then this error at the bottom is certainly unimportant. On the other hand, for erosion prediction around the foot of a gravity construction, this error may be very important.

#### 7.5. Breaking Criteria

Note from equation 7.07b that the theory used does not impose any limit on the height increase of a wave as it approaches a coast. On the other hand, we have all been to the beach at some time<sup>\*</sup> and have not seen any waves of infinite height. What, then, are the practical limitations on wave height? There are two: wave steepness, and wave height to water depth ratio.

##### Steepness Limit

Using the theory of solitary waves, investigators have shown that the maximum steepness of a non-breaking wave is  $0.142 = \frac{1}{7}$ . For this, the steepness is defined as the ratio of wave height to wave length,  $\frac{H}{\lambda}$ . This criteria normally governs the breaking of waves in deep water; and yet as Kinsman (1965) points out, many large storm waves do not break because they are too long<sup>†</sup>.

Values of wave steepness have been included in table 7.1. This breaking criteria indicates that the wave broke at a water depth somewhere between 0.77 and 1.00 m.

---

\* It is sincerely hoped that this assumption is correct!

† A wave of 15 second period, for example, would have to be 50 m high before it broke according to the steepness criterium. Luckily, we don't find this sort of wave too often.

### Wave Height: Water Depth Limit

The second criteria for breaking applies to the ratio of wave height to water depth  $\frac{H}{h}$ , often called the breaking index. A theoretical limit for this ratio (again for a solitary wave) is 0.78. This limit ratio is sometimes denoted by  $\gamma$ . A practical value for  $\gamma$  is about 0.6. Occasionally, an individual wave has even been observed for which  $\frac{H_{br}}{h_{br}} > 1.2$ . Thus, the limit is not an absolute surety. Generally, this criteria governs the breaking of waves on a shore. More thorough investigations, to determine  $\gamma$  from known physical parameters of the shore and wave have been carried out. See, for example, Swart (1974).

Values of  $\frac{H}{h}$  have been included for our example in table 7.1 as well. The wave would break according to this criteria in a water depth somewhere between 2 and 3 m. Indeed, the wave has broken by exceeding the maximum ratio  $\frac{H}{h}$ , rather than the maximum steepness. Now that breaking criteria and the effect of shoaling on a wave are known, we can think about the following questions: "How high is our wave in the example problem after it has passed over a shoal area having a minimum depth of 5 meters and has continued into water which is once again 100 meters deep?" What might be a good answer if the minimum depth of the shoal was 2 m?

In the first of these cases the shoal 5 m deep is not sufficient to cause the wave to break. Since the other effects are reversible, the wave height in deep water after the shoal will be, again, 2 meters.

In the second case, the wave which gets over the shoal will have a height of about  $0.6 \times 2 = 1.2$  m. As this wave progresses on into deeper water its wave height will decrease in the ratio  $\frac{2}{2.22}$  (see table 7.1). Thus, the resulting wave height in deep water will be  $1.2 \times \frac{2}{2.22} = 1.08$  m.\*

---

\* This is only a rough approximation. Other effects of the shoal such as transfer of energy to other (new) waves have been neglected.

## 8. TYPES OF BREAKERS

W.W. Massie

### 8.1. Introduction

In chapter 7 the criteria for wave breaking have been presented. Now, the breaking process itself can be examined. Obviously, when a wave breaks, its height diminishes and some of the energy of the wave is dissipated in turbulence and bottom friction; some is reflected back out to deep water, and some of the energy generates sound, other waves, heat, and currents. This last item, currents within the breaker zone, play a very important role in the morphological changes which occur along a coast. This current generation is reviewed in chapter 26 and treated in detail in volume II.

Patrick and Wiegell (1955) list three main types of breakers. These are described in the following paragraph.

### 8.2. Breaker Types

#### Spilling Breaker

Spilling breakers are usually found along very flat beaches. Waves begin breaking at a relatively great distance from shore and break very gradually as they approach still shallower water. A foam line develops at the crest during breaking and leaves a thin layer of foam over a considerable distance. Kinsman (1965) shows this very impressively on page 50 of his book. A less spectacular example is shown in figure 8.1. The breaker height decreases rather uniformly as we approach the coast. There is very little reflection of momentum back toward the sea.



Figure 8.1  
SPILLING BREAKER  
GENTLE BEACH SLOPE  
MAY CAUSE SEVERE  
EROSION

### Plunging Breaker

This is type of breaker often found on the travel posters for the Pacific Islands; it is spectacular. The curling top is characteristic of these waves. When one breaks much energy is dissipated in turbulence; little is reflected back to sea, and not much of a new wave is generated in the shallower water. This last is in contrast to what happens with a spilling breaker. Figure 8.2 shows a plunging breaker.



**Figure 8.2**  
PLUNGING BREAKER  
STEEP BEACH SLOPE

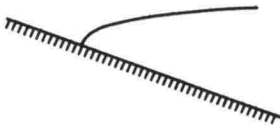
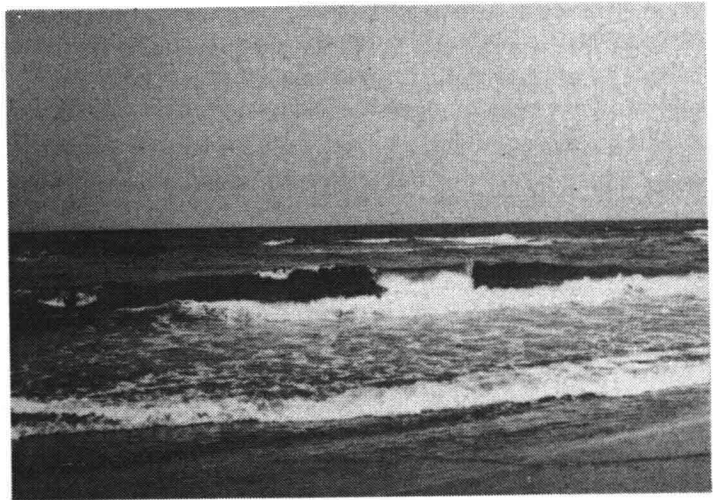


**Figure 8.3**  
SURGING BREAKER  
EXTREMELY  
STEEP SLOPE

### Surging Breakers

Surging breakers occur along extremely steep shores such as might be encountered along rock coasts. The breaker zone is very narrow, and much (more than half, usually) of the wave energy is reflected back out to deeper water. Figure 8.3 shows such a breaker. These breakers form up, much like plunging breakers, but the toe of each wave surges up the beach before the crest can curl over and fall.

### 8.3 Quantitative Classifications

Battjes (1974) reviewed the data available and parameters used for the classification of breaking waves into the above three main categories. Most of these parameters involve both wave properties such as height,  $H$ , and length,  $\lambda$ , as well as beach properties such as slope,  $m$ , and depth at the breaker line,  $h_{br}$ .

Battjes concludes that most of the earlier results can be collected via a single parameter involving three of the above four variables:

$$\xi_0 = \frac{m}{\sqrt{H_0 / \lambda_0}} \quad (8.01)$$

where:

- $H_0$  is the deep water wave height,
- $m$  is the beach slope,
- $\lambda_0$  is the deep water wave length, and
- $\xi_0$  is a breaking parameter.

The above parameter is determined purely on the basis of deep water wave conditions and the beach slope; it is valid for classifying breakers only if nothing strange happens to the waves between deep water and the beach. If, for example, waves break on a shoal far offshore then even though  $\xi_0$  can be evaluated, its relation to wave conditions at the beach - behind the offshore shoal - may, at best, be abnormal.

The fourth variable in the breaking process, the water depth in the breaker zone, can be included via the breaker index:

$$\gamma = \frac{H_{br}}{h_{br}} \quad (8.02)$$

where:

- $H_{br}$  is the wave height where breaking takes place, and
- $h_{br}$  is the water depth at that same location.

Battjes found a weak positive correlation between  $\log(\gamma)$  and  $\log(\xi_0)$ . Crudely fitting an equation to data he presents yields:

$$\gamma \approx \xi_0^{0.17} + 0.08 \quad (8.03)$$

which has been fitted over the range

$$0.05 < \xi_0 < 2$$

Further, there is still a wide spread in  $\gamma$  values for any given value of  $\xi_0$ ; a spread of  $\pm 0.1$  in  $\gamma$  is not enough to include all the data points. This can be explained, at least to some extent, by observing how difficult it can be to determine  $\gamma$  values via an experiment.

Another approach was used by Swart (1974). He defined a parameter  $p$  which ranges between 0.0 for spilling breakers and 1.0 for plunging breakers. (It is valid only for these two types.) He states that  $p$  can be determined with reasonable accuracy but does not elaborate how, except that he mentions "visual observation".

Swart, too, related the breaker index,  $\gamma$ , to his parameter,  $p$ :

$$\gamma = 0.33 p + 0.46 \quad (8.04)$$

Battjes (1974) related a number of additional properties of the breaker zone to the parameter,  $\xi_0$ ; these are all summarized in table 8.1. As one would expect from the comment concerning values of  $\gamma$ , above, values listed in table 8.1 are at best indicative rather than absolute. The reflection coefficient listed in that table is defined as the ratio of the height of the reflected wave to that of the incident wave. The number of breaking waves is the number of waves one can expect to find in the breaker zone at any instant.

Table 8.1 Breaker Zone Properties

Item	Values and remarks							
$\xi$	$\approx 0.1$	0.5	1.0	2.0	3.0	4.0	5.0	
breaker type	spilling		plunging		surging		(no breaking)	
$p$	0.0		1.0		(invalid)			
$\gamma$	0.5 to 0.8	0.7 to 1.0	0.8 to 1.1	1.2				
no. of waves breaking	6 to 7	2 to 3	1 to 2	0 to 1	0 to 1			
reflection coefficient	$10^{-3}$	0.01	0.1	0.4	0.8			
	absorption (progressive wave)						reflection (standing wave)	

9.1. Introduction

Until now, this discussion of waves has been restricted to two-dimensional phenomena; only motions which occurred in the vertical x-z plane were considered. Waves propagating into shallower water were assumed to be moving with their crests parallel to the depth contours. Further, until now, no partial obstacles have been allowed to interrupt the path of the waves. These restrictions will now be relaxed. Consider what happens when waves approach shoaling water with their crests at an angle to the depth contours.

9.2. Wave Refraction

When waves approach shallower water with their crests at an angle to the depth contours, the wave crests appear to curve so as to decrease this angle. This results from the fact that the wave celerity decreases as the water depth decreases - see equation 5.05 or 5.05b. In deep water refraction does not take place, since the wave speed is independent of water depth, there.

This phenomena is much like that in geometrical optics, where Snell's Law describes the behavior of light rays passing from one medium to another having a different transmission velocity. In the present case there is a gradual change in wave speed instead of an abrupt one encountered in optics. This gradual change leads to the curved wave crests shown in figure 9.1.

In figure 9.1, wave orthogonals (always perpendicular to the wave crests) have been sketched as well. These orthogonals are sometimes called rays. A bit of geometry quickly reveals that the distance between these rays increases as the water becomes shallower.

The effect of refraction on wave height is computed by assuming that the power transmitted between two adjacent wave orthogonals remains constant. In equation form:

$$U_1 b_1 = U_2 b_2 \quad (9.01)$$

where U is the power per unit crest length and b is the distance between orthogonals at points 1 and 2 respectively.

This should be compared to equation 5.10. Using this equation, we get:

$$E_1 n_1 c_1 b_1 = E_2 n_2 c_2 b_2 \quad (9.02)$$

where: E is the wave energy,  
n is the ratio of group velocity to wave celerity, and  
c is the wave celerity.

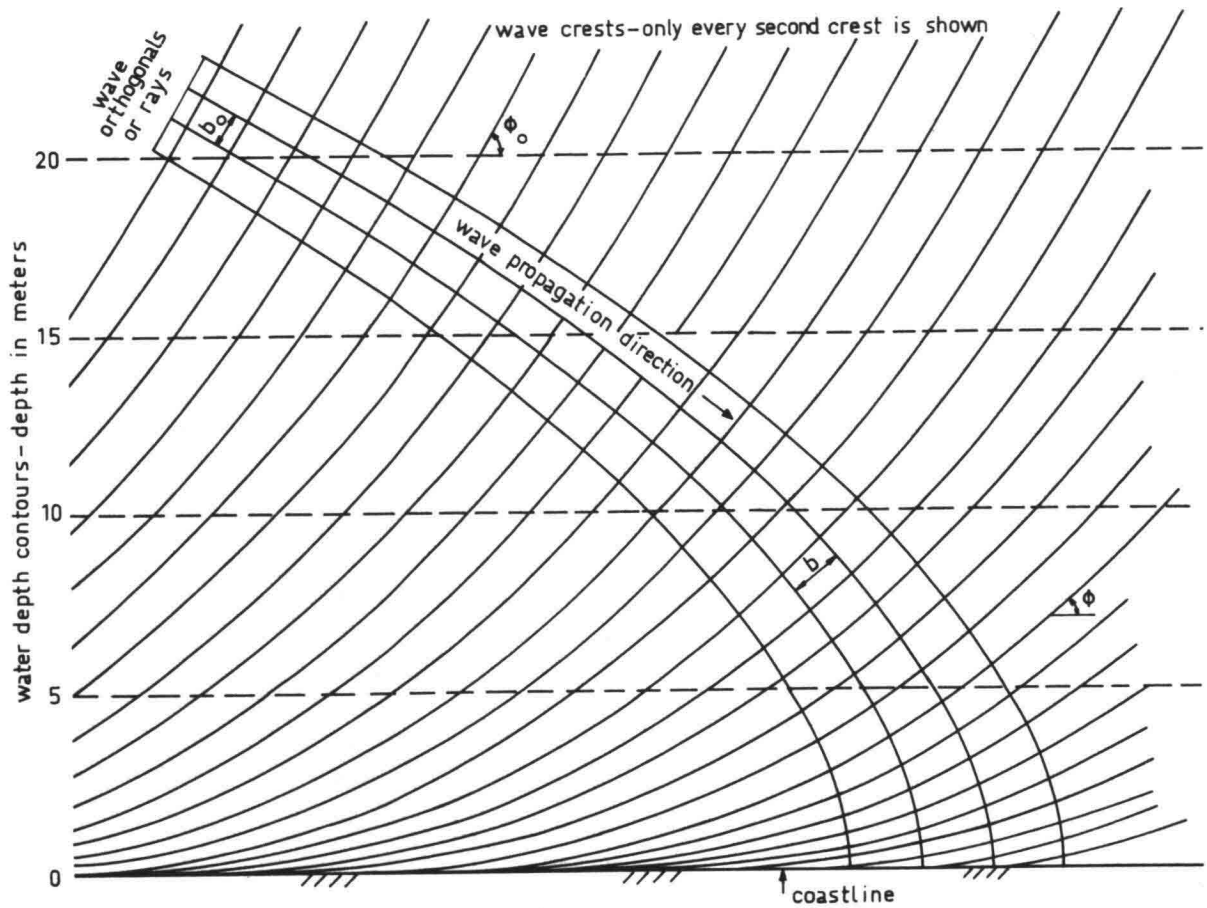


Figure 9.1 REFRACTION PATTERN

Substituting for  $E$  from (5.09) and choosing one measurement point in deep water leads to:

$$\frac{H_1}{H_0} = \sqrt{\frac{1}{2n_1} \frac{c_0}{c_1} \frac{b_0}{b_1}} = K_{sh} K_r \quad (9.03)$$

where:  $H$  is the wave height,  
 $K_{sh}$  is the shoaling coefficient, and  
 $K_r$  is the refraction coefficient.

$$K_r = \sqrt{\frac{b_0}{b_1}} \cdot$$

Only the problem of evaluating the ratio  $\frac{b_0}{b_1}$  remains. This is accomplished using geometry and Snell's Law. In equation form:

$$\frac{\sin \phi_0}{\sin \phi} = \frac{c_0}{c} \quad (9.04)$$

or:

$$\sin \phi = \frac{c}{c_0} \sin \phi_0 \quad (9.05)$$

where  $\phi$  is the angle between the wave crest and the depth contour.

From geometry given that the distance between given wave orthogonals measured parallel to the depth contours remains constant:

$$\frac{b_0}{b_1} = \frac{\cos \phi_0}{\cos \phi_1} \quad (9.06)$$

These relationships make it possible to complete the computations in a specific case. Table 9.1 shows the effect of refraction on the same wave as was chosen for table 7.1. ( $T = 7$  seconds,  $H_0 = 2$  m). Values from this table were used when drawing figure 9.1.

From table 9.1 it is obvious that refraction decreases the wave height as the water becomes shallower. What would be the angle between the wave crest and the depth contour if the depth were allowed to become zero? On the other hand, what happens when our waves pass over a shoal and again into deep water? The refraction process is reversible.

The computation procedure listed above is easily carried out for simple coasts where the bathymetry is simple. For more realistic hydrographic conditions, such a computation can be extremely laborious. For this reason a graphical solution technique has been developed. The construction of the necessary templates and their use is well described in the *Shore Protection Manual*, volume I, chapter 2.

TABLE 9.1. WAVE REFRACTION COMPUTATIONS

$T = 7.0$  s ;  $H_0 = 2.0$  m ;  $\rightarrow c_0 = 10.93$  m/s ;  $\lambda_0 = 76.53$  m.  
 $\lambda_0 = 76.53$  m

(1)	(1)	(1)	(1)	(1)	(2)	(2)	(1) (3)			
Water Depth h (m)	Wave Length $\lambda$ (m)	$c/c_0$ (-)	$K_{sh}$ (-)	$\phi$ (deg)	n (-)	$K_r$ (-)	$\frac{H}{H_0}$ (-)	H (m)	H' (m)	$b_1/b_0$ (-)
100	76.53	1	1	60.0	0.500	1.00	1.00	2.00	2.00	1.00
19.13	76.53	1	1	60.0	0.500	1.00	1.00	2.00	2.00	1.00
15	67.63	0.8839	0.9172	49.9	0.6724	0.8815	0.8085	1.62	1.83	1.29
10	59.74	0.7824	0.9166	42.7	0.7606	0.8245	0.7558	1.51	1.83	1.47
5	45.70	0.5966	0.9808	31.1	0.8713	0.7642	0.7495	1.50	1.96	1.71
3.82	42.86	0.5599	0.9450	29.0	1.000	0.7561	0.7145	1.43	1.89	1.75
3.0	37.98	0.4968	1.004	25.5	1.000	0.7442	0.7472	1.49	2.01	1.81
2.0	31.01	0.4053	1.111	20.5	1.000	0.7307	0.8118	1.62	2.22	1.87
1.0	21.93	0.2864	1.321	14.4	1.000	0.7184	0.9490	1.90	2.64	1.94
0.77	19.24	0.2516	1.410	12.6	1.000	0.7158	1.009	2.02	2.82	1.95

Wave Broken!!

NOTES

- (1) Data taken directly from table 7.1
- (2) Includes both refraction and shoaling influences, but not breaking!
- (3) Includes only shoaling

A further alternative to hand computations or graphical constructions is the use of large scale digital computer models. These models are currently under development; many still have occasional problems.

### 9.3. Wave Diffraction

Diffraction is a three-dimensional effect arising as a result of a "shadow" being formed by an obstacle. Diffraction is the phenomenon responsible for the spread of waves into this shadow zone

When diffraction occurs, wave energy seems to be transferred along the wave crests (across the orthogonals). This is in contrast to the assumption made in the previous section of this chapter.

How does diffraction occur? The following physical explanation has some strict theoretical difficulties, but is sufficient to give an insight to the process involved.

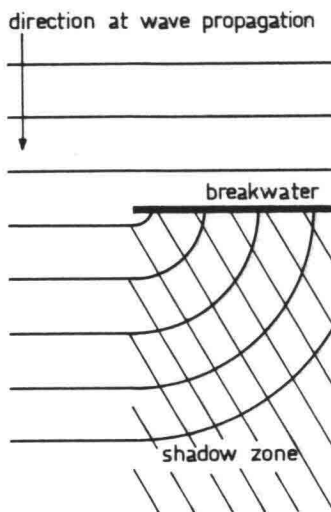


Figure 9.2  
WAVE DIFFRACTION  
PATTERN

As a wave passes the end of the obstacle shown in figure 9.2, the end of the breakwater may be considered as a source which generates arc shaped waves in the shadow zone behind the breakwater. The wave height decreases as we proceed along a wave crest arc in this shadow zone. Diffraction computations based upon this simple model might be easy but would generally be useless. The wave reflected by the seaward side of the breakwater (obstacle) is also partially diffracted into the shadow zone. Further, diffracted waves, hitting the shadow side of the breakwater are also reflected.

Even with all of this, plus a finite width of opening in a breakwater, numerical or graphical computations can often be used to determine wave heights at selected points in the vicinity. The theory is difficult, and will not be presented here; it is well treated in the courses and literature on short wave theory. One of the resulting graphical methods is based upon the Cornu Spiral. Graphs, showing wave height ratios as a function of position are given in the *Shore Protection Manual*, volume I, section 2. From these graphs it is obvious that the wave height distribution along a shore within a harbor can be quite irregular.

## 10. WAVE STATISTICS RELATIONSHIPS

E. Allersma  
E.W. Bijker  
W.W. Massie

### 10.1. Introduction

Until this point in our discussion all waves have been considered to be sinusoidal with constant period. It has already been indicated that this is not true in nature. Indeed, the sea surface can appear to be very irregular. Figure 10.1 shows a dramatic example of this.

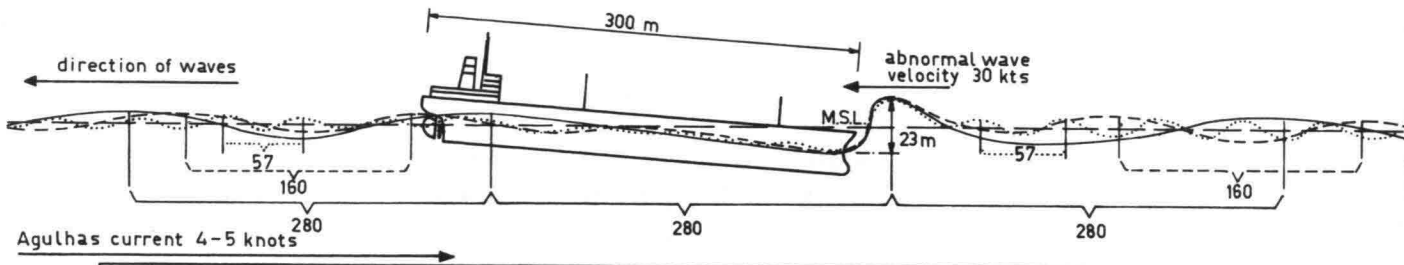


Figure 10.1

DIAGRAMATIC PROFILE SHOWING SINUSOIDAL CURVES OF THREE WAVE TRAINS HAVING WAVE LENGTHS OF 280, 160 AND 57 METERS WHICH BECOME IN-PHASE FOR A SHORT PERIOD THEREBY CREATING AN ABNORMAL WAVE ABOUT 23 METERS HIGH. IN ADVANCE OF THE WAVE IS A LONG DEEP TROUGH.

In this, and the following two chapters, we shall attempt to describe this sea surface irregularity more carefully.

Reference information is provided on these topics by Kinsman (1964), and Neumann and Pierson (1966). This chapter is largely abstracted from Allersma and Massie (1973), in which many more references are also listed.

### 10.2 The Phenomenon and its Characterizations

The motion of the sea surface is irregular. The water level is a stochastic variable. Generally, measurements of water level are made only at a fixed location. This yields a stochastic record of water levels as a function of time. This record could be presented as a graph of measurements carried out over a number of years or even decades. Unfortunately, such a long graph is rather cumbersome to use; statistics can be used to condense this data into more usable form without the loss of valuable details. Thus, the problem becomes twofold:

- The determination of the statistical parameters necessary to characterize a portion of our wave record representing an interval of constant sea conditions (usually a few hours).
- The determination of the frequency with which these statistical characterizations of the earlier mentioned sea state occur. When these two things are known, then the theory of the previous chapters (5 through 9) and a statistical model can be used to accomplish the design of our project.

What, specifically, are the statistical parameters needed? Civil Engineers are most often interested in wave heights. Therefore, it would seem most convenient to consider the statistical distribution of wave heights. The common statistical parameters can be used to describe such a distribution; the mean value is the most simple of these. In coastal engineering practice, however, the smaller waves are generally neglected and the mean value of the highest 1/3 of the waves (which are of the most interest) is chosen. This mean is called the significant wave height, denoted by  $H_{sig}$ . By comparing significant wave heights determined from actual wave records to visual estimates made while recording it has been found that these correspond rather well; an experienced observer can usually estimate  $H_{sig}$  rather closely.

Another wave height characterizing parameter of use in energy relationships is the root-mean-square wave height. For a group of  $N$  waves it is defined as:

$$H_{rms} = \sqrt{\frac{\sum_{i=1}^N H_i^2}{N}} \quad (10.01)$$

Similarly, a characteristic wave period can be determined; the average of the periods of the higher waves in the group is often chosen.

The value of  $H_{sig}$  determined from a wave record will be influenced to some extent by the duration of that record. Consider the following situation: A small sea is exposed to a constant light wind for a long time, so that a stable wave height has developed. Additionally, during a period of only 1/2 hour a severe thundersquall with high winds passes over the area. During this short but intense storm higher waves will be generated which will then die out after the storm. If a significant wave height is determined using a record lasting an entire day, then the influence of the thunderstorm will be more or less lost in the rest of the data while, on the other hand, a significant wave height based upon, say, a single hour of record which includes all of the storm will be somewhat higher.

The length of the record used to determine  $H_{sig}$  must, on the one hand, be long enough to determine a dependable average (20 minutes is about a minimum) while the records must not be so long that the wave conditions vary dramatically during the observation period. Often times significant wave heights are determined every 3, 6, or 12 hours, with 6 hours, corresponding to the interval between many other meteorological observations, being the most popular.

A disadvantage of such a simple parameter such as  $H_{sig}$  is that it gives only a very global description of the wave heights in the record. This would indeed be true if the wave height distribution was completely random. Luckily, many stochastic processes can be described by theoretical distributions having certain properties. For example, if a variable has a Gaussian Distribution then all of the statistical information can be condensed into two parameters: the mean, and the standard deviation.

Fortunately, within reasonable accuracy, wave heights of natural irregular waves also can be described via a theoretical distribution model: the Rayleigh Distribution. This distribution is completely characterized by a single parameter. Thus, the significant wave height,  $H_{sig}$ , (or any other average such as  $H_{rms}$ ) is sufficient to completely characterize the distribution. Taking  $H_{sig}$  as the characteristic parameter, the Rayleigh Distribution can be described by

$$P(H) = e^{-2\left(\frac{H}{H_{sig}}\right)^2} \quad (10.02)$$

where  $P(H)$  is the probability of exceedance of wave height  $H$ ,  
 $H_{sig}$  is the significant wave height of the record,  
 $e$  is the base of natural logarithms.

Values of  $P(H)$  versus  $\frac{H}{H_{sig}}$  computed from equation 10.02 are given

in table 10.1. Special graph paper is available which transforms equation 10.02 into a straight line. This is shown in figure 10.2. Obviously, using either the table, graph, or 10.02 we can determine the probability of exceedance of any desired wave height occurring in an interval characterized by a given significant wave height. For example, according to the Rayleigh Distribution 13.5% of the waves are higher than  $H_{sig}$ .

Some other handy relationships, also based upon the Rayleigh Distribution are listed below:

$$H_{sig} = 1.414 H_{rms} \quad (10.03)$$

$$\bar{H} = 0.886 H_{rms} \quad (10.04)$$

where  $\bar{H}$  is the average of all waves.

$$\sigma_H = 0.463 H_{rms} \quad (10.05)$$

where  $\sigma_H$  is the standard deviation of the wave height.

$$H_{sig} = 1.596 \bar{H} \quad (10.06)$$

We have now answered part of the problem posed at the beginning of this section, namely, we have the statistical parameters necessary to describe an interval of our total wave record.

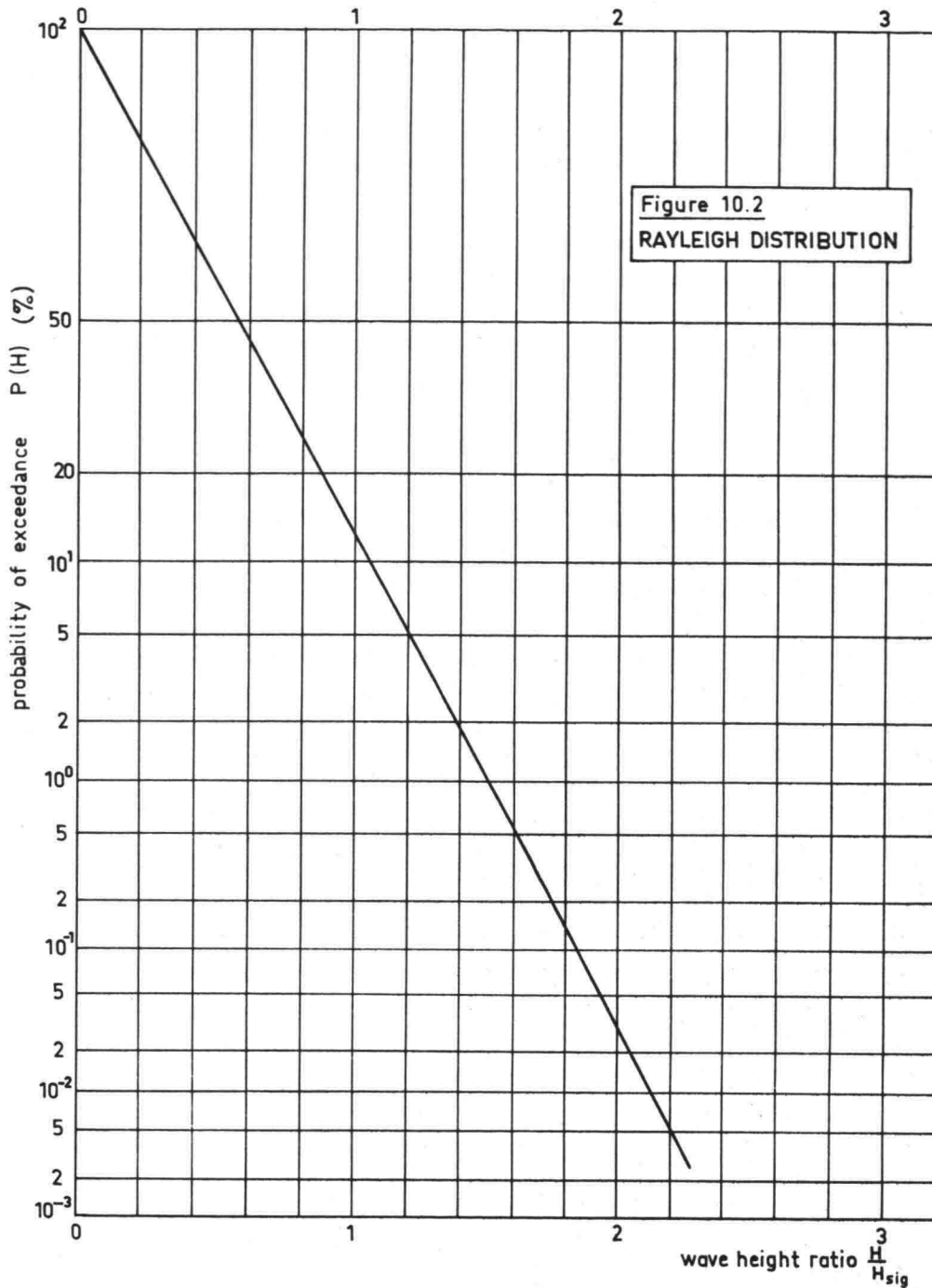
Table 10.1

Values of  $\frac{H}{H_{sig}}$  for various values of  $P(H)$

Probability of exceedance $P(H)$	$\frac{H}{H_{sig}}$
$10^{-5}$	2.40
$2 \times 10^{-5}$	2.33
$5 \times 10^{-5}$	2.22
$10^{-4}$	2.15
$2 \times 10^{-4}$	2.06
$5 \times 10^{-4}$	1.95
$10^{-3}$	1.86
$2 \times 10^{-3}$	1.77
$5 \times 10^{-3}$	1.63
0.01	1.51
0.02	1.40
0.05	1.22
0.10	1.07
0.125	1.02
0.135	1.00 *
0.20	0.898
0.50	0.587
1.00	0.000

---

\* Follows from definition of  $H_{sig}$



### 10.3 Determination of Chance of Occurrence

Once the statistical characterizations of one interval of a long record have been completed, this process can be repeated for each interval in the recording period which could extend over a period of years or even decades. Obviously, each interval produces a single value of  $H_{sig}$  and this collection of significant wave height values can also be studied statistically.

Isaacson and Mackenzie (1981) present a convenient review of the various statistical models often used in such work. One of the more common of these is the Weibull Distribution given by (in our case):

$$P(H) = e^{-\left(\frac{H-c}{a}\right)^b} \quad (10.07)$$

where:

$P(H)$  is the chance that  $H$  is exceeded, and  
 $a, b,$  and  $c$  are constants.

Of these  $c$  can be interpreted as the lower bound on the range of values for  $H$  - a minimum wave height in the current application. (There is also an upper bound form of Weibull Distribution, but that is less interesting for this application.) For most wave height applications,  $c$  will obviously be zero. With  $c = 0$ , (10.07) can be transformed to a straight line which can be fitted in order to determine the remaining constants  $a$ , and  $b$ . This is still quite a bit of work, and one often finds that  $b$  has a value close to 1.0. This reduces the fitting problem even further, since (10.07) now reduces to:

$$\ln (P(H)) = -\frac{1}{a} H \quad (10.08)$$

which is a straight line if  $\log (P(H))$  is plotted versus  $H$ .

Such a simplified fit usually works pretty well for practical problems for values of  $P(H)$  less than, say, 10 or 20 percent - the area which is of most interest.

An example of such a long term distribution - based upon data for the northern North Sea is shown in figure 10.3. This figure is compiled for "storms" - intervals over which a single value of  $H_{sig}$  has been determined-lasting 6 hours. It is unimportant whether the observations were made using a continuous set of exact six hour intervals - such as a meteorological office might do - or whether the measurements were made in a true random way. In both cases it is just as necessary to know the length of time during which a single value of  $H_{sig}$  has been determined as explained in the previous section.

If  $H_{sig}$  is being determined only at irregular intervals, these must be selected truly at random. An attitude of "It's a nice day, today; let's go measure waves!" can distort the results considerably.

Some users express the chance of occurrence of the (significant) wave height in units other than a pure probability (value ranging from 0 to 1). One form often encountered combines the storm duration and the chance to form a frequency,  $f$ , usually expressed in storms per year:

$$f = M P(H) \quad (10.09)$$

with:

$$M = \frac{(365) (24)}{\text{storm duration in hr}} \quad (10.10)$$

$M$  is, thus, the number of storm intervals in one year. Values of  $f$  can obviously be larger than 1; something which statisticians do not appreciate.

Going a step further - and compounding the confusion even more - the recurrence interval,  $R$ , is sometimes encountered.

$$R = \frac{1}{f} \quad (10.11)$$

$R$  usually has units of years and some speak of a storm which occur "every 15 years" or "with a recurrence interval of 15 years". This does not say - as more naïve readers might think - that such a storm will only occur at regular intervals of  $R$  years. Indeed, three separate storms, each with a recurrence interval of more than 10 years, all occurred during the same winter in the North Sea recently.

#### 10.4. Wave Periods

Just as wave heights have been characterized by statistical parameters, the wave period can also be treated as a statistical variable. The exact theory is a bit too comprehensive to discuss here. Allersma and Massie (1973) do treat this topic more thoroughly.

On the other hand, more or less empirical relationships have been derived which relate wave period to some other easily determined parameter. Many of these relations have been derived for application in a certain geographical area; they are not generally applicable. Examples of such relations are,

For the North Atlantic Ocean:

$$T = 2.5 H \quad (10.12)$$

For the Mediterranean Sea:

$$T = 4 + 2 H^{0.7} \quad (10.13)$$

For the North Sea:

$$\bar{T} = 3.94 H_{sig}^{0.376} \quad (10.14)$$

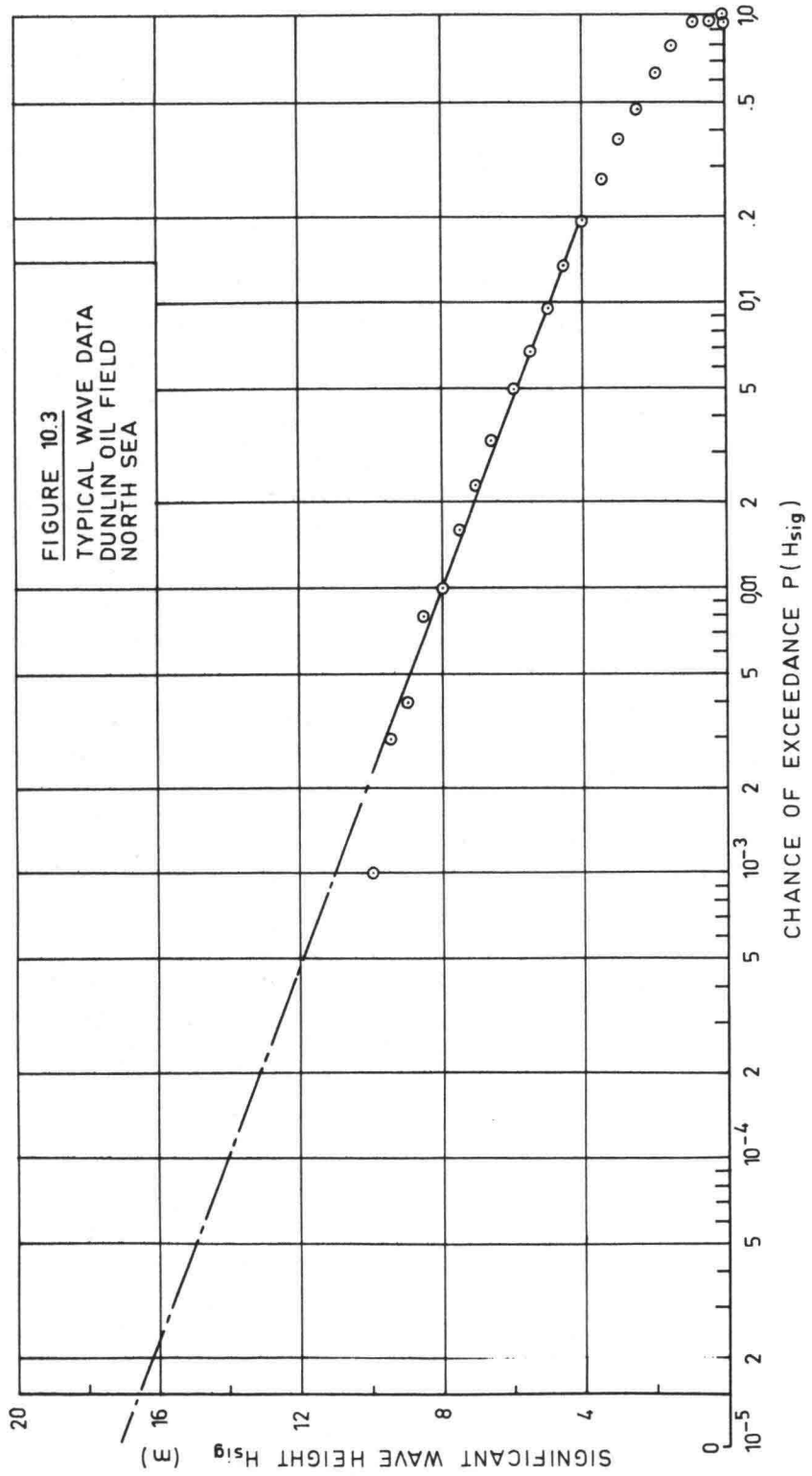
where  $\bar{T}$  is the average of all wave periods.

These equations are *not* dimensionless; the constants stated are for period,  $T$ , in seconds and wave heights,  $H$ , in meters.

Wiegel (1964), on a slightly different path shows theoretically that:

$$T_e = 1.23 \bar{T} \quad (10.15)$$

where  $T_e$  is the wave period of the regular wave train having the same energy as the irregular train having average period  $\bar{T}$ .



## 11. APPLICATION OF WAVE STATISTICS

E.W. Bijker

W.W. Massie

### 11.1 Introduction

The information provided in the previous chapter is fine for those interested only in condensing wave data. We, as engineers, need to apply that information to make a responsible design.

In this chapter a distinction is made between two similar situations which require different approaches from a statistical point of view.

In the first type of problem, the strength or stability of a structure may be evaluated in terms of a certain characterizing parameter of the waves, such as  $H_{sig}$ , the significant wave height. The construction is then subjected, either in a physical or mathematical model, to the entire Rayleigh Distribution determined by the chosen parameter value.

An example of such a design occurs with rubble mound breakwaters. (See volume III of these notes). When the structure is tested in a physical model, then the entire Rayleigh Distribution of wave heights should be reproduced. If, on the other hand, a mathematical model is used, then the fact that our characteristic wave represents an entire population of waves is taken into account in the formula preparation. This is done, for example, in formulas for breakwater armor unit weights.

This type of problem is relatively easy to handle. The probability of occurrence of the design parameter comes directly from the long term wave height distribution. Since this type of problem is treated in detail in the sections on breakwater design (volume III) we shall not consider it further, here.

In the second type of problem the structure is designed using just a single wave, the design wave. The objective in the remainder of this chapter will be to determine the probability of exceedance of a given design wave height. Why do this; don't we want to design a structure to withstand the biggest possible wave? Unfortunately, this is impossible, since it follows from the wave height distributions presented earlier that *any* chosen wave height - no matter how high - has a certain, finite chance that it will be exceeded. *Some* risk must be accepted. The problem of determining how much risk to accept is the subject of chapter 13 of this volume. For now, we shall only attack the problem of determining the chance that a given wave height will be exceeded in a given time interval. For many problems such as the deck elevation of an offshore structure, the number of times the design wave height is exceeded is not important; if the deck is hit by a wave crest then the structure will fail and it does not matter at all whether one, two, or even ten of these extreme waves come along.

There is another class of problems for which it *does* matter how many "waves" come along. An example of this involves the statistics of vertical ship motions so necessary for determining the depth of a ship channel. It is obviously more of a problem if ten ships get into difficulty in a channel than if this happens to only one ship.

The deck elevation problem is much less complex than the channel depth type problem. The first of these is handled in the remainder of this chapter; the channel problem is discussed in more detail in volume II.

### 11.2 Problem Statement and Assumptions

The precise problem statement is: "what is the chance that a chosen design wave height,  $H_d$ , is exceeded one or more times during the life,  $\ell$ , of a structure?" This chance is equal to the sum of the chances that  $H_d$  is exceeded  $n$  times with  $n \geq 1$ . This sum can be extremely difficult to evaluate. Using the property of probabilities:

chance something happens + chance something doesn't happen  $\stackrel{\text{def}}{=} 1$   
and realizing that what we want is "the chance that something happens" we can evaluate this using the above identity simply by evaluating the chance that it never happens; this will be used frequently in the following sections.

Each storm which occurs can be characterized by a given value of  $H_{sig}$ , the significant wave height. This wave height characterizes a set of  $N$  waves to which the structure is exposed during the storm. These  $N$  waves are distributed according to a Rayleigh Distribution characterized by the single value of  $H_{sig}$ .

Lastly, it is assumed that the significant wave heights obey a long - term frequency distribution such as that shown in figure 10.3 of the previous chapter.

### 11.3 The Numerical Treatment

First, let us discuss how the value of  $N$  associated with a particular value of  $H_{sig}$  is determined. Sometimes, values of  $N$  are tabulated from actual wave records during processing to determine  $H_{sig}$ , etc. An alternative is to divide the duration of the storm by the characteristic wave period listed with the reduced wave data. In any event,  $N$  is known for each  $H_{sig}$ .

First, consider a single storm containing  $N$  waves characterized by  $H_{sig}$ . We choose an arbitrary design wave height  $H_d$ . The chance that  $H_d$  is exceeded by any given wave is:

$$P(H_d) = e^{-2\left(\frac{H_d}{H_{sig}}\right)^2} \quad (10.02) \quad (11.01)$$

The chance that this wave is not exceeded is:

$$1 - P(H_d) \quad (11.02)$$

The chance that this wave is not exceeded in a series of  $N$  waves is:

$$\left[1 - P(H_d)\right]^N \quad (11.03)$$

Finally, the chance that this wave height,  $H_d$ , is exceeded at least once in our single storm containing  $N$  waves is:

$$E_1 = 1 - [1 - P(H_d)]^N \quad (11.04)$$

As an alternative, some prefer to use a Poisson approximation to evaluate  $E_1$ . As long as  $P(H_d)$  is small (usual for our problems) the difference is not important. In this case:

$$E_1 = 1 - e^{-N P(H_d)} \quad (11.05)$$

The next step is to combine this chance,  $E_1$ , with the chance that the value of  $H_{sig}$  used above also occurs. This chance that  $H_{sig}$  occurs must come from a long term distribution of significant wave heights. The data presented in a graph such as figure 10.3 provides information on the chance that any given value of  $H_{sig}$  is exceeded. We need to determine at least approximately what the chance is that  $H_{sig}$  occurs. This value,  $p(H_{sig})$ , can be seen as the chance that some wave height,  $H_{sig} - \Delta H_{sig}$  is exceeded minus the chance that the height  $H_{sig} + \Delta H_{sig}$  is exceeded:

$$p(H_{sig}) = P(H_{sig} - \Delta H_{sig}) - P(H_{sig} + \Delta H_{sig}) \quad (11.06)$$

$p(H_{sig})$  is the chance that  $H_{sig}$  falls in the interval:

$$(H_{sig} + \Delta H_{sig}) > H_{sig} > (H_{sig} - \Delta H_{sig}) \quad (11.07)$$

This interval having a width of  $2 \Delta H_{sig}$  has been characterized by its midvalue. Obviously, the value of  $p(H_{sig})$ , so obtained, is dependent upon the chosen value for  $\Delta H_{sig}$ . This dependence turns out to be small as will be pointed out later in this section. As a rough guide, one should choose  $\Delta H_{sig}$  such that the  $E_1$  value computed in (11.05) is not changed appreciably if  $H_{sig} \pm \Delta H_{sig}$  is used instead. A  $\Delta H_{sig}$  value of about 0.5 m is often used.

Now that the chance that our chosen value of  $H_{sig}$  used to compute  $E_1$  above, is known, we can now determine the chance that  $H_d$  occurs during any single storm period. Since the chance  $E_1$  is totally independent of  $p(H_{sig})$ :

$$E_2 = p(H_{sig}) E_1 \quad (11.08)$$

This is only the beginning of our solution, however. Indeed, it is very possible that  $H_d$  occurs as well in another wave field characterized by a different value of  $H_{sig}$ , completely outside the interval described in (11.07) used until now. Since a different value of  $H_{sig}$  will be used to designate this other storm condition, another value of  $E_1$  will also have to be computed. In order to keep the bookkeeping straight, an additional subscript,  $i$ , will be added to the characterizing values of  $H_{sig}$  chosen as well as to  $E_1$  and  $E_2$ . Equation 11.08 now becomes:

$$E_{2 i} = p(H_{sig i}) E_{1 i} \quad (11.09)$$

In theory, we must choose enough values of  $H_{sig\ i}$  to cover the entire range of possible storm wave heights - from zero to some maximum possible wave height. The number of these intervals,  $N'$ , will, of course, depend upon the value of  $\Delta H_{sig}$  chosen earlier. As  $\Delta H_{sig}$  increases,  $N'$  will decrease resulting in fewer values of  $E_{2\ i}$ . In practice, as will be demonstrated in the example of section 11.4, one does not always need to choose characterizing values of  $H_{sig\ i}$  over the entire wave height range. For a given value of  $H_d$  - this has been constant for our entire problem - one will find that  $E_1$  increases, while, on the other hand,  $p(H_{sig\ i})$  will decrease as  $H_{sig\ i}$  increases. The resulting products  $E_{2\ i}$ , will be small near both  $H_{sig\ i}$  extremes and once an  $E_{2\ i}$  value has become negligibly small, further computations with either very large or very small  $H_{sig}$  values are unnecessary. This is discussed further along with the example in section 11.4.

Since a given single storm condition is characterized by only a single value of  $H_{sig\ i}$ , two different storms cannot occur simultaneously; the values of  $H_{sig\ i}$  are mutually exclusive, but, of course, different values of  $p(H_{sig\ i})$  are related. Indeed, the sum of all the possible  $p(H_{sig\ i})$  values must be identically equal to one.

The overall chance that the chosen design wave height,  $H_d$ , is exceeded at least once in the single storm period is:

$$E_3 = \sum_{i=1}^{N'} E_{2\ i} \quad (11.10)$$

Using the philosophy explained in the previous section, the chance that this design wave is *not exceeded* is, of course:

$$1 - E_3 \quad (11.11)$$

Knowing, additionally, - see chapter 10 - that there are  $M$  storms per year possible and that our structure has a design life of  $\ell$  years, then this structure must be exposed to  $M \ell$  possible storms. The chance that  $H_d$  is *not exceeded* at all during the entire span of  $\ell$  years is, thus:

$$(1 - E_3)^{M\ell} \quad (11.12)$$

and, finally, the chance that the design wave height,  $H_d$ , is exceeded at least once during the life span of the structure is:

$$p(H_d) = 1 - (1 - E_3)^{M\ell} \quad (11.13)$$

This is our objective for now. If, of course, we find this value of  $p(H_d)$  to be undesirable - too large or too small - the only thing left to do is to choose (guess) another value of  $H_d$  and repeat this entire procedure - see section 11.6. Such a procedure can be carried out in a tabular form as is illustrated for a single value of  $H_d$  in the next section.

#### 11.4 Example Problem

Determine the overall chance that a design wave height,  $H_d$ , of 30 meters occurs at least once during the lifetime,  $\ell$ , of 25 years for a structure placed in the Northern North Sea such as near the Dunlin field. This design wave height and structure lifetime were quite common for the North Sea, by the way.

We choose  $\Delta H_{sig}$  to be equal to 0.5 m and choose  $H_{sig i}$  values at integer meter values as listed in column 1 of table 11.1. Note that the interval limits - column 2 of the table - are at exact half meter points except at each end of the table.

$P(H_{sig})$  values listed in column 3 follow from the graph (extrapolated as necessary) in figure 10.3, and  $p(H_{sig})$  - column 4 - are differences between adjacent values in column 3.

Average wave period values,  $\bar{T}$ , listed in column 5 are evaluated using equation 10.14 and the given values for  $H_{sig}$  from column 1. If anything, the resulting periods in column 5 seem a bit short; this will cause the end result,  $P(H_d)$  to be a bit high, and thus conservative. The reader should verify this conclusion. Values of  $N$  follow from:

$$N = \frac{6 \times 3600}{\bar{T}} \quad (11.14)$$

and are listed in column 6.

Now that  $H_{sig i}$  (col.1),  $H_d = 30$  m, and  $N$  (col.6) are known,  $P(H_d)$  and then  $E_1$  can each be evaluated using (11.01) and (11.04) respectively. The values are listed in columns 7 and 8.  $E_2 i$  follows from equation 11.09, then, and is listed in column 9. This column can then be summed yielding:

$$E_3 = 81.59 \times 10^{-6} \quad (11.15)$$

with, now  $M = 1460$  (6 hour storm duration, given in figure 10.3) and  $\ell = 25$  years; one can compute using (11.13) that:

$$P(H_d) = 0.949 \quad (11.16)$$

or nearly a 95% chance that at least one wave in the Northern North Sea will exceed 30 meters height during a period of 25 years. This seems like a rather high chance for a design wave condition! Part of the reason for this chance being high is that the rather short computed wave periods result in relatively large values of  $N$  and thus, also  $E_1$ . A philosophy for determining an acceptable chance that a design condition will be exceeded is presented in chapter 13.

One can see from examining table 11.1 further that in this case the computations for  $H_{sig} \leq 8$  m do not contribute values  $E_2 i$  - at least not within the number range of the calculator used. In hindsight, these computations could have been skipped. At the other end

of the table we see that computations were stopped with an interval ranging from 19.5 m to  $\infty$ , characterized by  $H_{sig} = 20$  m. In this case, since  $E_1 = 1.000$  and would remain that for all higher values of  $H_{sig}$ , the values of  $E_{2 i}$  are identical to the values of  $p(H_{sig})$ . If more intervals above  $H_{sig} = 20$  m had been used the sum of the terms for  $H_{sig} \geq 20$  would still have been the same for both  $p(H_{sig})$  and  $E_{2 i}$ .

The computations carried out in a table such as this have to be done quite precisely; some form of digital computer is a must (a pocket calculator is sufficient). Further, to reduce the influence of round-off errors, it can be wise to compute columns 7, 8, and 9 as well as the sum,  $E_3$ , using the full number of significant figures available on the calculator. This was done in this table while rounded off intermediate values were written down.

Table 11.1 Design Wave Height Probability Computations  
Northern North Sea,  $H_d = 30$  m  $\lambda = 25$  years

(1)	(2)	(3)	(4)	(5)	(6)	(7)	(8)	(9)
$H_{sig}$	Interval limits	$P(H_{sig})$	$p(H_{sig})$	$\bar{T}$	N	$P(H_d)$	$E_1$	$E_{2 i}$
(m.)	(m)	(-)	(-)	(s)	(-)	(-)	(-)	(-)
	0	1.000						
0								
1			0.21	3.94	5480	0.00	0.00	0.00
2	1.5	0.79	0.32	5.11	4230	0.00	0.00	0.00
3	2.5	0.47	0.20	5.96	3620	$1.38 \times 10^{-87}$	0.00	0.00
4	3.5	0.27	0.137	6.64	3250	$0.139 \times 10^{-48}$	0.00	0.00
5	4.5	0.133	$66 \times 10^{-3}$	7.22	2990	$53.8 \times 10^{-33}$	0.00	0.00
6	5.5	$67. \times 10^{-3}$	$37 \times 10^{-3}$	7.73	2790	$0.193 \times 10^{-21}$	0.00	0.00
7	6.5	$30. \times 10^{-3}$	$15 \times 10^{-3}$	8.19	2640	$0.111 \times 10^{-15}$	0.00	0.00
8	7.5	$15. \times 10^{-3}$	$9.4 \times 10^{-3}$	8.61	2510	$61.0 \times 10^{-12}$	0.00	0.00
9	8.5	$5.6 \times 10^{-3}$	$2.1 \times 10^{-3}$	9.00	2400	$0.223 \times 10^{-9}$	$0.48 \times 10^{-6}$	$1.00 \times 10^{-9}$
10	9.5	$3.5 \times 10^{-3}$	$1.95 \times 10^{-3}$	9.36	2310	$15.2 \times 10^{-9}$	$35.1 \times 10^{-6}$	$68.5 \times 10^{-9}$
11	10.5	$1.55 \times 10^{-3}$	$830 \times 10^{-6}$	9.71	2220	$0.346 \times 10^{-6}$	$0.768 \times 10^{-3}$	$0.638 \times 10^{-6}$
12	11.5	$720. \times 10^{-6}$	$350 \times 10^{-6}$	10.03	2150	$3.73 \times 10^{-6}$	$7.98 \times 10^{-3}$	$2.79 \times 10^{-6}$
13	12.5	$370. \times 10^{-6}$	$210. \times 10^{-6}$	10.34	2090	$23.7 \times 10^{-6}$	$48.3 \times 10^{-3}$	$10.1 \times 10^{-6}$
14	13.5	$160. \times 10^{-6}$	$88. \times 10^{-6}$	10.63	2030	$0.103 \times 10^{-3}$	0.188	$16.6 \times 10^{-6}$
15	14.5	$72. \times 10^{-6}$	$37. \times 10^{-6}$	10.91	1980	$0.335 \times 10^{-3}$	0.485	$18.0 \times 10^{-6}$
16	15.5	$35. \times 10^{-6}$	$19. \times 10^{-6}$	11.17	1930	$0.884 \times 10^{-3}$	0.819	$16.0 \times 10^{-6}$
17	16.5	$16. \times 10^{-6}$	$8.8 \times 10^{-6}$	11.43	1890	$1.97 \times 10^{-3}$	0.976	$8.59 \times 10^{-6}$
18	17.5	$7.2 \times 10^{-6}$	$3.7 \times 10^{-6}$	11.68	1850	$3.87 \times 10^{-3}$	0.999	$3.70 \times 10^{-6}$
19	18.5	$3.5 \times 10^{-6}$	$1.9 \times 10^{-6}$	11.92	1810	$6.83 \times 10^{-3}$	1.000	$1.90 \times 10^{-6}$
20	19.5	$1.6 \times 10^{-6}$	$1.6 \times 10^{-6}$	12.15	1780	$11.1 \times 10^{-3}$	1.000	$1.60 \times 10^{-6}$
	$\infty$	0.00						
		$\Sigma =$	1.000	check			$E_3 = \Sigma E_{2 i} =$	$81.59 \times 10^{-6}$

### 11.5 Further Development

The general philosophy behind the previous sections of this chapter can be extended appreciably. Some examples have already been indicated - the analysis of ship keel clearance in a channel, for one. The ultimate in the development of this philosophy combines information on environmental and other loading statistics with statistical information concerning the construction materials and even the quality of workmanship to arrive at an overall chance that a given structure will fail. This general topic is treated in separate courses on probabilistic design and will not be treated further here.

Before leaving this type of problem, however, it should be pointed out that the method just used was, perhaps a bit oversimplified. In many problems - a design wave force or beach sand transport are examples - the resulting condition is dependent upon more detailed wave period and direction data as well as wave height. It can be very important how many of the 1 meter high waves are a long period swell and how many are a short choppy sea. Extension of the method of section 11.3 to include both directional and more detailed period data is possible, but will not be done here.

### 11.6 The Inverse Problem

The method outlined in section 11.3 determines the chance that a given design wave height,  $H_d$ , is exceeded during the lifetime,  $\ell$ , of the structure. A more common problem is the inverse one: What wave height,  $H_d$ , occurs with a given chance,  $p(H_d)$ , of being exceeded during the given lifetime,  $\ell$ , of the structure? This inverse problem cannot be solved directly. Working backwards through section 11.3, one can easily solve equation 11.13 for  $E_3$ , but equation 11.10 cannot be solved. None of the values  $E_2$  are known, and the inverse solution cannot proceed further.

In practice, then, one must simply carry out a whole series of computation runs such as in section 11.3 for a series of chosen values of  $H_d$ . This allows the relationship between  $p(H_d)$  and  $H_d$  to be established. This can be represented in a graph, if desired, to facilitate interpolation.

### 11.7 A Second Type of Problem

An entirely different type of problem is often encountered as well. Via a design code it is sometimes specified that a structure be designed to withstand the *maximum* wave occurring in a storm having some given chance of being exceeded. A statement such as "Design for the maximum wave in a 100 year storm" is all too common. Based upon the knowledge of this and the previous chapter, one can see that such a discussion of a maximum wave is fundamentally impossible and statements such as quoted above can be troublesome for engineers and lucrative for lawyers.

As engineers, we have two possible approaches. In the first approach, we can, rather directly, determine a wave height,  $H_d$ , having a given chance of exceedance,  $E_1$ , in *some particular storm* having, for example, some given chance of exceedance. We can, for example, find  $H_d$  corresponding to a chance of exceedance of, say, 1/1000 in

a single "100 year storm" in the Northern North Sea. This "100 year storm" will first have to be interpreted using section 10.3. Apparently, R equals 100 years and f, then, is equal to 1/100, and with 1460 possible storms per year:

$$P(H_{\text{sig}}) = \frac{1}{(1460)(100)} = 6.849 \times 10^{-6} \quad (11.17)$$

Using once again data from figure 10.3, this means that:

$$H_{\text{sig}} = 17.6 \text{ m} \quad (11.18)$$

and, using (10.14):

$$\bar{T} = 11.58 \text{ s} \quad (11.19)$$

yielding, via (11.14):

$$N = 1860 \quad (11.20)$$

Knowing that  $E_1$  in this problem is to be 1/1000, we can determine  $P(H_d)$  by solving equation 11.04:

$$P(H_d) = 1 - \left[ 1 - E_1 \right]^{1/N} \quad (11.21)$$

or, substituting values:

$$P(H_d) = 1 - \left[ 1 - \frac{1}{1000} \right]^{1/1860} = 0.538 \times 10^{-6} \quad (11.22)$$

Equation 11.01 can now be solved for  $H_d$ .

$$H_d = H_{\text{sig}} \sqrt{-\frac{1}{2} \ln P(H_d)} \quad (11.23)$$

This yields:

$$H_d = 47.3 \text{ m.}$$

The second approach is to compute the most probable maximum wave height in the "design storm" chosen. The best - but difficult, due to lack of information - way to accomplish this would be to examine a large number of wave records, each lasting a given time (6 hours, for example) and each characterized by our chosen value of  $H_{\text{sig}}$ . Each record will contain about the same number of waves, N. If we had these records, it would be simple enough to pick out the maximum wave in each record and to subject these to a statistical analysis. The most probable maximum wave height is usually taken as the one with the highest probability density out of this sample of

maximum waves. If each of the wave records behaves in accordance with the Rayleigh Distribution, this problem can be attacked theoretically. The result is then:

$$H_d = \frac{1}{\sqrt{2}} H_{sig} \sqrt{\ln N} \quad (11.24)$$

Using this equation and the data used above yields:

$$H_d = \frac{1}{\sqrt{2}} 17.6 \sqrt{\ln (1860)} = 34.15 \text{ m} \quad (11.25)$$

By the way, the same result can be obtained by putting  $P(H_d) = 1/N$  into equation 11.01.

## 12. WAVE DATA

W.W. Massie

### 12.1 Introduction

In chapters 10 and 11 we used wave height data without saying too much about the practical problem of obtaining this information. In this chapter we shall indicate briefly how this necessary information can be obtained.

### 12.2 Existing Data

Government agencies in many countries accumulate data on waves and currents in areas under their jurisdiction. Some of this data is published, most of it is available upon request; occasionally, some is secret. The booklet by Dorrestein (1967) is an excellent example of published data. The information is presented in tabular form.

In general, the type of information needed is accumulated by the weather service or the hydrographic office on a national scale. Locally, measurements made specifically for a given project may be available from local agencies such as departments of public works.

Some of the the major hydrographic offices have wind, wave, and current data for nearly the entire world. Much of this is readily available. Probably the most important source of world-wide hydrographic information is the British Admiralty. The United States Naval Hydrographic Office also has an impressive collection.

### 12.3 Measurement Program

There are, of course, areas of the world for which no readily available wave data exist. What then? One solution, provided that sufficient time and money is available, is to conduct a specific measurement program. The length of time available for measurements is seldom, if ever, sufficient. Sometimes, the required measurement period can be shortened by correlating our few measurements with simultaneous measurements - part of a much longer record - at a nearby location\*.

Various types of wave height meters are available. Some measure water surface elevation directly with reference to a fixed staff, while others ride the waves and record the vertical water surface acceleration. A third type measures pressure differences at some point in the water. It is beyond the scope of this brief summary to discuss these various instruments in detail.

---

\* The second long-term set of measurements need not even be wave measurements. In many cases, a correlation with local wind data may be possible.

#### 12.4 Use of Substitute Data

It is sometimes advantageous to artificially generate wave data from available meteorological data. This information, gathered from ship's logs, is often published in special atlases of wind or barometric pressure data. The wind data can be used in a wave forecasting technique to predict the waves.

Is there *always* a correlation between wind and waves? No. When is it possible to have waves without wind or wind without waves? \*

How do we get wave data from barometric pressure information? The wind can often be predicted from the pressure gradients. Equilibrium between pressure gradient, Coriolis, and centripetal forces yields a wind velocity. The computation is similar to that used for ocean currents in chapter 3 of this volume. Once the wind is known, a wave forecasting technique can be used.

The advantage of predictions over our own site measurements is that they can be done more quickly and in a comfortable office. Even so, such a prediction can involve a lot of tedious work, and is probably less dependable than some on-site measurements.

#### 12.5 SMB Prediction Method

Bretschneider (1952) revised the semi-empirical wave forecasting relationships presented by Sverdrup and Munk (1947). The technique is thus called the Sverdrup-Munk-Bretschneider (SMB) method.

Three dimensionless equations form the basis of the method:

$$\frac{g H_{sig}}{U_w^2} = 0.283 \tanh [0.0125 \phi^{0.42}] \quad (12.01)$$

$$\frac{g T_{sig}}{U_w} = 7.540 \tanh [0.077 \phi^{0.25}] \quad (12.02)$$

$$\frac{g d}{U_w} \geq 6.5882 \exp \{ [0.0161 (\ln \phi)^2 - 0.3692 \ln \phi + 2.2024]^{\frac{1}{2}} + 0.8798 \ln \phi \} \quad (12.03)$$

also:

$$\phi = \frac{g F}{U_w^2} \quad (12.04)$$

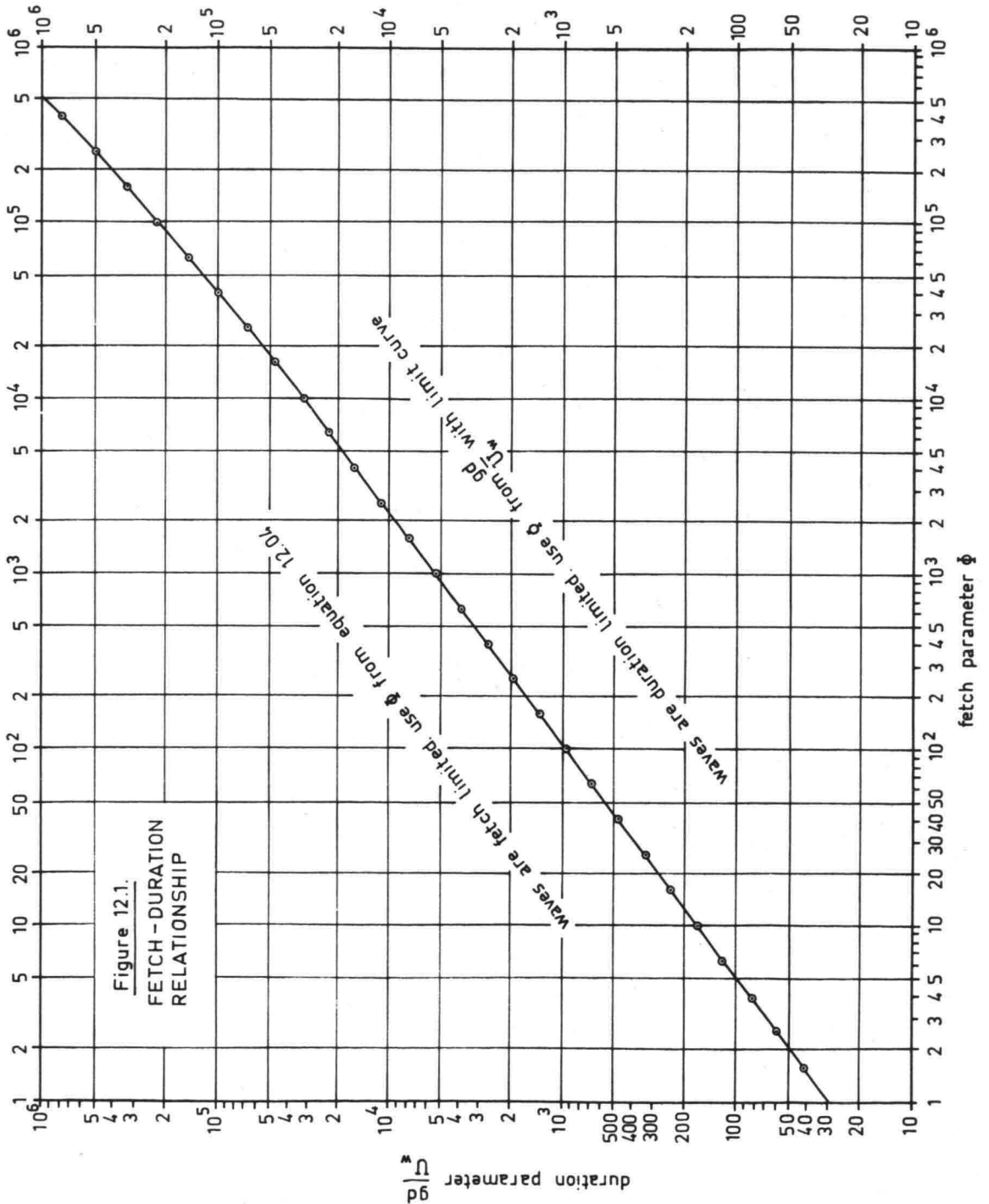
---

\* Swell is an example of waves without wind. This is most often found along coasts bordering on the larger seas. On the other hand, a wind blowing from the shore will not generate much of a wave along a coast.

in which:

- F is the fetch length,
- g is the acceleration of gravity,
- $H_{sig}$  is the significant wave height,
- d is the duration of the wind,
- $T_{sig}$  is the period of the significant wave,
- $U_w$  is the wind speed, and
- $\phi$  is the fetch parameter defined in (12.04).

Since equation 12.03 is rather cumbersome to handle and it is often necessary to determine a  $\phi$  corresponding to a given value of  $\frac{g d}{U_w^3}$ , this equation is represented in figure 12.1.



These equations are valid for *deep water* only. Their use, in practice, goes somewhat as follows:

- a. The fetch distance,  $F$ , the wind speed,  $U_w$ , and the duration,  $d$ , of this wind are determined from the available data.
- b.  $\phi$  is determined from 12.04 - be careful to use consistent units!
- c. Compute the parameter  $\frac{g d}{U_w}$  in the same set of units.
- d. Enter figure 12.1 with the parameters evaluated in the two previous steps. If these parameters locate a point above the plotted curve, then the wave height is determined by the fetch - use the value of  $\phi$  determined in step b, above. If, on the other hand, a point is below the line, the wind duration determines the wave height - proceed by using a smaller value of  $\phi$  determined using the duration parameter and the plotted limit curve.
- e. Using the verified (or corrected) value of  $\phi$ , the wave parameters,  $H_{sig}$  and  $T_{sig}$  can be determined via equations 12.01 and 12.02.
- f. Wave heights with other probabilities of occurrence can easily be determined using methods outlined in chapter 11.

Another, purely graphical solution to this problem is given in volume I of *Shore Protection Manual* (1973).

Table 12.1 adapted from Saunders (1965) lists some typical data for fully developed sea conditions. The wave conditions listed for wind speeds above about Beaufort force 8 won't be found too often - at least not with the corresponding wind speeds. It is, of course, possible to generate a significant wave height of, say, 15 m with a wind force 11 in a relatively short (compared to force 9) time and distance.

A limiting assumption inherent in the work above is that the wind velocity and direction remains constant for the entire wave generation period over the entire fetch length. This is an important limitation if one is making a wave forecast for a large body of water. Recent research is beginning to yield improved wave prediction methods which can allow the above limitations to be relaxed.

TABLE 12.1 Wave Generation Data

Conditions corresponding to a fully developed sea

Beau- fort	Wind Speed range (m/s)	Min. Fetch range (km)	Min. Duration range (hrs)	Significant wave ht. range (m)	Wave Per. range (s)	Ave. Period (s)	Sea State Description	Beau- fort
No.								No.
0	up to 0.5	-	-	-	-	-	Mirror surface	0
1	0.5 - 1.5	up to 9	up to 0.3	up to 0.02	up to 1.2	0.5	Small ripples	1
2	2.1 - 3.1	10 - 15	0.3 - 0.7	0.03 - 0.09	0.4 - 2.8	1.4	Small non-breaking wavelets	2
3	3.6 - 5.2	18 - 19	1.0 - 2.4	0.3 - 0.4	0.8 - 6.0	2.6	Large wavelets; crests begin to break	3
4	5.7 - 8.3	30 - 75	3.8 - 6.6	0.7 - 1.4	1.0 - 8.8	4.0	Frequent white caps	4
5	8.7 - 10.8	100 - 140	8.3 - 10	1.9 - 2.4	2.5 - 11	5.4	More pronounced wave form; many whitecaps	5
6	11.3 - 14.0	180 - 330	12 - 17	3.0 - 4.6	3.4 - 15	6.8	Large waves; extensive foam; some spray	6
7	14.4 - 17	420 - 630	20 - 27	5.5 - 7.9	4.5 - 18	8.5	Foam begins to blow	7
8	17 - 21	780 - 1300	30 - 42	9.1 - 13.7	5.5 - 22	10.5	Foam blows in streaks Spray affects visibility	8
9	21 - 24	1500 - 2100	47 - 57	15 - 20	7.0 - 25	12.5	Dense foam streaks; visibility restricted	9
10	24 - 28	2300 - 3300	63 - 81	22 - 29	7.5 - 30	14.7	Overhanging wave crests; entire surface white	10
11	29 - 33	3900 - 4600	88 - 101	31 - 38	8.5 - 32	16.7	Wave crests blown with wind	11
12	above 33						Air filled with foam visibility seriously restricted	12

13. OPTIMUM DESIGN

E.W. Bijker

A. Paape

13.1 Introduction

It has become obvious in chapter 11 that some risk in the design of engineering works must be accepted. The prime question, now, is, "what is the most responsible risk to assume?"

In this chapter we shall only discuss this problem in a general way. Specific coastal engineering applications will be taken up in later volumes of these notes. The optimum design technique can be used for a broad spectrum of projects.

13.2 Project Criteria

The project suitable for the optimum design technique must satisfy certain criteria:

1. There must be alternative solutions for the design available. It is sufficient to have similar structures which vary only in some detail such as size or strength.
2. It must be possible to evaluate the economic construction cost of each project alternative.
3. It must be possible to determine the chance of damage or failure of each alternative.
4. The economic loss resulting from damage to or the failure of our construction must be determinable.

We have seen in chapter 11 how item 3 of the above list can be evaluated for certain types of offshore constructions. The most difficult decision making is involved in the evaluation of item 4, above. The technical consequences of a "failure" are reasonably easy to evaluate; the social, environmental, or esthetic consequences are usually much more difficult to express in economic terms. However, we shall proceed, for now, assuming that the necessary costs can be expressed in economic units.

13.3 Optimization Procedure

The optimization process proceeds as follows:

- a. A design from among the alternatives available from step 1, above, is chosen.
- b. For this design, the total capital investment involved in construction is determined in convenient units such as current money value.
- c. By multiplying the chances of damage or failure found in item 3, above, by the economic consequences of such damage we can obtain the current capitalized monetary value of total damage to be expected during the lifetime of the project.
- d. we can repeat these three steps for each of the alternative designs available.

Once these steps have been carried out, we can choose that design which has the lowest total (sum of construction plus capitalized damage) cost. This is then our optimum.

An alternative reasoning is also possible which proceeds more or less as follows:

- a. Choose a design from among the alternative designs available from step 1, above.
- b. For this design determine the capitalized annual cost of the damage (failure) and the construction cost. Express both quantities in equivalent economic units.
- c. Choose a second design from among those available and determine its damage cost and construction cost.
- d. Evaluate the second design with respect to the first by comparing the *change* in capitalized construction cost to the *change* in capitalized damage cost.
- e. Obviously, only if the capitalized construction cost increase is less than the capitalized damage saving is it economical to choose the second design, assuming that the second design is the more costly to build. Repeated application of this procedure should lead to the same optimum as the first procedure listed.

Specific examples of the optimum design technique are given in volumes II, III and IV of these notes.

#### 13.4 Implicit Assumptions

It should be fully understood that the damage costs include both direct and indirect costs. Not only the structure must be repaired or replaced; there will usually be other losses due to interruption of production or even loss of human lives.

Also, the assumption has been made above that sufficient money was available to carry out the optimum solution. It is possible that when only a limited amount of capital is available now, one must choose a solution which costs less to build, but which has a greater capitalized damage cost. Since such evaluations involve some more complex economic and financial principles such as cash flow, we shall not develop this discussion further.

Another boundary condition to consider in optimization problems is the existence of design codes. Obviously, all designs must satisfy all applicable design codes specified by law. It is conceivable that such a code may dictate the design of a construction which is too conservative (overdesigned) to meet our optimization criteria.

### 14.1 Introduction

Now that the background information has been presented in the first 13 chapters, we are prepared to start applying this to specific coastal engineering problems. We shall begin this study of applications by examining the oldest of the three major subdivisions mentioned in chapter 1, the problem of providing safe harbors for ships. Various details of harbor problems form the subject of this and the next 10 chapters of this volume. Some further details are deferred to volume II; breakwaters form the topic of volume III of these notes.

The remainder of this story is adapted from Bijker (1974).

### 14.2 Early History

Originally, harbors were built at locations where both good hinterland connections and protection from the evils of the sea were naturally available. These evils of the sea include both natural (waves and currents) and human (pirates) enemies. Since settlements developed around the harbors, sites were usually inland at least far enough to assure dry land. Harbors developed sometimes well inland along rivers or estuaries. New Orleans, for example, is more than 100 km up the Mississippi River from its mouth.

Since ships were small some hundreds of years ago, their shallow draft allowed them to navigate easily over and around the numerous shoals found in these natural watercourses. This meant, even so, that local knowledge of the waterway was needed. Was this a disadvantage or an advantage for shipping? The use of pilots did hinder commerce somewhat, but it hindered pirates even more!\*

As time passed, and ships became larger and deeper, the difficulties with shoals increased. The use of pilots became more common; they knew the deepest channels. Inventive people even developed strange-seeming devices to reduce the draft of ships. One of the successful devices, a "ship camel" was designed and used to help ships cross the bar near the island of Pampus as they approached the port of Amsterdam. Such a camel is shown schematically in figure 14.1; this was really the predecessor of the floating drydock.

### 14.3 The influence of Dredging

More than 100 years ago another inventor came upon the idea of artificially deepening the shallow areas by means of underwater excavation - dredging. Sometimes even whole new channels were excavated. Both major ports in The Netherlands, Rotterdam and Amsterdam, have experienced this. Both have dredged entirely new artificial channels or canals to reach the sea. Interestingly, both harbors have abandoned their original artificial channels in favor of larger, improved ones.

---

\* Lord Nelson's fleet shipyard and harbor at Buckler's Hard on the Beaulieu River would have been a juicy prize if it could have been successfully attacked.

Amsterdam abandoned the North Holland Canal linking it with Den Helder in favor of the present North Sea Canal forming a much shorter link to IJmuiden. The Rotterdam Waterway is also a major man-made construction.

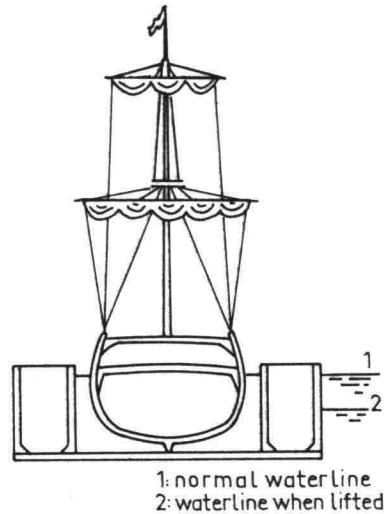


Figure 14.1.  
SHIP CAMEL

#### 14.4 Modern Developments

As ships become even larger the dredging required to open and possibly maintain such a channel over a long distance becomes a formidable economic burden. Also, the long sailing distance through such canals by the modern very large oil tankers presents a hazard to navigation. Since these canals pass close by densely populated areas, as well, the risk of social damage from calamities increases. Moreover, as ships carry higher value cargo such as containers, the time lost in navigating along a long canal has an increasing economic impact. In general, goods move faster over land than over water.

These factors, along with the decreasing threat by pirates have led to decisions to expand the harbors nearer to the shoreline. The Maasvlakte and Europoort in Rotterdam are examples of this. Many other harbors, such as London, Amsterdam, and Hamburg, are also at least planning similar developments. Many of these new harbor areas are developing on artificially filled land. The scarcity of land in the older urban areas has contributed to this harbor migration toward the sea.

This migration has not ended. Specialized facilities offshore are also developing rapidly. We need only to think of the plans for island harbors at sea or of the development and use of Single Buoy Moorings which can replace conventional harbors for some cargos.

In the next 10 chapters we shall examine some of the more specialized harbor problems in more detail.

## 15. APPROACH CHANNELS

W.W. Massie

### 15.1 Introduction

We might easily conclude from the previous chapter that all necessary dredging work needed to accommodate even larger ships takes place within the harbor or estuary. This is certainly not the case. Considerable dredging work is now carried out in more or less open sea in order to provide safe approaches for the largest ships. The improved channel for the Port of Rotterdam, for example, extends more than 35 km seaward from the harbor entrance; this is a rather extreme example. What are the consequences of such channels in sea? This is answered below.

### 15.2 Problems Encountered

When a river channel is deepened in order to accommodate larger ships, we need to contend with currents and sediment transport which are directed along the axis of the channel. While some sedimentation can be expected, much and often most of the sediment which enters a channel reach is merely swept along by the current and out the other end. Ships navigate easily either with or against the current and have little difficulty manoeuvring.

Does this situation change at sea? Yes, usually it does. Currents and sediment transports are often directed at a considerable angle to the axis of the channel. Sediment transport rates perpendicular to the channel axis are often very high where the channel cuts through the shallowest coastal regions. This results from the high sediment transport caused by the breaking waves along the adjacent shores. These breaking waves can also generate a crosswise current in the approach channel which can be dangerous for shipping, especially if the ships are moving slowly - they are harder to steer, then. One of the reasons to construct breakwaters out from the coast at a harbor or river entrance is to cut off, or at least reduce or possibly divert, the long-shore current and sediment transport. Breakwaters are given a separate discussion in chapter 18 of these notes. The causes and effects of long-shore current and sediment transport are highlighted briefly in chapter 26. Detailed treatment of this is taken up in volume II.

Farther at sea, outside the area where waves are breaking nearby, the problems are less severe. There are still currents and thus sediment transport caused by tides, but these usually do not create such serious problems as we encounter nearer to shore.

Other problems can become increasingly important farther offshore however. Position determining and navigation systems become less accurate; wider channels are needed to assure that ships do not run aground. Wave action can be more severe. This leads to more severe ship motion which requires a deeper channel to assure that the ship does not hit the bottom. Dredging is hampered in the same way by these problems too, of course.

### 15.3 The Optimization Problem

It should be obvious that design decisions must be made with regard to approach channels. Alternative solutions - various widths and depths - are available for a given problem. This problem lends itself well to an optimization procedure. This optimization will be discussed in detail in volume II. A constructional aspect, dredging, is taken up in the next chapter.

### 16.1 Introduction

Dredging is necessary at sea and in rivers and harbors for nearly all of the modern ports of the world today.\* What equipment is best suited to carry this out? After briefly explaining some general principles common to most all sorts of dredges, the most commonly available types will be listed and described. Neither part of this discussion is intended to be complete. Other courses specifically on dredging serve their purpose well.

### 16.2 General Principles

Most dredging is done by hydraulic dredgers. These machines are equipped with centrifugal pumps capable of pumping a mixture of soil and water. The soil is moved as a suspension in the moving water.

The ratio of soil to water in this suspension is an important factor establishing the efficiency of the operation. This ratio depends both upon the equipment used and the soil material. The amount of mixture required to move one part by volume of in situ soil varies from 1 to 2 for mud to 3 to 5 for medium sand ( $d \approx 250 \mu\text{m}$ ). For gravel and rock this ratio can be as high as 10 to 12.

Since the type of pump and the installed power more or less fix the quantity of mixture that can be moved, the productive output of the dredge is strongly dependent upon the ratio listed above.

The head loss in the pipelines increases with increasing soil grain size. The maximum length of discharge pipeline decreases with increasing grain size, since the maximum head (pressure) of the dredge pump is more or less constant. Some rather inaccurate empirical formulas have been developed to predict the head loss in dredge pipelines. See Führeböter (1961), for example.

The head loss can be reduced, in theory, by reducing the flow velocity. This can only be done to a certain extent, since a minimum velocity must be maintained in order to assure that the dredged material remains in suspension.

This minimum velocity increases with increasing grain size, grain specific weight, and pipe diameter.

### 16.3 Plain Suction Dredge

This is one of the most common types in Holland. Fig. 16.1 shows such a dredge designed to discharge through a floating pipeline. Fig. 16.2 shows a modified form designed for loading barges alongside.

---

\* Another purpose of dredging can be to obtain fill material for land reclamation. This type of dredging is often conducted completely independently of harbor development.

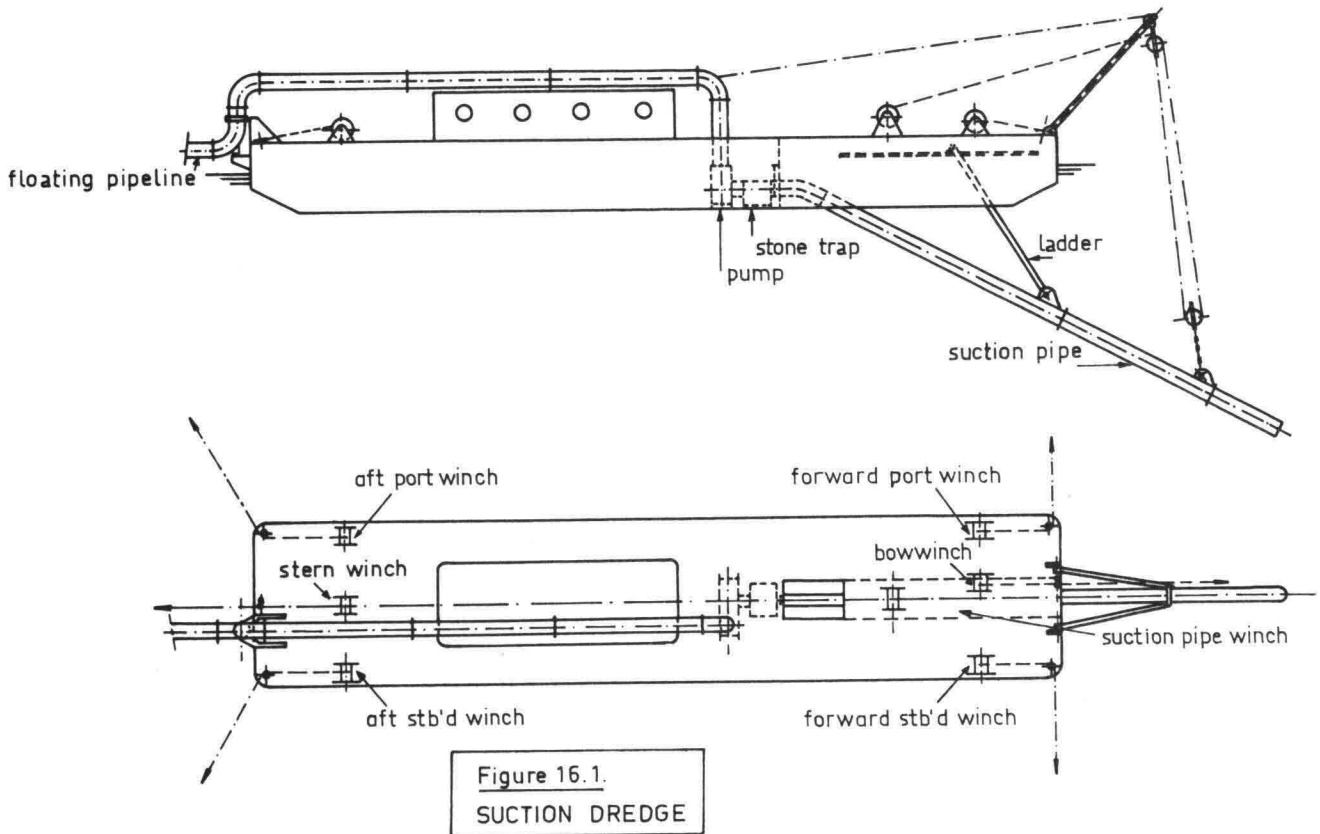


Figure 16.1.  
SUCTION DREDGE

These dredges are very efficient when dredging loose material such as sand. If a water jet is added at the end of the suction pipe to help loosen the in - situ material, then layers of clay can be penetrated to reach deeper sand layers.

These dredges are kept in place by six anchors and move very slowly in the direction of the bow anchor. This type of operation results in a very uneven bottom bathymetry making these dredges more useful for reclamation works.

The cost of transporting one unit of soil with this type of dredge is relatively low.\*

The production from such a dredge depends upon many factors including the sand grain size and porosity as well as the suction pit geometry.

In order to increase the depths attainable with suction dredges, it has become necessary to place the pump deeper under water. Often, the pump is located along the suction pipe instead of in the hull as shown in the figures. Sometimes, even, two pumps are used in series - one on the suction pipe and one in the hull. The inter-relationship between the factors affecting dredge performance is revealed by the so-called "suction equation". It is derived by examining the pressure change along the inside of the suction pipe between the inlet and the pump. See figure 16.3.

\* Exact cost figures are not given since they can vary too rapidly.

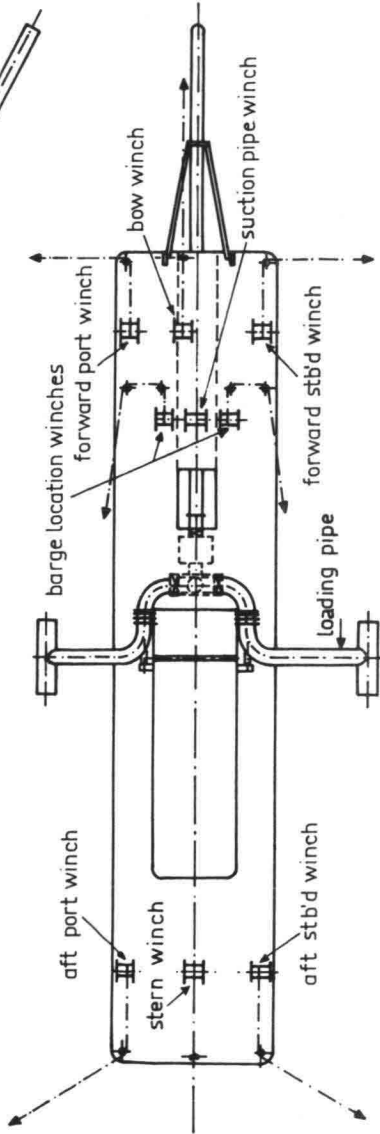
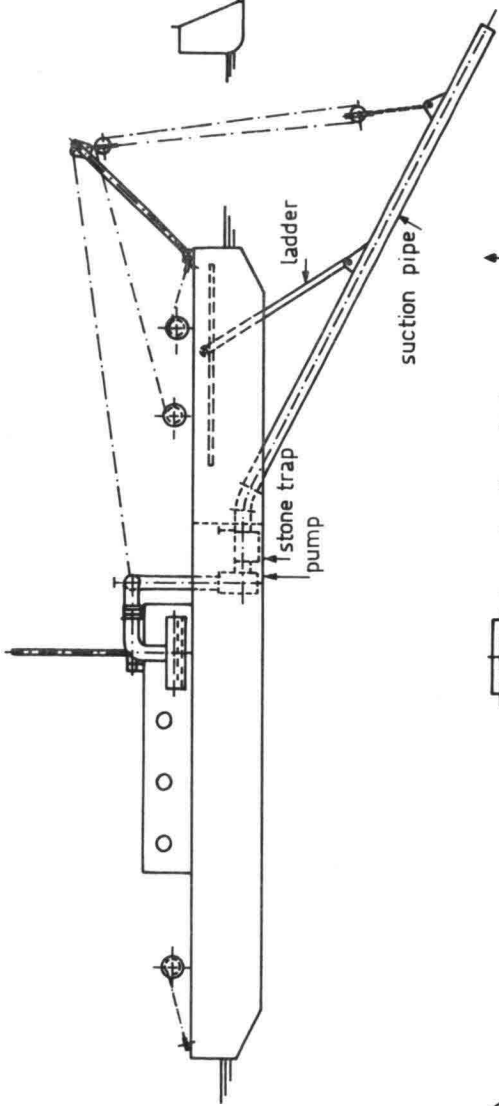
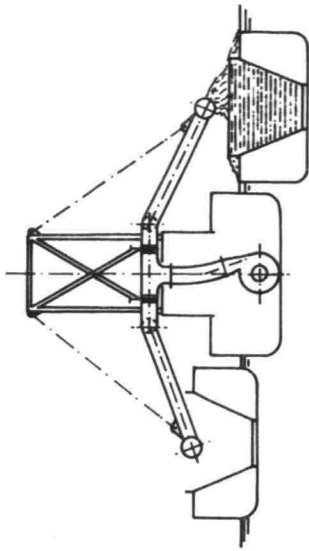


Figure 16.2  
BARGE LOADING  
SUCTION DREDGE

$$(p^* + Z_s) \gamma_w = (Z_s - Z_p + f \frac{V_s^2}{2g}) \gamma_m \quad (16.01)$$

where:

- $f$  is the hydraulic loss coefficient from suction pipe entrance to pump,
- $g$  is the acceleration due to gravity,
- $V_s$  is the flow velocity in the suction pipe,
- $p^*$  is the vacuum at the pump entrance expressed as head of water,
- $Z_p$  is the depth of submergence of the pump,
- $Z_s$  is the depth of the suction pipe entrance,
- $\gamma_m$  is the specific weight of the mixture, and
- $\gamma_w$  is the specific weight of water.

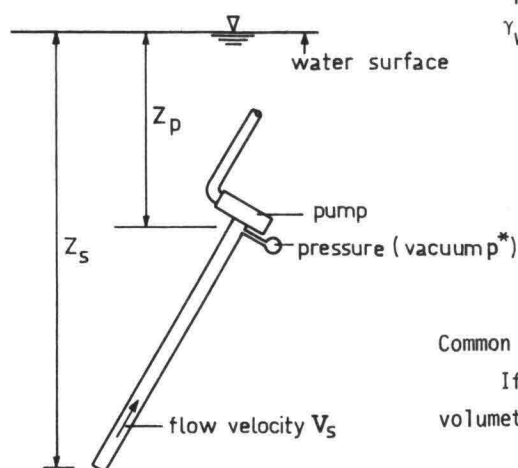


Figure 16.3  
DEFINITION OF  
SUCTION EQUATION  
TERMS

Common values for  $f$  range between 2.5 and 3.5 .

If the concentration of soil in the mixture measured on a volumetric basis is  $c_v$ , then:

$$\gamma_m = c_v \gamma_g + (1 - c_v) \gamma_w \quad (16.02)$$

where  $\gamma_g$  is the specific weight of the dry sand grains.

Solving for  $c_v$  yields:

$$c_v = \frac{\gamma_m - \gamma_w}{\gamma_g - \gamma_w} \quad (16.03)$$

Combining equations 16.01 and 16.03 yields:

$$c_v = \frac{\gamma_w}{\gamma_g - \gamma_w} \left[ \frac{p^* + (Z_p - f \frac{V_s^2}{2g})}{Z_s - (Z_p - f \frac{V_s^2}{2g})} \right] \quad (16.04)$$

The capacity of the dredge increases as the vacuum,  $p^*$ , and the depth of pump submergence,  $Z_p$ , increases. Increasing suction submergence,  $Z_s$ , and friction factor,  $f$ , tend to decrease capacity.

With submerged pumps, these dredges can work with very deep suction depths (70 meters can be reached when necessary).

A slight modification of the standard suction dredge is the barge unloading dredge shown in figure 16.4. Their principle of operation is the same as that for a suction dredge; their use is also very common in Holland.

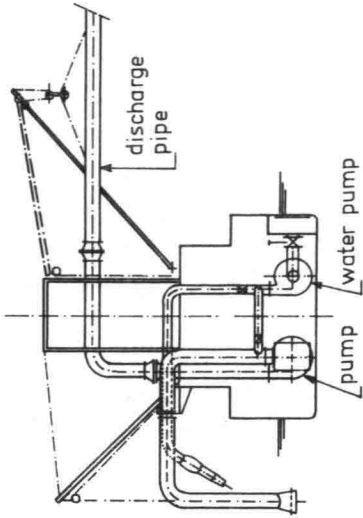
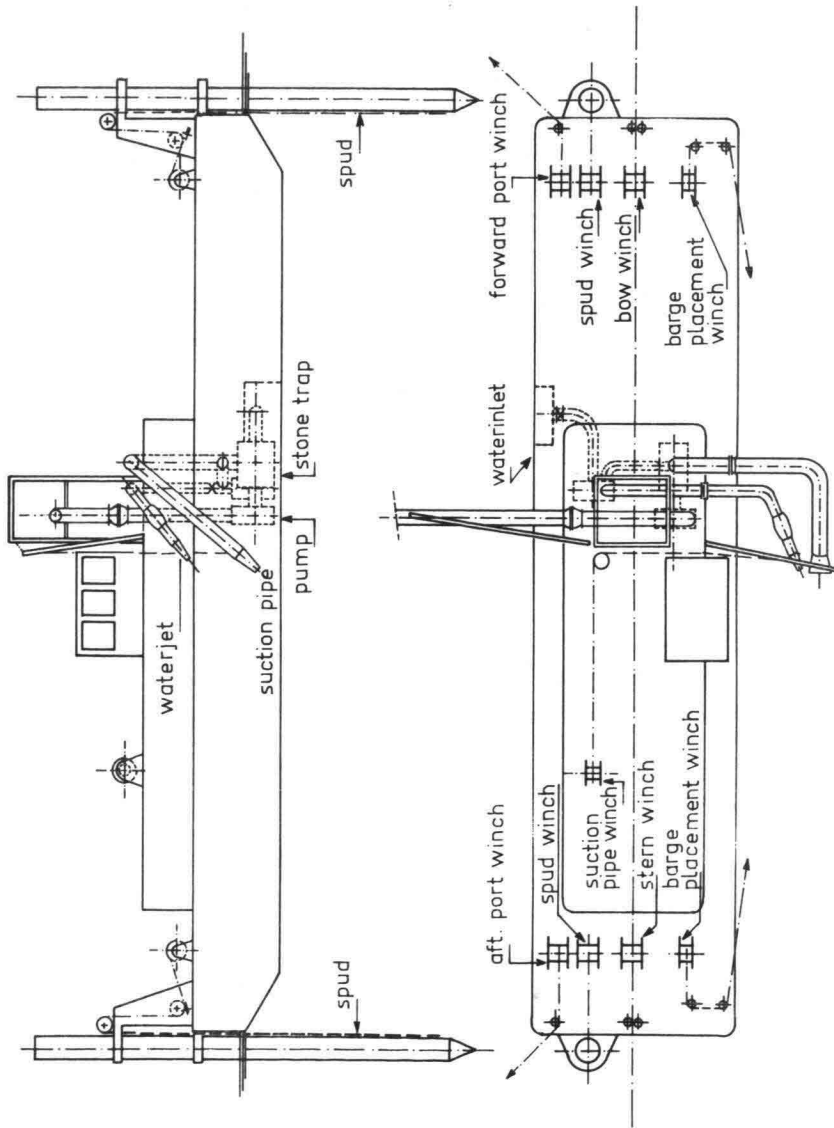


Figure 16.4  
BARGE UNLOADING  
DREDGE



#### 16.4 Cutter Suction Dredge

The cutter suction dredge is a more versatile form of suction dredge and is shown in figure 16.5. It can handle materials ranging from mud to soft rock. The soil in front of the suction tube is loosened by the cutter. The dredge moves into new material by swinging back and forth about one of the two anchoring spuds using the port and starboard forward winches and anchors. The dredge moves forward by changing the position of one spud while the dredge is held in place by the other. This moves its center of rotation forward a bit.

Equations 16.01 through 16.04 apply to the cutter suction dredge as well. Additional limiting factors are possible, however. These include the cutting capacity of the cutter and the hauling force and speed of the forward winches.

Since the suction dredge takes its material from a small area, it is capable of being accurately controlled. A depth accuracy of  $\pm 0.25$  m can be achieved, and side slopes can be cut.

Smaller cutters are used in soils such as sand, peat, and soft clay\* which require relatively little cutter or side winch power. Bigger, more powerful cutters are used with stiff clay and soft rock. Rock having a compressive strength of up to about  $5 \times 10^7$  N/m<sup>2</sup> can be attacked successfully with a cutter suction dredge. Harder rock must be handled with explosives.

The maximum depth which can be obtained is about 25 meters. This limit is imposed by structural stiffness limits of the spuds and ladder.

Typical production capacities for a "big" cutter suction dredge are listed in table 16.1.

To achieve the productions listed in this table, the dredge with submerged pump was operating as follows:

dredging depth : 20 m  
 pipeline diameter : 0.8 m  
 installed power : 5600 kw (7500 HP)

Table 16.1 Typical Cutter Suction Dredge Production

Material (see text)	Production (m <sup>3</sup> /hr in situ)	Maximum discharge distance (km)
sand	1500	3 to 6
soft clay	1750	6
stiff clay	750	3
soft rock	400	1.5

\* Soft clay has a cohesion of less than  $3 \times 10^4$  N/m<sup>2</sup>.

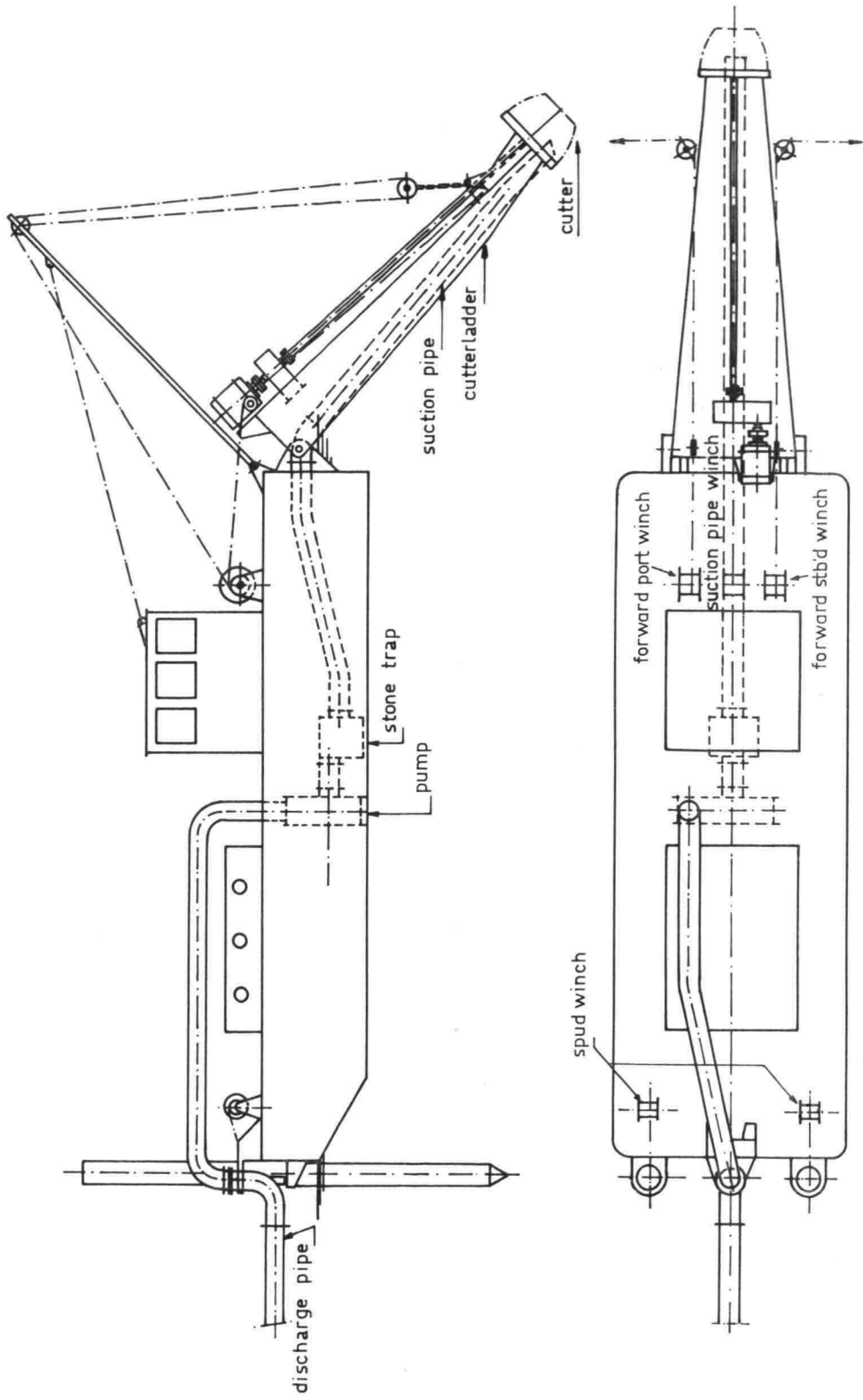


Figure 16.5 CUTTER SUCTION DREDGE

### 16.5 Trailing Suction Hopper Dredge

This type of dredge, shown in figure 16.6, is a ship with towed suction tubes. These ships pick up their load while traveling slowly (a few knots) forward. This ability to load while underway makes it an ideal dredge for work in waterways with heavy traffic. Furthermore, unlike stationary dredges, it can operate in moderate to high seas\*. Thus, this is the most suitable dredge for work in exposed harbor approach channels and at sea. These dredges can handle either mud or sand.

It usually takes 1 to 3 hours to fill the hopper of such a dredge with sand. This time is dependent upon the dredging depth, and grain size and porosity of the sand layer. Only  $\frac{1}{2}$  to 1 hour is needed to fill the hopper with mud.

After filling the hopper, the ship sails to a dumping site at a speed of about 11 knots (20 km/hr). The production achieved by such a dredge is dependent upon its pumping and hopper capacity, sailing distance to the unloading site, and the time required to unload. The maximum hopper capacity available in 1975 is about 10000 m<sup>3</sup>.

These dredges can work with a depth accuracy of about  $\pm 0.5$  m. up to a maximum depth of about 35 m.

### 16.6 Bucket Dredge

Unlike the preceding types, this is a purely mechanical dredge. It loosens the soil and transports it upward by means of a continuous conveyor chain of buckets. See figure 16.7. At the top of the chain of buckets, they dump their load of material into a chute which directs it into a barge moored along side.

The bucket dredge is positioned by six anchors. It moves in an arc around its bow anchor, drawn by its side winches, in order to reach new material. The bottom profile accuracy is of the order of  $\pm 0.2$  m.

A great variety of soils can be excavated with such a dredge. All materials ranging from mud to soft rock can be handled directly. Also, they are well suited for cleaning up the broken stone after explosives have been used. This is because they can handle larger pieces than other types of dredges (up to about 1 m diameter).\*\*

---

\*A very few of the large, modern plain suction dredges can operate even when they are exposed to light wave action.

\*\*By comparison, other dredges are limited by the pump impeller dimensions to about 0.4 m.

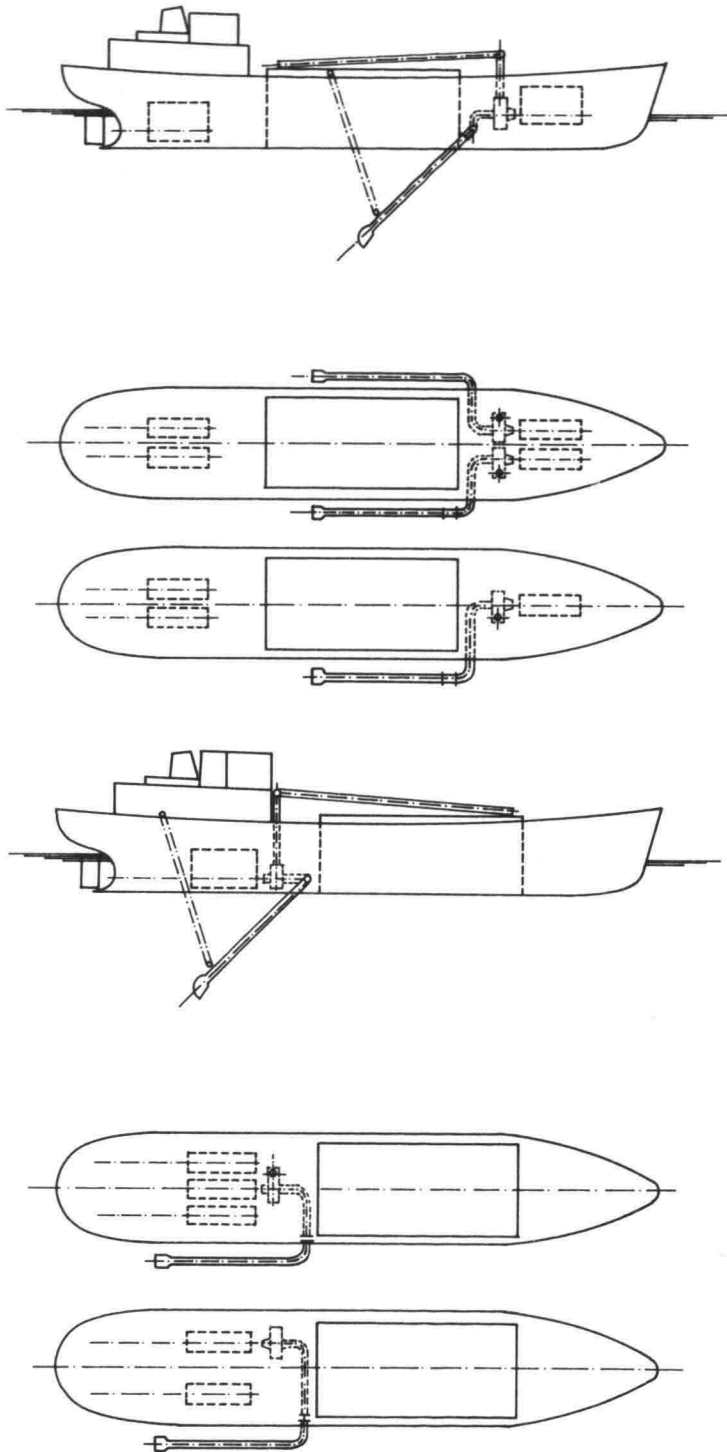


Figure 16.6  
TRAILING SUCTION HOPPER DREDGES

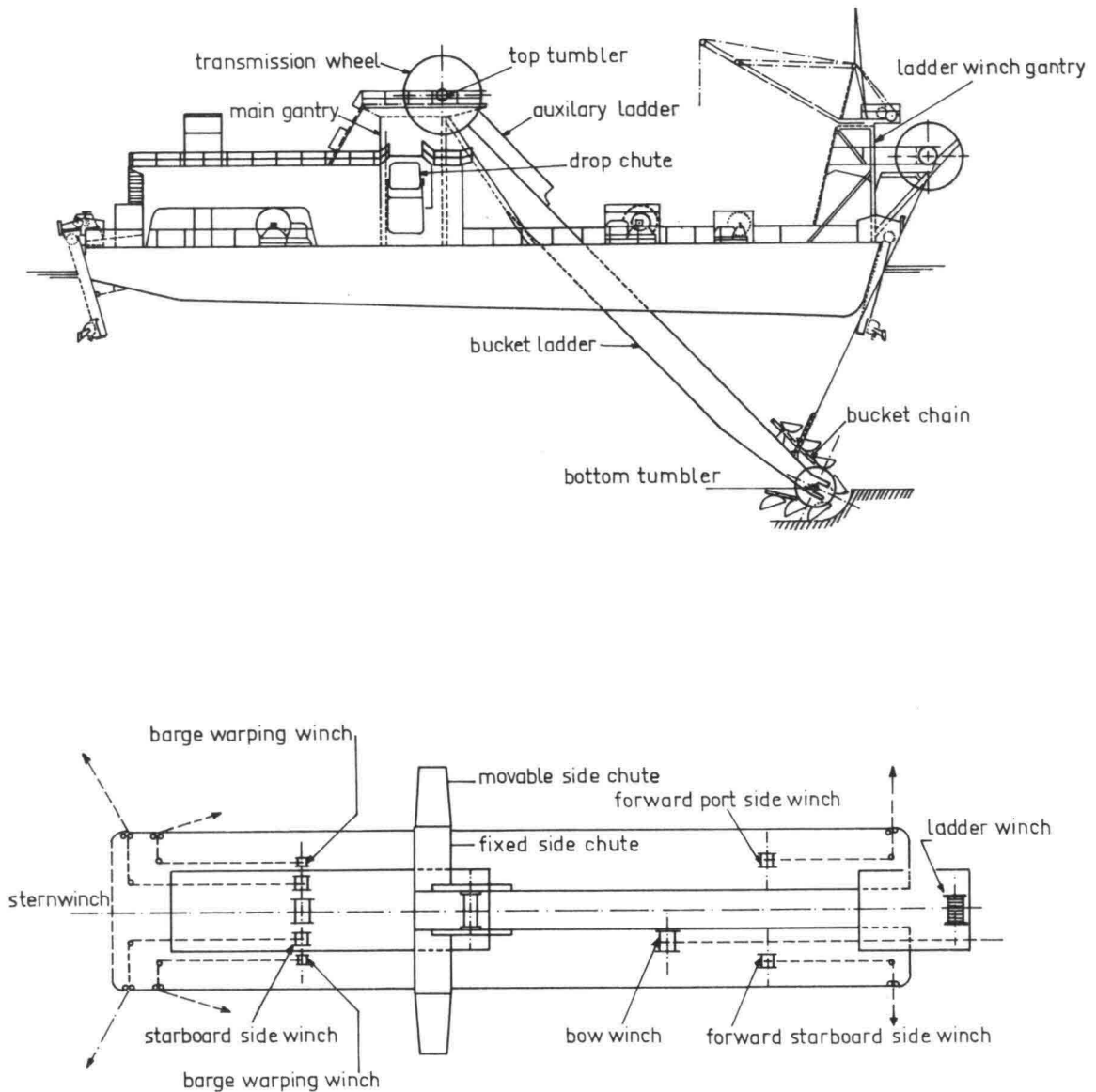


Figure 16.7  
BUCKET DREDGE

The maximum depth attainable with these dredges is about 40 m. Bucket sizes range up to about  $1 \text{ m}^3$  volume, and a bucket chain speed of about 30 buckets per minute is a maximum. Typical production capacities for a bucket dredge are listed in table 16.2. These productions are listed for the following condition:

bucket volume :  $0.75 \text{ m}^3$   
dredging depth : 15 m  
installed power : 375 kw (500 HP)

Table 16.2 Typical Bucket Dredge Production

Material	production in m <sup>3</sup> /hr in situ
mud	1000
clay	500
sand	350
broken rock	75
soft rock	50

### 16.7 Further Developments

Only the most commonly used dredges have been listed. Other types such as side casting and dipper dredges are sometimes used for special applications. Developments in dredging are aimed at achieving economics of scale or at increasing the productivity of equipment under adverse conditions. One of the recent developments in this field has been the addition of swell compensation to an articulated suction pipe on a plain suction dredge - see figure 16.8. The size of these dredges has been increased, too, increasing their seaworthiness. They can continue working in wave conditions previously considered unsuitable for this type of dredge and they can ride out an even heavier storm on their own anchors. The floating discharge pipe, if used, may prove to be the most vulnerable component of the system.

A second newer development shown in figure 16.9 combines a cutter suction dredge with a jack-up platform often used in the offshore industry. Such a dredge, according to its builder, should be able to work with fairly close tolerances (less than 0.5 m) even in waves of up to 3 to 4 meters. Once again, the discharge pipeline will probably be the weakest link in the production chain.

Recently, concern for the environmental consequences of dredging and spoil disposal has increased sharply, especially in the United States. Spoil disposal is the subject of the next chapter.

The proceedings of the various World Dredging Conferences (WODCON) are helpful when attempting to keep abreast of the latest developments.

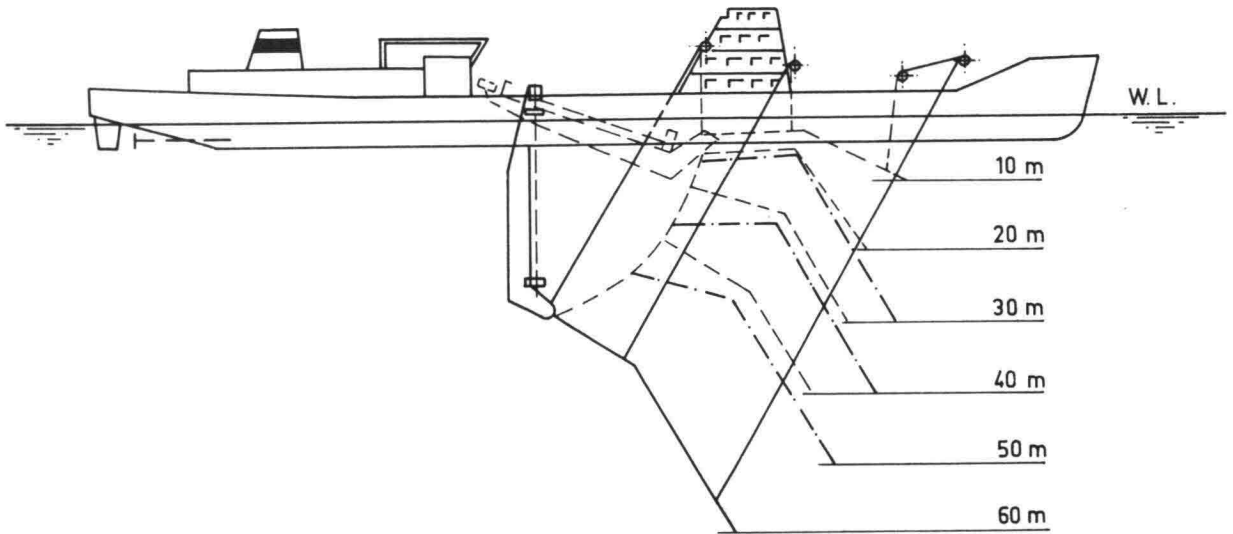


Figure 16.8  
Seagoing suction dredge

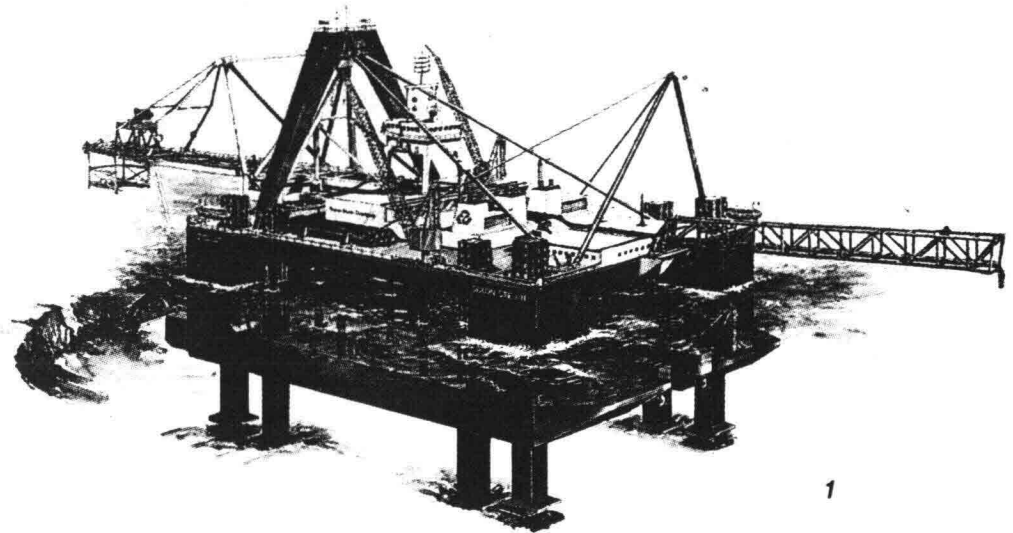


Figure 16.9  
Jack-up cutter suction dredge

Extra Notes

### 17.1 Introduction

It has been described in the previous chapter how material can be dredged from the oceans, lakes, and waterways. When this spoil material is obtained for a specific purpose such as land reclamation or use as concrete aggregate, then there is usually little direct spoil disposal problem. Cressard (1975)\* describes some of the indirect environmental consequences of such dredging, however. The dredging operation itself is usually carried out at a location dictated by the quality of the bottom material rather than by navigational considerations.

When navigational considerations do dictate the site of the dredging, we are often faced with a substantial spoil disposal problem. Because the type and quality of material dredged is no longer a chosen variable, we are often faced with the problem of disposing of a relatively poor quality spoil (one for which there is no immediate use). This material may be disposed of on land or dumped into another body of water.

### 17.2 Marine Disposal

Obviously, the disposal of a large quantity of foreign material in a body of water - even an ocean - can have serious consequences for the marine biology<sup>†</sup>. Many of the deleterious consequences can be avoided by disposing of the material only in the deepest ocean trenches. Unfortunately, the prohibitive shipping costs make transport to such sites uneconomical except for disposal of the most lethal materials such as certain radioactive wastes.

Research is only now beginning on the impact of the disposal of dredged material in the areas nearer to shore. This work is being carried out primarily by biological oceanographers.

---

\*The journal in which this article appears, serves as a current awareness journal for the dredging industry.

<sup>†</sup>This is an example of how coastal engineering relates to biological oceanography. See chapter 3.

### 17.3 Land Disposal

It is sometimes more economical or desirable to dispose of mud, clay, and sand dredged from harbors reasonably nearby on land rather than at sea. In this case, the spoil material mixed with water is pumped ashore via a pipeline. The further disposal procedure is dependent upon the type of material.

If the material is sand having a grain size greater than about 100  $\mu\text{m}$ , then it is possible to simply discharge the mixture at the disposal area and let the excess water flow away directly. This technique works well, provided that the layer of sand to be built up is at least 0.75 m thick. The sand layer develops sufficient bearing capacity almost immediately to allow construction equipment to work and extend the discharge pipeline.

With finer sands containing some mud and clay, the bearing capacity of the filled area often does not develop rapidly enough to allow construction equipment to work. Work must sometimes be stopped for a time before the discharge pipeline can be extended.

As the dredged material becomes finer, it has a greater tendency to be washed away with the drainage water. Sometimes, it is sufficient to use a bigger discharge area or to take special measures to prevent the discharge of fine material in suspension in the drainage water.

When very fine material such as mud or clay is being handled, it is often discharged into an area which has been dammed off from its surroundings. Only after most of the solid material has settled is the surplus water allowed to flow away. After the surface water has flowed away, a layer, optimally about 1.3 m thick, of saturated mud remains. Drainage channels are made through this to allow the remaining pore water to escape. After a period of a bit more than a year, the layer has consolidated to a thickness of about 0.9 to 1.0 m. At this time new dikes can be built in order to add an additional layer of mud, or the created land surface may be developed for other uses such as agriculture or recreation.

18.1 Introduction

We have just seen in the previous three chapters that as ships become larger the dredging problems associated with harbors become greater. This often necessitates that we continue dredging operations in much more open water. Since the wave action in this open water can complicate the dredging problem, it is often economical to take measures to protect the harbor entrance channel. Protection can be provided to make dredging operations more efficient or to reduce the amount of dredging necessary. Of course, breakwaters can occasionally serve other purposes as well such as providing quay facilities for ships.

Details of breakwater construction are the subject of volume III of these notes. We are concerned here only with their use with regard to morphological problems.

18.2 Morphological Functions of Breakwaters

How can breakwaters be used to help solve approach channel dredging problems? There are several ways:

a. They can reduce the wave action in the approach channel so that dredging equipment can operate more efficiently. Most dredging equipment must remain stable in the waves in order to operate effectively. Reduced wave action may make it possible to select and use more efficient equipment for the dredging operation.

b. By extending through the breaker zone breakwaters can block the longshore transport of sand which could otherwise settle into the dredged channel. By blocking this transport of material by wave action, the amount of necessary maintenance dredging can be significantly reduced in many cases. Obviously, we must be careful when we interrupt this longshore sand transport. Material which once simply passed along the coast (before the channel was built) will now pile up against the breakwater; coast erosion can be expected on the opposite site of the approach channel.

c. When there is a large sediment supply from a natural river flowing through the harbor, then a shoal can often be expected slightly offshore from the river mouth\*. This shoal can form a major obstacle for shipping, especially during a severe storm when waves can be breaking on this shoal. Many ships have been wrecked attempting to cross such a bar under these circumstances. Breakwaters built out in such a way that the entrance is kept narrow until deeper water is reached increase the entrance current velocities; the resulting increased sediment transport capacity tends to keep the entrance open. Where does this material then go? Some of it will probably be

\*Such a shoal can also form after the accretion mentioned in item b, above, has reached the end of the breakwater and material passes around the end.

deposited in deeper water offshore while some may settle out further upstream in the river. Indeed, since the river has in effect been made longer by building the breakwaters, the slope must slightly decrease and a siltation problem can appear inland from the entrance. At least, this material can be dredged out under excellent conditions - no wave action and often less shipping traffic. An example of a harbor entrance where breakwaters are being built to constrict the entrance is shown in figure 18.1. The channel dredged through the shoal is shown by the dashed lines. In this case, the river is the Columbia discharging into the Pacific Ocean on the west coast of the United States.

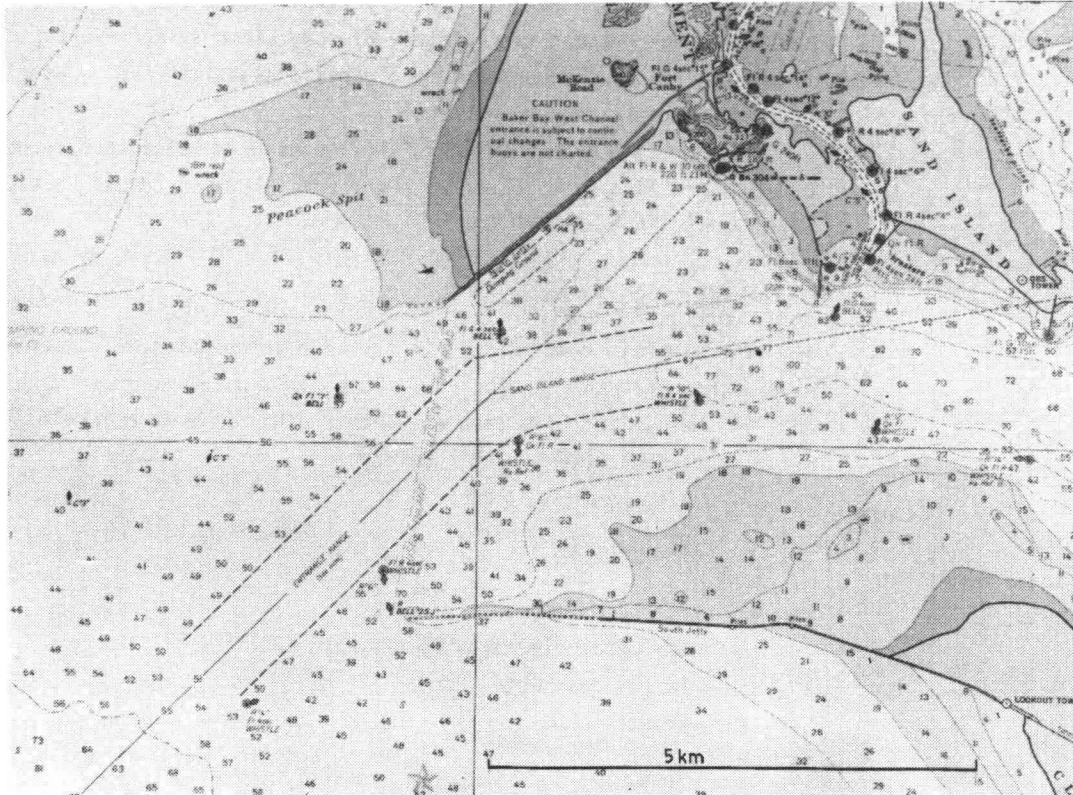


Figure 18.1 COLUMBIA RIVER ENTRANCE, U.S. WEST COAST  
Scale : as shown                      depths in feet

### 18.3 Other Considerations

Another interesting question is, "What is the optimum depth of such an approach channel?" This is one of the topics discussed in volume II. By reducing wave action in a channel, ship motion is reduced and it can be possible to let ships enter a bit shallower channel than would be possible otherwise.

Of course, breakwaters extend and alter the shape of our harbor. These changes will, thus, also modify the natural resonant period of standing waves in the harbor. If the new resonant period should happen to correspond with that of a tidal component, a multiple of a persistent ocean swell, or a gust oscillation, then some significant problems can be expected in the harbor. These resonances, or seiches, are treated in the following chapter.

19.1 Definition

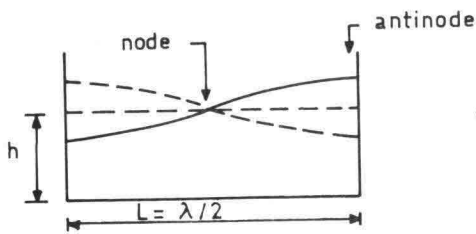
Strictly speaking, seiches are free standing wave oscillations in a closed body of water. The surges occasionally experienced in Lake Geneva fit this strict definition, for example. This type of phenomena can be caused by, for example, atmospheric pressure variations, or abrupt in or out flow of large quantities of water.\*

The term seiche is also used to describe standing wave action sometimes found in harbors. These waves have relatively long periods and low amplitudes when compared to the waves described in chapter 5. In harbors which are not completely closed, other driving forces can be present. Tidal influences and long period swell in the adjacent ocean can excite seiches in harbors.

Another term, "range action", is often used to refer to seiches. This term is also used to refer to the motion of moored ships resulting from seiches.

19.2 Simple Cases

The simplest true seiche (in a closed water body) is a standing wave with a node in the middle of the basin and an antinode at each end. The basin length is then equal to one half the wave length as shown in figure 19.1. For such a long wave:



$$c = \sqrt{gh} \tag{5.05 b} \tag{19.01}$$

where: c is the wave speed,  
g is the acceleration of gravity, and  
h is the mean water depth.

Applying this to the basin in the figure, the wave period, T, can be computed:

$$T = \frac{2 L}{\sqrt{gh}} \tag{19.02}$$

Using Lake Geneva as an example, we find, with

L = 90 km and h = 200 m that T is about 1 hour 8 minutes.

When a harbor is connected to the sea, a node can be found at the entrance and an antinode will be found at the end of the harbor basin. In this case, the wave length can be 4 times the harbor basin length as shown in figure 19.2. In this case:

$$T = \frac{4 L}{\sqrt{gh}} \tag{19.03}$$

Figure 19.1  
STANDING WAVE IN  
CLOSED BASIN  
(distorted scale)

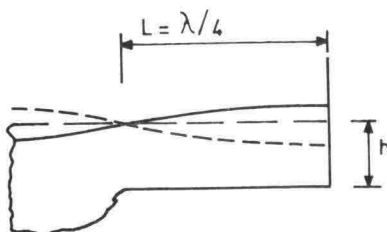


Figure 19.2  
SEICHE IN  
HARBOR BASIN  
(distorted scale)

\* Seiches are often observed in shipping locks on a small scale.

Other possibilities are also possible, however. In general:

$$T_i = \frac{4 L}{(i) \sqrt{gh}} \quad (19.04)$$

where  $i$  is an odd integer: 1, 3, 5, ..; note that as  $i$  increases the period of the  $i^{\text{th}}$  harmonic wave decreases. Also, equation 19.03 is the same as 19.04 with  $i = 1$ ; this yields the first harmonic, or primary wave. An example with  $i = 5$  is shown in figure 19.3. Thus, seiches having several periods can be sustained in a given harbor basin. In practice,  $i$  in equation 19.04 will usually be small; most often 1.

### 19.3 Effects of Seiches

Usually, the vertical amplitude of a seiche, even at an antinode, is small. However, especially at a node, the *horizontal* displacement of the water can be very significant. Since moored ships are simply drawn along with the water, they can have mooring difficulties if they happen to be near a seiche node. Another related influence on the large ships is the effect of the water surface slope.

### 19.4 Seiche Prevention

Seiches have long periods and small amplitudes. The waves cannot be broken on a shore and since they have so much momentum, there is little that can be done to damp them in an existing basin. Often, too, the driving force for a seiche cannot be removed either, since it can well be a tidal wave component or very long natural swell which drives it. However, since we are dealing with a resonant vibration with little damping, we may remember from dynamics that we need change the natural period only slightly to cause a significant reduction in the response. From equation 19.04, it is seen that the periods of the seiches in the harbors are dependent upon both the depth and the length. Either, or both, may be varied to change the response of the harbor to a given driving period. As another trick, many harbors are laid out with irregularly shaped basins, in the hope that direct reflections will be reduced.

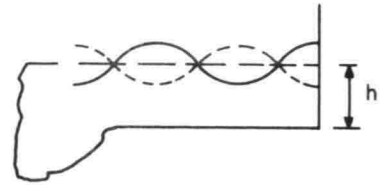


Figure 19.3  
FIFTH HARMONIC  
SEICHE  
(distorted scale)

20. TIDAL RIVERS20.1 Introduction

It has already been indicated in chapter 14 that harbors were often originally developed along rivers, sometimes rather well inland. London, England, Portland, Oregon, U.S.A., Antwerp, Belgium, Rotterdam, The Netherlands and Hamburg, Germany are obvious examples of such harbors. In some cases the distance to the sea has become too much of an obstacle for shipping and the prosperity of the harbor has suffered. Deventer, in The Netherlands exemplifies this.

In this chapter, we examine the effects of tides on the lower reaches of rivers and the consequences for dredging and navigation.

20.2 River Mouths

River mouths on flat coasts handle not only the fresh water run off from their drainage basin, there is also a tidal flow through the mouth. Escoffier (1940) studied the stability of tidal inlets. His predominantly qualitative study led to an expression for the maximum entrance channel velocity,  $V_m$ , for a given estuary as function of the hydraulic radius of the channel,  $R$ , its cross sectional area,  $A$ , and the tidal range in the estuary,  $\Delta h$ . Since this is done for a given estuary, then other variables such as the channel bed roughness, its length, the surface area of the estuary, and the tidal range at sea have all become more or less constant.

Escoffier combined the variables for a given estuary into a single parameter,  $x$ , such that a larger entrance cross-section will result in a larger value of  $x$ . Qualitatively, he found that  $V_m$  varied as a function of  $x$  more or less as shown in figure 20.a.

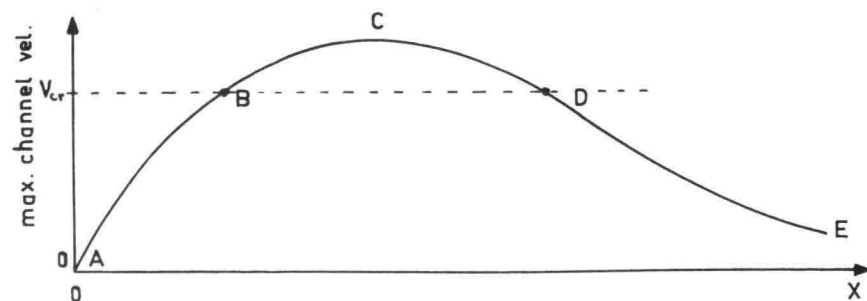


Fig. 20.a channel velocity geometry relationship

In the range from A to C on this curve, the entrance channel is so small that it "chokes off" the tidal flow so that the tidal difference within the estuary will be less than at sea. On branch C-E of the curve this is no longer true and the maximum current velocity decreases as the channel becomes larger.

Escoffier's next step was to introduce the concept of a critical maximum velocity,  $V_{cr}$ , below which the velocity in the channel is too low to cause erosion. This critical velocity is more or less independent of the channel geometry, according to Escoffier, and he plotted it as a horizontal line on figure 20.a.

The fate of an estuary can now be predicted by examining the curve A C E in relation to  $V_{cr}$ . Obviously, if  $V_m$  is always less than  $V_{cr}$  - for all values of  $x$ , then any sediment deposited in the entrance will remain there and the estuary will be closed off eventually. If on the other hand, a curve of  $V_m$  versus  $x$  intersects the  $V_{cr}$  line such as at B and D in the figure, then a variety of situations can exist. If, for example, the channel dimensions place it on branch A-B of the curve in figure 20.a, then the channel is too small to maintain itself; it will be closed by natural processes. If the channel geometry places it on branch D-E of the curve, it will also become smaller, but as it does so, the velocity,  $V_m$ , will increase; sedimentation continues until point D is reached. Lastly, if the channel configuration places it on branch B-D of the curve, then erosion takes place until point D is again reached; point D represents a stable situation.

With this insight, it is now possible to evaluate the influence of changes in an estuary mouth. Since point D represents a naturally stable situation, most natural estuaries will tend to lie more or less in that region. A severe storm can, of course, largely fill the entrance moving it suddenly to branch A-B of the curve. In such a situation, immediate dredging is called for to prevent complete closure. One need not restore the original situation, however; once the entrance geometry places it on branch B-C-D of the curve in the figure, nature will do the rest of the work given enough time.

Shipping interests can make it desirable to enlarge a given estuary entrance to accommodate larger ships. If such an expansion scheme places the channel on branch D-E of the curve, then the dredging industry will remain profitable for the foreseeable future. It may be possible to carry out the expansion and still prevent perpetual dredging by changing the channel alignment and artificially constricting its width - techniques often used in rivers - so that the larger channel cross-section remains stable. Translating such changes into a figure such as 20.a means that a new curve of  $V_m$  versus  $x$  has been generated which generally yields a bit higher value of  $V_m$  for a given  $x$  value. This results in point D, the equilibrium situation, being moved to the right in the figure.

One of the most important questions to be answered in order to use the above approach by Escoffier is, "what is the stable equilibrium condition of an estuary?" or in other words, "when has point D in figure 20.a been reached?" Several investigators O'Brien (1969), Jarrett (1976) and Shigemura (1980) have devoted special attention to the determination of the equilibrium cross sectional area of an estuary entrance. Their results for sandy coasts do not differ too much from those of O'Brien (1969). He found that the minimum equilibrium cross sectional area of the entrance,  $A$ , was linearly related to the volume of the tidal prism. In equation form:

$$A = 6.56 \times 10^{-5} P \quad (20.01)$$

where  $A$  is the minimum equilibrium cross section area of the entrance in  $m^2$ , and

$P$  is the tidal prism volume in  $m^3$ .

In this equation,  $P$ , the tidal prism, is the storage volume of the estuary between the low tide and high tide levels. It is usually determined by multiplying the mean surface area of the estuary by the mean tide range in the estuary. Since a river flow will also contribute to the filling of the tidal prism, this volume is not equal to the time integral of either the inflow or the outflow during flood or ebb respectively. The coefficient in equation 20.01 is *not* dimensionless. Indeed, it has dimensions of  $1/L$  and in foot - lb - s units:

$$A = 2 \times 10^{-5} P \quad (20.01)$$

where  $A$  is in  $ft^2$  and  $P$  in  $ft^3$ .

Tidal prism volumes in O'Brien's data ranged from about  $1.4 \times 10^7 m^3$  ( $5 \times 10^8 ft^3$ ) to about  $3 \times 10^9 m^3$  ( $1.1 \times 10^{11} ft^3$ ). There is some indication that equation 20.01 would tend to yield too great a cross section area for smaller tidal prisms.

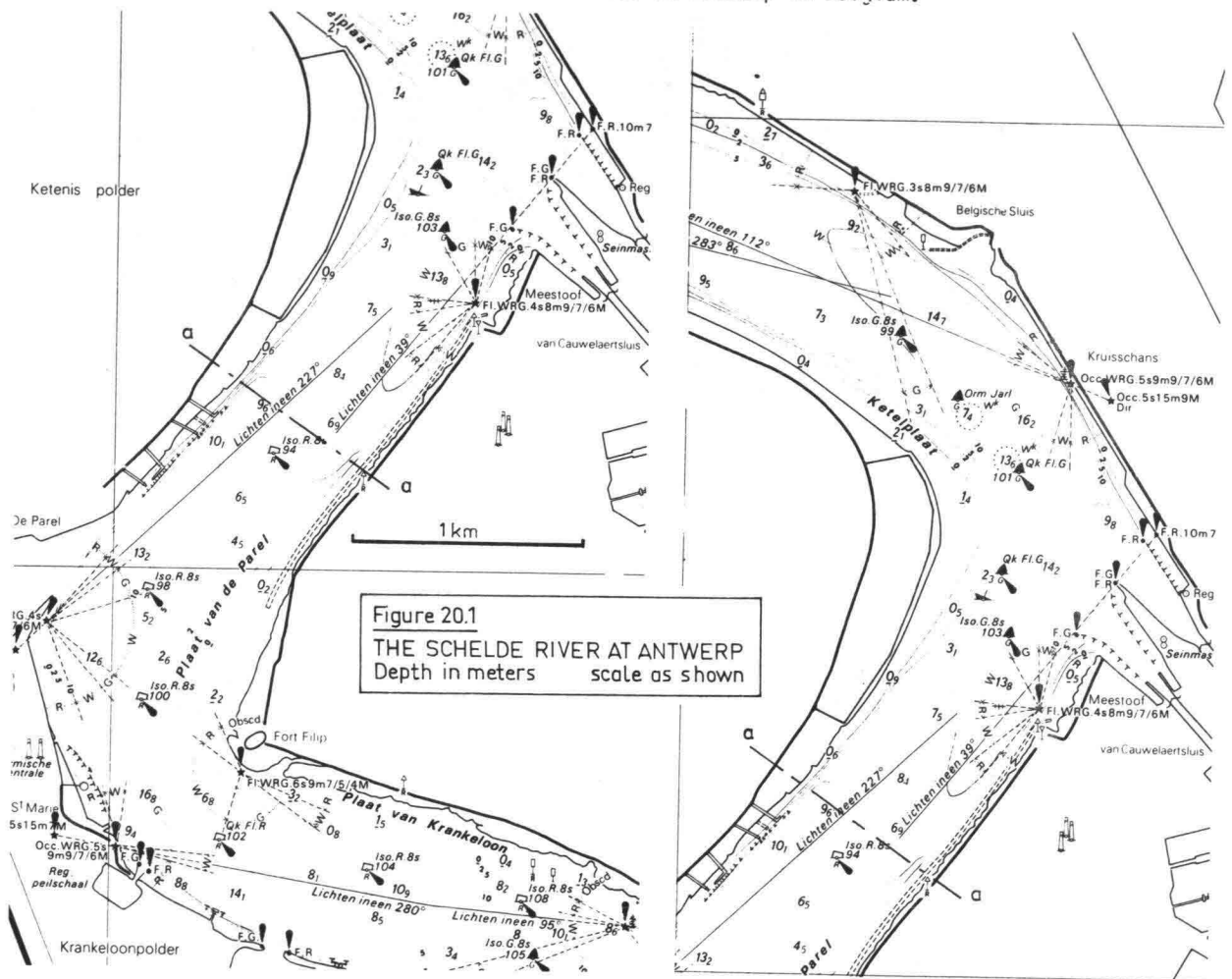
O'Brien found, as well, that there was little influence on equation 20.01 from the bed material size. Further, the equation seemed equally valid for both large river mouths and for bays and tidal lagoons. A restriction, however, is that (20.01) is valid only for inlets having a predominantly semi-diurnal tide. This last bit of information, combined with the realization that the tidal prism is filled and emptied once during each tidal period of  $12^h 25^m$ , leads to a simple but only crude conclusion that the average of the absolute value of the current velocity in the estuary mouth is constant, a result which certainly does not disagree with that of Escoffier more than 30 years earlier!

Obviously, the *form* of the mouth *is* influenced by many other factors. The discussion of these is postponed until chapter 29, however.

### 20.3 River channels

The geometry of natural channels and shoals in rivers is discussed in courses in river engineering. The deepest channel sections develop along the outside of the river bends with the channel shifted somewhat down stream from the shoreline bend. How is this modified by the presence of tidal action?

When there is an alternating current direction in a narrow channel the only influence of the tide on the river bathymetry is to make the location of the deeper channel in the river bends correspond more closely to that of the shoreline bend. The position represents a compromise between the development to be expected with only an ebb current and that expected with only a flood current. An example of such a channel development is shown in figure 20.1 - the Schelde River at Antwerp in Belgium.



In areas where the river width is not restricted, an entirely different pattern can develop. These tidal river reaches often have two rather independent channel systems. The ebb current concentrates in one set of channels while the flood current is often strongest in another set of channels. This pattern is most completely developed near river bends. Figure 20.2 shows this pattern clearly at another section of the Schelde River less than 50 km downstream from Antwerp (fig. 20.1).

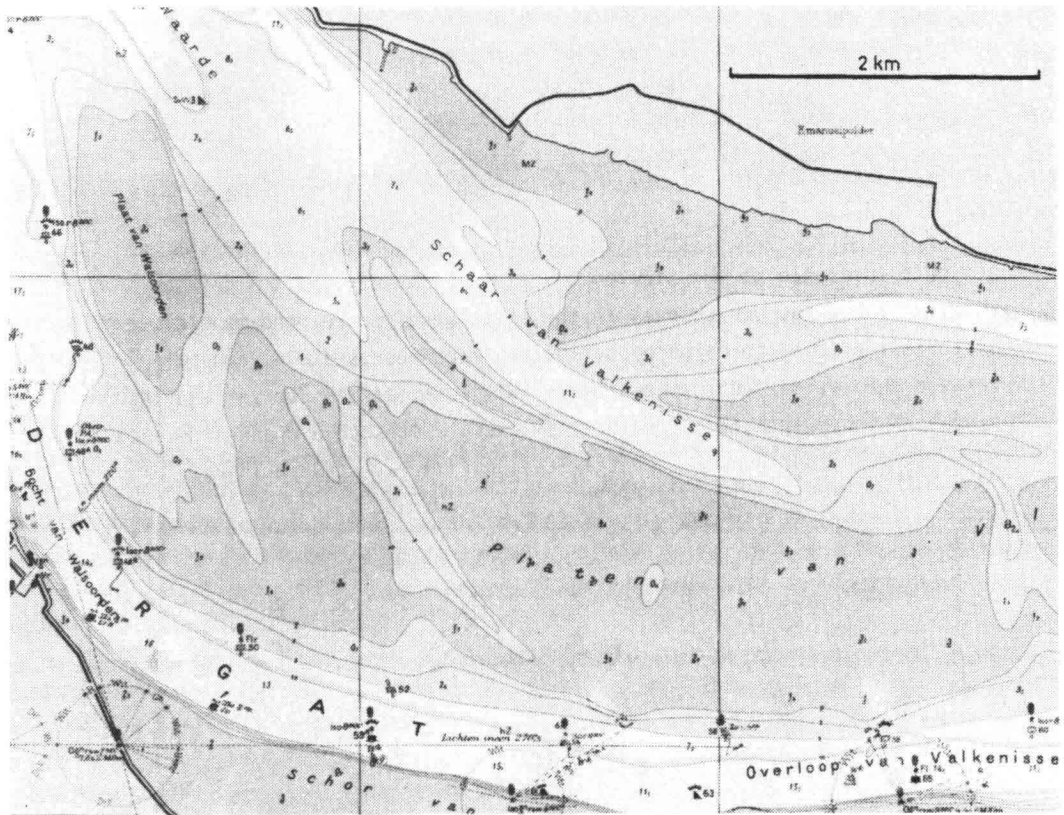


Figure 20.2  
THE SCHELDE RIVER EAST OF HANSWEERT  
Depth in meters scale as shown

Flood channels can usually be recognized by the following characteristic features:

- a. They tend to be shallower than ebb channels.
- b. They tend to "die out" - they lead to progressively shallower water and finally spread out on a shoal.

Ebb channels, on the other hand, are continuous and tend to be deeper. The reasons for these characteristic differences are explained in the following section.

#### 20.4 Tidal Currents

One factor which helps to account for the characteristic differences between flood and ebb channels is that the quantity of water discharged during the ebb is always greater than the quantity entering the river during the flood. This is because the river runoff plus the ocean water which entered during the flood tide must be discharged during the ebb. This tends to make ebb currents stronger, and hence, ebb channels deeper. An example of this is shown in table 20.1 and figure 20.3 which shows the current at Rotterdam. If a similar graph were made of the current some greater distance upstream, the ebb current would become more important. As some point, even, the current would always flow downstream with a velocity which varied according to the tide. How far up a river can a tidal influence still be detected? Theoretically all the way unless there are rapids (reaches with supercritical flow).

TABLE 20.1 TIDE AND CURRENT DATA ROTTERDAM.

Time (hrs)	Average Current* (m/s)	Tide level (m)
0	-0.15	-0.69
1	+0.08	-0.50
2	0.60	-0.03
3	0.75	+0.52
4	0.44	0.91
5	+0.07	1.04
6	-0.44	0.91
7	-0.73	0.61
8	-1.03	+0.25
9	-1.05	-0.15
10	-0.85	-0.47
11	-0.52	-0.58
12	-0.30	-0.62

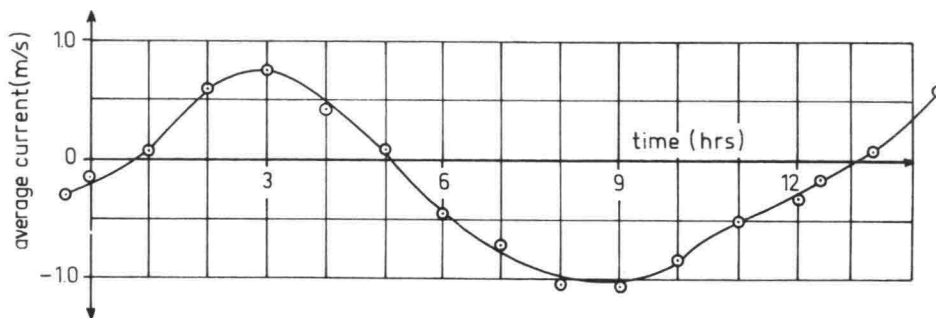


Figure 20.3 CURRENT AT ROTTERDAM

Another phenomenon in a tidal river is a tide-dependent variation in water level. The current and the level are related by the equations used to describe long waves. In such a case, conservation of momentum yields:

$$V \frac{\partial V}{\partial x} + \frac{\partial V}{\partial t} = -g \frac{\partial z}{\partial x} - g \frac{V|V|}{C^2 h} \quad (20.02)$$

in which:

- C is the chezy friction coefficient,
- g is the acceleration of gravity,
- h is the depth,
- t is time,
- V is the flow velocity,
- x is the coordinate measured along the river, and
- z is the absolute water surface elevation.

\* Flood currents are considered positive.

In this equation, it has been assumed that the river slope is small and the runoff is negligible. If the friction - the last term in equation 20.02 - is also negligible (this can be the case with a short surface wave or with a tide in the deepest ocean basin), the vertical tide (water level) and horizontal tide (current) are in phase with one another as shown in figure 20.4.

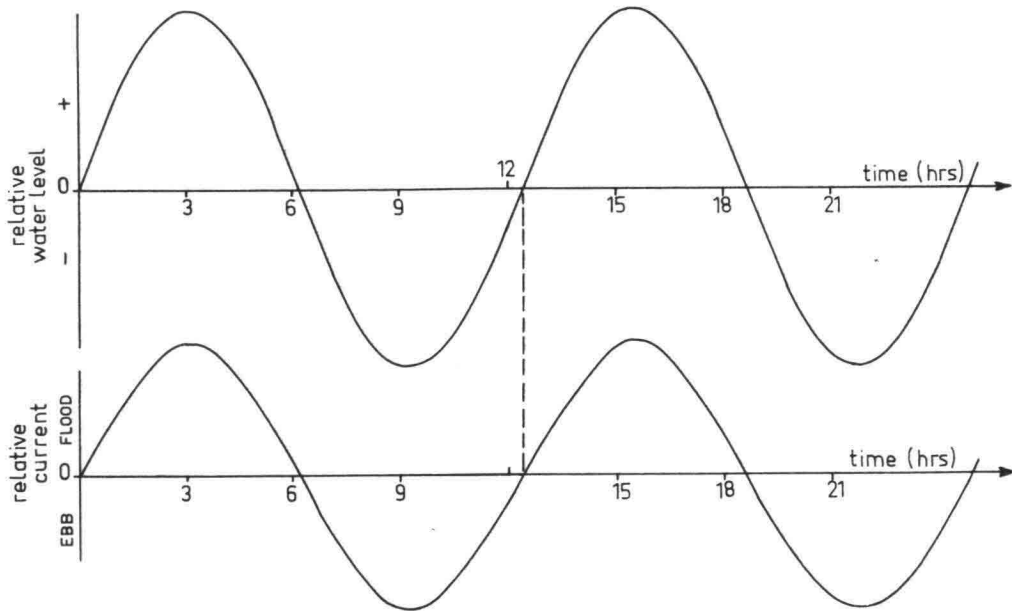


Figure 20.4 IDEALIZED VELOCITY-LEVEL RELATIONSHIP

In a real situation, the friction term in equation 20.02 will be relatively large with respect to the inertia terms. Since some of the momentum is then lost to friction, the velocity will be reduced. Figure 20.5 shows the relationship between the vertical and horizontal tides at Rotterdam. The current curve is the same as that in figure 20.3. The right hand portion of these graphs is plotted by adding one tide period ( $12^h 25^m$ ) to the times listed in table 20.1. The time of high tide (high water) and low water are indicated along with the times of slack water (zero current).

Note that the low tide slack comes much later relative to low water than is the case at high tide. This is partially caused by the fresh water river flow acting to fill the most inland portion of the tidal prism during a rising tide. This enhances the development of a water surface slope to retard the tide wave, while at low water on the other hand, the river flow tends to prolong the ebb current.

A second reason why ebb channels are deeper and more continuous is indicated in figure 20.5. Note that the maximum ebb current occurs when the tide level is lower than that corresponding to the maximum flood current. The combined effect of higher total ebb flow and the lower stage during this flow tends to increase the velocity and enhances erosion in ebb channels.

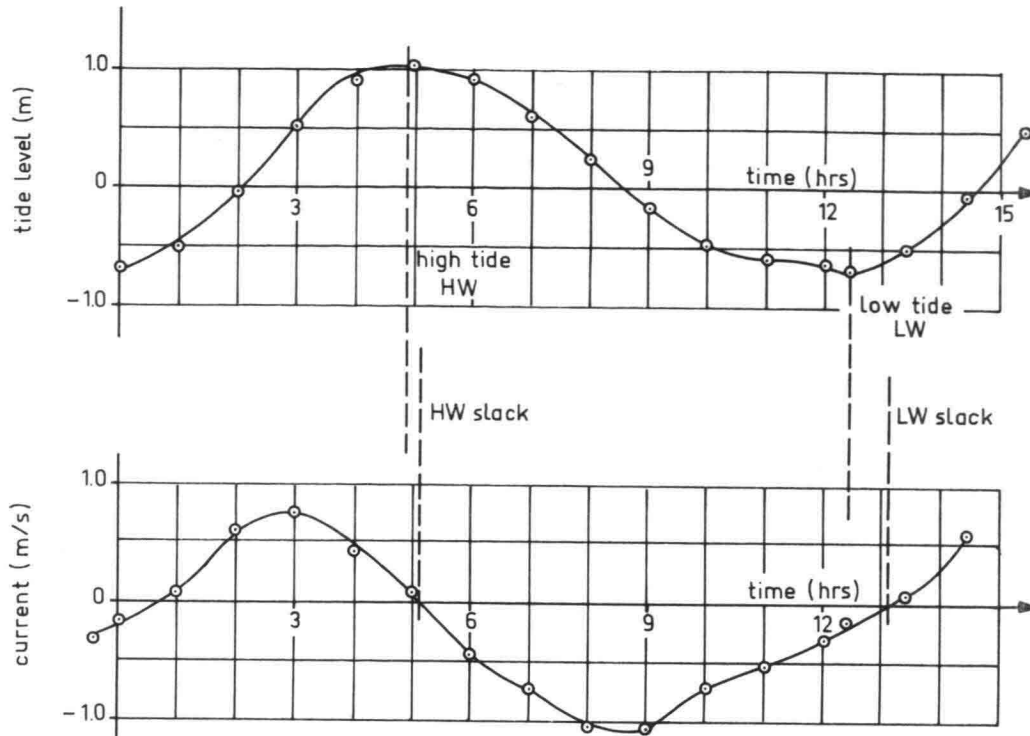


Figure 20.5 VERTICAL AND HORIZONTAL TIDE AT ROTTERDAM

This discussion has been limited until now to measurements made at a single river cross-section. A tidal wave also travels along a river. As an example of this, the high tide wave reaches Antwerp about 1<sup>h</sup> 45<sup>m</sup> after it passes Vlissingen. Tidal data for the Western Schelde Estuary between Vlissingen and Schelle, Belgium, are presented in table 20.2 and figure 20.6. This estuary has a very small fresh water flow, in contrast to the situation in Rotterdam. Figure 20.6 gives a clear indication of how a tide wave propagates along the estuary. This phenomenon can sometimes be utilized by ships, as outlined in the following section.

Why are the maxima of the flood currents in table 20.2 greater than the ebb current maxima? This is caused, in this case by the distortion of the vertical tide curves; for a rising tide the sharp increase in water level in a short time causes higher velocities.

TABLE 20.2 Tidal Data for Western Schelde

Time (hrs)	Vlissingen		Hansweert		Schelle, Bel.
	level (m.)	current (m/s)	level (m.)	current (m/s)	level (m.)
0	1.72	-0.14	2.43	+0.50	1.60
1	1.14	-0.66	1.76	-0.95	2.83
2	+0.20	-0.94	+0.80	-1.07	2.92
3	-0.80	-0.87	-0.30	-1.07	2.00
4	-1.63	-0.71	-1.29	-0.99	0.90
5	-2.07	-0.44	-2.08	-0.72	+0.03
6	-1.78	+0.04	-2.32	-0.28	-0.75
7	-1.33	0.32	-1.60	+0.60	-1.44
8	-0.81	0.45	-0.90	0.66	-2.04
9	-0.10	0.63	-0.28	0.84	-1.85
10	+1.30	1.24	+0.73	1.14	-0.65
11	2.10	0.88	2.11	1.74	-0.17
12	1.77	+0.09	2.52	+0.80	+1.10
13	1.35	-0.53	2.00	-0.70	2.60

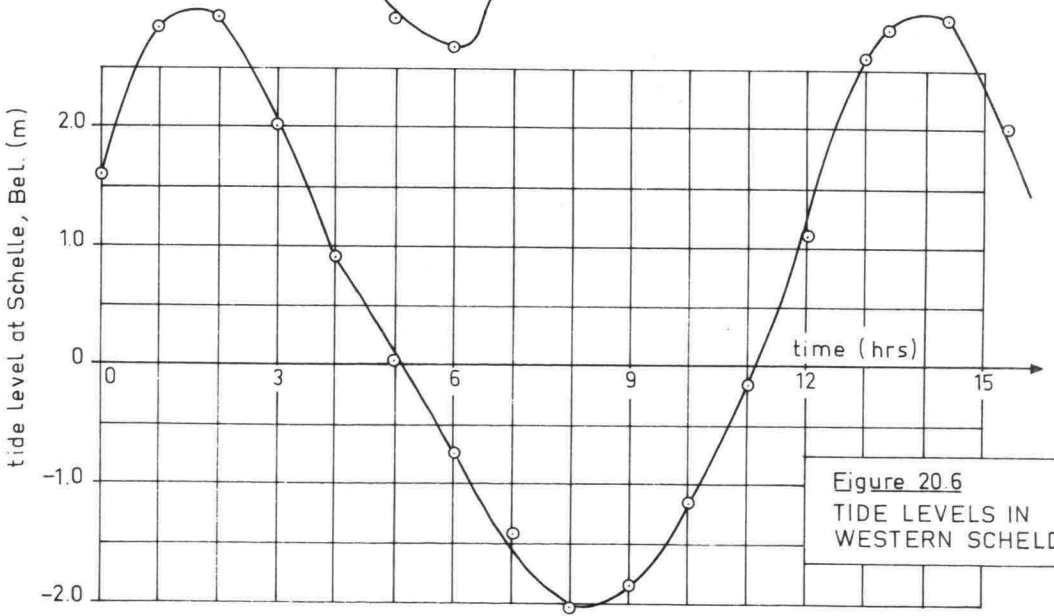
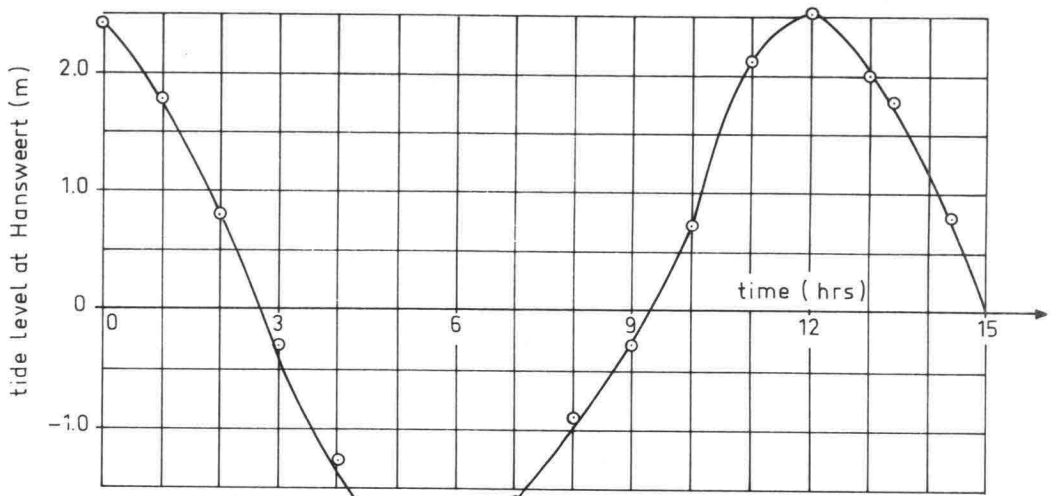
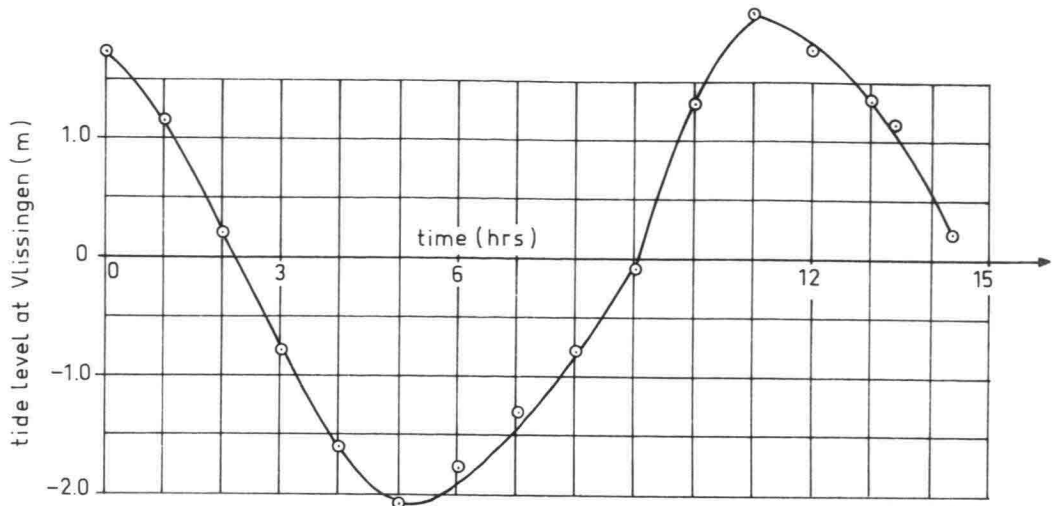


Figure 20.6  
TIDE LEVELS IN  
WESTERN SCHELDE

### 20.5 River Navigation

The reasons for locating harbors well upstream along rivers have been indicated in chapter 14. The dredging problems have also been indicated. How can the tides be used to reduce the amount of necessary dredging and to help the shipping on a river? After all, it is not always economical to dredge away shoals along a river to sufficient depth so that *all* ships can navigate at *all* tide stages. It may be possible to allow larger, deeper ships to wait at the entrance for high tide and then to "ride" this high tide wave up the river. Unfortunately, the ships of concern here are not able to attain a speed as high as that of the tidal wave. Thus, even though they may enter a river at high tide, they cannot keep up with the tide wave as they progress up the river; interruption of their travel may be necessary, therefore. In order to determine the best strategy for a pilot on a ship, it is necessary to predict the water depth at each shallow channel reach at the time of arrival of the ship. To accomplish this the propagation velocity of the tide wave must be determined. Since friction tends to slow the tide wave, equation 5.05 b is not sufficiently accurate. Instead:

$$c = \sqrt{g\bar{h} (1 - \tan^2 \theta)} \quad (20.03)$$

where:

$\bar{h}$  is the average depth

$\theta$  is a friction factor computed from:

$$\theta = \frac{1}{2} \arctan \left\{ \frac{T' 8g V_{\max}}{6\pi^2 C^2 \bar{h}} \right\} \quad (20.04)$$

where:

$C$  is the Chézy friction factor,

$T'$  is the tide period,

$V_{\max}$  is the maximum flood current, and

$\arctan \{ \quad \}$  indicates the angle whose tangent is  $\{ \quad \}$ .

The procedure outlined above will be demonstrated via an idealized example.

### 20.6 Example

A pilot needs to bring a ship needing a minimum channel depth of 11.5 meters up a 250 km channel to a harbor. Three shoals are located along this channel as shown in figure 20.7. The depth over each of these shoals is only 11.0 m relative to the mean water level. The rest of the river is 13.0 m. deep. The Chézy friction factor for this river is  $60 \text{ m}^{1/2}/\text{s}$ .

The tide is semidiurnal (period =  $12^{\text{h}} 25^{\text{m}}$ ) and is assumed to be sinusoidal. The tide range is 3 meters and the maximum current is 1.2 m/s. It is assumed that this tidal form is valid for the entire river reach. The tidal information is also shown in figure 20.7.

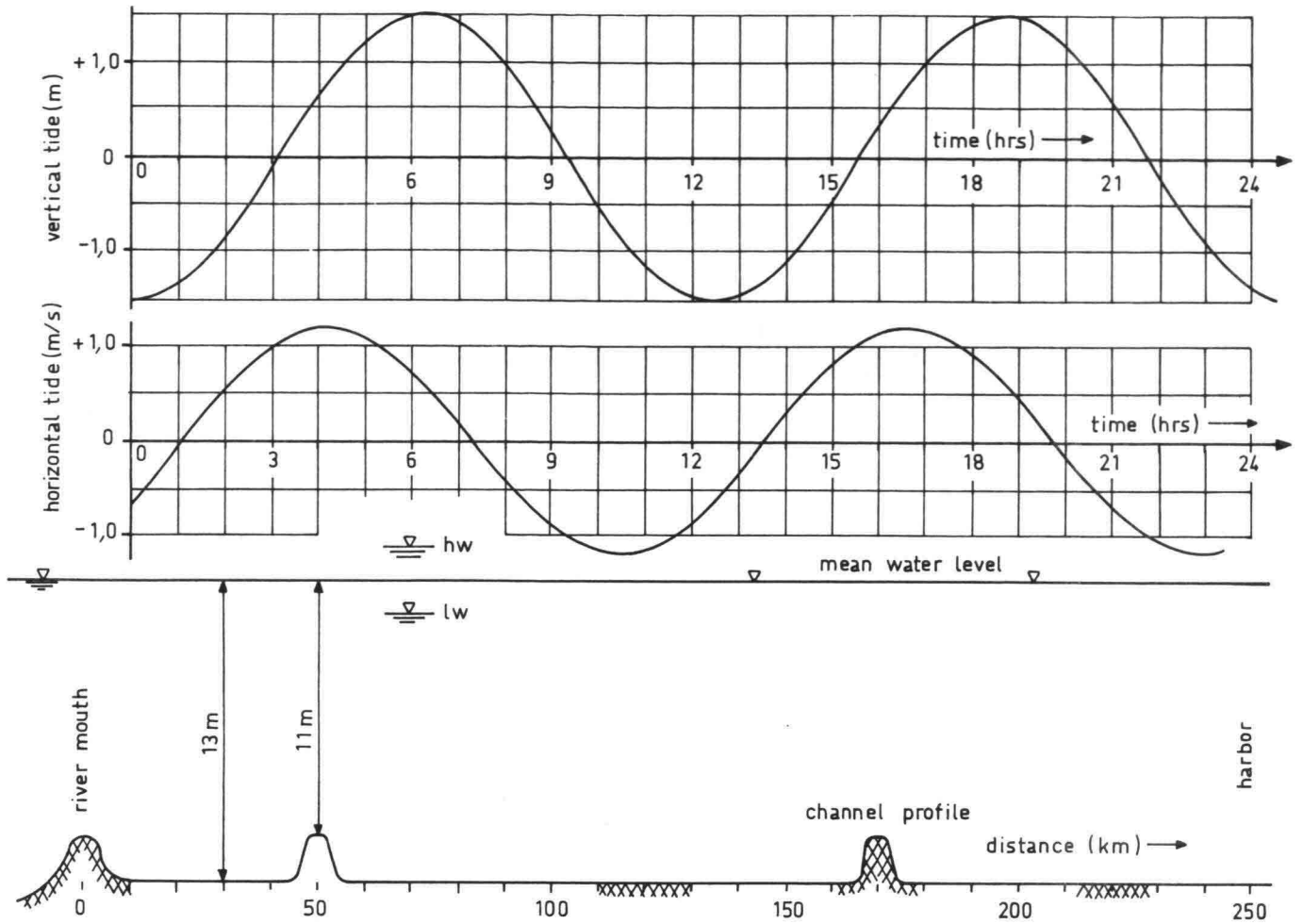


Figure 20.7 EXAMPLE PROBLEM DATA

As an additional limitation, the ship must maintain a minimum speed of 5 kt. (9.26 km/hr) relative to the water. Her maximum speed is 8 kt (14.82 km/hr).

The solution begins by determining the speed of the flood tide wave through the channel. Using 20.04,

$$\theta = \frac{1}{2} \arctan \left\{ \frac{(12.42)(3600)}{6\pi^2} \frac{(8)(9.81)}{60^2} \frac{1.20}{13} \right\} \quad (20.05)$$

$$= \frac{1}{2} \arctan \{1.52\} \quad (20.06)$$

$$= 28.33^\circ. \quad (20.07)$$

Thus, from (20.03):

$$c = \sqrt{(9.81)(13)(1 - \tan^2 28.33^\circ)} \quad (20.08)$$

$$= 9.51 \text{ m/s} = 34.2 \text{ km/hr} \quad (20.09)$$

The determination of the location of the ship at any time can be accomplished by integrating the velocity of the ship with respect to time. This can be most easily done by numerical integration in a tabular form, as shown in table 20.3. In this table two identical ships are considered, one moving at a minimum and one at maximum speed through the water.

In table 20.3, the ship velocity with respect to the ground is integrated with time steps of one hour. In order to determine the absolute velocity of the ship, the tidal current *at the ship's location* at the end of each hour must be known. Since the horizontal and vertical tides are known only at the entrance, the assumption is made that the tide wave propagates along the channel at speed  $c$  and is unchanged in amplitude and form. (Figure 20.6 shows that this last part of the assumption is not always true in practice). The depth and current at the ship can be obtained from the tidal curves in figure 20.7 by converting the distance between the ship and the crest of the tide wave into an equivalent time. Thus, the time listed in the left hand column of the table is an absolute time, while the "tide time" listed in the first column for each ship is determined by this distance between ship and tide wave crest. Since all tide times are related to a single high water crest, the times can have values greater than one tide period. Obviously, adding or subtracting a multiple of the tide period to these times would not affect the result of the computation.

The first line of table 20.3 is computed as follows:

The start time is arbitrarily chosen as zero. Since the water depth over the first shoal must be 11.5 m, the corresponding tide level must be +0.5. From figure 20.7 this tide corresponds to a tide time of 3.8 hours. At this time, the current is +1.2 m/s, from fig. 20.7. The time interval between the tide time and High Water is  $6.21 - 3.8 = 2.41$  h. With a tide wave speed of 34.2 km/h, the tide wave crest is located at -82.4 km at the time the ship crosses the first shoal.

In each succeeding hour, the tide wave progresses 34.2 km.

A typical line, for the time interval 16 -17 hrs goes as follows: At  $t = 16$  hrs, the ship is at 151.0 km and the tide crest is at 464.8. The tide phase in figure 20.7 is then:

$$\frac{464.8 - 151.0}{34.2} + 6.21 = 15.4 \text{ hrs.} \quad (20.10)$$

Entering figure 20.7 with a time of 15.4 hrs yields a tide level of - 0.1 m and a current of + 1.0 m/s. The tide level gives a depth of 12.9 m. The incremental distance for the ship in one hour is:

$$(1.0 \text{ m/s})(3.6) + 9.3 = 12.9 \text{ km.} \quad (20.11)$$

resulting in a distance after 17 hours of 163.9 km.

The results of table 20.3 can be visualized more easily in a graph of position versus time. In figure 20.8, the positions of the ships and of the tide wave crest are shown, along with the positions of the three shoals. The time intervals during which the shoals can be crossed are also shown.

TABLE 20.3 TABULATED INTEGRATION COMPUTATION

Time (hrs)	Pos. of H.W. (km)	SHIP MOVES 9.3 km/hr.				SHIP MOVES 14.8 km/hr.				Ship $x$ (km)	Ship $\Delta x$ (km)	Comments
		Tide Time (hrs)	Tide Level at ship (m)	Depth (m)	Current (m/s)	Tide Time (hrs)	Tide Level at ship (m)	Depth (m)	Current (m/s)			
0	-82.4	3.8	+0.5	11.5	+1.2	3.8	+0.5	11.5	+1.2	0.0	19.1	Both ships start when depth is 11.5 m with rising tide.
1	-48.2	4.4	+0.9	13.9	+1.2	4.2	+0.8	13.8	+1.2	13.6	19.1	
2	-14.0	5.0	+1.2	14.2	+1.1	4.7	+1.1	14.1	+1.2	13.3	19.1	
3	20.2	5.6	+1.4	14.4	+0.9	5.1	+1.3	12.3	+1.1	12.5	18.8	Fast ship passes second shoal.
4	54.4	6.2	+1.5	12.5	+0.7	5.6	+1.4	14.4	+0.9	11.8	18.0	Slow ship passes second shoal.
5	88.6	6.9	+1.4	14.4	+0.3	6.0	+1.5	14.5	+0.8	10.4	17.7	
6	122.8	7.6	+1.2	14.2	-0.2	6.5	+1.5	14.5	+0.5	8.6	16.6	
7	157.0	8.3	+0.8	13.8	-0.6	7.0	+1.4	14.4	+0.2	7.1	15.5	
8	191.2	9.1	+0.2	13.2	-0.9	7.6	+1.2	14.2	-0.2	6.1	14.1	
9	225.4	10.0	-0.5	12.5	-1.1	8.2	+0.8	13.8	-0.5	5.3	13.0	Fast ship arrives just too late to cross third shoal. Must wait until next tide!
10	259.6	10.8	-1.0	12.0	-1.2	8.8	+0.4	11.4		5.0	171.0	
11	293.8	11.7	-1.4	11.6	-1.0					5.7		
12	328.0	12.5	-1.5	11.5	-0.6					7.1		
13	362.2	13.3	-1.4	11.6	-0.2					8.6		
14	396.4	14.0	-1.1	11.9	+0.3					10.4		
15	430.6	14.7	-0.6	12.4	+0.7					11.8		
16	464.8	15.4	-0.1	12.9	+1.0					12.9		
17	499.0	16.0	+0.3	11.3	+1.1							Slow ship arrives at third shoal just too early to cross

Apparent errors in this table result from numerical round-off.

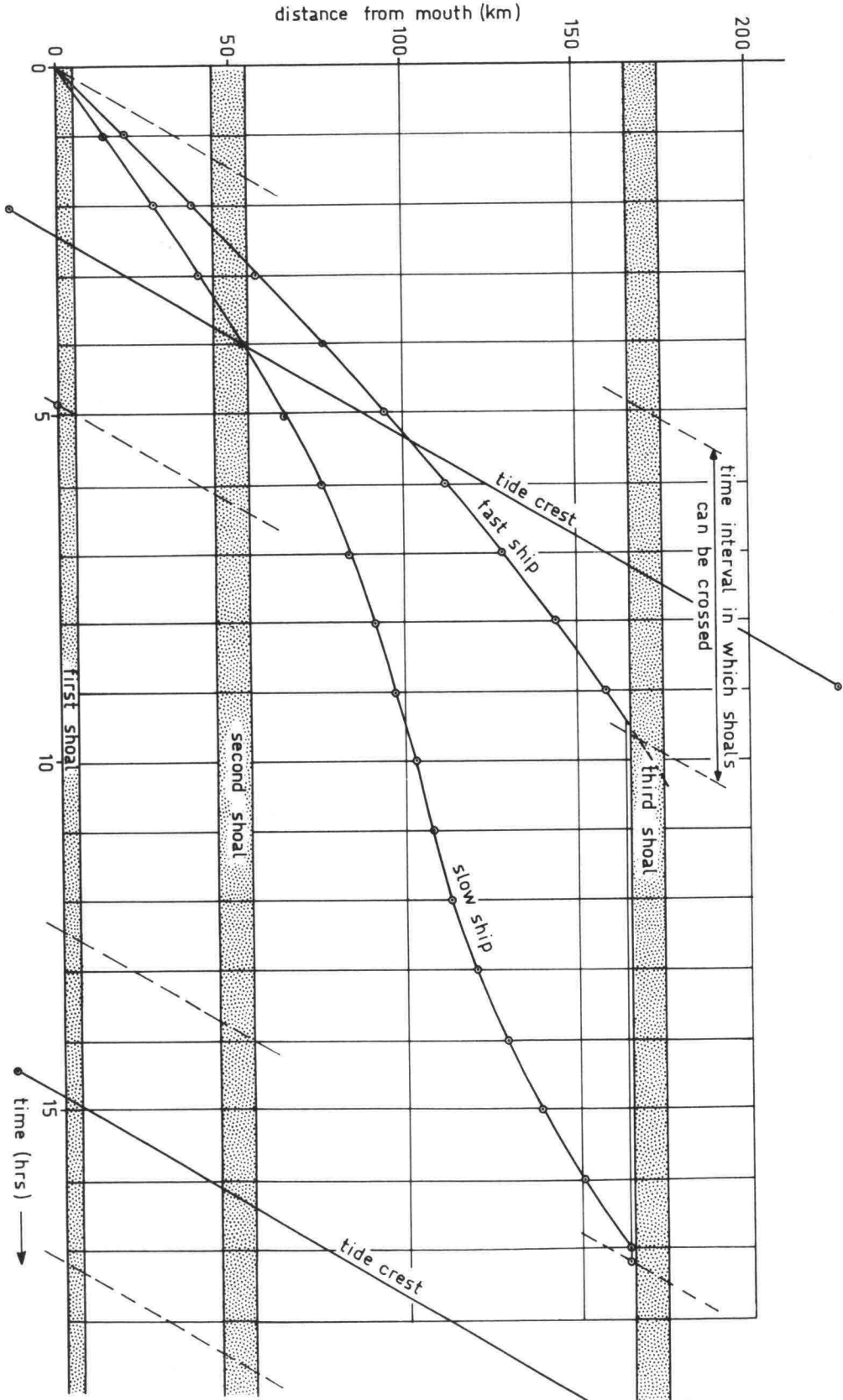


Figure 20.8 DISTANCE - TIME CURVES FOR TIDE AND SHIPS

Several interesting conclusions can be drawn from figure 20.8:

- a. Both ships must wait for the second tide to cross the third shoal. The extra speed of the fast ship makes no difference to the time needed to navigate the first 170 km of the estuary.
- b. The slow ship could avoid stopping at all by delaying her departure a short time. This would (approximately) move the curve for this ship a bit to the right in figure 20.8. The second shoal would still be cleared on the first tide and the ship would arrive late enough at the third shoal to navigate it easily as well.
- c. Dredging away the third shoal would be nearly as effective as dredging out both the first and second shoals for improving the navigation.
- d. Dredging only the outer bar would allow the fast ship to cross both the second and third shoals on the first tide.
- e. Dredging of the second bar would not change the pilot strategy for either ship.

The choice of which shoals and bars to dredge and how deep to make the channel through them is a problem lending itself well to economic optimization techniques as were outlined in chapter 13. The problem of determining the optimum depth for a channel is taken up in detail in chapter 5 of volume II.

#### 20.7 Other Tidal Effects

When the fresh water of a river meets salt sea water, the density differences caused by variations in salinity cause additional currents. Also, the salinity variations can affect the physical chemistry of fine sediments. All of these phenomena related to salinity are discussed, together, in chapters 22 and 23.

### 21.1 Introduction

One of the most important bits of data needed for surveying work in a tidal river is a datum elevation. Measurements of tides, channel depths and terrain topography can all be related to this datum.

Such a datum is easily determined from a coastal tidal record from which a mean sea level datum can be determined. Of course, this datum can be transferred inland along a river by conventional differential leveling techniques, but such work can be tedious, especially in rather inaccessible tropical areas where, it seems, an accurate datum is most often lacking.

An alternative method for transferring a datum level inland along a river is described in the next sections of this chapter. It uses the river, itself, as a level.

An important assumption in this whole chapter is that the fresh water flow in the river may be neglected.

### 21.2 Precise Problem Statement

It is a simple matter to determine a mean sea level (M.S.L.) datum at the river mouth (coast) from a tide record. We can also easily measure water level changes using a tide gauge some distance upstream from the river mouth (A in figure 21.1). Our problem is one of determining the datum level for this second tide gauge located at B in that figure. The time scales of these two records agree.

This problem really reduces to determining the time at which the river reach A-B has no surface slope. Then, the absolute levels of the two tide records would be identical.

The horizontal tide at C, midway between A and B is also needed for this problem solution. All of this data is shown in table 21.1 and figure 21.2 for a hypothetical reach of river.

### 21.3 A Simple Method of Solution

The tidal motion in the river reach is governed by:

$$V \frac{\partial V}{\partial x} + \frac{\partial V}{\partial t} = -g \frac{\partial z}{\partial x} - \frac{g |V| V}{C^2 h} \quad (21.01)$$

where:

C is the chézy friction coefficient,

g is the acceleration of gravity,

h is the depth,

t is time,

V is the flow velocity,

x is the coordinate measured along the river, and

z is the absolute water surface elevation.

This equation is the same as equation 20.02 in the previous chapter.

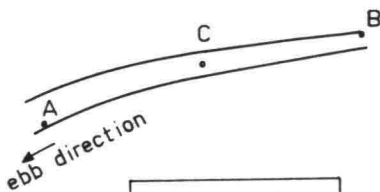


Figure 21.1  
RIVER PLAN

TABLE 21.1 Tide and Current Data

Time (hrs)	Tide level at A (m)	Relative	
		Tide level at B (m)	Current at C (m/s)
0	+0.15	+0.99	-0.10
1	-0.35	+0.69	-0.35
2	-0.75	+0.22	-0.52
3	-1.00	-0.06	-0.60
4	-1.00	-0.21	-0.57
5	-0.75	-0.13	-0.45
6	-0.20	+0.15	-0.24
7	+0.30	+0.49	+0.10
8	+0.72	+0.91	+0.38
9	+0.95	+1.14	+0.50
10	+0.98	+1.32	+0.50
11	+0.80	+1.31	+0.37
12	+0.37	+1.11	+0.07
13	-0.18	+0.77	-0.25
14	-0.68	+0.39	-0.44

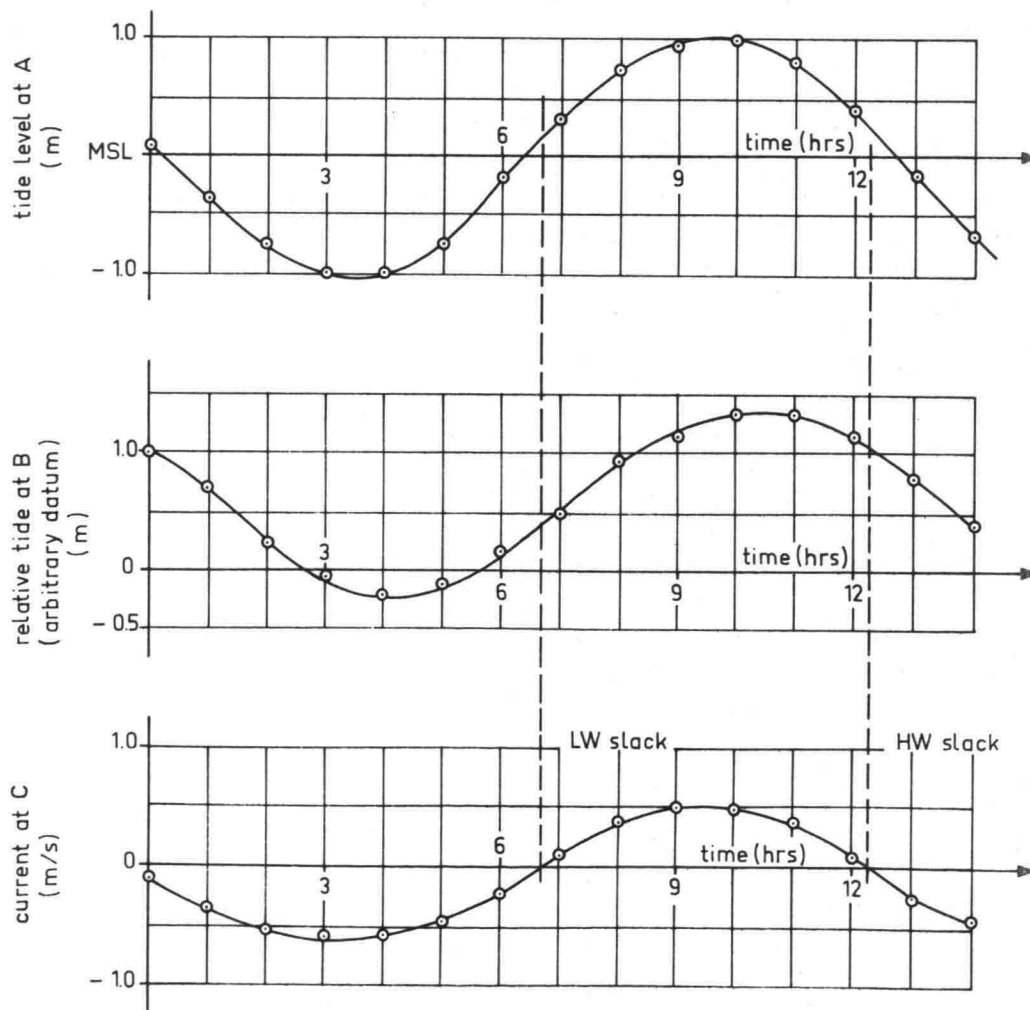


Figure 21.2 TIDE AND CURRENT DATA

If the inertia terms on the left in equation 21.01 could be neglected, then the water surface slope would be zero at the time of slack water.

Unfortunately, this is too simple. Since inertia is important, the water will continue flowing until an adverse surface slope has been generated. This means that the water surface slope will be zero some time,  $\Delta t$ , before slack water. Making a further essential assumption that the inertia influence at high tide is the same as at low tide leads to a conclusion that:

$$\Delta t_f = \Delta t_e \tag{21.02}$$

In other words, at some time,  $\Delta t_f$  before the flood slack and  $\Delta t_e$  before the ebb slack the absolute water levels of the two tide curves must be the same (They must cross when superimposed).

The assumption stated by equation 21.02 is valid if there is no fresh water flow in the river. A relatively large runoff flow can upset this assumption very much. Probably, in such a case, the improved method outlined in the following section will yield somewhat better results. Even so, such a flow can disturb the results appreciably.

The problem is solved graphically by moving the curve of the tide at B vertically over the tide curve at A. Moving curve B vertically over curve A will increase one value of  $\Delta t$  while decreasing the other. When the position is found yielding equal values of  $\Delta t$ , the water levels at A and B are equal and the arbitrary vertical scale at B can be related to the scale at A. The two tide curves, in their proper relative positions, are shown in figure 21.3.

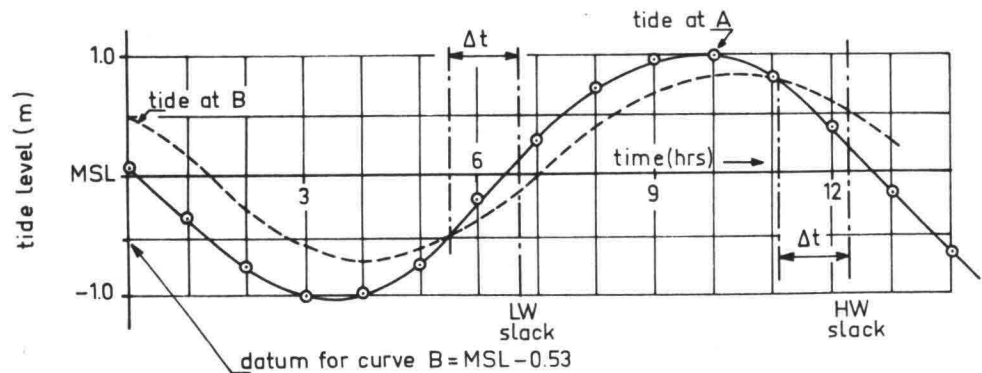


Figure 21.3 ADJUSTED TIDE CURVES.

In this figure the tide curve at A is shown with the solid line. The superimposed tide curve for point B is drawn as a dashed line and times of slack water are the same as in figure 21.2. The actual values of  $\Delta t$  found are not important. What is important is that the zero of the arbitrary scale used for the tide record at B corresponds to - 0.53 m with respect to M.S.L. Thus, the tide record at B can be related to M.S.L. by subtracting 0.53 m from the given values tabulated in table 21.1.

#### 21.4 A Better Solution

An essential assumption in the solution just presented was that the two time intervals  $\Delta t_f$  and  $\Delta t_e$  were equal (eqn. 21.02). This assumption is often invalid, especially when the current curve at point C in figure 21.1 is asymmetrical.

The theory is based, again, upon equation 21.01 which is repeated here for convenience:

$$V \frac{\partial V}{\partial X} + \frac{\partial V}{\partial t} = -g \frac{\partial z}{\partial X} - \frac{g}{C^2 h} |V| \quad (21.01)$$

For tidal problems:

$$V \frac{\partial V}{\partial X} \ll \frac{\partial V}{\partial t} \quad (21.03)$$

This is especially true when the velocity is low near slack water. Also, at the time of interest:

$$\frac{\partial z}{\partial X} = 0 \quad (21.04)$$

Thus, when we substitute 21.04 and neglect the smaller acceleration in equation 21.01, it becomes:

$$\frac{\partial V}{\partial t} = - \frac{g}{C^2 h} |V| \quad (21.05)$$

The partial derivative can now be replaced by a total derivative in 21.05:

$$\frac{dV}{dt} = - \frac{g}{C^2 h} |V| \quad (21.06)$$

The variables can be separated:

$$\frac{dV}{V|V|} = - \frac{g}{C^2 h} dt \quad (21.07)$$

Integration yields:

$$|V|t = \frac{C^2 h}{g} \quad (21.08)$$

Equation 21.08 gives the relationship between  $V$  and  $t$  near the time of slack water and when  $\frac{\partial z}{\partial X} = 0$ . Obviously, it gives a relationship for  $\frac{dV}{dt}$  as well.

Since the water depth,  $h$ , at both points A and B can be measured at the time of local slack water, we need only to estimate the Chézy friction factor in order to work with equation 21.08. After this is estimated a graph of  $|V|t = \text{constant} = \frac{C^2 h}{g}$  for a high tide slack at B and a low tide slack at A can be constructed. These curves can then be placed on the measured velocity curve at C such that the origins of the velocity axes are the same and the slopes of the two curves are equal where they are tangent to each other (osculate). The  $V t$  curve from equation 21.08 is moved horizontally along the time axis in

order to accomplish this osculation. The time on the horizontal scale of the current curve corresponding to the point of osculation is the time at which  $\frac{\partial Z}{\partial x} = 0$  and hence, the tide curves for A and B must cross.

This procedure is demonstrated in the following hypothetical example.

### 21.5 Example

This improved method will be applied to the same type of river as shown in figure 21.1. This time, however, the tidal data is given in table 21.2 and figure 21.4. Further the Chézy coefficient is  $60 \text{ m}^{1/2}/\text{s}$ .

TABLE 21.2 TIDE AND CURRENT DATA

Time (hrs)	Time level at A (m)	Relative Tide level at B (m)	Current at C (m/s)
0	+0.45	0.75	+0.21
1	0.00	+0.33	+0.07
2	-0.33	-0.04	-0.08
3	-0.67	-0.35	-0.21
4	-0.90	-0.55	-0.37
5	-0.98	-0.62	-0.50
6	-0.79	-0.47	-0.60
7	-0.30	-0.15	-0.62
8	+0.40	+0.35	-0.20
9	+0.83	+0.75	+0.40
10	+1.00	+0.98	+0.50
11	+0.87	+1.05	+0.42
12	+0.60	+0.87	+0.32
13	+0.25	+0.55	+0.14
14	-0.15	+0.15	-0.05

The depth,  $h$ , at B during the high tide slack is 8 m and the depth at A during low tide slack is 7 m. Thus, for point A:

$$\frac{c^2 h}{g} = \frac{(60)^2 (7)}{9.81} = 2568 \text{ m} \quad (21.09)$$

and for B:

$$\frac{c^2 h}{g} = \frac{(60)^2 (8)}{9.81} = 2935 \text{ m} \quad (21.10)$$

Curves of equation 21.08 using the constants evaluated in the two above equations are shown in figure 21.5.

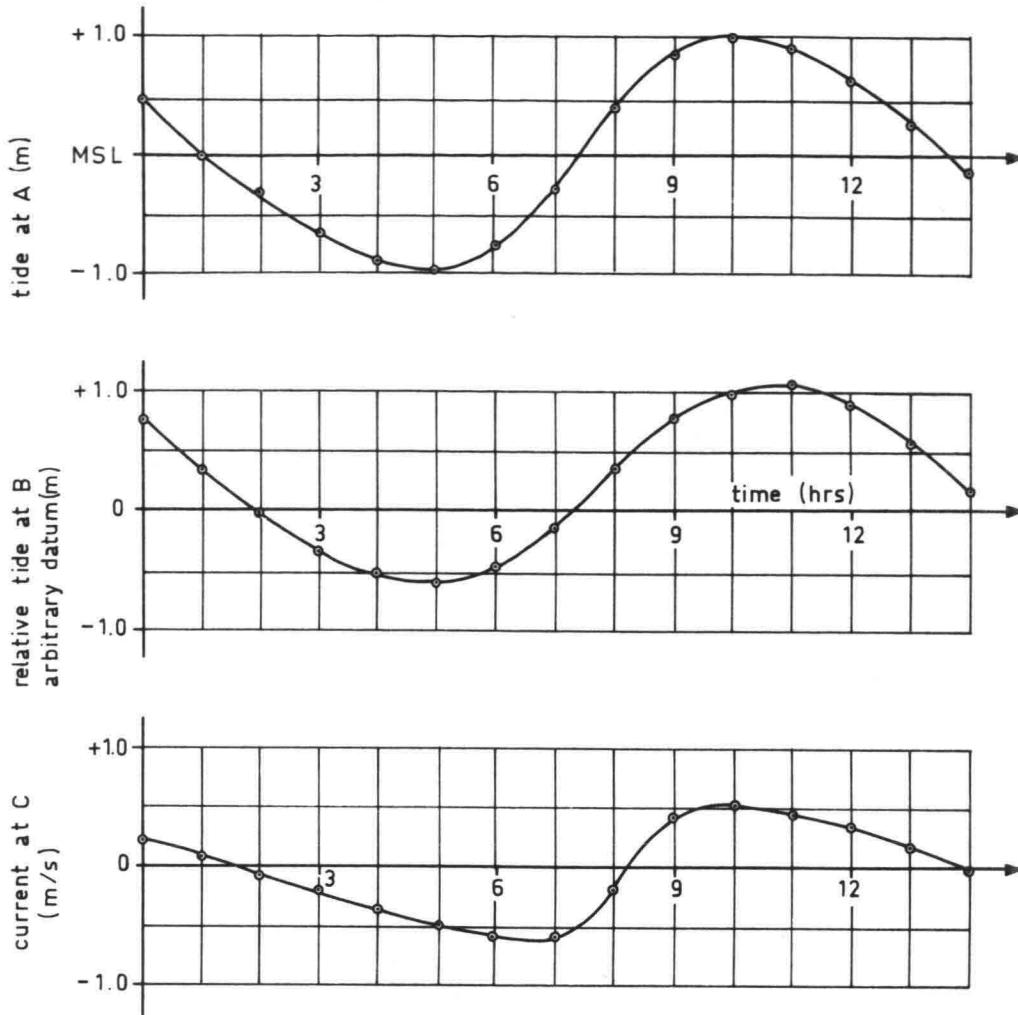


Figure 21.4 TIDE AND CURRENT DATA

Each of the curves in figure 21.5 is then placed individually on the current curve in figure 21.4. The V-t curve is moved *horizontally* along the current curve time axis until the two curves are just tangent to each other at one point (osculate). This point of osculation is projected upward to the tide curve at A. The same procedure with the second V-t curve yields a second point on the tide curve at A.

If all of the theory and assumptions were exactly correct, then the tide curve at B could be superimposed on the curve at A such that the two curves intersected at the two points just determined. Generally, this will not be possible; we make a final adjustment by moving the tide curve at B *vertically* such that the time intervals between the actual and theoretical crossing points are equal.

Figure 21.6 shows the current curve with the superimposed V-t curves. The osculating points are projected on to the properly superimposed tide curves. The two equal time intervals are also shown. The datum for curve B turns out to be 0.21 m below M.S.L.

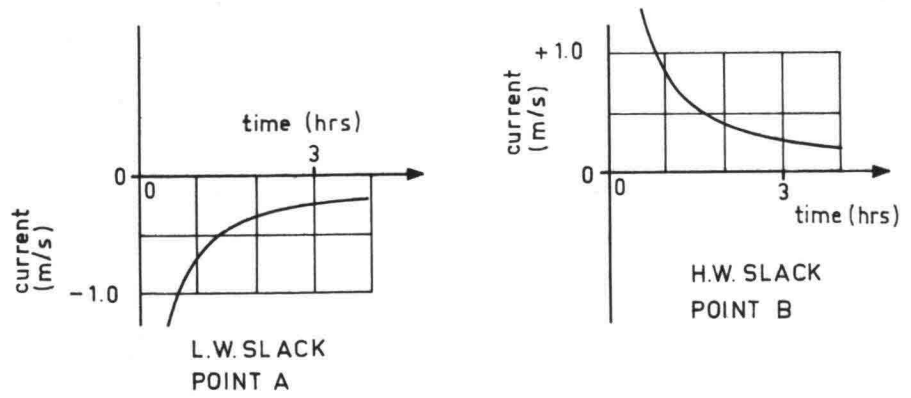


Figure 21.5 VELOCITY TIME CURVES

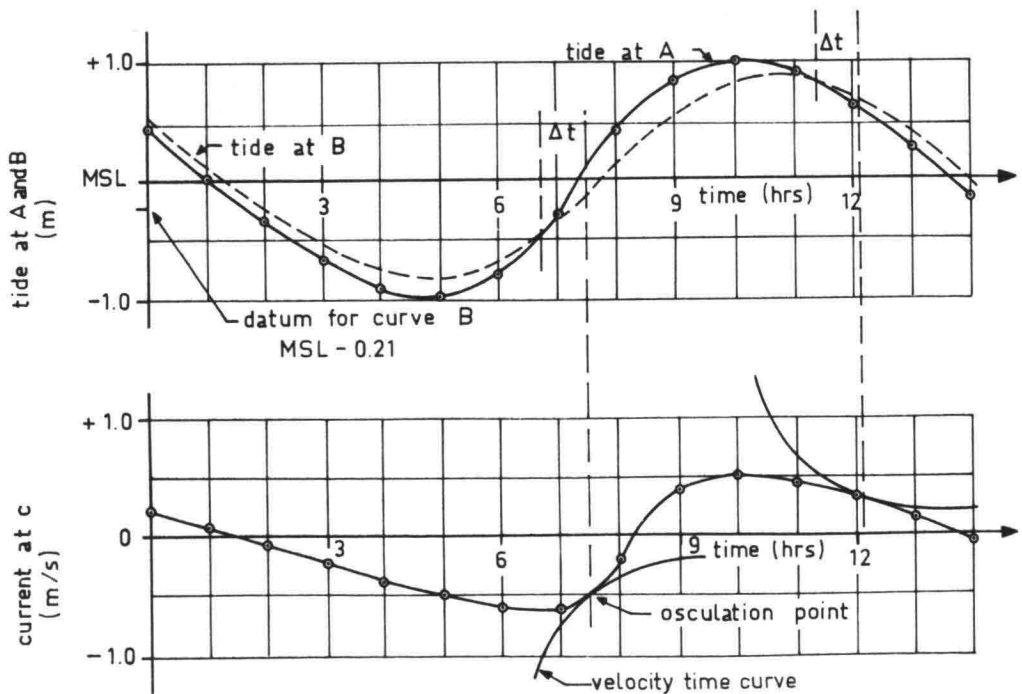


Figure 21.6 GRAPHICAL SOLUTION

### 21.6 A Reexamination

It must be remembered that even at its best, the methods outlined in this chapter give only approximate results. Even so, these results are usually of sufficient quality for at least preliminary surveys.

The distance along the river between points A and B in figure 21.1 can vary between a few kilometers and more than 100 kilometers. It is important, however, that the current measurement station, C, be located midway between A and B.

As the depth becomes shallower, the importance of the friction term in equation 21.01 increases relative to that of the inertia terms. When the river is shallow enough, in fact, the inertia influences can be neglected and the water surface will be horizontal exactly at the moment of slack water. Thus, the vertical and horizontal tide curves will be  $\frac{1}{4}$  period out of phase.

Effects of density differences in estuaries are discussed next in the following chapter.

22. DENSITY CURRENTS IN RIVERS

E.W. Bijker  
 L.E. van Loo  
 J. de Nekker

22.1 Introduction

The previous two chapters have considered tidal influences on rivers without regard to the fact that the river water is relatively pure while the ocean water is essentially salty. The effects of these salinity differences between ocean and river water form the major subject of this chapter. Chapter 23 will consider the additional influences on harbors located along rivers.

The approach used in these chapters will be purely practical. Derivations of many of the equations used can be found in the literature or other courses on theory of density currents.

22.2 Salinity Variations with Tide

Salt water enters an estuary during a rising tide unless there is more than enough fresh water flow in the river to completely fill the entire tidal prism during the rising tide phase. Few rivers have sufficient flow over the entire year to prevent the intrusion of salt water at least occasionally. Indeed, the opposite is more often true, there is seldom sufficient flow to prevent the intrusion of salt water.

The salinity at some point in a river can be expected to vary according to the tide. Also, since the salt water comes from the sea, the maximum salinity should be expected at about the time of the high tide slack. This is illustrated in table 22.1 and figure 22.1 for Rotterdam. The current data is the same as that listed in table 20.1. Again, flood currents are considered positive.

TABLE 22.1 Tidal Data for Rotterdam

Time (hrs)	Current (m/s)	River Salinity ( <sup>0</sup> /oo)
0	-0.15	2.48
1	+0.08	2.47
2	+0.60	2.83
3	+0.75	3.64
4	+0.44	5.08
5	+0.07	7.25
6	-0.44	8.06
7	-0.73	7.16
8	-1.03	6.08
9	-1.05	4.90
10	-0.85	3.64
11	-0.52	2.65
12	-0.30	2.48

Note: The symbol <sup>0</sup>/oo denotes parts per thousand.

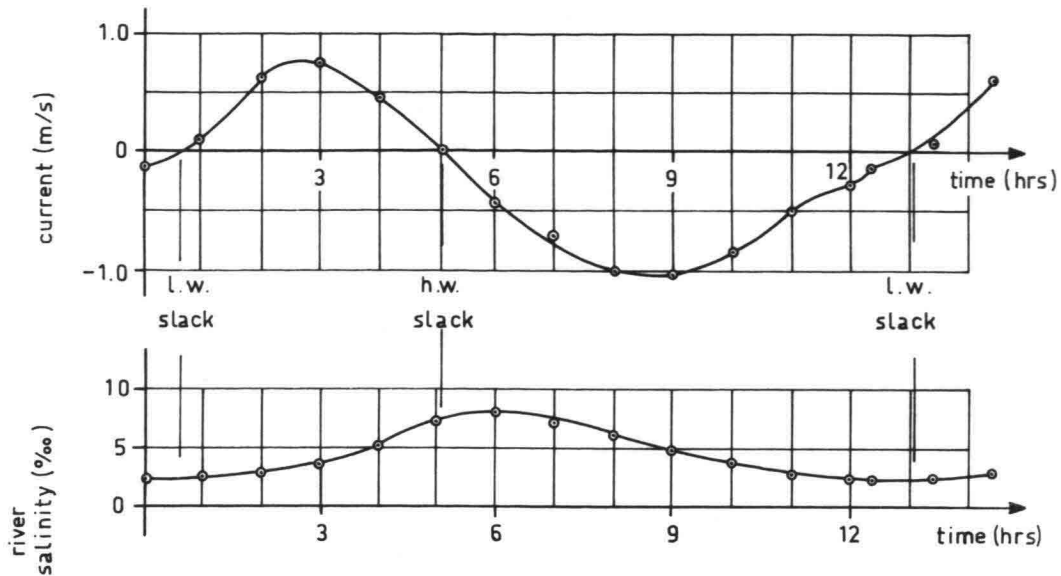


Figure 22.1 CURRENT AND SALINITY AT ROTTERDAM

In this example, the salinity maximum is reached shortly after the high water slack. The explanation for this is given in section 6 of this chapter.

Recalling from chapter 3 that sea water has a salinity of about 35 ‰, we see that pure sea water never really reaches Rotterdam. Mixing has already dispersed the incoming sea water through the fresh river water forming a brackish mixture. If we were to measure salinities at a point nearer to the sea, then we could expect to find higher maximum salinity values. Further inland, the maximum salinity becomes still lower.

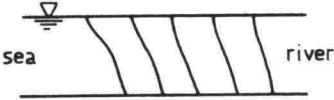
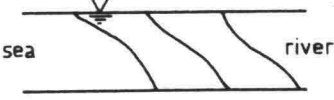
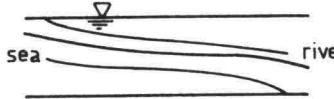
The degree of mixing in an estuary can be approximately related to the ratio between the volume of the tidal prism and the river flow. In table 22.2, the mixing parameter,  $M$ , is:

$$M = \frac{Q_r T'}{P} \quad (22.01)$$

where:  $M$  is the mixing parameter,  
 $P$  is the volume of the tidal prism,  
 $Q_r$  is the fresh water river flow, and  
 $T'$  is the tide period, here in seconds.

In each of the sketches of river profiles, the sea is assumed to be to the left, haloclines (lines of constant salinity) are shown.

TABLE 22.2 River Mixing Criteria

<u>M</u>	<u>description</u>	<u>sketch</u>
0	Mixed Estuary	
0.1	Partially Mixed Estuary	
1.0	Stratified Estuary	

Note: Sketches are not to scale.

In each sketch, salinity increases toward the left.

A more fundamental approach to the problem used by Ippen and Harleman (1961) investigates the mixing process through use of a dimensionless stratification number. This is defined as:

$$\frac{\text{rate of energy dissipation}}{\text{rate of potential energy gain}}$$

where this is done for a unit mass of fluid. The energy dissipation in the numerator results from the damping of the tidal wave in the estuary; the denominator reflects the potential energy gain as water increases in density (salinity) moving downstream.

Harleman and Abraham (1966) related the stratification number uniquely to a dimensionless estuary number, defined by

$$E = \frac{P F^2}{Q_r T'} = \frac{F^2}{M} \quad (22.02)$$

where:

F is the Froude number based upon the maximum flood current velocity at the estuary mouth.

The estuary number has the advantage over the stratification number that its parameters can be rather easily evaluated. In contrast to the mixing parameter, estuary mixing increases with increasing estuary number values. Well mixed estuaries have estuary numbers greater than about 0.15.

Another independent problem related to estuaries is the determination of the salinity distribution within the estuary. Harleman and Abraham (1966) attempted this determination using a one-dimensional theoretical model for the salinity distribution in an estuary. In their model, the x axis extends positively upstream from the estuary entrance

along the channel axis. In keeping with a one-dimensional model, the salinity is assumed to vary only as a function of time and position along this channel axis. Further, they assume that the salinity distribution is determined by an equilibrium between inward diffusion and outward convection with the fresh water flow.

Since the extreme situations of salinity distribution (maximum and minimum intrusion) occur at moments of slack water (high water slack and low water slack, respectively, we can examine these situations using a simplified ordinary differential equation:

$$V_r S_s = D \frac{d S_s}{dx} \quad (22.03)$$

where:

- $S_s$  is the salinity at the moment of slack water,
- $V_r$  is the fresh water velocity (which is negative),
- $x$  is the coordinate along the channel, positive upriver from the mouth, and
- $D$  is the apparent dispersion coefficient which includes all mixing effects.

To integrate this further, an equation for  $D$  as a function of  $x$  is needed. The following function was assumed:

$$D = \frac{D_0 B}{x + B} \quad (22.06) *$$

where:

- $B$  is the distance outside the estuary at which the salinity reaches that of the ocean, and
- $D_0$  is the diffusion coefficient at  $x = 0$ .

At  $x = -B$ ,  $D = \infty$ , which is not inconsistent; infinite mixing would be required to maintain a constant salinity.

Substituting 22.06 into 22.05 and integrating yields:

$$\ln S_s + \text{constant} = \frac{V_r (x + B)^2}{2 D_0 B} \quad (22.07)$$

---

\* Equations 22.04 and 22.05 have been dropped during revision.

The constant is evaluated using the definition of B:

$$S_s \Big|_{x = -B} = S_0 = \text{ocean salinity} \quad (22.08)$$

Thus, 22.07 becomes:

$$\frac{S_s}{S_0} = \exp \left[ \frac{V_r}{2 D_0 B} (x + B)^2 \right] \quad (22.09)$$

$S_s$  decreases with increasing  $x$ , since  $V_r$  is negative.

For a given estuary, the two unknowns in 22.09,  $D_0$  and  $B$ , can be evaluated if values of  $S_s$  are known - from measurements - at two different locations. It is sometimes even possible to reduce 22.09 further by including the dependence of  $D_0$  and  $B$  on  $V_r$ . This has been done, for example, for the Chao Phya Estuary in Thailand. The resulting equation for the low water slack is:

$$S_s = S_0 \exp \left[ - (18)(10^{-6})Q_r x^2 - 0.045 Q_r^{1/2} \right] \quad (22.10)$$

Equation 22.10 is *not* dimensionless.  $Q_r$  is in units of  $\text{m}^3/\text{s}$  and is positive,  $x$  is in km.

### 22.3 Density - Salinity Relationship

Salinity variations cause variations in water density, just as do temperature variations. The relationship between water density and temperature and salinity is given in chapter 3. The influence of salinity on density is greater than that of temperature, at least over the range of values normally encountered.

Density differences within bodies of water will be the independent variable for the rest of our discussion. These differences may result from either temperature or salinity variations. While the cause of the density differences can be of importance from a thermodynamic or pollution point of view, it is unimportant for the mechanics of the flow. Therefore, little further consideration will be given to the cause of the density variations, except in certain specific instances.

### 22.4 Statics of Stratified Water Masses

Two limiting cases of static equilibrium between bodies of water having different densities can be considered, depending upon the orientation of the separating surface.

The simplest case has a horizontal interface between the two layers. If the upper layer is less dense than the lower layer this stratification will be in equilibrium. In fact, such an interface can remain stable even though both layers of water are in motion. This stratification, caused either by salinity or temperature differences is found in the oceans and in all but the shallowest lakes.

The second case has a vertical interface, and is unstable. Such interfaces do exist, however; across the door of a lock, for example. Figure 22.2 shows the pressure distribution on such a door. If the resultant horizontal force on the door is zero, then:

$$\frac{1}{2} \rho_1 g h_1^2 = \frac{1}{2} \rho_2 g h_2^2 \quad (22.11)$$

where:

$g$  is the acceleration of gravity,

$h$  is the depth,

$\rho$  is the mass density of water, and

the subscripts, 1, 2, refer to the two water masses.

When  $\rho_2 > \rho_1$ , then 22.11 yields:

$$\frac{h_1}{h_2} = \sqrt{\frac{\rho_2}{\rho_1}} \quad (22.12)$$

while the resultant horizontal force is zero, figure 22.2 shows clearly that the resultant moment on the door is not zero.

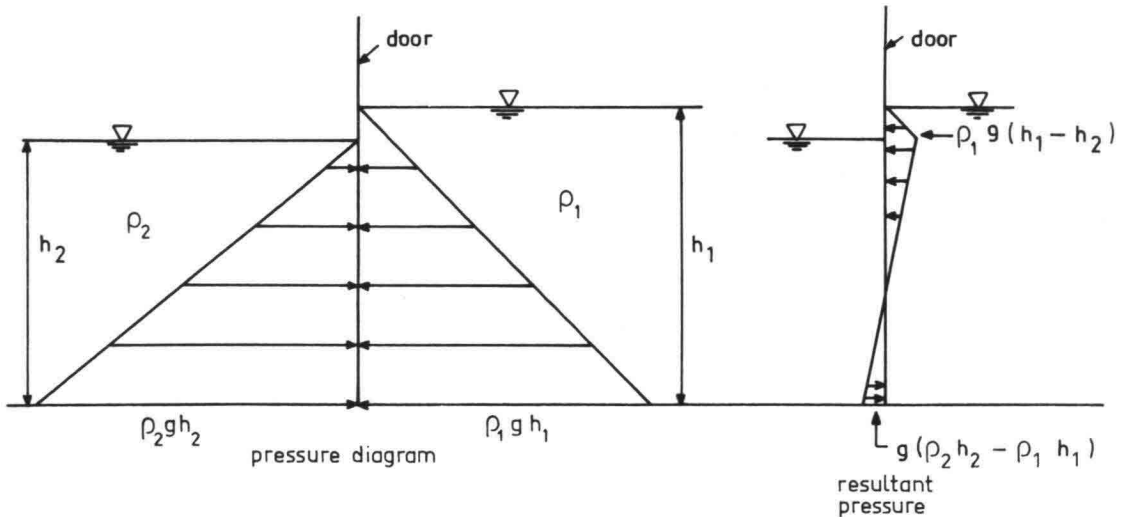


Figure 22.2 PRESSURES ON VERTICAL INTERFACE

This form of density stratification also represents an idealization of a phenomenon in nature when the salinity in a river at the mouth of a harbor or tributary suddenly changes at some time during a tide cycle. This phenomenon, its theory, and consequences will be the subject of chapter 23.

### 22.5 Internal Waves

When a horizontal stratification surface exists within a body of water (case one of the previous section), then waves can be generated at this interface, just as on the upper surface. Indeed, the upper surface of a body of water is also an interface between two

fluids—water and air. However, for internal waves on an interface between water layers, the density of the upper fluid is nearly the same as the density of the lower fluid. The resulting low density difference will have a strong influence on the phenomena involved, especially when these are compared to wind waves.

Internal waves can be caused by a disturbance such as a ship, earthquake or underwater landslide. They can also result from shear forces along an interface between two layers in relative motion.

The celerity of a wave on an interface is given by:

$$c = \sqrt{\frac{(\rho_2 - \rho_1)g \theta_1 \theta_2}{\rho_2 \theta_1 + \rho_1 \theta_2}} \quad (22.13)$$

where:

$c$  is the wave speed,

$\theta$  is the layer thickness, and

subscripts 1, 2, refer to the two layers.

See figure 22.3, in which the arrows show the direction of water movement. Equation 22.13 reduces to equation 5.05b when  $\rho_1 = 0$ .

Since  $\rho_2$  is nearly equal to  $\rho_1$  in equation 22.13, it can be approximated by:

$$c \approx \sqrt{\frac{(\rho_2 - \rho_1)g \theta_1 \theta_2}{\rho_1 h}} \quad (22.14)$$

$$c \approx \sqrt{\frac{\delta g \theta_1 \theta_2}{h}} \quad (22.15)$$

in which:

$\delta = \frac{\rho_2 - \rho_1}{\rho_1}$  is the relative density of the water masses,

and

$h$  is the total depth =  $\theta_1 + \theta_2$ .

These waves can be very high, since the gravitational influence on them is small. They are accompanied by much smaller negative waves on the water surface, as shown in figure 22.3. Indeed, as a first approximation, the ratio of surface wave height to internal wave height is equal to  $\delta$ .

These internal waves can absorb a considerable energy from a ship causing the so-called "dead water". This is explained via an example.

A ship of 4 m draft sails into a stratified harbor having a surface layer 3 m thick of relatively fresh water (salinity,  $S$ , = 5 ‰ and temperature,  $t$ , = 2°C) above a deeper layer 7 m thick with  $S = 36$  ‰ and  $T = 4$  °C\*. What is the maximum speed that this ship can attain?

\* This stratification is quite common in northern harbors during the spring snow-melt runoff.

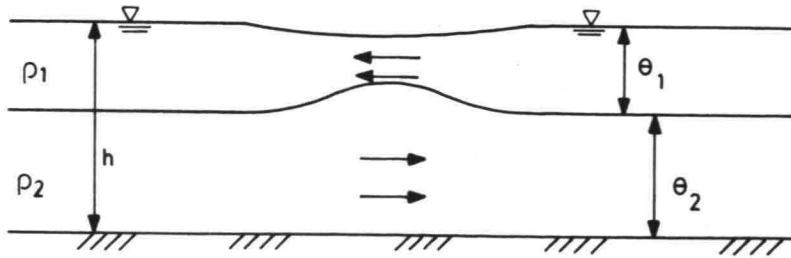


Figure 22.3 INTERNAL WAVE

From table 3.3, chapter 3,

$$\sigma_{t1} = 4.00 : \rho_1 = 1004.00 \frac{\text{kg}}{\text{m}^3} \quad (22.16)$$

$$\sigma_{t2} = 28.70 : \rho_2 = 1028.70 \frac{\text{kg}}{\text{m}^3}$$

Further,  $\theta_1 = 3$  m,  $\theta_2 = 7$  m. Using (22.13):

$$c = \sqrt{\frac{(1028.7 - 1004)(9.81)(3)(7)}{(1004)(7) + (1028.7)(3)}} \quad (22.17)$$

$$= 0.709 \text{ m/s} = 1.38 \text{ kt.}$$

The only way the ship can move faster than this wave is to cut through it or climb over it; neither is very likely!

This dead water phenomenon also played an important role in a naval battle near Copenhagen some centuries ago. In this area the rather fresh Baltic Sea water flows over more dense water from the Skagerrak.

### 22.6 The "Static" Salt Wedge

A salt wedge occurs in a fresh water river which discharges into a saline sea. The sea water intrudes along the river bottom under the fresh discharge water. The length of the intruding wedge is determined by an equilibrium between the friction,  $\tau_I$ , along the interface and the horizontal pressure gradient resulting from inclination of the interface. When this equilibrium is strictly satisfied, the salt wedge will be in a stable position with the fresh water flowing seaward on the surface and spreading out in a thin surface layer at sea. The length of this wedge is of great importance as will be pointed out in more detail later in this chapter.

Schijf and Schönfeld (1953) derived an expression for the length of such a wedge in a prismatic, horizontal, rectangular channel discharging into an infinite, non-tidal sea. If no mixing occurs across the interface, then their equation is:

$$L_w = \frac{2h}{f_I} \left[ \frac{1}{5F^2} - 2 + 3F^{2/3} - \frac{6}{5}F^{4/3} \right] \quad (22.18)$$

$$\text{with: } f_I = \frac{8\tau_I}{\rho(V_1 - V_2)(V_1 + V_2)} \quad (22.19)$$

$$\text{and: } F = \frac{V_r}{\sqrt{\delta g h}} \quad (22.20)$$

in which:

$L_w$  is the length of the wedge,  
 $V_r$  is the velocity in the river upstream from the wedge,  
 $V_1$  is the velocity in the fresh water above the wedge,  
 $V_2$  is the velocity in the salt wedge, and  
 $\tau_I$  is the friction stress along the interface.

This is all shown in figure 22.4.

This expression illustrates the influence of water depth,  $h$ , the river discharge velocity,  $V_r$ , and the density differences on the salt intrusion. A reasonable value for  $f_I$  is in the order of 0.1. A nomographic solution of the above equations has been worked out by Partheniades et al. (1980).

Of course, in the idealized equilibrium state,  $V_2 = 0$ . This is why no friction stress on the bottom is shown in figure 22.4. The data used to plot this figure were:  $f_I = 0.08$ ;  $h = 10$  m;  $V_r = 0.2$  m/s; and  $\delta = 0.0246$ , giving  $L_w = 2689$  m. The figure is drawn with a distortion of 1 : 100.

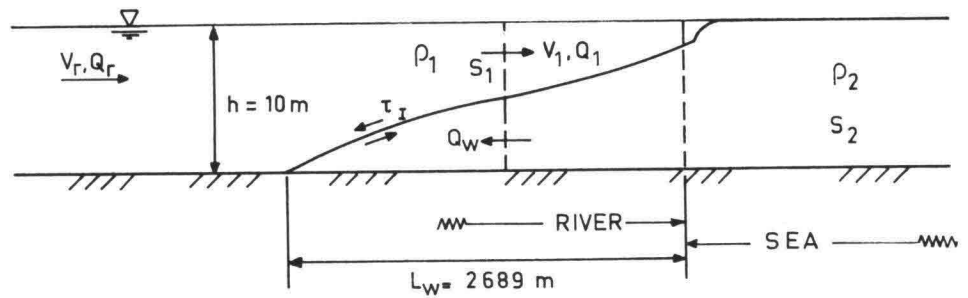


Figure 22.4 "STATIC" SALT WEDGE IN RIVER MOUTH (distortion 1:100)

The word static is enclosed in quotation marks since there is, in a real situation, more a state of dynamic equilibrium. Mixing will take place along the interface between the water masses. Salt and sea water will be transported along with the river water back to the sea. This is indicated in figure 22.4 at the vertical dashed line part way along the wedge. Since the total net flow out the river must be equal to the fresh water runoff:

$$Q_1 = Q_r + Q_w \quad (22.21)$$

in which:  $Q_w$  is the inflow flow in the wedge,  
 $Q_r$  is the fresh water river flow, and  
 $Q_1$  is the net outflow through the cross section.

Continuity of salt must also be maintained. This implies that:

$$Q_1 S_1 = Q_w S_2 \quad (22.22)$$

where  $S_1$  and  $S_2$  are the respective salinities.

If one substitutes different values of  $V_r$  into equation 22.18 (via 22.20) he will find that  $L_w$  decreases as  $V_r$  increases; indeed,  $F = 1$  yields  $L_w = 0$ . Remembering that increasing  $V_r$  implies also an increasing  $Q_r$  we seem to discover a contradiction with the rules of thumb presented in equation 22.01 and table 22.2. According to that table, increasing  $Q_r$  should lead to a more stratified estuary, and hence, a longer instead of a shorter salt tongue (wedge). This dilemma is explained by realizing that all tidal influences have been neglected in formulating equation 22.18; thus, this comparison is invalid.

In a real estuary the salt wedge intrusion problem is much more complex. The river flow,  $Q_r$ , varies, tidal influences are present, and the estuary is certainly not prismatic.

Generally, the tidal influence is most important - it leads to an incessant oscillatory motion of the entire two-layer system over an uneven bottom. This motion, of course, increases mixing across the interface. Indeed, in estuaries with strong tidal influence and little fresh water flow the stratification can be essentially destroyed, leading to a well mixed estuary. The Western Schelde is an example of such an estuary. At a given time and place there is little vertical salinity gradient. In such an estuary, the average seaward transport of salt by the river flow is an equilibrium with transport of salt into the estuary by diffusion.

The effect of this diffusion (which is always present to some extent) combined with the momentum of a possible inward flowing salt tongue can delay the time of maximum average salinity at a point on a tidal river until a bit later than the H.W. slack, as observed with the data from Rotterdam, figure 22.1.

As has already been indicated, the tides cause the salt tongue or the haloclines to move back and forth in the river as a function of the tide. The consequences of this presence and movement of the salt tongue for the river and its surroundings are discussed in the next section.

### 22.7 Siltation Problems

The most direct consequence of a salt tongue in a river is its effect on the siltation pattern of the estuary. Obviously, from figure 22.4, the current along the estuary bottom is drastically changed by the presence of the salt tongue. Upstream from the tip of the tongue, the velocity along the bottom is toward the sea, while within the wedge there is often a small velocity into the estuary. Since the bottom velocity at the tip of the tongue must be zero, it can be expected that material will be deposited there. In estuaries where there is little tidal influence and the position of the salt wedge remains relatively stable, this local sedimentation can form a pronounced shoal in the river. While the cause of this tongue has been attributed to salt, above, this phenomenon can also be found in an estuary having a density difference caused by other factors such as thermal gradients. This phenomenon might, for example, also be observed in the cooling water discharge channel from a power station, even one located on a fresh water lake.

When the suspended sediment in a river consists of clay and the density tongue is caused by salinity differences, then physical chemical processes can also strongly influence the siltation pattern in the estuary.

Suspended clay in fresh water consists of flat or needle - shaped particles having a maximum dimension less than a few micrometers. Because of their form, large surface area and the crystal structure of the clay minerals, these particles are negatively charged on the surface. Since the particles are so small, the electrostatic forces rather than the gravity forces control the behavior of the clay particles, and work to keep the particles separated and in suspension.

As the salinity of the water increases, the positive ions ( $\text{Na}^+$ ,  $\text{Mg}^{++}$ ,  $\text{Ca}^{++}$ , etc.) present tend to neutralize the electrostatic forces, thus allowing the clay particles to flocculate, and settle. A salinity of about 3 ‰ is critical in this process. The physical chemical influences are only important for salinity variations below this value.

The flocculation caused by an increase in water salinity is at least partially reversible. When, later in the tide cycle, the salinity decreases, the flocs of clay particles exposed to the fresh water can "explode" dispersing the individual particles once again in suspension. This process can provide disturbing influences on suspended sediment measurements in areas where low, variable salt concentrations can be found.

An impression of the magnitude of this influence on siltation can be gained by comparing the fall velocity\* of clay particles in fresh water to the fall velocity of flocs of particles in salt water ( $S > 5$  ‰). Allersma, Hoekstra and Bijker (1967) report that the apparent ratio between these fall velocities was more than 1 : 50.

The quality of the material forming the river bed in such an area is not the same as the usual form of compact clay. Indeed, the sediment which forms as a result of flocculation contains a large quantity of water. The volume of the sediment (solid particles plus water) can be 5 to 10 times the volume of the particles. (In soil mechanics terminology, the void ratio can be as high as 10). Obviously, such a high volume of water will keep the sediment density low - usually between 1100 and 1250  $\text{kg/m}^3$ . The material behaves as a viscous fluid with a viscosity of in the order of 100 to 5000 times that of water; this is comparable to yoghurt (except for color!).

This material, often called sling mud, is difficult to detect when making soundings. It appears as a faint reflection on an echogram. The sediment is so soft that ships can often sail through it.

The consolidation process for such a soft silt is very slow. Layers up to 2.5 m thick remain fluid for several weeks - even in a laboratory settling tube.

---

\* The fall velocity is the velocity at which sediment particles drop through still water.

This sling mud can be brought into suspension once again when the current velocity above it reaches a critical value ranging between 0.2 and 1.0 m/s.

Sling mud will be discussed again in more detail in chapter 27 about the morphology of mud coasts.

The influence of the salinity on the suspended silt concentration at Rotterdam is demonstrated in figure 22.5. Data used to plot this figure for Rotterdam is listed in tables 22.1 and 22.3.

TABLE 22.3 Suspended Load At Rotterdam

Time (hrs)	Suspended material (mg/l)
0	60
1	58
2	68
3	90
4	116
5	95
6	61
7	54
8	77
9	90
10	93
11	81
12	66

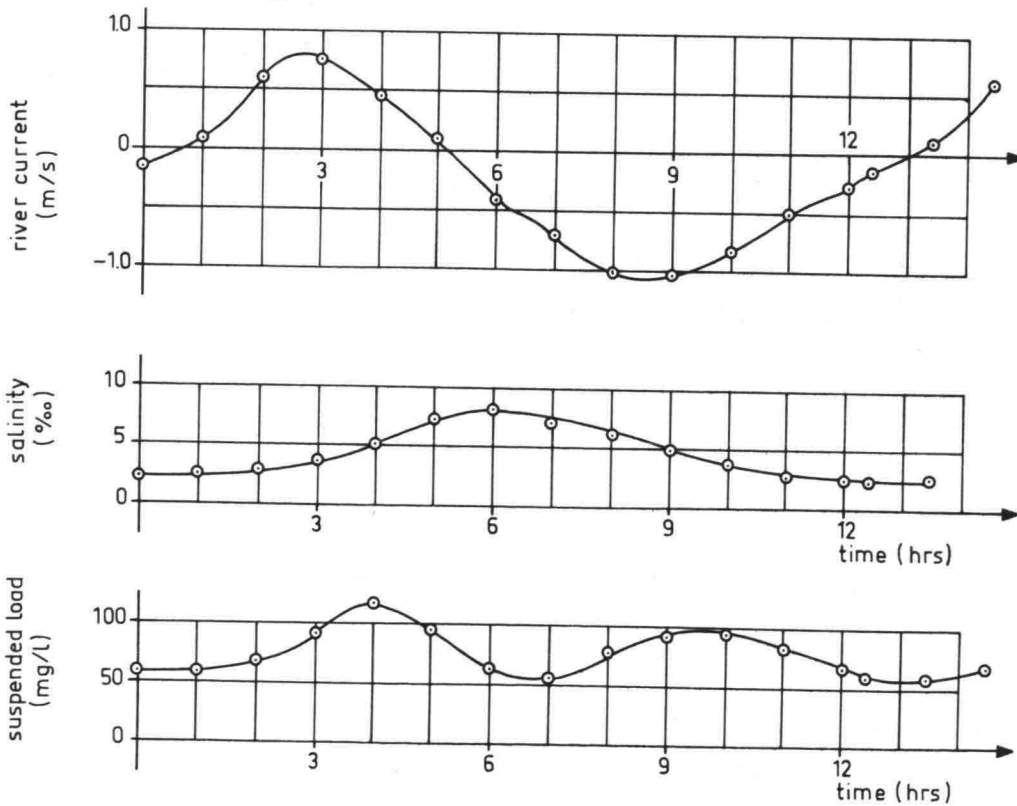


Figure 22.5 SUSPENDED LOAD AT ROTTERDAM

In the time interval between 5 and 7 hours the relatively high salinity causes the suspended sediment concentration to decrease, even though the current is becoming stronger. Between  $8\frac{1}{2}$  and 10 hours, the reverse is true; decreasing salinity increases the suspended sediment even though the velocity is becoming weaker. On the other hand, near 0.6 hours and again at 13 hours, the sediment concentration minima are caused by the low current velocity.

Even without local flocculation taking place, it is still possible to form and maintain layers of sling mud. Such layers can be found, for example, in Rotterdam Europoort even though the salinity there is always higher than 5 ‰. These layers, their formation and removal will be discussed in section 27.6.

### 22.8 Rotterdam Harbor Entrance

Extensive layers of soft mud have recently been reported in the entrance to Europoort and even in the Rotterdam Waterway. With modern echo sounding devices it is possible to estimate the density of layers of mud on the bed. Figure 22.6 shows an example of such a profile measured near the entrance to Rotterdam. At the mud surface the density of the mud is about  $1030 \text{ kg/m}^3$ . This material is so soft that ships simply steam through it. The reported depth of the channel is often taken to be the contour line with  $\rho = 1200 \text{ kg/m}^3$ .

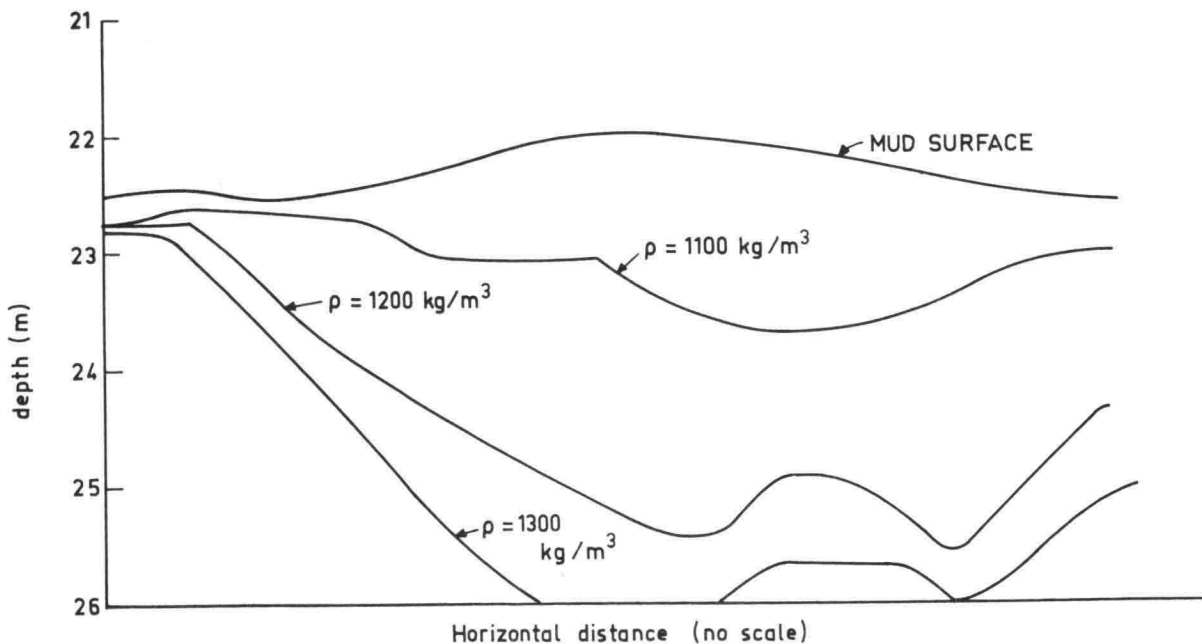


**Figure 22.6** Channel Bed Profiles

The upper portions of the mud layer behave as a viscous fluid and while it is easy to pump with a dredge its extremely low density results in poor dredge productivity measured in terms of quantity of solids

moved per hour. One means of improving this situation is to dredge a deep pit so that the silt layers can move to that pit and consolidate slowly there. Mud of higher density can then be withdrawn from the deepest part of the pit using a dredge. Now, one has only a problem of getting the mud layer to move to the pit. There are two possibilities:

If sufficient bed surface slope is available, gravity forces will cause the sling mud to flow toward and into the pit. The second approach relies on the shear stress exerted by water flowing above the bed - the tide, for example - to provide a driving force for the mud movement. A danger in this approach is that if the surface shear stress becomes too high, the boundary between mud and water becomes turbulent stirring the mud into suspension. Mud in suspension will, of course, simply pass over the nicely prepared pit.

Laboratory tests carried out on mud from the Rotterdam Waterway by den Hartog (1979) and prototype measurements both indicate that the mud in Rotterdam behaves as a viscous fluid. In such cases one can even consider dredging a catching pit at a given location and maintaining it using a permanent dredging installation.

Overconsolidation (too high a mud density) in the bottom of such a dredging pit can be disadvantageous. If the density becomes too high, so much extra dredging power is needed that the economies expected from higher production are lost - Cox (1981).

## 22.9 Pollution Problems

In addition to increasing the siltation problems in an estuary, density currents can also cause problems of environmental pollution.

The most obvious source of environmental pollution is the infiltration of salt water into the surrounding ground water along a river. The deleterious effects of water salinity on the growth patterns of plants have been well documented by agricultural specialists. The prediction of the severity of saline pollution for a given location is a topic of study for specialists in ground water hydrology.

Another, often less obvious, pollution problem can be caused by the presence of thermal density currents. Marine life such as shellfish often is unable to adapt to rapidly varying water temperatures experienced when the edge of a thermal plume drifts over it at some time in a tide cycle. Several large and elaborate model studies have been conducted in various laboratories, both in the United States and the Netherlands to determine the extent and severity of thermal plumes from steam power stations to be located along estuaries. Demonstration that the plume of discharged cooling water will not harm the surrounding marine life is often required before a construction permit will be granted.

Techniques used to combat the deleterious effects of density currents are discussed in the next section.

## 22.10 Methods to Combat Density Current Influences in Rivers

There are relatively few techniques which are economical for combatting the intrusion of a salt tongue in a river. Many more techniques are available for more restricted areas such as harbor basins and canals; these will be discussed in the following chapter.

It has been indicated via equations 22.18 through 22.20 that the length of the salt wedge can be reduced by decreasing the water-depth and by increasing the fresh water flow. In the Netherlands, the discharge of fresh water through the New Waterway has been increased as a result of the completion of the northern part of the Delta Project (Volkerak dam and locks, and the Haringvliet Sluice). In addition, the development of the Europoort harbor area has eliminated the necessity for bringing large, deep ships into the New Waterway past the Europoort entrance. In recent times, therefore, parts of the New Waterway in Rotterdam have been partially filled in order to decrease their depth and drive the salt water tongue back toward the sea to a greater extent.

Thermal density currents can be combatted by either enhancing the mixing of the two water layers or stimulating the heat transfer process between layers or to the atmosphere.

Although not too common in use, mixing can be enhanced, for example, by increasing the turbulence in the thermal discharge or artificially generating an unstable stratification. Increasing discharge velocity and construction of a pile supported jetty in front of the discharge flume of a power station have been suggested as means to increase mixing by increasing turbulence.

Naturally unstable stratifications are often artificially generated when warm, low salinity sewage is discharged near the bottom of the sea. As the lighter sewage rises through the sea water the resulting turbulence helps to disperse it.

Obviously, another solution to thermal pollution problems is to re-cool the discharge water before it is released. This may be accomplished by retention in shallow pools or by circulation through a cooling tower. Sometimes, simply a long wide discharge channel can serve the purpose. The objective in all of these solutions is to transfer the heat to the atmosphere.

Extra Notes

23. DENSITY CURRENTS IN HARBORS23.1 Tide Flow in Harbor

In this chapter the tide and density current influences on a harbor built along a tidal river will be discussed. The information presented in this section, however, will be of general use, even for harbors located along a coast far away from a river or on an estuary without fresh water runoff.

The construction of a harbor along a tidal river will obviously increase the tidal prism of the estuary. Usually, unless there is a very significant and extensive harbor development, the influence of the additional harbor area on the total tidal prism will not be enough to cause significant changes in the river itself.

We have already seen in chapter 20 (figure 20.5) how inertia effects maintain a flood current in a river even after high water. For a harbor, on the other hand, the inertia terms are much less important and the current in the harbor mouth will be slack just at the time of high and low water. This is true when no density effects are involved. Table 23.1 lists the data used to plot figure 23.1 showing this phenomenon for the 2e Petroleumhaven in Rotterdam. (The density current influences have been eliminated from the data listed in the table). Since the currents are so small, they are listed in centimeters per second.

TABLE 23.1 HARBOR TIDE AT ROTTERDAM (2e Petroleumhaven)

Time (hrs.)	Harbor Tide level (m)	River Current (m/s)	Harbor Filling Current (cm/s)
0	-0.69	-0.15	0.9
1	-0.50	+0.08	2.2
2	-0.03	0.60	3.2
3	+0.52	0.75	2.2
4	0.91	0.44	1.1
5	1.04	+0.07	0
6	0.91	-0.44	-1.5
7	0.61	-0.73	-2.1
8	+0.25	-1.03	-1.6
9	-0.15	-1.05	-1.1
10	-0.47	-0.85	-1.5
11	-0.58	-0.52	-0.8
12	-0.62	-0.30	0

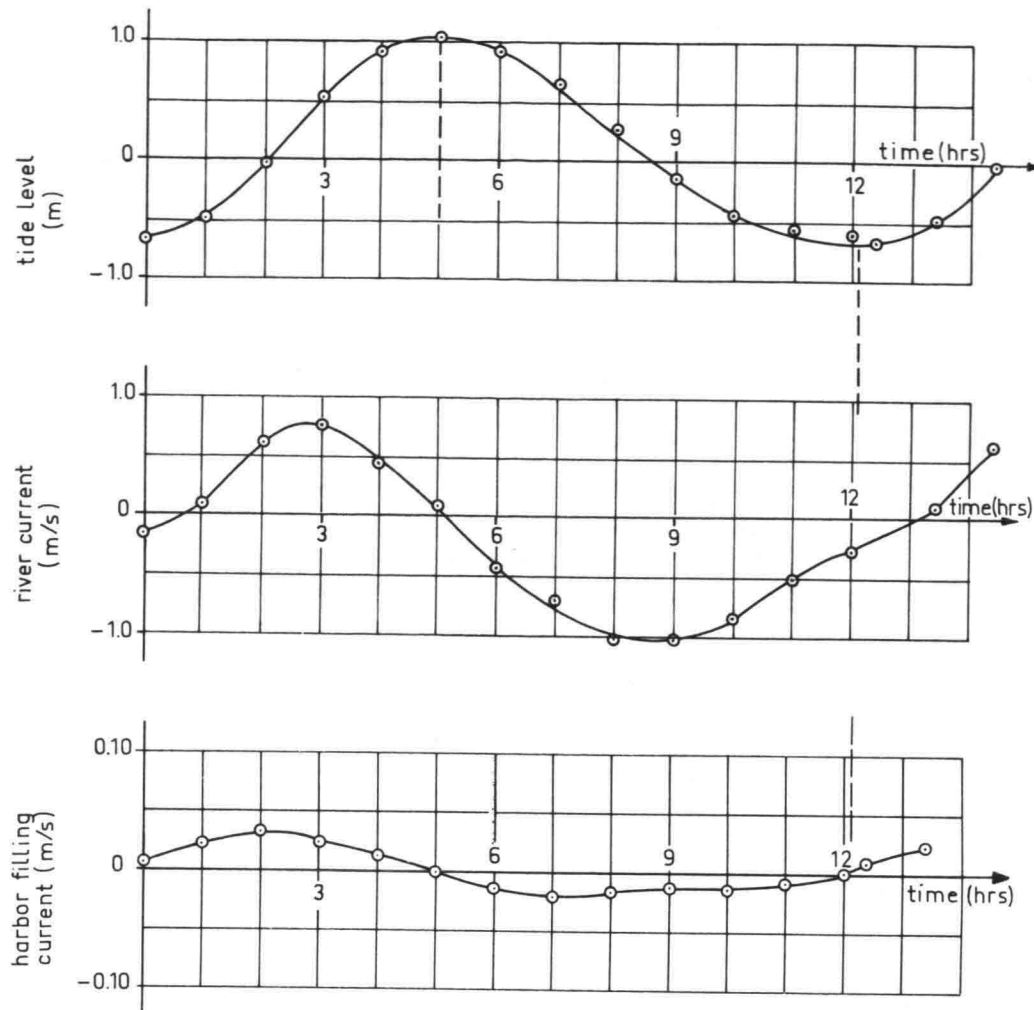


Figure 23.1 HARBOR LEVEL AND CURRENT, 2<sup>e</sup> Petroleumhaven, Rotterdam

### 23.2 Density Currents in Harbors

The density stratification at the mouth of a harbor basin just after the river salinity has changed can be schematized by a vertical interface such as was shown in figure 22.2 in the previous chapter. As was already pointed out, there, this condition is unstable and leads to a current pattern as is shown in figure 23.2. The flow of the more dense layer can be compared to the flow of water down a river valley just after a dam has burst. Such a profile of the interface is, therefore, sometimes called a dry bed curve. The toe of the dry bed curve is held back slightly by the friction along the bottom.\*

Since the volume of water in the harbor remains constant - neglecting filling or emptying - the harbor inflow must equal the outflow caused by the density difference. Since the usual assumption is that the flow in each direction occurs over half the depth, then the two flow velocities must be equal for a rectangular channel.

\* Compare to figure 22.4 in which there is no bottom friction.

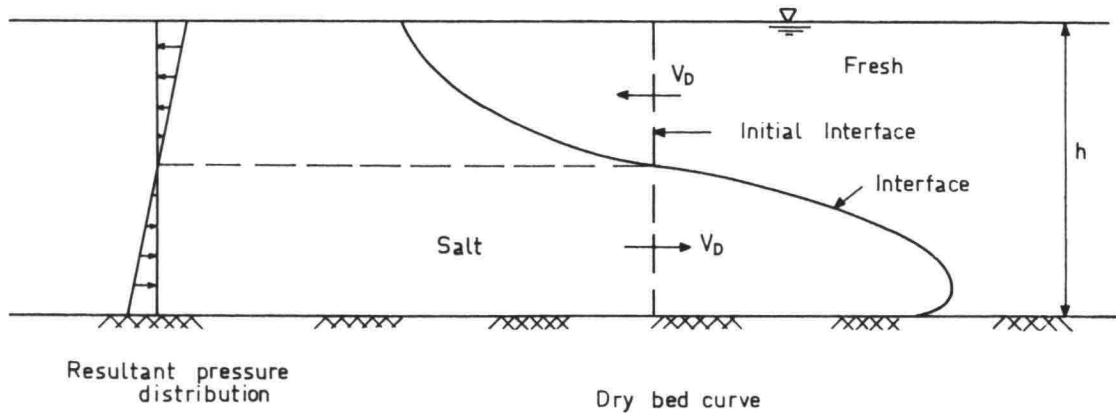


Figure 23.2 DENSITY CURRENT FORCES AND MOTION

Theoretically:

$$V_D = 0.45 \sqrt{\delta g h} \quad (23.01)$$

in which:

$\delta$  is the relative density (ch. 22),

$g$  is the acceleration of gravity,

$h$  is the water depth, and

$V_D$  is the velocity in the dry bed curve.

In practice, the coefficient, 0.45, is a bit too large; a value somewhere between 0.3 and 0.4 usually gives better results. Equation 23.01 compares favorably, but not exactly, with equation 22.13 when  $\theta_1 = \theta_2 = \frac{h}{2}$ .

Table 23.2 lists river and harbor salinities for Rotterdam as well as the measured density current velocity. The values of  $\delta$  listed are computed from the salinity data assuming that both the river and the harbor are at a uniform temperature of 16°C. The density current velocities are given for the surface current with positive indicating a flow into the harbor. By symmetry, as already explained, the flow in the lower layer must be in the opposite direction with the same speed. Some of the data from this table are plotted in figure 23.3.

We see from table 23.2 that the magnitude of the density current velocity more or less follows the value of  $\delta$ . If theory and practice always agreed, then there should be a perfect correlation between  $|V_D|$  and  $\sqrt{\delta}$  (from equation 23.01). The correlation coefficient for  $|V_D|$  against  $\sqrt{\delta}$  for the data in table 23.2 is only 0.58, however. This does not make the theory look too good, but this comparison shall be re-examined in section 23.4.

TABLE 23.2 SALINITY AND DENSITY CURRENTS AT ROTTERDAM

Time (hrs.)	River S (‰)	Harbor S (‰)	$\delta$	$V_D$ at surface (cm/s)
0	2.48	3.96	$1.149 \times 10^{-3}$	3.0
1	2.47	3.30	$5.952 \times 10^{-4}$	4.0
2	2.83	3.04	$1.619 \times 10^{-4}$	1.2
3	3.64	2.63	$7.830 \times 10^{-4}$	-5.0
4	5.08	3.01	$1.600 \times 10^{-3}$	-8.0
5	7.25	3.91	$2.567 \times 10^{-3}$	-10.7
6	8.06	5.23	$2.180 \times 10^{-3}$	-10.3
7	7.16	6.56	$4.616 \times 10^{-4}$	-1.4
8	6.08	6.69	$4.679 \times 10^{-4}$	+2.1
9	4.90	6.37	$1.128 \times 10^{-3}$	2.5
10	3.64	5.43	$1.379 \times 10^{-3}$	2.5
11	2.65	4.36	$1.325 \times 10^{-3}$	2.1
12	2.48	3.82	$1.039 \times 10^{-3}$	2.1

$\delta$  computed from salinities at  $T = 16^{\circ} \text{C}$  using table 3.3

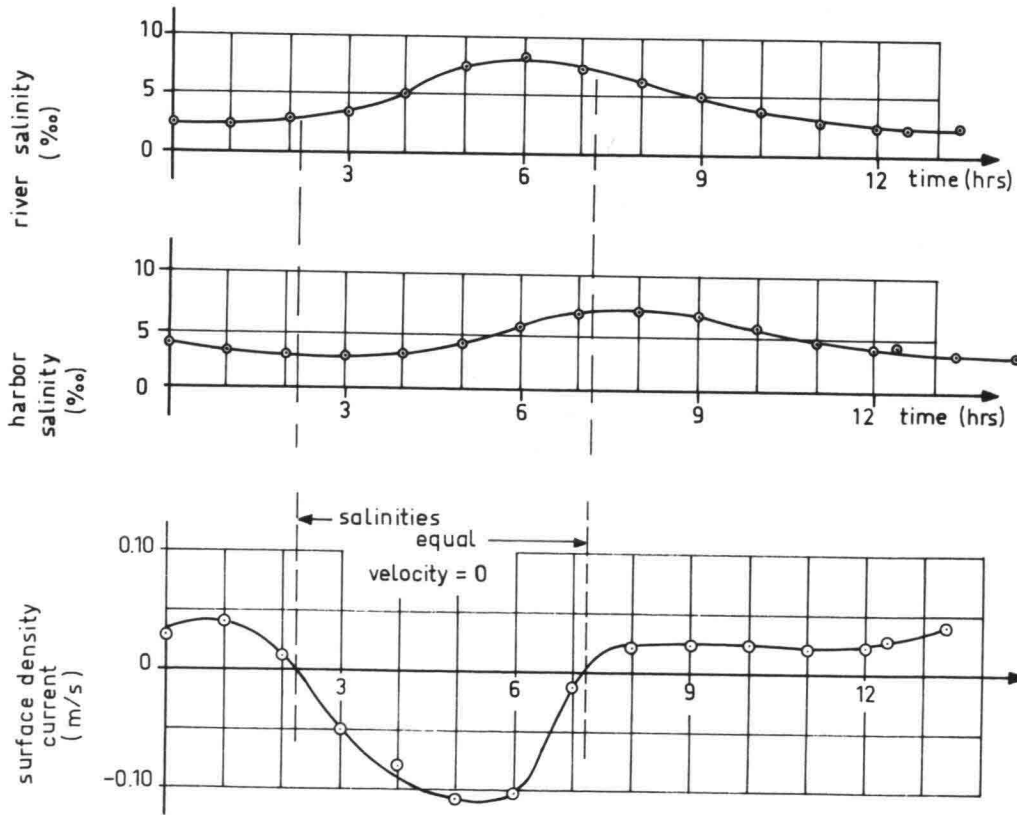


Figure 23.3 HARBOR SALINITY AND DENSITY CURRENT (2<sup>e</sup> Petroleumhaven, Rotterdam)

23.3 Superposition of Current Components

In a real harbor on a tidal river, the flow in the harbor will be a superposition of the filling flow and that caused by the density current. Figure 23.4 shows the idealized current profiles and their superposition for various times listed in tables 23.1 and 23.2. When  $|V_D| < V_f$ , the presence of a density current component does not affect the total volume of water entering the harbor. This is demonstrated in figure 23.4 by the velocity profiles for time equals 2 hours. The implication of this observation is that velocity distributions can be superimposed while the sediment transports cannot be simply added except when the sediment concentration is constant over the entire depth. This discussion comes up again in later sections of this chapter.

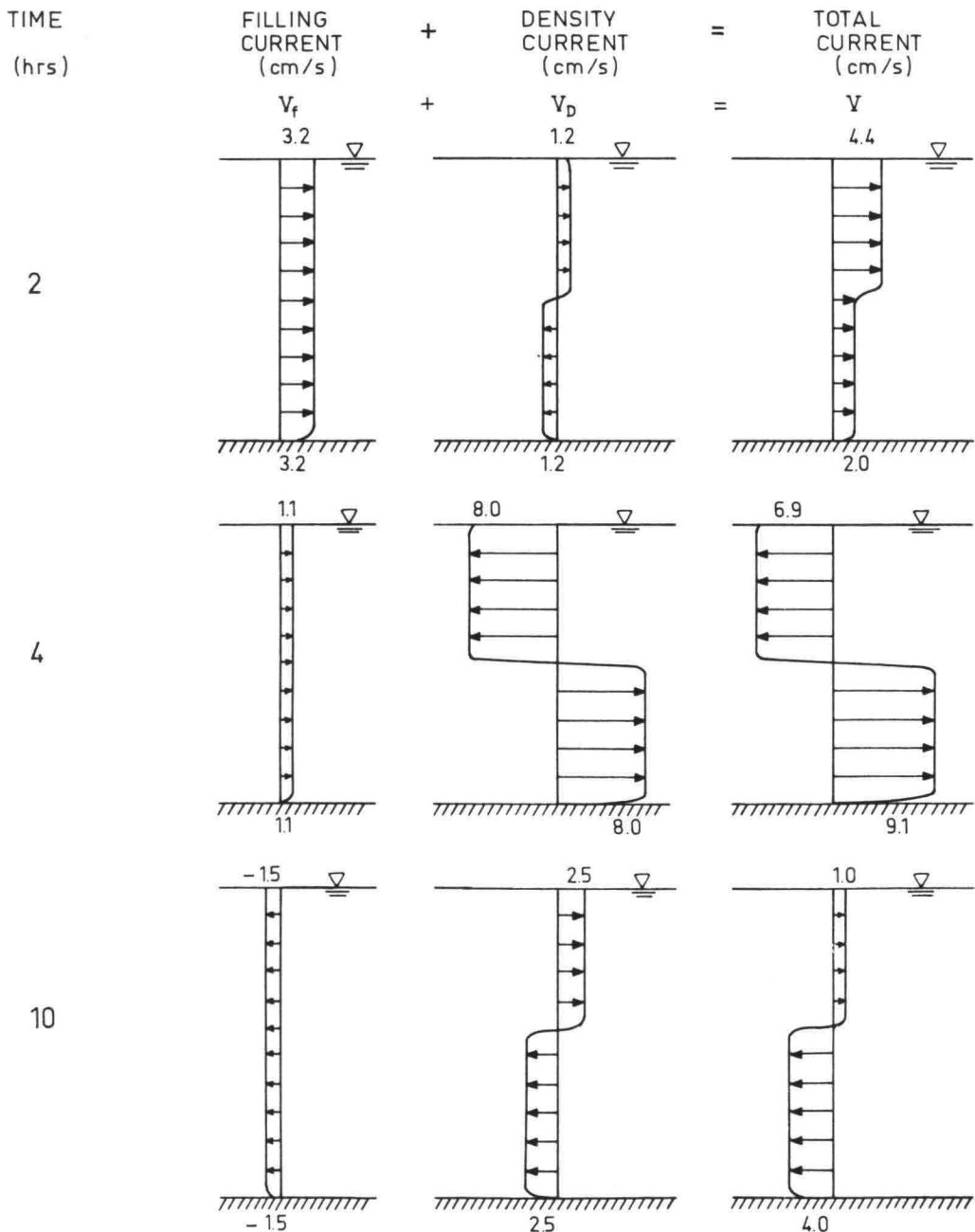


Figure 23.4 HARBOR ENTRANCE VELOCITY PROFILES

Until now, the assumption has been made that the harbor had an infinite length. In the next section, we examine the extra conditions imposed upon this theory by the finite length of a harbor.

### 23.4 Currents in Finite Harbors

The dry bed curve of a density tongue rushing into a harbor has been shown in figure 23.2. Equation 23.01 described its velocity. How far does such a tongue penetrate into a harbor?

Two conditions must be satisfied for a density tongue to continue progressing in a harbor basin:

- it must have somewhere to go, and
- the driving force (density difference) must still exist.

The first of these is dependent only upon the harbor geometry while the second criterium depends upon the water alone. In order to separate these conditions for discussion, let us first assume that initially all of the water in a harbor basin and the adjacent river has a density of  $1005 \text{ kg/m}^3$ . At some instant, the density of the water in the river increases to  $1015 \text{ kg/m}^3$ , and maintains that value indefinitely; thus, the driving force (item b, above) is maintained. There is no tide. The harbor has a rectangular form and has depth  $h = 7 \text{ m}$  and length  $L = 2500 \text{ m}$ . (see figure 23.5).

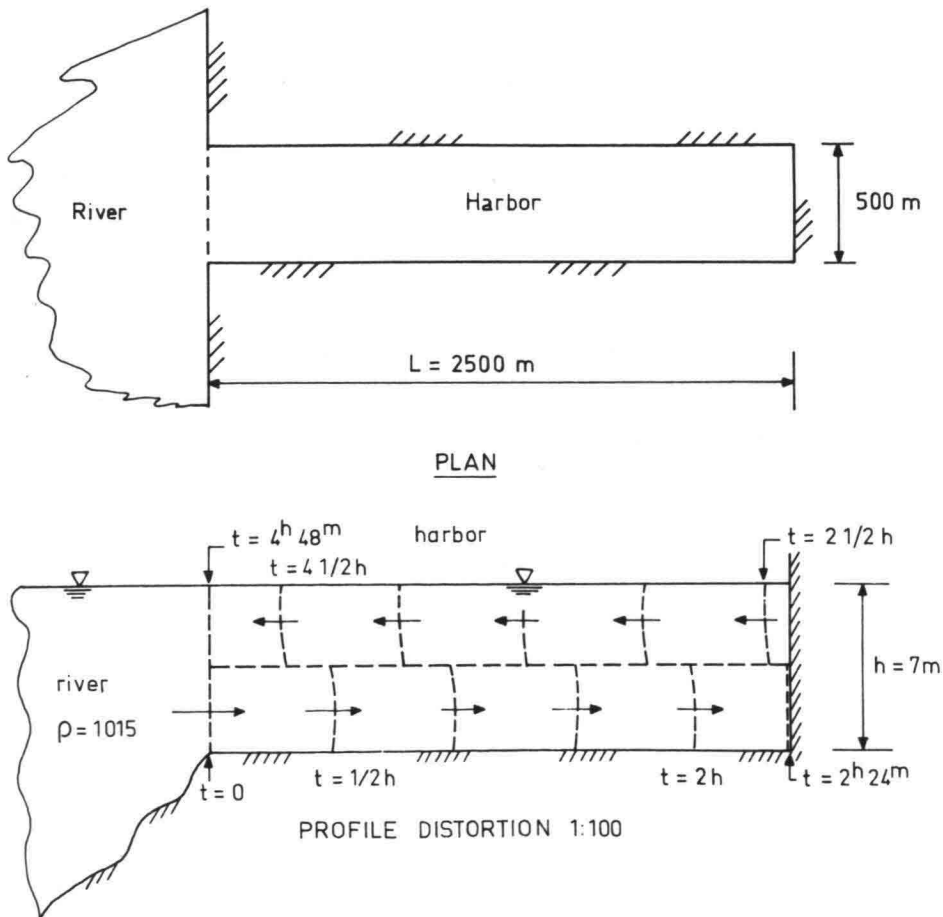


Figure 23.5 PROGRESS OF DENSITY CURRENT IN HARBOR

Using 23.01 with improved coefficient, we find the density current speed:

$$V_D = 0.35 \sqrt{\left(\frac{1015 - 1005}{1005}\right)(9.81)(7)} \quad (23.02)$$

$$= 0.289 \text{ m/s} \quad (23.03)$$

$$= 1042 \text{ m/h} \quad (23.04)$$

With this speed, the tongue progresses without hinderance over the length of the basin - 2500 m - arriving at the inner end in 2<sup>h</sup> 24<sup>m</sup>. The wave then reflects from the inner end of the harbor, just as does any other long wave, and propagates back toward the entrance at the same speed arriving there 4<sup>h</sup> 48<sup>m</sup> after the cycle started. The progress of the tongue after each half hour interval is shown by the dashed lines in figure 23.5.

After 4<sup>h</sup> 48<sup>m</sup> the tongue has returned to the harbor entrance. The harbor is now filled with more dense water - the same density as the river - and the process stops, since there is no longer a density difference across the harbor entrance.

What has happened to the less dense water that was originally in the harbor? That water has spread over a large area of the river in a thin layer, where wave action enhances its mixing with deeper water.

This example also yields some additional insight into the data presented in table 23.2 and figure 23.3. The average salinity (if the density difference is of saline origin) in the harbor increases linearly with time during 4<sup>h</sup> 48<sup>m</sup> in the example above, but the density current remains constant over this time period; it is completely determined by the density difference at the harbor entrance. Thus, the direct correlation between  $\sqrt{\delta}$  and  $|V_D|$  is really incorrect when  $\delta$  is determined based upon *average* salinities.

The time required for the density current to enter a harbor and exchange the contents explains the phase lag between the peak salinities in a river and in an adjacent harbor - see figure 23.3. Does a complete water exchange take place? Most likely, it does in this case even though the maximum harbor salinity is less than that in the river. By the time the harbor exchange has taken place, the river salinity is no longer maximum. Additional evidence that a complete exchange takes place is given by the abrupt change in density current velocity in figure 23.3 between 6½ and 7 hours. Since there is no abrupt change in salinity at that time, the velocity decrease must be caused by removal of the effective driving force.

The second type of problem, in which there is insufficient time for a complete exchange, is somewhat more complex. This is illustrated via the following example.

This example is exactly the same as the previous one in that the harbor initially contains water having  $\rho = 1005 \text{ kg/m}^3$  and the river abruptly changes density from 1005 to 1015  $\text{kg/m}^3$ . This time however, this higher density will be maintained in the river for only 1<sup>h</sup> 12<sup>m</sup>, after which the river density will again become 1005  $\text{kg/m}^3$ . Indeed, the problem is exactly like the previous example in all respects for the first 1<sup>h</sup> 12<sup>m</sup>. This is shown in figure 23.6A.

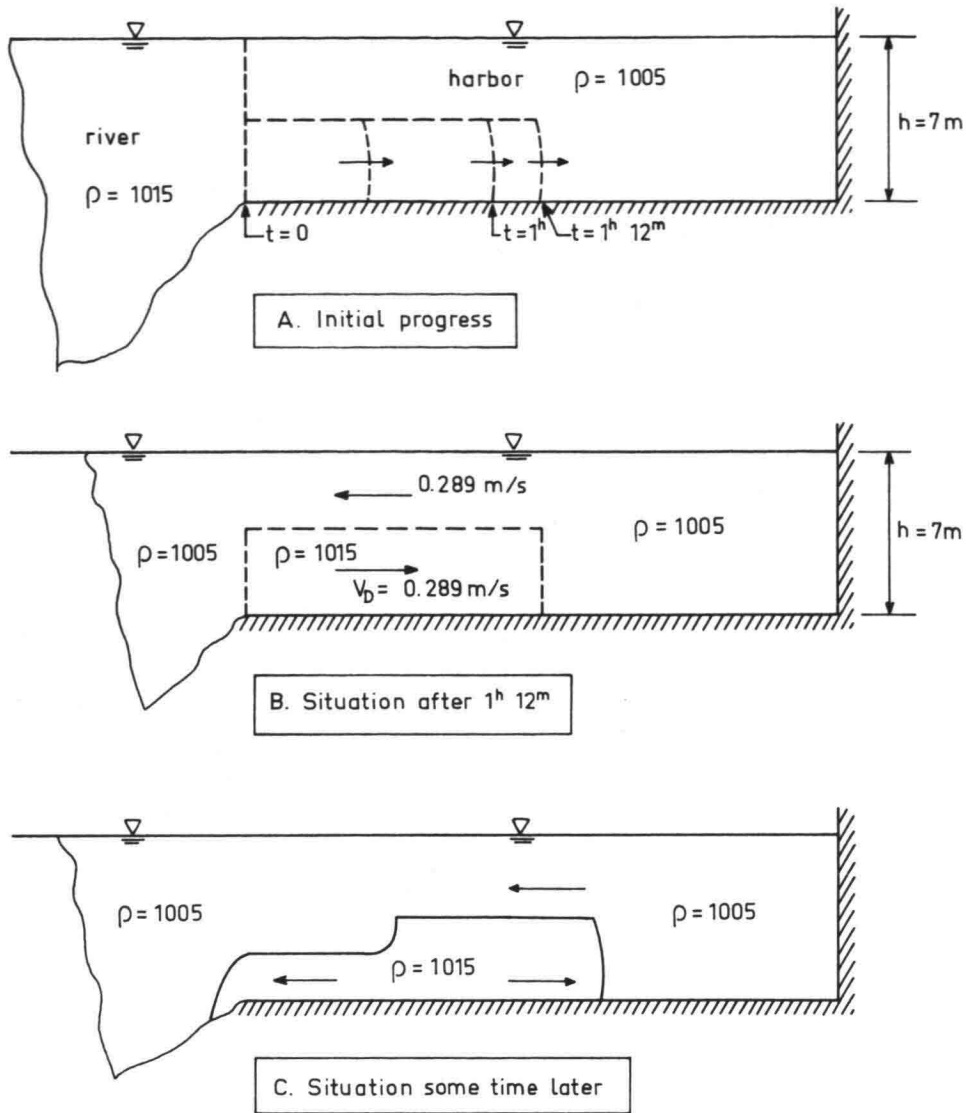


Figure 23.6 DENSITY CURRENTS IN HARBOR

After  $1^{\text{h}} 12^{\text{m}}$  the situation will be as shown in figure 23.6B. The driving force is no longer present. Momentum will keep the slug of salt water moving for a time, but other influences become important since the trailing end of the slug of dense water is unstable. A dry bed curve will develop at this end of the 3.5 m thick lower layer causing the slug of water to spread out in a thinner layer along the harbor bottom. Ultimately, of course, this thin layer could retreat entirely to the deeper river. Quantitative evaluations of all these processes are beyond the scope of this course and are not necessary for our main purpose - the determination of the quantity of silt which enters the harbor along with the more dense water. An impression of the form of the interface between the two water masses at some later time is shown in 23.6C.

### 23.5 The Practical Problem

The discussion just presented holds true only to the extent that its assumptions are satisfied. A glance at figure 23.3 is sufficient to see that the assumption that the river density changes abruptly does not hold true in nature. Secondly, many harbors are not rectangular in form. A dependable theoretical computation of the water exchange in a harbor of arbitrary shape on a given river is extremely time consuming at best. For this reason, physical model studies are often used; a significant portion of the Delft Hydraulics Lab is devoted to the modeling of saline density currents.

A second approach to the problem is to develop a semi-empirical equation for the water exchange and to determine its coefficients based upon experience with existing harbors. Such an equation can then be used to predict the exchange taking place in a similar harbor under the same conditions. Since a volume,  $\Psi$ , can be expressed as a velocity times a cross-section area times a time, one can expect to find a square root of a relative density times a water depth representing the velocity multiplied by the entrance area,  $A_E$ , in the equation. The constant tide period as well as the other coefficients can be combined into one constant. Such an approach has been taken at the harbor of Rotterdam. Using measurements made in several of the larger harbors there (Botlek, 1e, 2e petroleumhaven) the following relationship results:

$$\Psi_D = G A_E \sqrt{\delta' \bar{h}} \quad (23.05)$$

in which:

$A_E$  is the cross sectional area of the entrance in  $m^2$ ,  
 $G$  is a coefficient depending on the harbor,

$\bar{h}$  is the average depth of the harbor in meters, and  
 $\delta'$  is the relative density defined as:

$$\delta' = \frac{\rho_{\max} - \rho_{\min}}{\bar{\rho}} \quad (23.06)$$

in which

$\rho_{\min}$  is the minimum river density,  
 $\rho_{\max}$  is the maximum river density, and  
 $\bar{\rho}$  is the average river density over one tide period, and  
 $\Psi_D$  is the *total* water volume exchanged by the density current during the *entire* tide period.

The method just described depends upon having an existing harbor along the tidal river. Further, the size and geometry of a projected harbor is not always comparable to that of an existing harbor. In such cases, the above scheme is of little help, since the coefficient  $G$  cannot be determined.

The density current can be of major importance for harbor siltation resulting in maintenance dredging costs. An estimate of the density current, therefore, can be of vital importance for feasibility studies. Even a crude computation can be helpful in such cases. The following approach

is suggested in an anonymous report (1960) by the Delft Hydraulics Laboratory. The expected accuracy of the method is in the order of  $\pm 50\%$ .

The anonymous author's - in fact Gersie and Bijker - attack the problem by defining a coefficient,  $\alpha$ , which gives the ratio of total water exchange volume to harbor volume. Since there are two influences involved, filling plus density current,  $\alpha$  is split into two components:

$$\alpha = \alpha_f + \alpha_D \quad (23.07)$$

where:

$\alpha$  is the ratio of water volume entering the harbor per tide to the harbor volume,

$\alpha_f$  is that portion caused by the filling, and

$\alpha_D$  is caused by the density influence.

$\alpha_f$  can be evaluated by comparing the tidal prism of the harbor to the total harbor volume.

$$\alpha_f = \frac{P}{V_H} = \frac{\Delta h}{\bar{h}} \quad * \quad (23.08)$$

where:

$\bar{h}$  is the average harbor depth

$\Delta h$  is the difference between the high and low tide levels,

$V_H$  is the total harbor volume based upon depth  $\bar{h}$ , and

$P$  is the tidal prism of the harbor basin.

$\alpha_D$  is not independent of the harbor filling - see section 23.3 - but is dependent upon the filling current component as well.

$$\alpha_D = \frac{(V_D - |V_f|) T_D}{2L} \quad (23.09)$$

where:

$V_D$  is the density current velocity,

$V_f$  is the filling current velocity,

$L$  is the length of the harbor, and

$T_D$  is the time interval over which the density difference exists.

Now some problems begin to appear! What density ratio,  $\delta$ , should be used to compute  $V_D$ ? How is  $T_D$  determined? What is  $L$  for a complex harbor?

Starting with this last question, we are working, in fact, with a schematized rectangular harbor with cross sectional area equal to that of the entrance. The length follows from our schematization, and is usually just about the longest distance from the entrance to an extremity of the harbor. A bit of experience is very helpful in making this schematization.

$T_D$  is the time during which a density difference is present. It is related only to the density - time curve for the estuary and is not necessarily directly related to the tide level. Also,  $T_D$  during the time of increasing harbor density may be different from that for decreasing density.

\* The second step is valid if the sides of the harbor are vertical.

The most difficult question is one of determining the proper value of  $V_D$ . The following approach is suggested:

- a. Compute  $V_D$  based upon a  $\delta$  corresponding to the extreme values of the schematized density in the river using 23.01.
- b. Using this value of  $V_D$  compute  $\alpha_D$  and then  $\alpha$ .
- c. If  $\alpha < 1$ , then the maximum harbor density will be less than the river maximum and our assumption in step a is violated. In that case, repeat steps a and b using a new value of  $\delta$  one half as large as the original one.

In equation 23.09 the absolute value of the filling current has been averaged over the time  $T_D$ . Note that the absolute value has been taken before the average. The value of  $V_f$  for use here is determined from the vertical tide in the river.

$$V_f = \frac{A_H}{A_E} \frac{dh}{dt} \quad (23.10)$$

where:

$A_H$  is the surface area of the harbor, and  
 $A_E$  is the cross sectional area of the entrance.

Actually, equation 23.09 does not tell the whole story. The following inequality must also be satisfied:

$$0 \leq \alpha_D \leq 1 \quad (23.11)$$

Thus, the influence of the density current may not be negative; it may be zero. The upper limit on  $\alpha_D$  is imposed by the schematization of the density - time curve.

The value of  $\alpha_D$  can be corrected for the fact that the harbor has been schematized by multiplying it by the ratio of surface areas of the schematized and actual harbors, respectively.

The volume of water entering the harbor during a complete tidal period can best be determined as the sum of its components. The harbor filling current contributes a volume of water equal to  $\alpha_f$  times the harbor volume. This same volume of water flows out when the water level falls. During the period that the river density is high,  $\alpha_D^*$  times the harbor volume flows into the harbor. When the river density is low,  $\alpha_D^*$  times the harbor volume flows out.

Both computational techniques outlined in this section are illustrated in section 23.7.

### 23.6 Other Current Influences

The current pattern in a harbor mouth can be even more complicated than has already been described. The complication can exist in the form of an eddy rotating about a vertical axis in the harbor entrance. Water exchange between the harbor and eddy on one side and between river and eddy on the other can increase the transport of salt and suspended sediment into the harbor.

---

\* These two values of  $\alpha_D$  are not generally equal.

When a harbor is small, the density current can usually carry out a complete water exchange rather quickly, but then stops transporting silt laden water into the harbor. The eddy, on the other hand, continues functioning exchanging sediment laden river water for clearer harbor water. This cause can be the most important of all three causes for the transport of sediment into a small harbor.

Eddies form at the entrance to larger harbor basins as well. However, these tend to be excited by the other current components in the harbor entrance rather than the river current. As such, they contribute little to the supply of sediment to the harbor.

An attempt will be made in the next sections to quantify the amount of siltation to be expected in a harbor. Before attacking that, however, we should consider the effects of the presence of the harbor on shipping in the river.

It takes little imagination to realize that near the mouth of a harbor, where eddies, density currents, river currents and harbor filling currents are all competing with one another, the current pattern can be rather confused. Small, shallow draft ships will only be concerned with the surface currents. Larger, deeper ships which penetrate the interface between layers are subjected to an even more complex pattern of current forces. Add to this the dead water phenomenon described in the previous chapter, and we should realize easily the respect with which harbor pilots are usually treated. An enumeration of the various ways various ships can react to various current patterns would be too voluminous to include here. It is sufficient for our purpose to recognize that such ship maneuvering problems can and do occur and to have the sense to ask a pilot's advice about any extensive harbor changes.

### 23.7 Harbor Siltation

The same processes of siltation described for a tidal river in the previous chapter occur in adjacent harbors as well. Variations in salinity cause flocculation and rapid settlement of fine material in harbors just as in rivers. In addition, however, the settlement of material in harbors proceeds even faster because of the relative tranquility of the water in the basin. Obviously, all of the phenomena which cause water exchange between the harbor and river also increase the supply of sediment to the harbor.

The harbor siltation is computed by multiplying the volume of water exchanged in one tide cycle in the basin by the difference in sediment concentration between inflowing and outflowing water. The role of each of the current components will be examined in the following example.

A harbor is located along a river in which the average suspended sediment concentration is 77 mg/l (this agrees with the data in table 22.3). The harbor is 2000 meters long and has a prismatic cross section with side slopes of 1:4. The tide range is 1.7 meters and the harbor depth at low water is 13.5 meters. Figure 23.7 shows such a harbor,

having a bottom width of 400 m. Again using data from Rotterdam, the river has a maximum salinity of 8.06 ‰ and a minimum salinity of 2.47 ‰ (table 22.1) With a water temperature of 16°C and table 3.3, we find that the maximum density in the river is 1005.18 kg/m<sup>3</sup> and the minimum density is 1000.85 kg/m<sup>3</sup>, yielding:

$$\delta' = \frac{1005.18 - 1000.85}{1003.02} = 4.32 \times 10^{-3} \quad (23.12)$$

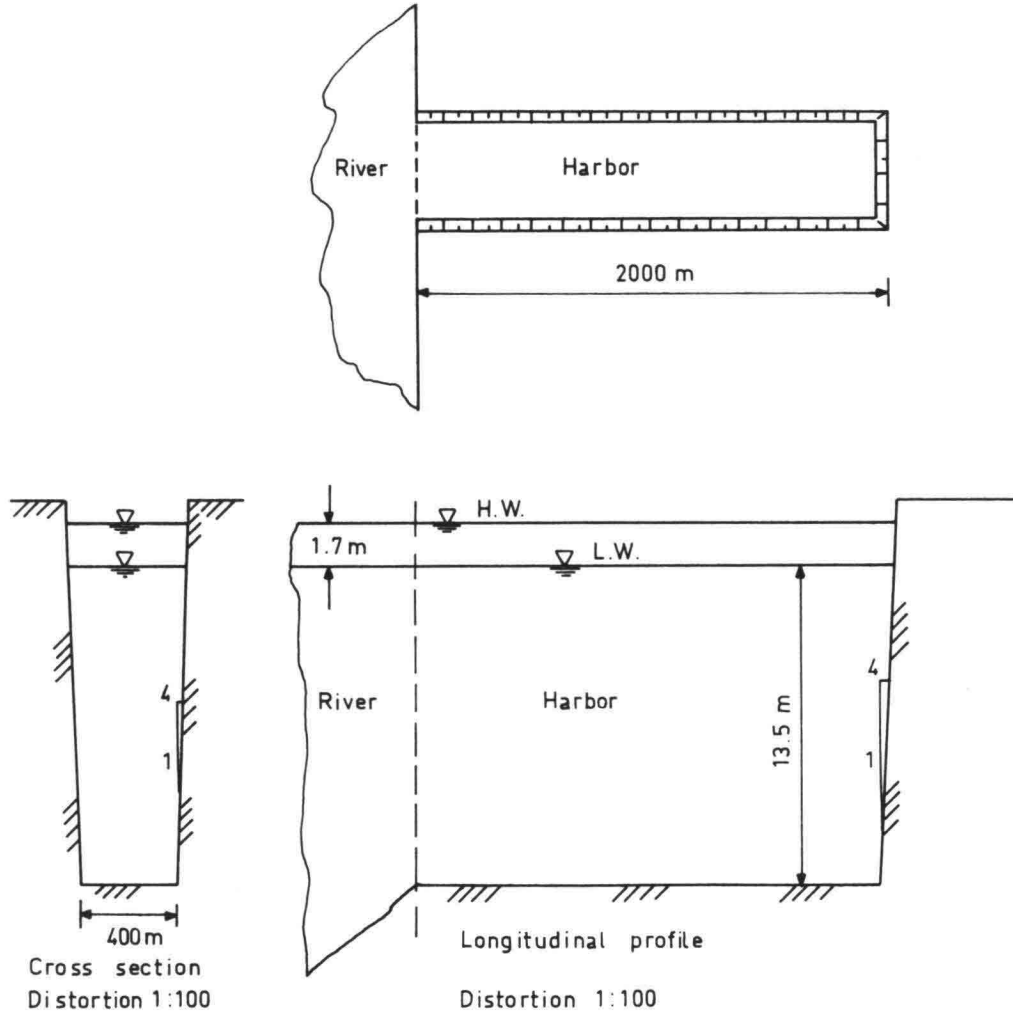


Figure 23.7 HARBOR EXAMPLE SKETCH

The average water depth in the harbor is:

$$\bar{h} = 13.5 + \left(\frac{1}{2}\right)(1.7) = 14.35 \text{ m} \quad (23.13)$$

Yielding a top width of:

$$400 + (14.35)(8) = 515 \text{ m} \quad (23.14)$$

The average flow area in the entrance is, then:

$$A_E = \left(\frac{1}{2}\right)(400 + 515)(14.35) = 6565 \text{ m}^2 \quad (23.15)$$

The tidal prism,  $P$ , of the harbor is the volume of water supplied per tide by the filling current.

$$P = (515)(2000)(1.7) = 1.75 \times 10^6 \text{ m}^3 \quad (23.16)$$

Each liter of this water carries 77 mg of dry sediment into the harbor. Probably not all of this material will settle in the limited retention time. The concentration of sediment in discharged water can be estimated from laboratory tests or from experience in similar local harbors. For this problem, let us assume that the discharge water from the harbor carries an average of 10 mg/l of dry silt. Thus, 67 mg/l is retained in the harbor.

The amount of sediment transported into the harbor by the filling current\* is then (with units conversion):

$$s_f = (1.75 \times 10^6) (67)(10^{-3}) = 1.17 \times 10^5 \text{ kg/tide} \quad (23.17)$$

The influence of the density current is computed using equation 23.05. The total volume of water exchanged by the density current during a tide period is, using  $G = 8000 \text{ m}^{\frac{1}{2}}/\text{tide period}$ :

$$V_D = (8000) (6565) \sqrt{(4.32 \times 10^{-3})(14.35)} \quad (23.18)$$

$$= 1.31 \times 10^7 \text{ m}^3/\text{tide} \quad (23.19)$$

Half of this water,  $6.53 \times 10^6 \text{ m}^3/\text{tide}$ , enters along the harbor bottom with the intruding salt tongue and brings:

$$s_{D_1} = (6.53 \times 10^6)(67)(10^{-3}) = 4.38 \times 10^5 \text{ kg/tide} \quad (23.20)$$

sediment with it.

The other half of the exchange water enters the harbor along the surface as the salt tongue retreats. Since the surface water in a river usually contains less sediment, it transports relatively less sediment into the harbor. For Rotterdam, it is assumed that this surface current transports only 20% of the sediment found in the other currents into the harbor. Since this material will be finer than the average of all the material, it will settle more slowly. Thus, we can still assume that 10 mg/l leaves the harbor later. These considerations yield:

$$s_{D_2} = (6.53 \times 10^6) [(0.2)(77) - 10] (10^{-3}) \quad (23.21)$$

$$= 3.53 \times 10^4 \text{ kg/tide} \quad (23.22)$$

\* Because the density current component dominates the velocity profile, this current is concentrated in the lower layer of the harbor.

The sedimentations are compared in table 23.3. We see that more than 80% of the harbor siltation is caused by the density current.

TABLE 23.3 HARBOR SEDIMENTATION SUMMARY

Component	Quantity (kg/tide)	Percent of total
Filling Current	$1.17 \times 10^5$	19.8
Salt Inflow	$4.38 \times 10^5$	74.2
Salt Outflow	$3.53 \times 10^4$	6.0
Density Subtotal	$4.73 \times 10^5$	80.2
Grand Total	$5.90 \times 10^5$	100

A very practical question remains for those responsible for the maintenance of the harbor. How much shallower will the harbor become as a result of siltation over the course of one year? This can be answered if the density of the dry sediment particles and that of the in situ sediment are known. Reasonable values for these are  $2650 \text{ kg/m}^3$  and  $1200 \text{ kg/m}^3$ , respectively. Then, if  $v_v$  denotes the volume of water filled voids in  $1 \text{ m}^3$  of sediment, then:

$$1200 = (2650)(1 - v_v) + (1000)(v_v) \quad (23.23)$$

from which  $v_v = 0.88$ . Therefore,  $1 \text{ m}^3$  of sediment contains

$$(1 - 0.88)(2650) = 318 \text{ kg} \quad (23.24)$$

of dry sediment particles.  $5.9 \times 10^5 \text{ kg}$  of sediment particles occupies a volume of:

$$\frac{5.90 \times 10^5}{318} = 1855 \text{ m}^3 \quad (23.25)$$

This volume of sediment accumulates in one tide period. There are:

$$\frac{(365.25)(24)}{12.42} = 706 \quad (23.26)$$

tides per year, so that in one year, the accumulation of sediment in the harbor is:

$$(1855)(706) = 1.31 \times 10^6 \text{ m}^3/\text{year!} \quad (23.27)$$

This volume is spread over the harbor bottom in a layer which is:

$$\frac{1.31 \times 10^6}{(2000)(400)} = 1.64 \text{ m} \quad (23.28)$$

thick.

It is usually not economical to dredge out a sediment layer less than about 2.5 m thick. In this case the harbor could be dredged about once every  $1\frac{1}{2}$  years.

This last figure dramatizes the importance of the density current. If the density current could be eliminated in the harbor, then the interval between dredgings could be increased by about a factor 5 (see table 23.3) or to about 7½ years. The economic savings involved are obvious.

As a check, the computations just carried out will be repeated using the second technique of section 23.5.

$\alpha_f$  can be computed from the data using 23.08:

$$\alpha_f = \frac{1.75 \times 10^6}{(6565)(2000)} = 0.133 \quad (23.29)$$

To compute  $\alpha_D$  we must first schematize the river salinity curve. We can attempt this by schematizing figure 23.3 for river salinity as being  $S = 2.5$  ‰ from  $t = 0$  to  $t = 3$  hrs and from  $t = 10$  to  $t = 12.4$  hrs. From  $t = 4.5$  to  $t = 7.5$  hrs  $S$  is assumed to be equal to  $7.5$  ‰. This yields  $T_D = 3$  hrs for increasing harbor salinity and  $T_D = 5.4$  hrs for decreasing salinity. (We assume that nothing happens during the rest of the tide period). The schematized curve is shown in figure 23.8.

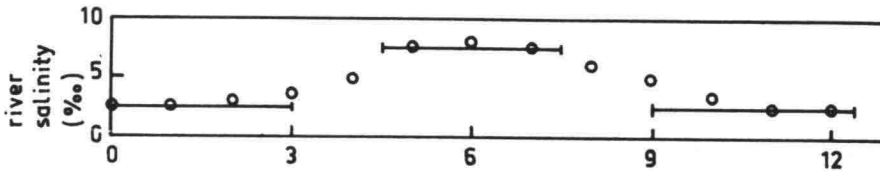


Fig. 23.8 SCHEMATIZED SALINITY CURVE

Since we are not aiming for high accuracy, values  $\alpha + \rho$  for computing  $V_D$  can be determined using equation 3.22. Thus:

$$\delta = \frac{0.75(7.5 - 2.5)}{1000 + (0.75 \times 2.5)} = 3.74 \times 10^{-3} \quad (23.30)$$

This results in a value of  $V_D$  from equation 23.01 with improved coefficient of:

$$V_D = 0.35 \sqrt{(3.74 \times 10^{-3})(9.81)(14.35)} \quad (23.31)$$

$$= 0.254 \text{ m/s} \quad (23.32)$$

$\overline{|V_f|}$  follows using 23.10 with data from table 20.1.

Time interval (hrs)	$ \Delta h $ (m)	$\Delta t$ (hrs)
0-3	1.21	3
10-12.4	0.22	2.4
4.5-7.5	0.55	3

Also, from figure 23.7, the area of the harbor is:

$$A_H = (2000)(515) = 10.3 \times 10^5 \text{ m}^2$$

and

$$A_E = 6565 \text{ m}^2$$

Thus, using 23.10 for increasing density:

$$|V_f| = \frac{10.3 \times 10^5}{6565} \times \left(\frac{0.55}{3}\right) \quad (23.33)$$

$$= 28.8 \text{ m/hr} = 8 \times 10^{-3} \text{ m/s} \quad (23.34)$$

and for decreasing density:

$$|V_f| = \frac{10.3 \times 10^5}{6565} \times \frac{1.43}{5.4} \quad (23.35)$$

$$= 41.5 \text{ m/hr} = 1.15 \times 10^{-2} \text{ m/s} \quad (23.36)$$

The two values of  $\alpha_D$  can now be computed using 23.09, in which  $L = 2000$  m. For increasing density:

$$\alpha_D = \frac{(0.254 - 8 \times 10^{-3})(3)(3600)}{(2)(2000)} = 0.664 \quad (23.37)$$

and for decreasing density:

$$\alpha_D = \frac{(0.254 - 1.15 \times 10^{-2})(5.4)(3600)}{(2)(2000)} = 1.179 \quad (23.38)$$

Since one resulting value of  $\alpha$  is somewhat less than one, our initial assumption that there was a complete harbor exchange in *both* directions (leading to the extreme density differences used above) is incorrect. Following the suggestion in section 23.5, we can recompute  $V_D$  and  $\alpha_D$  for a reduced  $\delta$ . Reducing  $\delta$  by 50% as suggested yields:

$$V_D = 0.35 \sqrt{(1.87 \times 10^{-3})(9.81)(14.35)} \quad (23.39)$$

$$= 0.180 \text{ m/s} \quad (23.40)$$

Since  $V_f$  remains the same, we can proceed directly to the computation of  $\alpha_D$ .

For increasing salinity:

$$\alpha_D = \frac{(0.180 - 8 \times 10^{-3})(3)(3600)}{(2)(2000)} = 0.464 \quad (23.41)$$

and for decreasing salinity:

$$\alpha_D = \frac{(0.180 - 1.15 \times 10^{-2})(5.4)(3600)}{(2)(2000)} = 0.819 \quad (23.42)$$

This seems reasonable.

The total harbor volume,  $V_H$ , is:

$$V_H = (6565)(2000) = 1.31 \times 10^7 \text{ m}^3 \quad (23.43)$$

Using the same silt concentrations as previously, the silt transport into the harbor by the filling current is:

$$s_f = (0.133)(1.31 \times 10^7)(67)(10^{-3}) = 1.17 \times 10^5 \text{ kg/tide} \quad (23.44)$$

The density current during increasing salinity transports:

$$s_{D_1} = (0.464)(1.31 \times 10^7)(67)(10^{-3}) = 4.07 \times 10^5 \text{ kg/tide} \quad (23.45)$$

and for decreasing salinity using the lower sediment concentration just as with the previous version:

$$s_{D_2} = (0.819)(1.31 \times 10^7)[(0.2)(77) - 10](10^{-3}) \quad (23.46)$$

$$= 5.79 \times 10^4 \text{ kg/tide} \quad (23.47)$$

These values are compared in table 23.4.

TABLE 23.4 Harbor Siltation Summary

Component	Quantity (kg/tide)	Percent of total
Filling Current	$1.17 \times 10^5$	20.1
Salt inflow	$4.07 \times 10^5$	69.9
Salt outflow	$5.79 \times 10^4$	10.0
Density Subtotal	$4.65 \times 10^5$	79.9
Grand total	$5.82 \times 10^5$	100.0

The remaining problem of determining the amount of siltation is exactly the same as was previously done and will not be repeated here.

The amazing agreement between the results of the two methods should be attributed more to luck than to accuracy of the method.

Methods to eliminate or reduce density current influences in a harbor are discussed in the next section.

### 23.8 Methods to Combat Density Currents in Harbors

Since it is not necessary to pass a runoff flow through a harbor entrance - in contrast to a river mouth, more technical possibilities are available to reduce the influence of density currents.

One of the simplest methods to reduce the density current water exchange in a given harbor basin is to narrow the entrance. As was shown in equation 23.05, the volume of water exchanged is directly proportional to the entrance area,  $A_E$ . Thus, reducing the entrance width should reduce the volume of exchanged water in direct proportion. In practice, such a narrowing will not be quite that effective. The intruding density current stream will spread in both horizontal directions in the wider harbor basin; this tends to increase the effective driving force by increasing the slope of the interface between the water masses. The density current flow will be greater than might otherwise be expected. This effect is difficult to quantify, however.

Another technique is to install a single set of doors at the entrance to the harbor. The harbor level is then maintained at a constant level - even the filling current is eliminated. The water level in the harbor remains constant; this is handy for the cargo handling operations. Does a density current cause a water exchange? It does not have to. If the doors are opened only once during the tide cycle and at the same time in the cycle when the water levels are equal, then the harbor water will eventually have the same density as the river water and no dredging problems will be experienced. On the other hand this means that the doors are opened only once every tide period and it may be unacceptable to force the shipping to wait so long to pass through the entrance.

What would happen if the doors were opened twice per tide cycle while the water levels were the same - once on a rising tide and once on a falling tide? There will still be no filling current, but there is no guarantee that the density in the river will be the same at both times. In general it will not be, and a density current and water exchange will take place during the time that the doors are open. Indeed, such a solution is of little value except when very great tide level variations might make cargo handling inefficient in an open basin.

If the single set of doors were replaced by a lock, then ships could enter and leave the harbor at any time irrespective of the water levels. Each locking operation can be accompanied by a water exchange within the lock, however. Since the lock is relatively small, this exchange progresses rather rapidly - 27 minutes for the large lock at IJmuiden, for example. Special facilities have been built at IJmuiden to trap this intruding salt water and retain it for later disposal. These special facilities consist of a deep pit just inside the lock connected via an equally deep channel to a sluice. Salt water coming through the inner door opening of the lock falls into the pit. Later, during low tide at sea, this salt water can be discharged through the sluice.

An additional device used at IJmuiden to reduce the salt intrusion is an air bubble curtain. This is a stream of rising air bubbles released from a perforated submerged pipeline at the end

of the lock near the door. The rising bubbles increase turbulence and hence mixing. The mixing reduces the driving force of the density tongue and reduces the intrusion.

Such a device could also have been used, of course, in combination with the single set of doors mentioned earlier. Its use for a harbor entrance which is always open is not usually economical, because of power consumption of the air compressors which drive the system.

Other more exotic devices have been proposed from time to time to combat density current intrusions into harbors. For example, a device looking like a giant brush with vertical buoyant rubber bristles fixed to the bottom has been conceived. The bristles bend in order to allow a ship to pass. Many other similar devices can be conceived using a bit of ingenuity.

### 23.9 Review

Many relationships between phenomena which take place in rivers and harbors have been presented in this and the preceding three chapters. It is instructive as review to gather together all of the information presented on a single graph sheet. This has been done in figure 23.9. All of the data, with the exception of the tide data for Hook of Holland has been presented earlier in these chapters. The tidal data for Hook of Holland is included for completeness in table 23.5.

TABLE 23.5 TIDAL DATA FOR HOOK OF HOLLAND

Time (hrs)	Water level (m)	Average Current (m/s)
0	-0.53	+0.13
1	-0.21	0.80
2	+0.40	1.17
3	0.80	1.43
4	0.88	0.80
5	0.67	+0.26
6	+0.19	-0.44
7	-0.25	-0.94
8	-0.58	-1.16
9	-0.58	-1.13
10	-0.63	-0.93
11	-0.69	-0.62
12	-0.62	-0.08

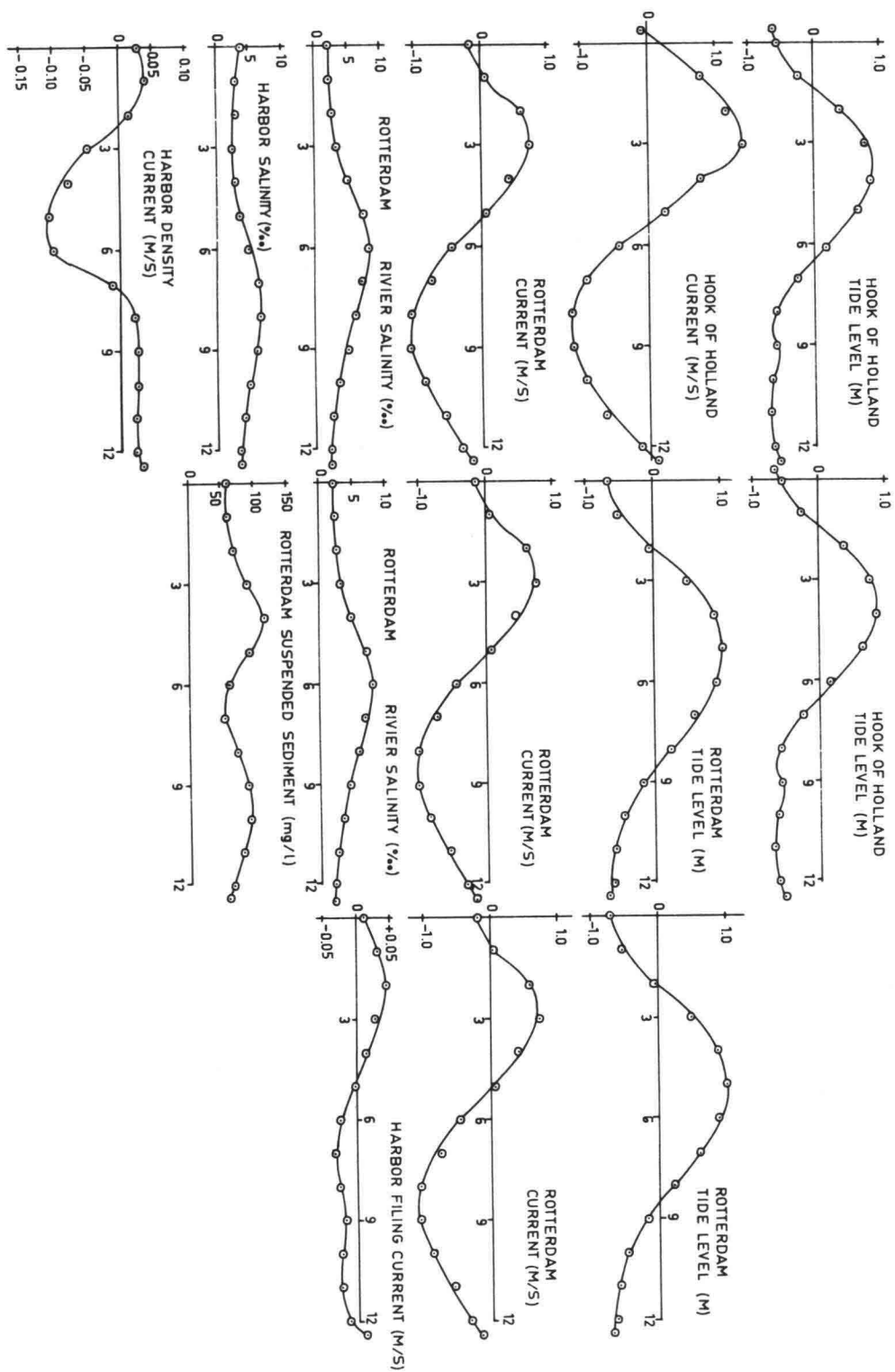


Figure 23.9 SUMMARY OF ALL DATA PRESENTED FOR ROTTERDAM

### 24.1 Definition

Pollution is defined by A.F. Spilhaus as "anything animate or inanimate that by its excess reduces the quality of living".\* This definition is extremely general; even overpopulation can be seen as a pollution problem under this definition. The important word in the above definition is excess. We often forget that many polluting substances occur and are transported naturally as well as by man.

A more restricted definition is provided by a report to the President and Congress by the U.S. National Water Commission in June, 1973: "Water is polluted if it is not of sufficiently high quality to be suitable for the highest use people wish to make of it at present or in the future".\*

This definition for use with regard to water quality is good in that it allows for variations in quality dependent upon water use.

It is the purpose of this chapter to create an awareness of marine pollution problems. Hopefully, an emotional discussion of this topic can be avoided.

The degree to which disagreement can develop is exemplified by two opposing articles which appeared in *Civil Engineering* - Gould (1973) and Thomas (1974). Both quote factual information and neither, really contradicts the other except on matters purely based upon opinion.

### 24.2 Polluting Materials

The materials causing marine pollution can be grouped into seven main categories. These are: human wastes, oil, halogenated hydrocarbons, other organic materials, heavy metals, heat, and radioactive materials. Each of these is described a bit below. (Dredging spoil material has been discussed separately in chapter 17.).

Human fecal waste is often first considered, since it raises such a great aesthetic problem - people do not like to see or smell it. On the other hand, it is certainly a natural product and fecal wastes are also produced in great quantity by marine life. Six million tons of anchovies off the California (U.S.A.) coast produce as much fecal material as 90 million people, according to Bascom (1974-1). Two aspects of the disposal of fecal wastes remain important, however: Fecal wastes can consume oxygen from the water and these wastes contain bacteria. The oxygen demand can lower the dissolved oxygen level below that needed by marine life. While most bacteria are killed soon by contact with sea water (within hours), it is not sure that this is true for all types, thus epidemiological problems can be conceived.

---

\* quoted by Bascom (1974-1)

Oil and petroleum products are perhaps the most controversial pollutants. The public reaction to oil spills by ships is usually emotional and vehement. Shipping is not the only source of marine oil pollution, however. Unknown quantities of it seep naturally into the oceans. A report compiled for the Connecticut (U.S.A.) State Legislature concludes that more than two thirds of the oil discharged by man into the seas comes from the crankcases of automobile engines and oil sumps of other machines.\* This oil causes no great problems, however, since its rate of input is low enough and it is sufficiently dispersed to be broken down by natural processes.

Oil pollution from major spills is usually a local and often temporary problem. The short term biological and esthetic influences can be severe, but the pre-existing natural situation usually restores it self without the intervention of man within a few years. This is not true of the next category of pollutants.

Halogenated hydrocarbons include the most common organic pesticides. While a few of these chemicals, such as TEPP lose their lethal properties rather quickly, others such as DDT seem to be virtually undestructable in nature. The process of concentration of pesticides in certain types of marine life is rather well known. Because of their indestructability, disposal of these types of materials should be especially carefully controlled.

The adverse effects of the discharge of nutrients into restricted bodies of water such as lakes are well documented elsewhere. On the other hand, the effect of such nutrients on the ocean can be beneficial. According to Isaacs, "The sea is *starved* of the basic plant nutrients, and it is a mystery to me why we should be concerned with their thoughtful introduction into coastal seas in any quantity that man can generate in the foreseeable future." \*\*

With proper management, nutrients may be successfully disposed of along the coasts. A by-product of this disposal would be the stimulation of marine life and thus of the fish life dependent upon these plants. This artificial nutrition amounts to the simulation of an upwelling responsible for the prosperous fishing industry in certain parts of the world (Japan, for example).

Since oxygen is consumed in the biodegradation of the nutrient materials, their discharge must be managed in such a way that dissolved oxygen levels do not become too low to support fish life.

Heavy metals such as copper and zinc are naturally present in sea water and in bottom sediments. Low concentrations of certain of these elements are beneficial or even essential for a number of organisms. For example, copper is an essential nutritional element for crabs.

Marine sediments contain much higher concentrations of heavy metals than sea water (Table 24.1). Heavy metals, ionically bound to sediment particles tend to go into solution in sea water as the ionic constituents of sea water itself disturb the physical chemistry of the sediment

---

\* Reported in *Scientific American*, Vol. 228, no. 2, Feb. 1973 page 48.

\*\* quoted in Bascom (1974-1)

particles - see section 7 of chapter 22. Table 24.1 compares heavy metal concentrations in sediments and sea water. Heavy metals also enter the sea from the atmosphere. Forest fires, for example, add metallic oxides to the atmosphere which deposits them over the whole world.

Just as with discharges of many pesticides, the influence of heavy metal discharges is cumulative. The indiscriminate addition of heavy metals to the sea should be avoided. An example of the cumulative action as influenced by man is shown in figure 24.1, which shows the lead concentration in layers of sediment in the ocean near Long Beach, California, U.S.A. The sharp rise in concentration in recent years is attributed to airborne lead from automotive emissions.

TABLE 24.1 Concentrations of Heavy Metals in sea water and sediments.

Element	Concentrations in parts per million at stated locations					
	Sea water Average	Ocean Sed. California upper 10 cm	Europoort silt	Botlek to Eemhaven silt	Waalhaven to Rijnhaven silt	Rhine River Silt
Cadmium	$1 \times 10^{-4}$	0.3	2.7	19.	36.	45.
Chromium	$4.5 \times 10^{-4}$	42.	185.	435.	870.	1240.
Cobalt	$4 \times 10^{-4}$	7.				
Copper	$3 \times 10^{-3}$	16.	55.	250.	450.	600.
Lead	$3 \times 10^{-5}$	8.	96.	304.	545.	800.
Manganese	$1.8 \times 10^{-3}$	290.				
Mercury	$2 \times 10^{-4}$	0.04				
Nickel	$6.6 \times 10^{-3}$	13.				
Silver	$3 \times 10^{-4}$	1.				
Zinc	0.01	32.	350.	1300.	2150.	2900.

Data from: Bascom (1974-1), and  
de Nekker & In't Veld (1975)

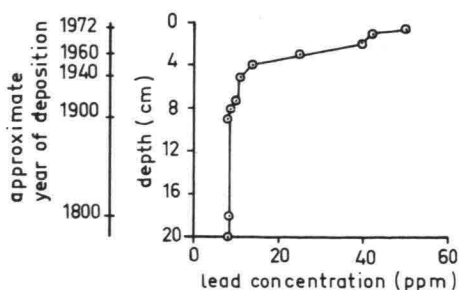


Figure 24.1 LEAD CONCENTRATION  
IN SEDIMENT BASCOM (1974-1)

Thermal discharges may be either warmer (power station cooling water) or cooler (liquified natural gas conversion) than the surrounding water. Most marine life can adapt to the modified thermal climate near such a heat source or sink, but are often killed either mechanically or as a result of abrupt temperature and pressure changes as they are drawn through the plant. Heat discharged into the oceans is only of local biological significance. It might well be combined in the future with the discharge of nutrients to stimulate marine life for the benefit of man.

Radioactive wastes form the seventh category of pollutants. Since water forms a relatively good shielding radioactive moderator, disposal of such wastes at sea can seem attractive. The direct danger to marine life is less than that to man because marine life can tolerate a larger radiation dose before it becomes fatal - van Staveren (1974). Such a reasoning can be dangerous, however, since man can conceivably ingest a fatal dose of radio poisons from seemingly healthy fish.

### 24.3 Control Measures

The most common control measures are legal sanctions applied against those who cause pollution. Starbird (1972) describes the success possible with a river. When rivers cross international boundaries, their cleanup can only be accomplished by all of the bordering nations working together. The attempts to clean up the Rhine exemplify the frustrations; the British have had much more success with the Thames.

Legal restrictions must be realistic, however. Pollution reduction levels must be attainable and consistent with other standards. Bascom (1974-2) points out an example of unrealistic restriction. "In Los Angeles (U.S.A.), the level of 'pollutants', such as arsenic and copper, in municipal drinking water is higher than can be legally discharged into the ocean." This is an example of a ridiculously strong restriction.

On a more humorous level, a common joke in yacht clubs in the U.S. in the early seventies was that anti-pollution laws were becoming so strict that diapers would soon be required on seagulls.

### 24.4 Proposed Disposal Systems

It has already been alluded that the oceans can be an ideal disposal place for some wastes. The most promising are heat and nutrients which could be harnessed in the sea to increase food production via fish farming.

Whether or not other wastes are dumped into the oceans, they must be disposed of in some way. Some people propose disposal of the more undesirable wastes by dumping in the deep sea. The consequences of such actions deserve careful study; unexpected things can happen as is reported by Jannasch and Wiersen, cited in *Scientific American* (1973). It appears that biochemical decay processes are greatly retarded by pressure. Thus, "since natural re-cycling processes are nearly at a stand still in deep water, these areas are not appropriate dumping grounds for organic wastes".

The above quotation is in contrast with the proposal of Bostrom and Sherif, also reported in *Scientific American* (1972). They propose compacting and then disposing of all sorts of wastes in ocean regions called subduction sinks. At these locations - usually deep ocean trenches - crust material is being drawn down to the earth's mantle. They indicate that all of man's wastes amount to less than 1/250 of the volume of material drawn into the mantle. They admit that there are several details yet to be worked out for this plan, however.

One of the more important of these problems is that this large volume of material is drawn downward over a large area at a very low rate - millimeters per decade. Thus, any unit of waste material deposited in one of these subduction sinks will remain exposed for such a long time that containment of the waste remains a serious problem.

### 25.1 Introduction

Sediment transport plays an important role in nearly every coastal engineering problem. Frequently a shortage of material occurs at some location (undesired erosion); at other places an overabundance of material can be just as troublesome (siltation of a navigation channel, for example). An important goal of coastal engineering research is to predict the sediment transport rates along a coast. Compared to similar predictions for rivers, coastal engineering calculations tend to be an order of magnitude more difficult; oscillating water movements under waves and the multitude of current-causing forces increase the number of variables involved to a considerable degree. Before discussing beach profile forms and offshore-onshore sediment transport, attention will first be directed toward the more general sediment transport relations involved along coasts.

### 25.2 Basis Principles of Sediment Transport

Sediment transport in a coastal zone can be treated, in principle, much like that in a river. In direct analogy to the situation in a river, the sediment transport rate can be described as the product of velocity,  $V$ , and sediment concentration,  $c$ , integrated over the water depth. In rivers, both  $V$  and  $c$  vary only very slowly as functions of time,  $t$ , or horizontal position,  $x$ . They do vary as a function of elevation, of course, and this variation makes the use of the integral necessary. In a coastal zone, where waves play an important role in the water motion, the water velocity,  $V$ , and even the concentration,  $c$ , usually vary strongly as a function of time - on a scale comparable to the wave period. A reliable computation of the sediment transport rate now becomes:

$$S(t) = \int_{-h}^0 c(z,t) V(z,t) dz \quad (25.01)$$

Unfortunately, insight regarding  $c(z,t)$  is at best very poor as is demonstrated in figure 25.1 which shows nearly 100 different records of  $c(t)$ , all measured at a constant elevation and under identical regular wave conditions.

Hardly anything is known about the behavior of  $c(z,t)$  under irregular breaking waves common along coasts.

Sediment transport calculations in the direction of wave propagation are essentially impossible (as of early 1982) based upon equation 25.01; too little is known about  $c(z,t)$  and the average value of  $V(z,t)$  is nearly zero making the computations involved very sensitive to small errors. Since refraction makes the angle of wave incidence small along a shore, onshore-offshore sediment transport is difficult to handle using 25.01. Empirical methods, entirely indepen-

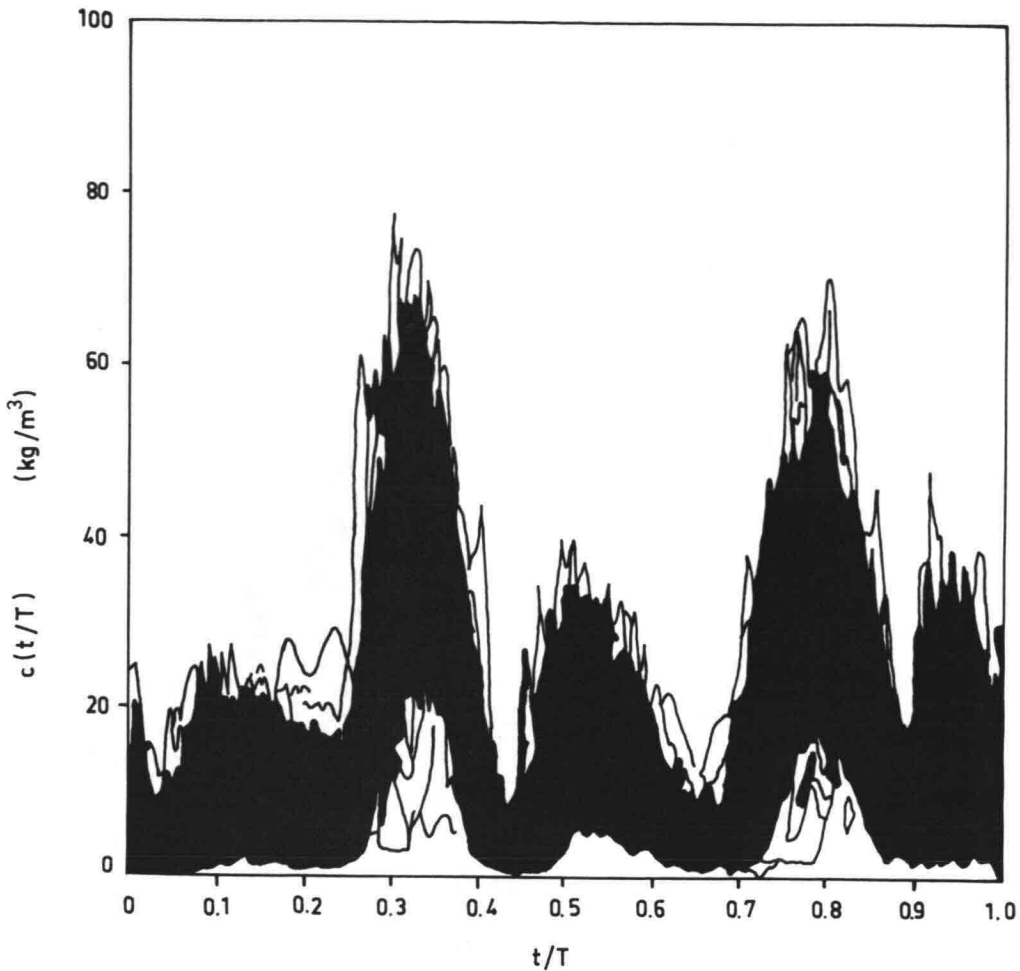


Fig. 25.1 Sediment concentrations as a function of time (99 individual records)

dent of equation 25.01 have been developed, however. One of these, by Swart (1974 and 1976) is discussed further in volume II; the remainder of this chapter will attempt to give only a qualitative description of shoreline profiles.

### 25.3 Beach Profile Form

A typical beach profile form has been sketched in figure 25.2; the frequently encountered nomenclature has also been included in that figure.

Waves approaching with crests parallel to a coast under constant boundary conditions (water level, wave height and wave period) will ultimately produce a stable beach profile. This type of situation can easily be reproduced in a wave flume where after an experiment has continued for a long enough time a stable, unchanging beach profile results. Beach material is still in suspension, but no net transport of material occurs along the profile under such stable conditions.

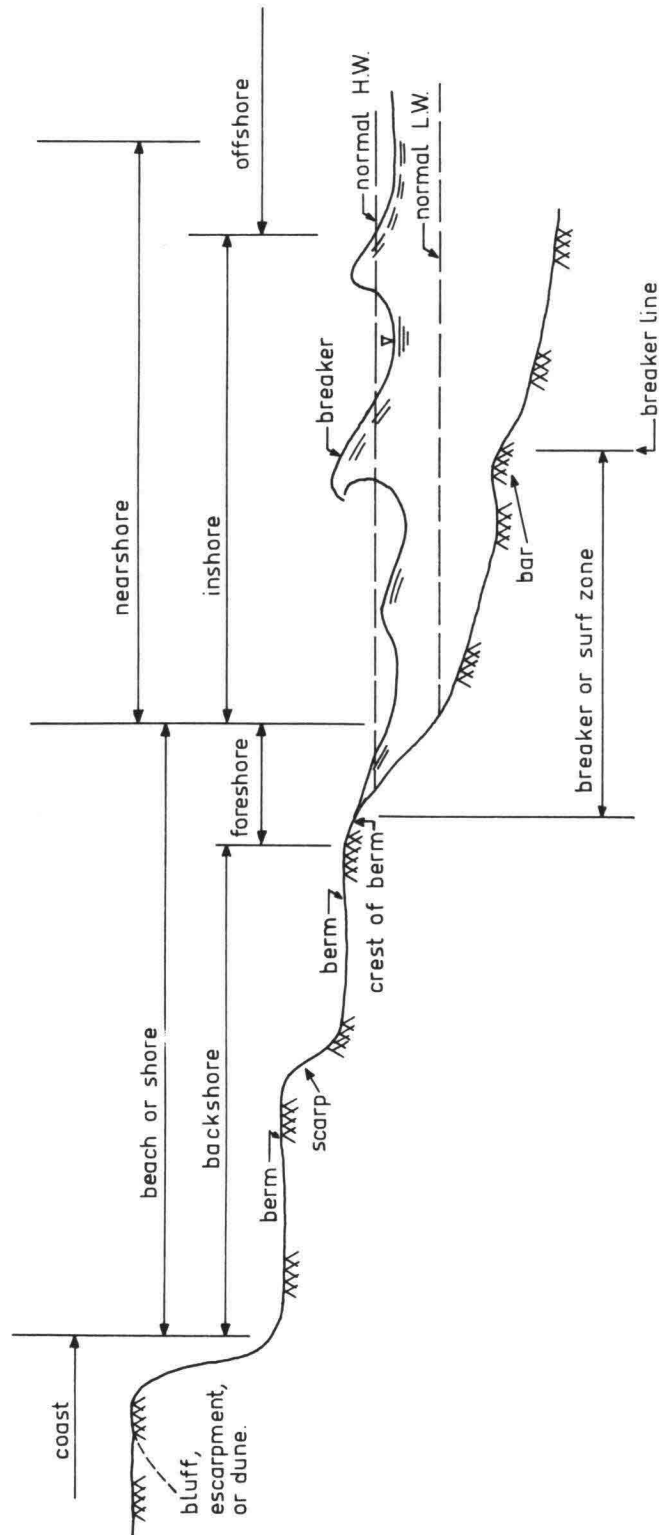


Figure 25.2 SANDY BEACH PROFILE NOMENCLATURE ( scales are distorted )

The form of such a stable beach profile depends upon the above-mentioned boundary conditions as well as on the sediment grain size. Given constant hydraulic conditions, coarser beach materials tend to form steeper beach slopes; gravel beaches are far steeper than are sand beaches. On the other hand, if the beach material is of a given diameter, then higher waves tend to result in flatter beach slopes.

Additionally, since the depth at the outer end of the beach profile - the breaker line in figure 25.2 - is also greater for higher waves, these two effects combine to produce much wider beach profiles under more severe wave conditions.

The time needed to establish an equilibrium beach profile is seldom provided in nature. Wave or water level (tide!) conditions change too rapidly for a real equilibrium ever to be reached. Indeed, a beach is always striving to attain an ever-changing equilibrium. Such changes are not always that obvious during a single tide period, but seasonal variations such as a "summer profile" or "winter profile" are rather well known to every regular beach visitor.

If one extends his period over which conditions are averaged to include several years, one finds that the hydraulic boundary conditions become very stable and the beach profile follows suit<sup>\*</sup>; long term beach profile form changes are usually very modest. Shorter term (seasonal or even single storm) beach profile changes can be seen as a sort of "noise". With a beach profile in such a state of dynamic equilibrium such "noise" can still be very important, however, as will be discussed later in this chapter and in chapter 30.

One should realize that in such a state of dynamic equilibrium, sediment movement is *always* taking place along the beach profile; material is constantly being eroded somewhere along the profile and deposited somewhere else. The occurrence and rates of such local erosion and deposition are nearly impossible to predict.

The seasonal profiles mentioned above (summer and winter profiles) are often referred to in the literature on coastal morphology. Summer profiles are usually described as accretion profiles. This last qualification is true only in the zone near the still water-line; the sediment deposited there is eroded further offshore to satisfy a mass balance. Winter profiles are often called erosion profiles. Such a distinction between profile types is most pronounced for beaches where there is little tide combined with sharp distinctions in wave climate over the year. Along the Dutch coast such seasonal distinctions in wave climate are not extremely pronounced and a reasonable tidal variation further obscures such a beach profile distinction.

Using the insight presented in this section one is frequently able to at least "understand" the processes occurring on a given beach after a bit of observation of that beach profile. Figure 25.3 shows typical sand and water movements on a beach.

---

\* Longshore transport (ch.26) can still cause the entire beach profile form to move horizontally, sometimes over considerable distances, however.

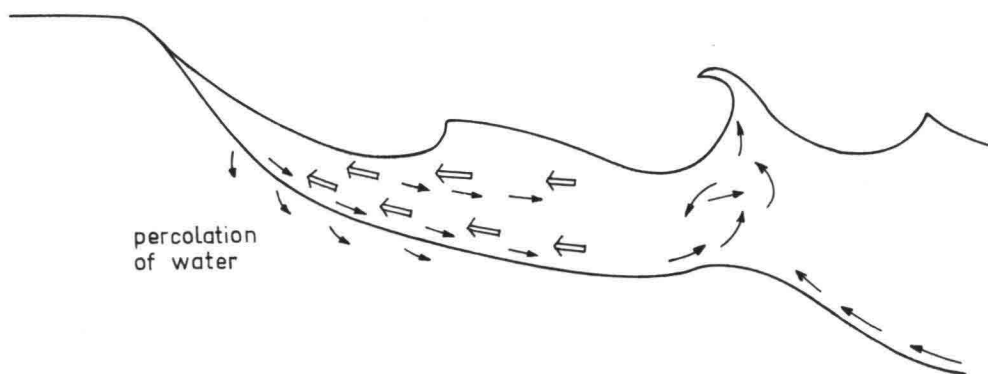


Figure 25.3 MOVEMENTS OF SAND AND WATER DURING CALM WEATHER IN THE BREAKER ZONE  
 ← movement under crest  
 → movement under trough  
 sketch not to scale

#### 25.4 Dune Formations

Dunes often form an important role in a more complete coastline profile. Under normal conditions the wind is the predominant cause of material transport on dunes. (This predominant role is fulfilled by waves and currents on the rest of the beach.) Dry and even wet sand can be transported by winds. Onshore directed winds blow sand grains from the beach into the dunes, and dunes in some areas can reach spectacular dimensions with heights of several tens of meters - see figure 25.4.

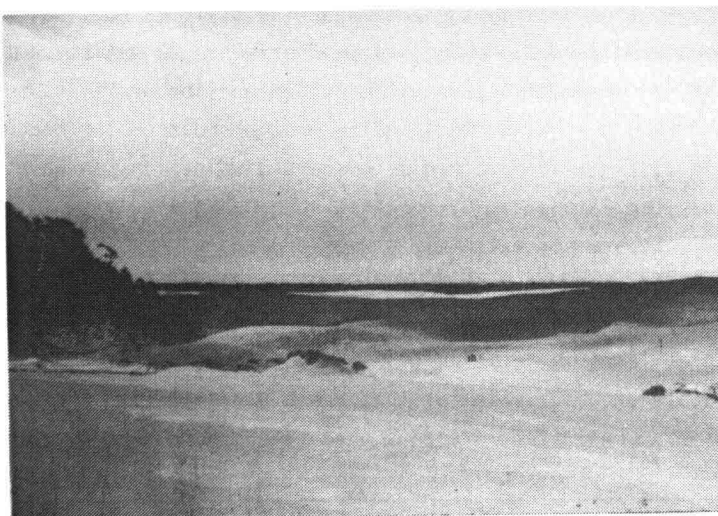


Figure 25.4  
 DUNES ALONG THE COAST OF OREGON, U.S.A

Dunes can play an important role in the protection of a low-lying hinterland from the sea. Under such conditions - such as in most of The Netherlands - proper dune management is essential. Dune stabilization using vegetation or small fences is a well-known technique used in many parts of the world.

The prevailing wind direction relative to the coastline also plays an important role in dune formation and integrity. This can be demonstrated along the Dutch coast where a predominantly south-west wind prevails. Well developed dunes can be found along the west coast of Holland where the wind blows more or less perpendicularly to the coast. By contrast, the dunes along the coast of the Wadden Islands in the North of The Netherlands are of much poorer quality. Here, the wind direction is nearly parallel to the coast.

### 25.5 Dune Erosion

Under "normal" weather conditions the dune portion of a coast profile behaves more or less independently from the rest of the beach. Under storm conditions - especially in areas such as the Southern North Sea where storms can increase the still water level considerably - this condition of independence is abruptly ended. Storm water level increases of up to a few meters occur more or less regularly along the Dutch coast. Storm surge levels about 3 m above normal were measured during the historic floods in 1953; 4.0 m is a commonly accepted design surge level today in Holland.

Under such conditions the dunes, themselves, are exposed to direct wave attack and erosion of the dunes will result - see figure 25.5. At the start of dune erosion the beach profile is much steeper than the equilibrium profile associated with the storm water level and waves. Material is thus eroded from the toe of the dunes and deposited further offshore in an attempt to restore equilibrium. The erosion of the dune toe causes the upper portion of the dune to cave in forming a steep scarp, so typical of eroding dunes. Usually (and

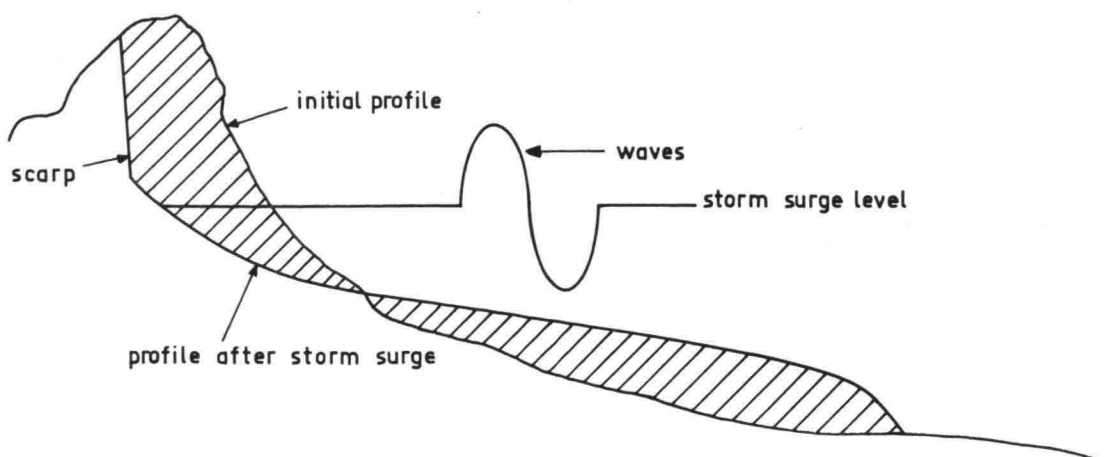


**Figure 25.5** Dune erosion. (distorted scale)

we can only be thankful for that) the storm conditions do not last long enough for the corresponding equilibrium beach profile ever to be reached. Even so, under extreme conditions along the Dutch coast (water level including tide about 5 m above MSL and a significant wave height of about 8 m) several hundred cubic meters of sand can be eroded along each meter of coastline in a period of only a few hours. Being a bit more specific, an erosion from above the still water level of  $300 \text{ m}^3/\text{m}$  can be expected within about 5 hours while some 25 hours are needed to erode a total of about  $400 \text{ m}^3/\text{m}$ .

A design code for dunes along the coast of The Netherlands is nearing completion in 1982. Even with the help of such a code, the proper design of a dune-based shore defense can be a challenging task.

When analysis shows that a given dune formation is inadequate to withstand a given design condition, then one must resort to the use of man-made extra protection. This will be discussed in chapter 30.

### 26.1 Introduction

The computation of sediment transport parallel to the coast can, in principle, also be handled via equation 25.01. This problem even turns out to be a bit simpler now, because a relatively constant longshore current velocity is usually present and the additional velocity components due to waves act nearly perpendicular to the sediment transport direction in the longshore transport situation. This latter, minor influence of the waves means that  $V(z,t)$  will now have a non-zero time average and will not vary too much in magnitude during a wave period. In turn, the concentration of sediment in the flow is also more stable now as a result of the constantly present current. This allows equation 25.01:

$$S(t) = \int_{-h}^0 c(z,t) V(z,t) dz \quad (25.01) \quad (26.01)$$

to be simplified without too much error by taking some time averages (denoted by the superscript bar):

$$\overline{S(t)} = \overline{S} = \int_{-h}^0 \overline{c(z)} \cdot \overline{V(z)} dz \quad (26.02)$$

The determination of the terms in equation 26.02 is considerably simpler than corresponding measurements needed for (26.01). An average longshore current velocity can be measured using a dye tracer or floats and an average concentration can be found by continuously extracting a water sample with a small pump.

The longshore current to be substituted in equation 26.02 can, in principle, have many different driving forces but in most beach situations this current is driven predominantly by breaking waves which approach the coast at some angle,  $\phi_{br}$ , measured at the outer edge of the breaker zone. This longshore current is concentrated more or less in the surf zone and occurs regardless of whether there is sediment transport. Methods to compute this current are outlined in volume II; it is sufficient, here, to realize that this longshore current in the breaker zone provides the transport medium for longshore sediment movement.

Since the wave motion in the breaker zone is nearly perpendicular to the resulting current, the major influence of the waves is to stir more material loose from the beach, thereby increasing the sediment concentration term in equation 26.02.

Even with this knowledge, computation of longshore sediment transport rates using equation 26.02 remains cumbersome. Since longshore transport plays such an important role in long term coastal erosion

or accretion problems, a considerable research effort has been expended to derive sediment transport formulas which are convenient to use. One of the simplest of these, the CERC\* Formula will be treated in some detail here. A more complete treatment of this and other formulas is included in volume II.

## 26.2 The CERC Formula

If one set of special conditions prevail, namely that the longshore current in equation 26.02 is driven exclusively by the waves, then both  $c$  and  $V$  in that equation can be related in some way to the incident wave conditions. Carrying this philosophy a bit further, a formula for the longshore sediment transport rate was derived by the Coastal Engineering Research Center having the form:

$$S = f(H^2, c, \phi) \quad (26.03)$$

where:

- $c$  is now the wave speed,
- $H$  is the wave height,
- $S$  is the sediment transport, and
- $\phi$  is the angle between the waves and the water depth contours.

Being a bit more specific,

$$S = 0.040 \left[ H_{sig}^2 \right]_{br} c_{br} \sin \phi_{br} \cos \phi_{br} \quad (26.04)$$

where:

- $H_{sig}$  is a significant wave height, and the subscript  $br$  refers to conditions determined at the outer edge of the breaker zone.

If the water depth contours in the area are all parallel, then equation 26.04 can be transformed, using information from chapters 9 and 5 to:

$$S = 0.020 \left[ H_{sig}^2 \right]_o c_o \sin \phi_{br} \cos \phi_o \quad (26.05)$$

where the subscript  $o$  now refers to deep sea conditions.

Some users prefer to use a root mean square wave height in equations 26.04 and 26.05. The constant coefficient must, of course, now be doubled - see equation 10.03.

The value of the coefficient to be used in the CERC Formula is a subject for continual controversy. The values used above reflect the best judgement as of early 1982.

Even though it is difficult to give a more exact physical derivation of the CERC Formula, it can be a helpful aid for understanding and even solving a number of practical problems. A price has been

---

\* Coastal Engineering Research Center, a U.S. Government coastal research institute.

paid to achieve its simplicity. One price has already been mentioned; it neglects all longshore current driving forces except those from the waves.

A second limitation is that the sand transport is independent of the sand properties such as grain size and density. Also, the beach slope, and hence the type of breakers, is ignored. This has happened because the observed data which led to the CERC Formula were made on sandy beaches having more or less the same properties. The accuracy of the data was not sufficient to allow inclusion of these variables in the computational model.

A last major limitation is that only the total sand transport in the breaker zone is given. It is often handy to know how this transport is distributed over the width of the breaker zone. Bijker and Svasek (1969) solved this by assuming that the longshore transport in some element of breaker zone width is directly proportional to the wave energy dissipation - or better, energy transformation - within that width element. This assumption exposes another basic objection to the CERC Formula (and all other energy - based formulas, too): Only a few percent of available energy is actually used to transport the sediment along the coast. Small changes in this percentage can result in large changes in sand transport; this is not healthy for the formula.

Another, entirely different approach has been developed in an effort to overcome the limitations mentioned above. This approach is described briefly in the next section.

### 26.3 The Bijker Formula

Bijker (1967) proposed that the combined effect of all of the possible force components be determined and that the longshore current and littoral transport be determined based upon this. The modern development of this idea is outlined very briefly here and is described in detail in volume II.

The influence of waves on the longshore current along a coast manifests itself via the gradient of the longshore component of momentum flux of the waves. This is explained in detail in volume II. In principle, this gradient of the longshore component of momentum flux, combined with other driving fluxes resulting from tides, etc., provides the driving force acting on a water mass. In a steady state condition, these forces are balanced by a bed friction force acting on the longshore current as it is disturbed by the waves. The development of this equilibrium is discussed in detail in volume II as well.

This technique allows all driving force components to be included in the longshore current determination, and its velocity distribution within the breaker zone is also revealed. With the details of the current known, it is a reasonably simple matter to combine this with a sediment transport formula in order to obtain a littoral drift prediction. Obviously, the distribution of this transport of sand is also revealed using such a method.

### 26.4 Applications

Longshore sediment transport calculations are seldom a coastal engineering objective in themselves. Usually such computations form only a step in the analysis of a larger coastal morphology problem. Most of these morphological problems involve long term coastal erosion resulting from longshore sediment transport processes. Accretion problems sometimes present themselves - beach houses that come to be too far away from the water - but usually cause less panic.

It is very important to realize that the presence of a longshore sediment transport does not, of itself, lead to either erosion or deposition. Indeed, if one considers a portion of a beach as sketched in plan in figure 26.1, the coastline will remain stable as long as  $S_{in}$  is equal to  $S_{out}$ . On the other hand, if  $S_{out}$  is greater than  $S_{in}$  ( $S$  increases as we move along the beach;  $\frac{\partial S}{\partial x} > 0$ ) beach material must be eroded in the area under consideration in order to maintain a mass transport balance. It should also, now, be obvious that accretion results from a decrease in sand transport:  $\frac{\partial S}{\partial x} < 0$ .

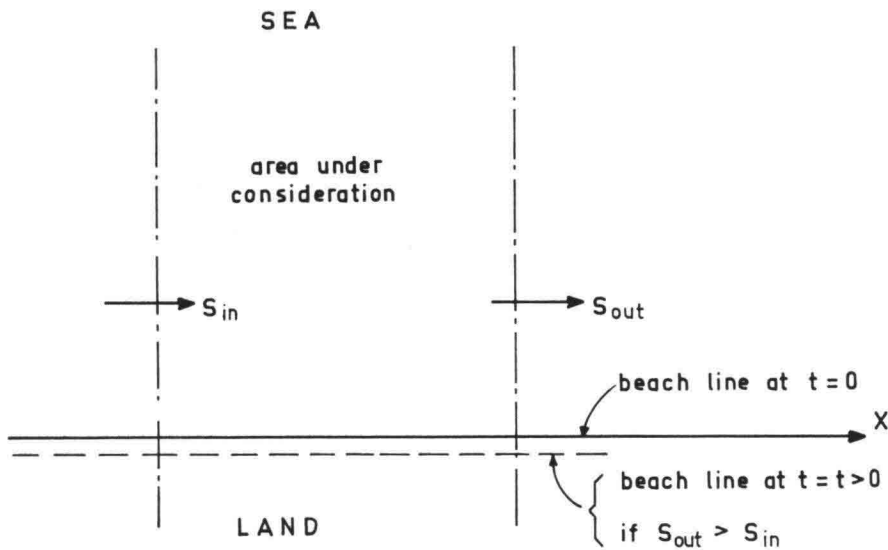


**Figure 26.1** Longshore Transport Continuity

A sand transport gradient is responsible for longshore coastal changes. By contrast, onshore and offshore transport from the previous chapter only moves material along the beach profile perpendicular to the coast; as such it has no direct influence on this conclusion concerning longer term changes in a beach position.

Gradients in the longshore transport can be caused by changes in any of the factors in equation 26.04 as one proceeds along a coast, but the angle of wave incidence usually changes the most easily although the wave height sometimes changes dramatically as well. A curved coastline will always be subject to a sand transport gradient assuming that the offshore wave conditions do not vary along the shore. A convex coast (as seen from the sea) will erode while a concave coast will accrete. In general, a coastline will attempt to re-orient itself parallel to the direction of the approaching wave crests.

Since erosion problems are usually more pressing than accretion problems, let us turn our attention to a segment of a convex coastline shown in plan figure 26.2a. The resulting sand transport is plotted as a function of distance along the coast,  $x$ , in figure 26.2b. As expected,  $S$  increases with  $x$  (line 1) and erosion of the entire coast segment - including the "shoreline of interest" in the figures occurs.

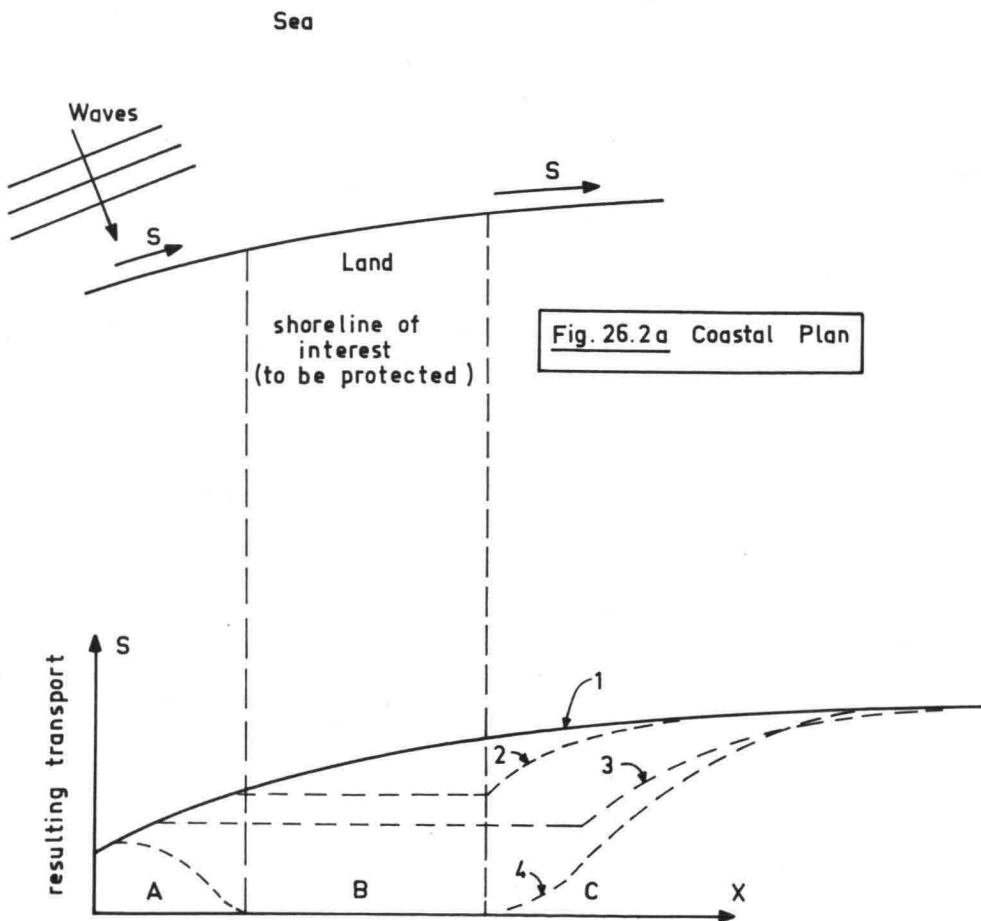


Fig. 26.2b Sediment Transport rates

A very common coastal morphology problem involves halting the effect of erosion on the shoreline of interest - segment B in figure 26.2b. There are two possible solutions to such a problem: nullification of the effects of erosion or modification of the longshore transport curve - figure 26.2b - by artificial means.

The first solution amounts to tolerating the natural erosion process and replacing the eroded material from time to time by supplying sand from elsewhere. Modern dredging technology makes such a solution technically feasible in many cases. Its friendliness for the total environment makes such a solution attractive as well. A disadvantage is that such a solution is not permanent; sand must be supplied from time to time forever.

The second solution approach involves changing the curve of  $S$  versus  $x$  - curve 1 in figure 26.2b - so that the sand transport gradient is zero along "our" stretch of coast. In other words, we want to get a constant sand transport along segment B of the coast. In figure 26.2b this means that segment B of the  $S$  curve must be horizontal; Lines 2, 3, and 4, all satisfy this requirement. Of these, line 2 represents the least complex solution, but notice that lines 3 and 4 will both have the same stabilizing effect on beach segment B. Since the seriousness of the problem is dependent upon  $\frac{\partial S}{\partial x}$ , lines 2, 3, and 4 will have different influences on the beach segments A and C.

Solution line 2 has no influence at all on area A. The erosion which occurs there is apparently not a problem. The steep slope  $\frac{\partial S}{\partial x}$  in region C near the boundary BC indicates that the erosion problem for our neighbor will become more severe locally, immediately adjacent to section B.

Solution line 3 stabilizes a portion of region A as well as region B and even part of C. Erosion ultimately takes place further along in region C as the original sand transport curve is restored.

What happens with line 4? Now, the negative sediment transport gradient means that sand will accumulate in region A adjacent to region B. There is now no sediment transport in region B - something which is not necessary for stability. Region C now is subjected to the most severe erosion of all the solutions, the rate of erosion will be highest where  $\frac{\partial S}{\partial x}$  is greatest.

One can conclude that solution line 2 is the best of these type of possibilities. It limits the area of beach change to a rather restricted area but will need some coastal defence structures - chapter 30 - in order to accomplish this solution.

Extra Notes

### 27.1 Physical Description

Mud coasts occur near the mouths of rivers which discharge great quantities of fine (clay) sediments into the sea. This supply must be greater than the capacity for the sea to disperse these materials toward deeper water offshore.

A pure mud coast is very low - seldom higher than a spring high tide level. Since the slope of the shore profile is very flat - 1:1000 is not uncommon - vast mud flats are found before the coast. Accretion, if present, leads to the formation of a broad, flat, poorly drained, swampy coastal plain. Vegetation eventually forms a layer of peat on the surface. These coastal plains can become very fertile agricultural land if drainage and protection from flooding are provided.

Some sand is also present along most mud coasts. Since the transport process for sand is basically different from that for mud (see section 2 of this chapter) the two materials tend to segregate. The sand can be found as isolated segments of beach, perhaps even with a berm and dunes as described in chapter 25. These berms and dunes are sometimes found isolated in the coastal plain - evidence of past coastal development.

### 27.2 Properties and Transport Process

Clay particles (smaller than 2  $\mu\text{m}$ ) are generally transported in suspension. Waves and strong currents can bring compacted clay into suspension, while only a weak current is needed to maintain this suspension. The sedimentation of suspended material is governed by the following equation

$$\text{Sedimentation} = \left[ Wc + \epsilon \frac{dc}{dz} \right]_{z=0} \quad (27.01)$$

where:

$c$  is the concentration of sediment at elevation  $z$  above the bed (in general),

$\epsilon$  is the eddy viscosity coefficient, and

$W$  is the particle fall velocity in still water.

In order to determine the sedimentation equation 27.1 is evaluated at the bed,  $z = 0$  as a special case. More generally, (27.01) can be used to describe the sediment concentration profile in, for example, a river.

The fall velocity,  $W$ , above is the important soil parameter in equation 27.01. In general,  $W$  increases with increasing soil particle size. However, the concentration of sediment, if high enough, also influences the fall velocity, as the adjacent particles interact. Initially, for concentrations below about 5000 ppm by weight, the fall velocity will increase as the particle concentration increases. Above

about 7000 ppm the concentration of grains apparently becomes so large that the water flow between the grains is restricted; the fall velocity then decreases with further increases in particle concentration. Salt water - being more viscous than fresh water - experiences this decrease of fall velocity of slightly lower concentrations than does fresh water.

Flocculation, an independent process, can accelerate the deposition process (see section 22.7). Deposition of flocculated clay forms a very soft material commonly called sling mud. Its classification based upon silt concentration is shown in table 27.1. For convenience, some of the data is also plotted in figure 27.1.

Table 27.1 Properties of Sling Mud

Concentration of solids (mg/l)	Mass density (kg/m <sup>3</sup> )	Water Content		Material classification (-)
		by volume (%)	by Weight (%)	
0	1000.00	100.00	100.00	
100	1000.06			
200	1000.12			
500	1000.31			
1 000	1000.62	99.96	99.90	
2 000	1001.25			
5 000	1003.11			
10 000	1006.23	99.62	99.01	
20 000	1012.45			
50 000	1031.13			
100 000	1062.26	96.23	90.59	
200 000	1124.53	92.45	82.21	
300 000	1186.79	88.68	74.72	
400 000	1249.06	84.91	67.98	sling mud
500 000	1311.32	81.83	61.87	
600 000	1373.58	77.36	56.32	
700 000	1435.85	73.58	51.25	
800 000	1498.11	69.81	46.60	
900 000	1560.38	66.04	42.32	
1 000 000	1622.64	62.26	38.37	
2 000 000	2245.28	24.53	10.92	clay
2 650 000	2650.00	0.00	0.00	

The expression for the concentration mg/l is not dimensionless. A dimensionless and widely used expression is ppm, denoting parts per million. For low values of the concentration the difference is negligible, since the concentration hardly changes the mass or the volume. For greater concentration there is a marked difference which again varies with the use of volume and mass concentrations. An

example for a concentration of 300,000 ppm worked out using mass units, volume units and mg/l illustrates this.

$$a. \quad 300,000 \text{ ppm } \underline{\text{by mass}} \quad \frac{300,000}{10^6} = 0.3$$

$$\begin{aligned} \text{Total mass} &= 1000 \text{ kg} \\ \text{Silt} &: 0.3 \times 1000 = 300 \text{ kg} \\ \text{Volume silt} &= 300/2650 = 0.113 \text{ m}^3 \\ \text{Volume water} &= 0.7 \text{ m}^3 \\ \text{total} &= 0.813 \text{ m}^3 \quad \rho = 1230 \text{ kg/m}^3 \end{aligned}$$

$$b. \quad 300,000 \text{ ppm } \underline{\text{by volume}}$$

$$\begin{aligned} 1 \text{ m}^3 \text{ material} & \\ 0.3 \times 1 &= 0.3 \text{ m}^3 \text{ silt} \\ \text{Silt mass} &= 0.3 \times 2650 = 795 \text{ kg} \\ \text{Water mass} &= 700 \text{ kg} \\ \text{total} &= 1495 \text{ kg} \quad \rho = 1495 \text{ kg/m}^3 \end{aligned}$$

$$c. \quad 300,000 \text{ mg/l}$$

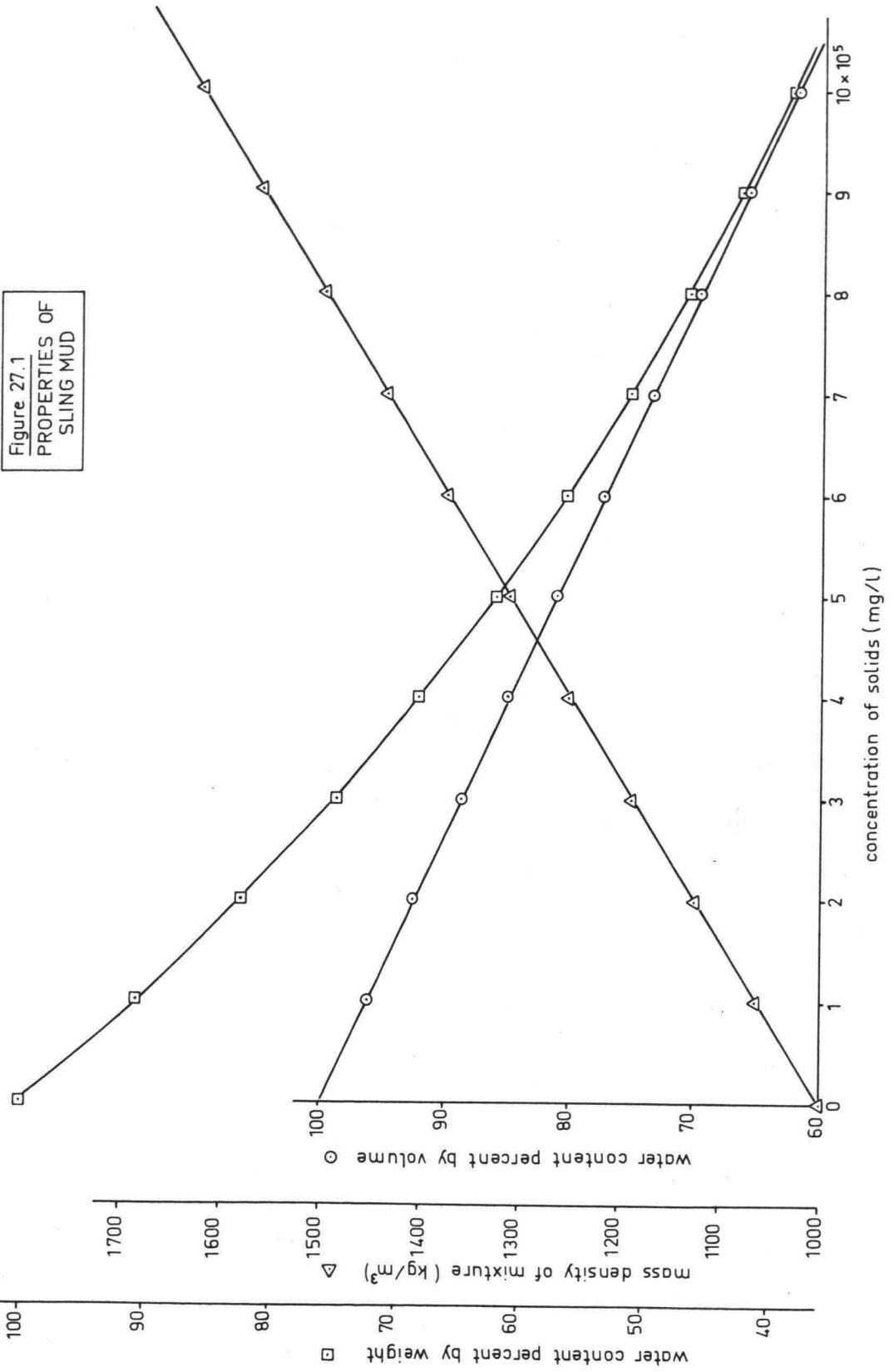
This is 300 kg silt per  $\text{m}^3$  volume

$$\begin{aligned} 300/2650 &= 0.113 \text{ m}^3 \text{ silt} \\ \text{rest is water} &= 0.887 \text{ m}^3 \\ \text{total weight} &= 887 + 300 = 1187 \text{ kg} \quad \rho = 1187 \text{ kg/m}^3 \end{aligned}$$

Another rather important question is: how much "dry material" is contained in  $1 \text{ m}^3$  of dredged material with a given bulk density  $\rho_s$ ? This can be answered after reviewing section 23.7.

As has already been pointed out in chapter 22, sling mud, a viscous water-clay mixture, can occur in large quantities along the coast and in channels. Ships can, with care, sail through it. It may even clean the barnacles off the ship's bottom! Its viscosity damps waves rapidly; even surface water waves are "absorbed" by it. Given enough time, this mud will eventually consolidate into a very soft soil.

Sand, on the other hand, is primarily transported as bed load rather than suspended load. This explains its tendency to segregate along a coast. Transport processes for sandy portions of mixed mud-sand coasts are the same as have been described in the previous two chapters. If much sand is present, it can form a nearly continuous layer covering a clay subsoil. Such a formation can be found, for example, in the Gulf of Venezuela.



### 27.3 Influence of Rivers

Rivers and estuaries discharging on a mud coast are characterized by deep (about 20 m) tidal estuaries which discharge over shallow bars at their mouths where the maximum depth is usually only 3 to 5 m.

Both the bars and the estuary are important for determining the sediment transport. Tidal currents, fresh water river discharge and its seasonal variations, as well as density currents are important. Generally, sediment is transported from the bars into the estuary during the dry season as the density tongue penetrates further upstream. As the river flow increases at the start of the high runoff season, these sediments are again spewed out of the estuary along with the sediment discharge of the upper river. This can lead to very rapid accretion in the bar area with all of its subsequent dredging and navigation problems.

### 27.4 Examples

Mud coasts can be found in many parts of the world, examples include:

- a. The coast of Languedoc, west of the mouth of the Rhône in southern France.
- b. The coast of Louisiana, west of the Mississippi River Delta on the Gulf Coast of the U.S.A. A chart of this delta is shown in chapter 29.
- c. The northern coast of the Gulf of Siam, near the mouth of the Chao Praya River in Thailand.
- d. The coast of the Gulf of Martaban with sediment supplied by the Irrawaddy, Sittang, and Salween Rivers in Burma.
- e. The northeast of South America, between the mouths of the Amazon and Orinoco Rivers. Some aspects of the coast of Suriname, a portion of this 1600 km coast, are so special they are discussed in the following section.

### 27.5 The Coast of Suriname

The coast of Suriname is unique in that an enormous supply of sediment from the Amazon River is distributed by a relatively calm sea. This description is abstracted from Allersma (1968).

The flow in the Amazon is in the order of  $200\,000\text{ m}^3/\text{s}$  (compared to the Rhine -  $2200\text{ m}^3/\text{s}$ ). The sediment supply is in the order of  $7 \times 10^8$  tons per year. Along the coast of Suriname, 98% of the bottom material has a diameter less than  $50\ \mu\text{m}$ , with a mean diameter of about  $1\ \mu\text{m}$ . The total transport of sediment toward the west along this coast is estimated to be  $100 \times 10^6$  tons per year. The mud coast extends to a depth of about 20 meters and is about 30 km wide with an average slope of about 1:1500.

This coast has a remarkable pattern of wave - like depth contours. Huge shoals extend from the shore at more-or-less regular intervals of about 45 km - figure 27.2A. Bottom slopes on these shoals range

from 1:500 to 1:3000. The shoals move along the coast toward the west with a speed of about 1.5 km/year. This is accomplished by erosion of material from the eastern side of the shoals combined with deposition on the western side. About  $100 \times 10^6 \text{ m}^3$  of sediment move along the coast in this way each year. This erosion and deposition is shown in figure 27.2C. The influence of waves on this process is evidenced by comparing figures 27.2C and 27.2D. Deposition generally can be associated with areas of lower wave height - indicated by more widely spaced wave orthogonals (See chapter 9).

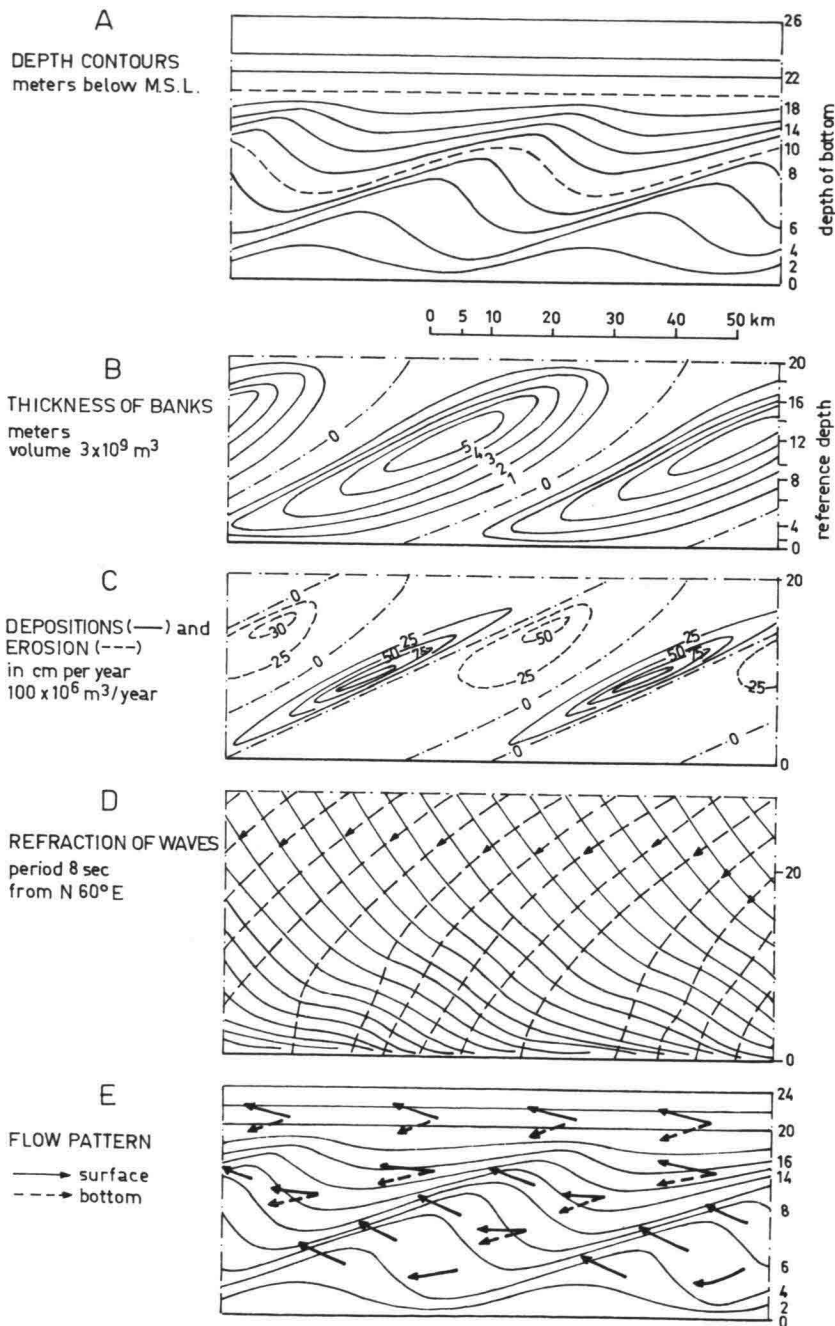


Figure 27.2 SCHEME OF FEATURES ABOUT MUD SHOALS

28. COASTAL FORMATIONS

L.E. van Loo

W.W. Massie

28.1 Introduction

The purpose of this and the following chapter is to illustrate the various coastal formations found in the world and to explain the reasons for their existence. Ideas developed in previous chapters describing the water and sediment movements in rivers and along coasts will now be combined to provide the necessary explanations.

Several additional photos and descriptions of coastal formations illustrated in this and the following chapter are included in the *Shore Protection Manual*. In addition, Shepard and Wanless (1971) provides a large collection of spectacular photos along with descriptions of the physical processes.

Also, much can be learned from a careful study of seamen's navigation charts. Portions of such charts are used in these chapters to illustrate many of the coastal formations.

One additional principle remains to be explained, however. Consider an infinitely long, straight sandy coast having parallel depth contours. Such a coast was sketched in chapter 9, figure 9.1. If waves approach this coast at a uniform angle along its entire length, and there are no other current driving forces such as tides, then there will be a constant, uniform transport of sand along this coast. There will be no erosion or deposition even though a continuous flow of sand passes along the coast. What, then, causes erosion or deposition? This is caused by a *change* in transport or transport capacity along a coast. This change may result from changing any of the factors influencing sand transport, such as wave height and direction of approach - see chapter 26.

Natural, continuous beaches will not get our main attention in this chapter even though some of the formations to be discussed will look - at first glance - like long, uninteresting beaches. Beaches can develop even along rocky coasts, however. Figure 28.1 shows such a beach, nestled between rock outcrops on the eastern shore of the Adriatic Sea in southern Yugoslavia.

28.2 Spit

A spit is a pointed tongue extending into the sea. Its direction is usually a continuation of the shoreline from which sediment is supplied. Such a spit is shown in figure 28.2a, the north end of Block Island on the Atlantic Coast of the United States. Waves coming predominantly from the southwest cause a sand transport toward the north along the western shore of the island. As the water becomes deeper at the north end of the island, the waves no longer break, the sediment transport decreases and the spit builds out further. Figure 28.2b shows an oblique aerial photograph of this island, showing the spit.

Sandy Hook, near the entrance to New York Harbor (U.S.A.) is also a spit; they are rather common.

Spits can also form where a river mouth interrupts an otherwise straight coast. This will be discussed in the following chapter.

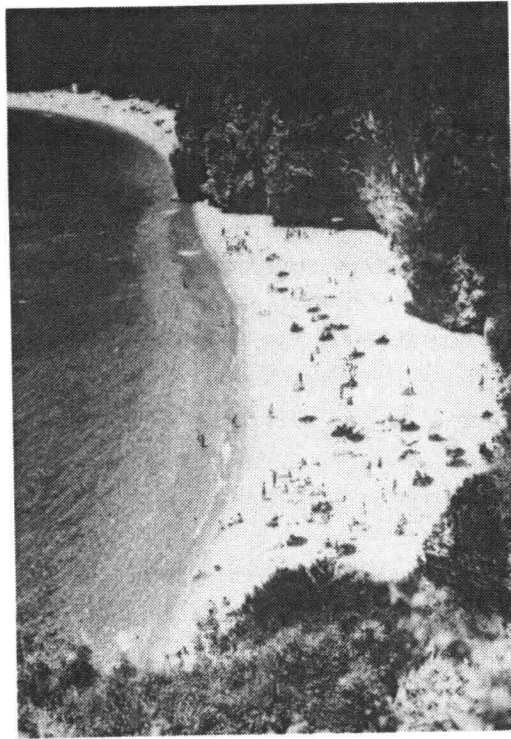


Figure 28.1  
A NATURAL BEACH ON THE ADRIATIC COAST OF YUGOSLAVIA

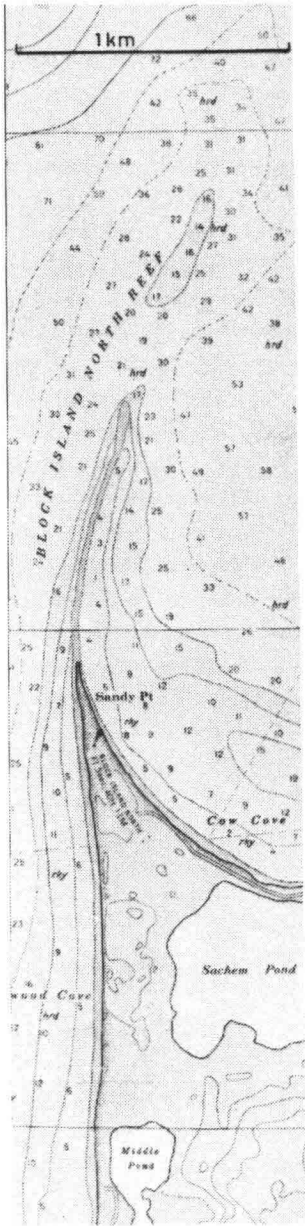


Figure 28.2a  
SPIT AT NORTH END OF BLOCK ISLAND, R.I., U.S.A.  
( depths in feet, scale as shown)



Figure 28.2b  
AERIAL PHOTO OF BLOCK ISLAND

### 28.3 Barrier

In contrast to a spit which is formed from material moving *along* the coast, barriers are built from material moving *perpendicular* to the coast - review chapter 25.

Barriers can form when there is sufficient supply of beach material from offshore, and the bottom bathymetry is such that the waves break at some distance from the coast, because of a broad shallow foreshore zone. A barrier will form at the outer edge of this shallow zone where the waves break; the supply of sand will eventually build up a berm - isolated from shore - which becomes the barrier. Storm waves can break over this barrier transporting sand into the shallows behind it. Severe storms can even break gaps in the barrier. If the variations in tide level are sufficient for the berm to become dry, then the wind can also transport material forming dunes along the barrier.

An excellent example of a barrier which has been broken is the string of Wadden Islands in the north of the Netherlands. (figure 28.3). A much more extensive nearly continuous barrier is found along the northwest coast of the Gulf of Mexico - figure 28.4. Cape Hattaras, North Carolina, on the U.S. Atlantic coast is another example of a barrier. When a barrier completely encloses an estuary, a salt or brackish lake usually results. Figure 28.5 shows such a barrier along the south coast of Martha's Vinyard Island on the U.S. Atlantic coast.

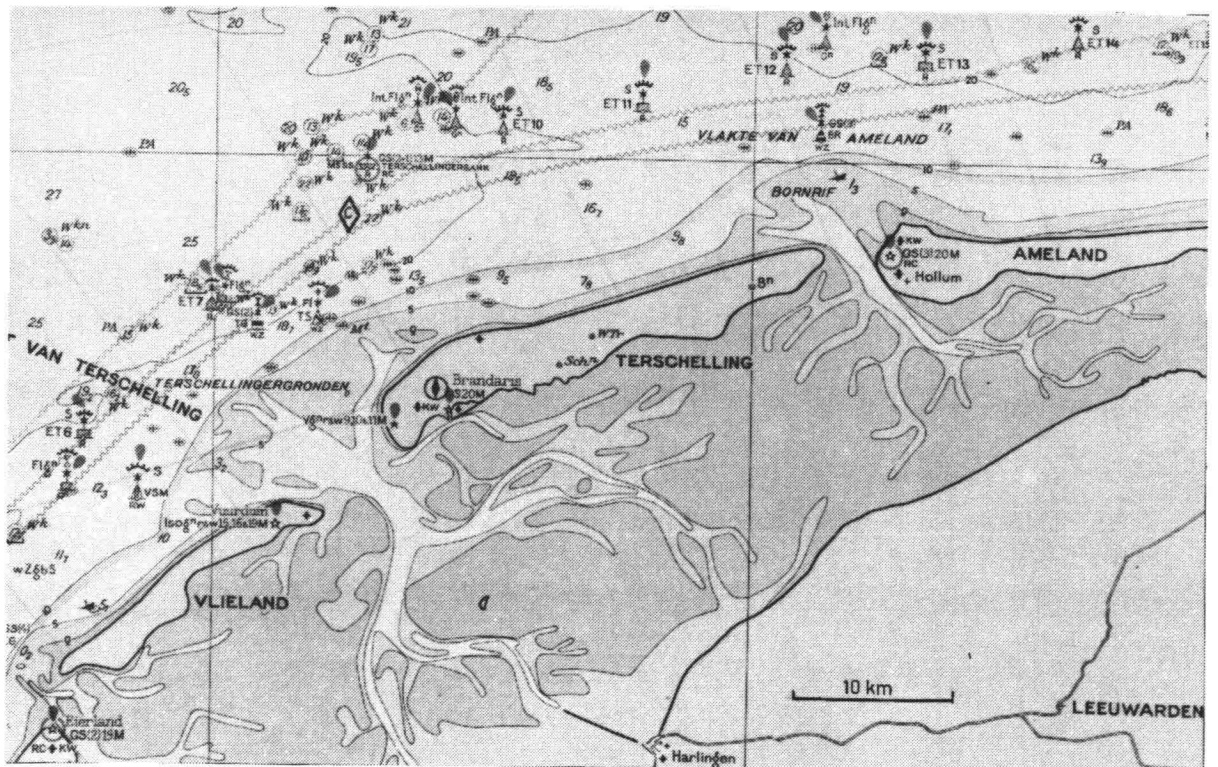


Figure 28.3  
PORTION OF WADDEN SEA AND ISLANDS,  
FRIESLAND, THE NETHERLANDS  
( scale as shown, depths in meters )

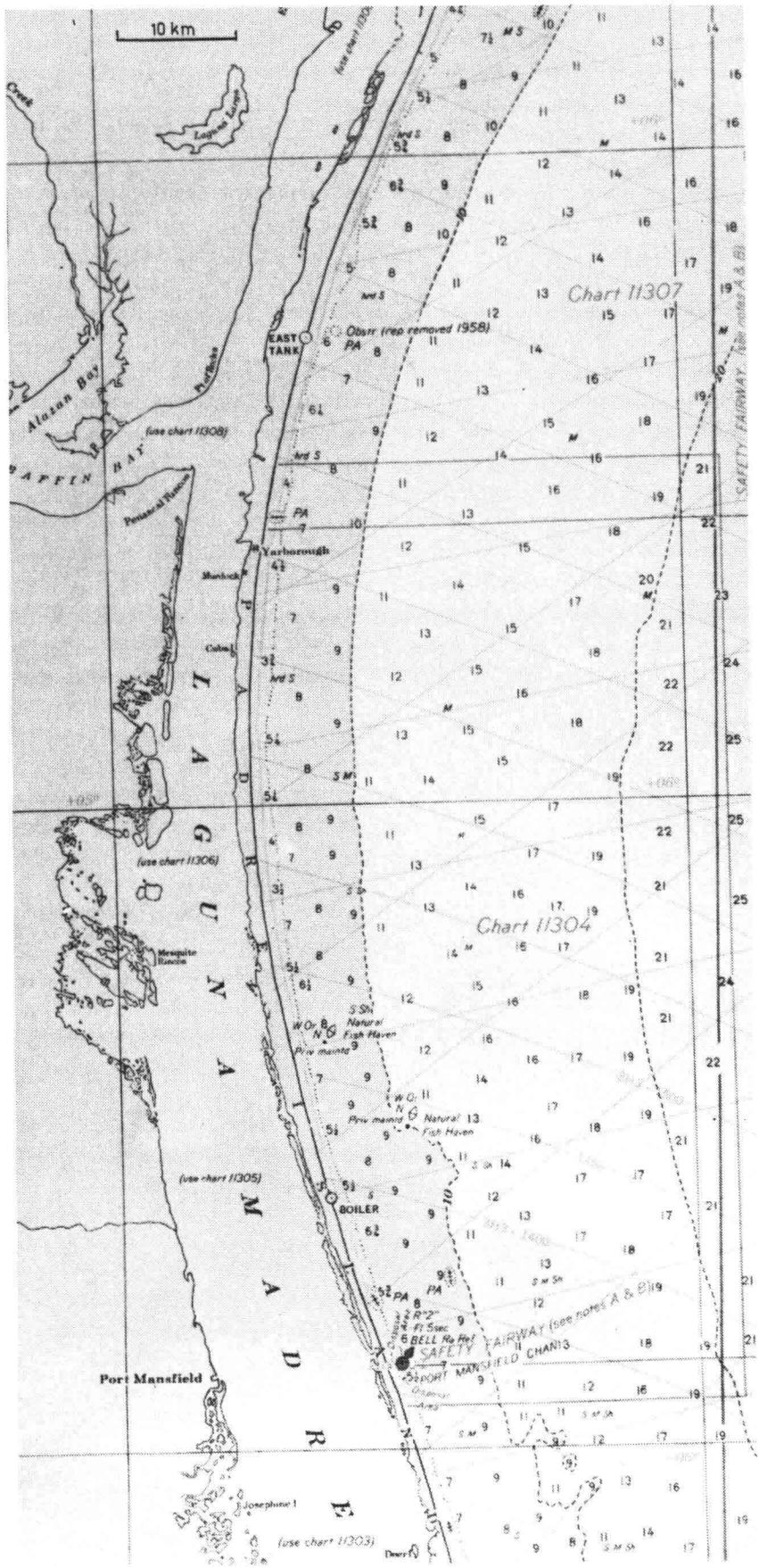
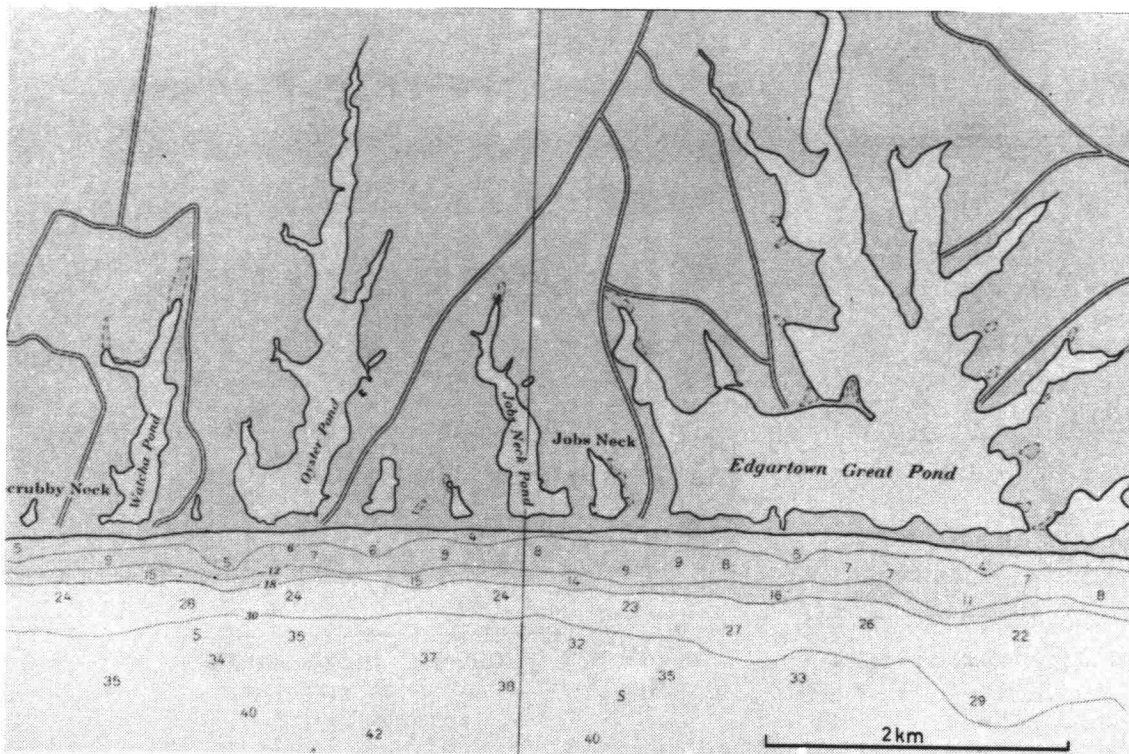


Figure 28.4  
BARRIER ALONG THE COAST OF TEXAS, U.S.A.  
( scale as shown, depths in fathoms )



**Figure 28.5**  
BARRIER ENCLOSING POND ON MARTHA'S VINYARD IS.  
( scale as shown, depths in feet )

#### 28.4 Tombolo

An obstacle before a coast such as a rock outcropping, an offshore breakwater, or even a shipwreck will reduce the wave activity in the zone of wave shadow between the object and the shore. Since the reduced wave activity in the shadow will result in a reduced sediment transport capacity, material being carried along the shore will be deposited in the shadow zone forming a tombolo. Initially, only a shoal will form. This can, however, develop into a point of land connecting the original shoreline to the obstacle. As with a spit, the development of a tombolo depends upon a transport of material parallel to the coast.

A small natural tombolo has developed behind Ram Island in Buzzards Bay on the North Atlantic coast of the United States. This area is protected from wave attack except from the south. This tombolo is shown in figure 28.6.

Figure 28.7a shows the start of a tombolo formation behind a series of offshore breakwaters. These were built, in this case, to stimulate and preserve a recreational beach. Figure 28.7b shows an aerial photo of this area, near Boston, on the U.S. Northeast coast. The pattern of wave diffraction is especially prominent in this photo.

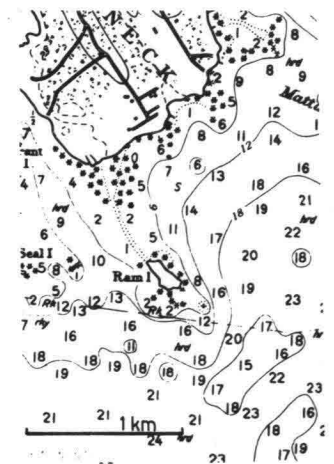
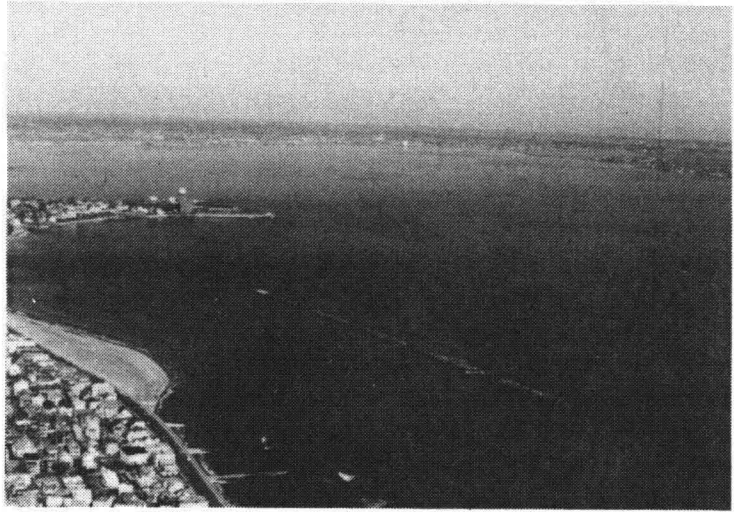
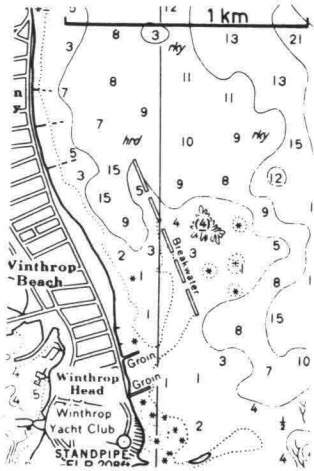


**Figure 28.6**  
TOMBOLLO BETWEEN RAM ISLAND AND  
MATTAPOISETT NECK, BUZZARDS BAY, USA.  
( scale as shown, depths in feet )



a. PLAN  
(scale as shown, depths in feet)

b. OBLIQUE AERIAL PHOTO

Figure 28.7  
WINTHROP BEACH, MASSACHUSETTS, U.S.A.

29. DELTAS

L.E. van Loo

W.W. Massie

29.1 Introduction

A delta develops around a location where an estuary discharges water and sediment through a coast. Because rivers transport more sediment, the most spectacular deltas develop near river mouths rather than at other forms of estuaries.

Several factors contribute to the form of a delta. Among these are,  
 Tide and fresh water runoff currents in the estuary,  
 Estuary sediment discharge and properties,  
 Coastal waves and currents,  
 Coastal sediment material transport and properties, and  
 Water level variations in the sea and estuary.

Most of these factors can be combined in a qualitative descriptive factor: the ratio between the supply of river sediment and the distribution capacity of the coastal processes. It seems most logical to start the discussion with an estuary discharging sediment and water into a body of still water; the distribution capacity of the coast is zero.

29.2 Deltas on Quiet Coasts

Consider a river discharging a constant flow  $Q_r$  and a constant sediment load  $S_r$  through an initially straight coastline. There are no waves, and only a river current. Such a situation is shown in figure 29.1a.

As the discharge passes the mouth, the flow will spread out, reducing the current strength and hence the sediment transport capacity. Material will be deposited in areas where the current is weakest - at the sides of the discharge. Shoals, which will eventually come above water level, will develop projecting into the sea. These can be compared to spits described in the previous chapter except that in this case the supply of material now comes from the river.

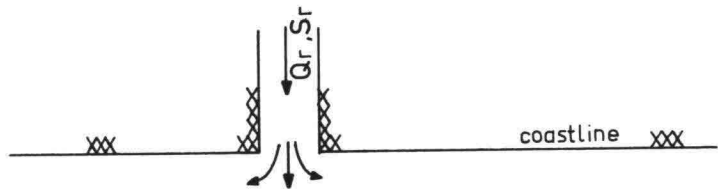
Such a development is shown in figure 29.1b.

This cannot go on forever, however. The consequences of such a formation are a topic for river engineering. The most important consequence for the delta is that the water level at the location of the original mouth becomes higher. Eventually, this will cause too high an hydraulic gradient *across* the spit and the river will break through, forming a new mouth - see figure 29.1c.

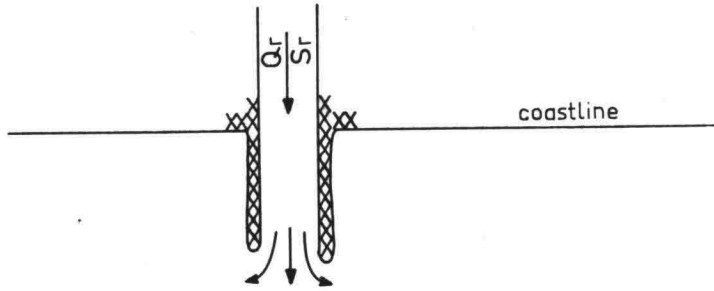
This process, of course, repeats itself. Figure 29.2 shows a natural example of such a delta - the Lyéna River delta on the north coast of Siberia, U.S.S.R. Both Érgye - Muóra - Sissye Island and Bärkin Island are parts of this delta.

Figure 29.3 shows a detail of a portion of the Mississippi River Delta on the Gulf of Mexico coast of the U.S.A. The pattern of repeated shoal breaks is evident. Only isolated portions of this delta remain dry during storm surges.

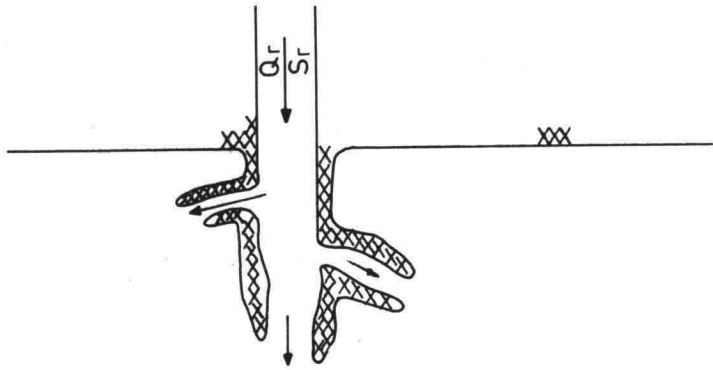
Such delta formations are often called "birdfoot deltas" because of their form. This is especially obvious in figure 29.4 which shows a major portion of the Mississippi River Delta.



a. INITIAL CONDITION



b. FIRST DEVELOPMENT



c. CONTINUING DEVELOPMENT

Figure 29.1  
DEVELOPMENT OF DELTA IN ABSENCE OF WAVE  
( no scale )

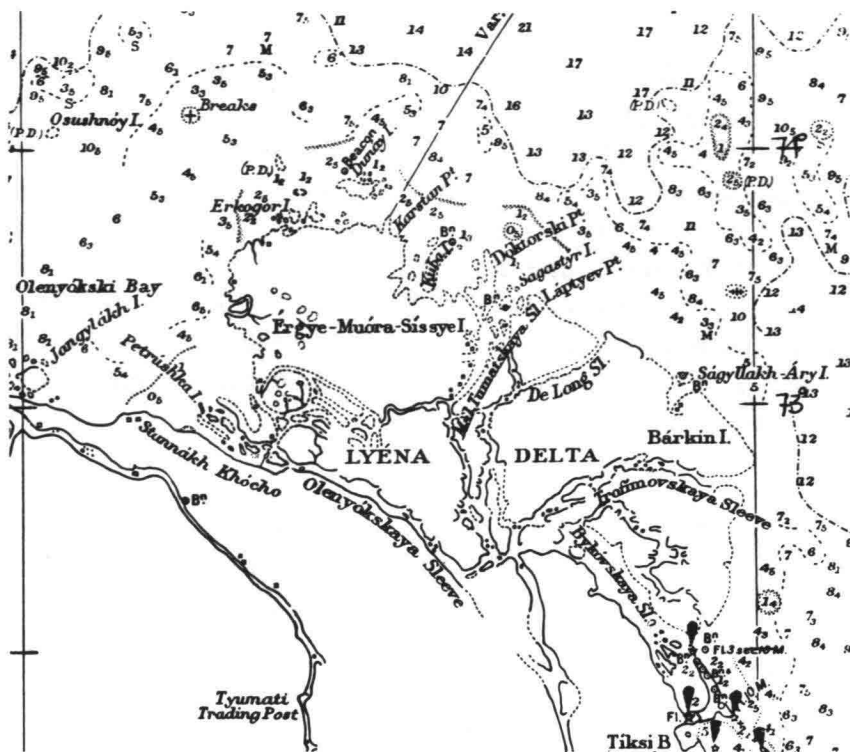


Figure 29.2  
 LYENA RIVER DELTA, SIBERIA, U.S.S.R.  
 ( scale as shown; depths in fathoms and feet )



Figure 29.3  
 DETAIL OF MISSISSIPPI RIVER DELTA, LOUISIANA, U.S.A.  
 ( scale as shown, depths in feet )

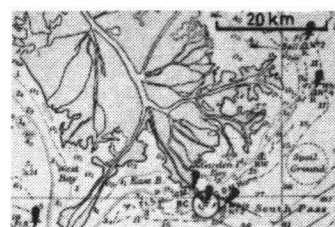
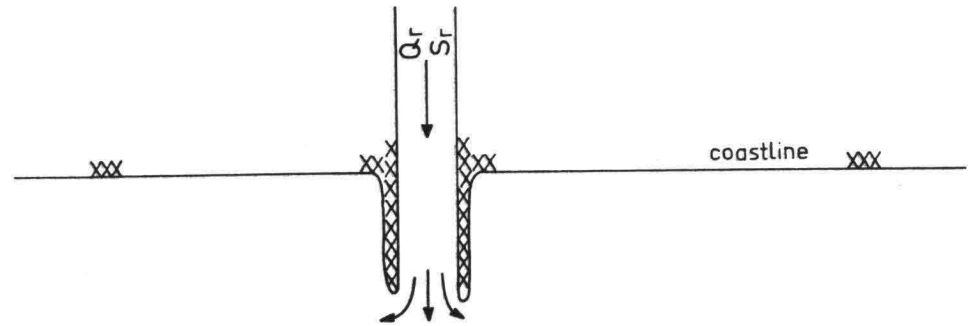


Figure 29.4  
 MISSISSIPPI RIVER DELTA REGION, LOUISIANA U.S.A.  
 ( scale as shown depths in fathoms and feet )

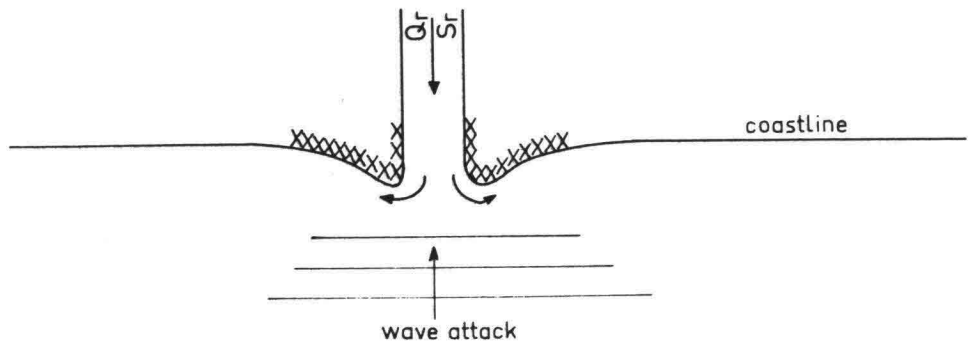
### 29.3 Deltas with Moderate Distributing Influences

If waves were to attack one of the deltas just mentioned, what would be their effect on the delta form? For simplicity, let us assume that the dominant wave propagation direction is perpendicular to the original straight coast, thus, there will be no sand transport along the original coast. Why? - see chapter 26!

The wave action will obviously attack the ends of the projecting shoals shown in figure 29.1b. Material from the shoals is transported toward and along the coast. Figure 29.5 shows the development with and without wave action.



a. REPEAT OF 29.1 b NO WAVES



b. EFFECT OF MODERATE WAVE ATTACK

Figure 29.5  
DELTA WITH MODERATE WAVE ATTACK  
( no scale )



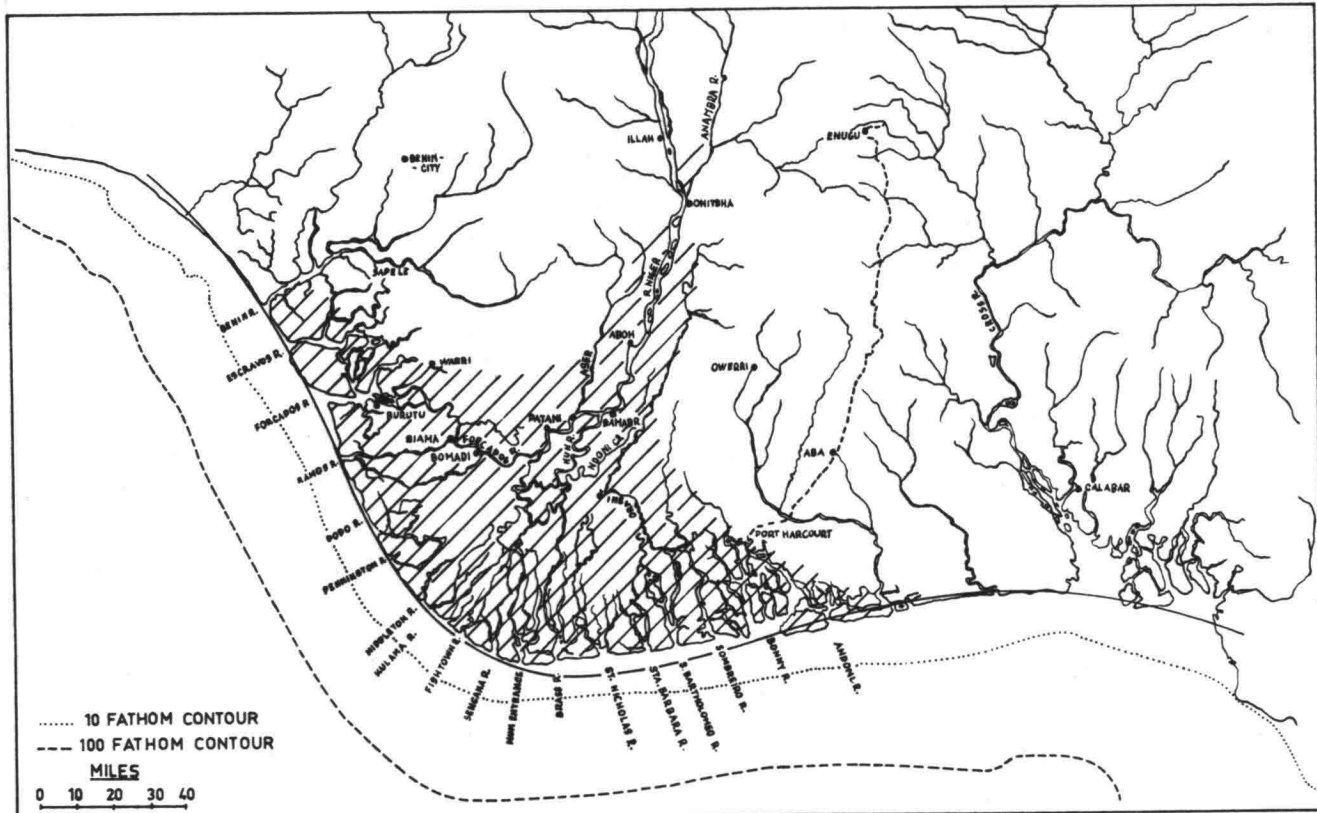


Figure 29.7 NIGER RIVER DELTA, NIGERIA

The maximum sand transport then occurs near the inflection points of the shore line. Material is supplied by the river through the mouths between these two points. More information about this delta is given by Frijlink (1959).

#### 29.4 Deltas with Strong Distributing Influences

As the distributing capacity of the coastal processes becomes relatively more important, the delta protrudes less and less into the sea. Even a river having a very large sediment transport can form such a delta if the coastal distribution capacity is high and/or the material is easily eroded.

An excellent example of such a delta is shown in figure 29.8 - the Amazon River in Brazil. Even though the sediment supply is enormous (ch.27) it is immediately swept away to the northwest. In this case a longshore current of up to 4 knots is caused by the South Equatorial current (see ch. 3). The current approaching the delta area from the southeast is not fully loaded with sediment as evidenced by the relatively steep shore slope in that area. To the north of the river mouth, the mud coast has developed as indicated in chapter 27.

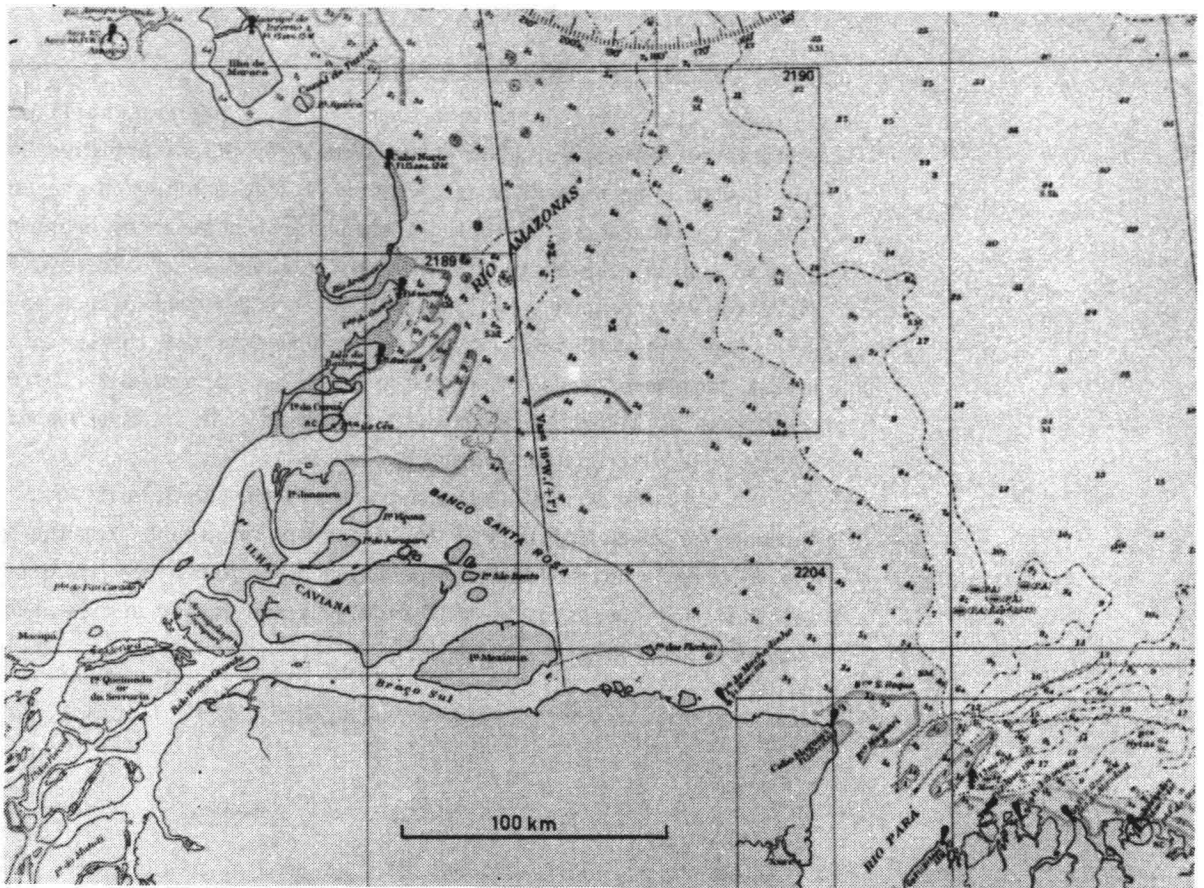


Figure 29.8  
 AMAZON RIVER DELTA, BRAZIL  
 (scale as shown, depths in fathoms and feet)

If the river sediment is heavier (sand instead of clay) even severe wave attack may not be sufficient to distribute this material along the coast. In such cases a somewhat horseshoe shaped shoal will develop just outside the river mouth. (This usually happens to some extent for every estuary). An example of such a river mouth bar has already been shown in figure 18.1, the mouth of the Columbia River, Oregon, U.S.A. As discussed in that chapter, breakwaters are being built here to narrow the river mouth and stimulate natural erosion of this bar. In effect, such works force the bar farther offshore.

In this and the previous sections, the sand transport along the coast independent of the river supply has been negligible. In the next section we examine the influence of this longshore sediment supply.

### 29.5 Influence of Longshore Transport

When a significant longshore transport is present, still other delta forms can develop. The estuary mouth is often sufficient to block the longshore transport. Coastal material is deposited on the up-drift side of the entrance, narrowing the mouth. This enhances erosion resulting in a slow displacement of the entire river mouth sideways in the direction of the longshore transport. Figure 29.9 shows such an estuary - the Coos River (Coos Bay), on the Pacific Coast of the U.S.A. A dominant longshore transport from the north has displaced the estuary mouth several kilometers toward the south so that it is now confined by the rock outcrop (Cape Arago; Coos Head).

What is the source of the material in the North Spit in this figure? This has all been supplied by the longshore transport from the north. The relatively unimportant sediment supply of the river has either remained within the estuary as it slowly became longer or has been swept away past Cape Arago.

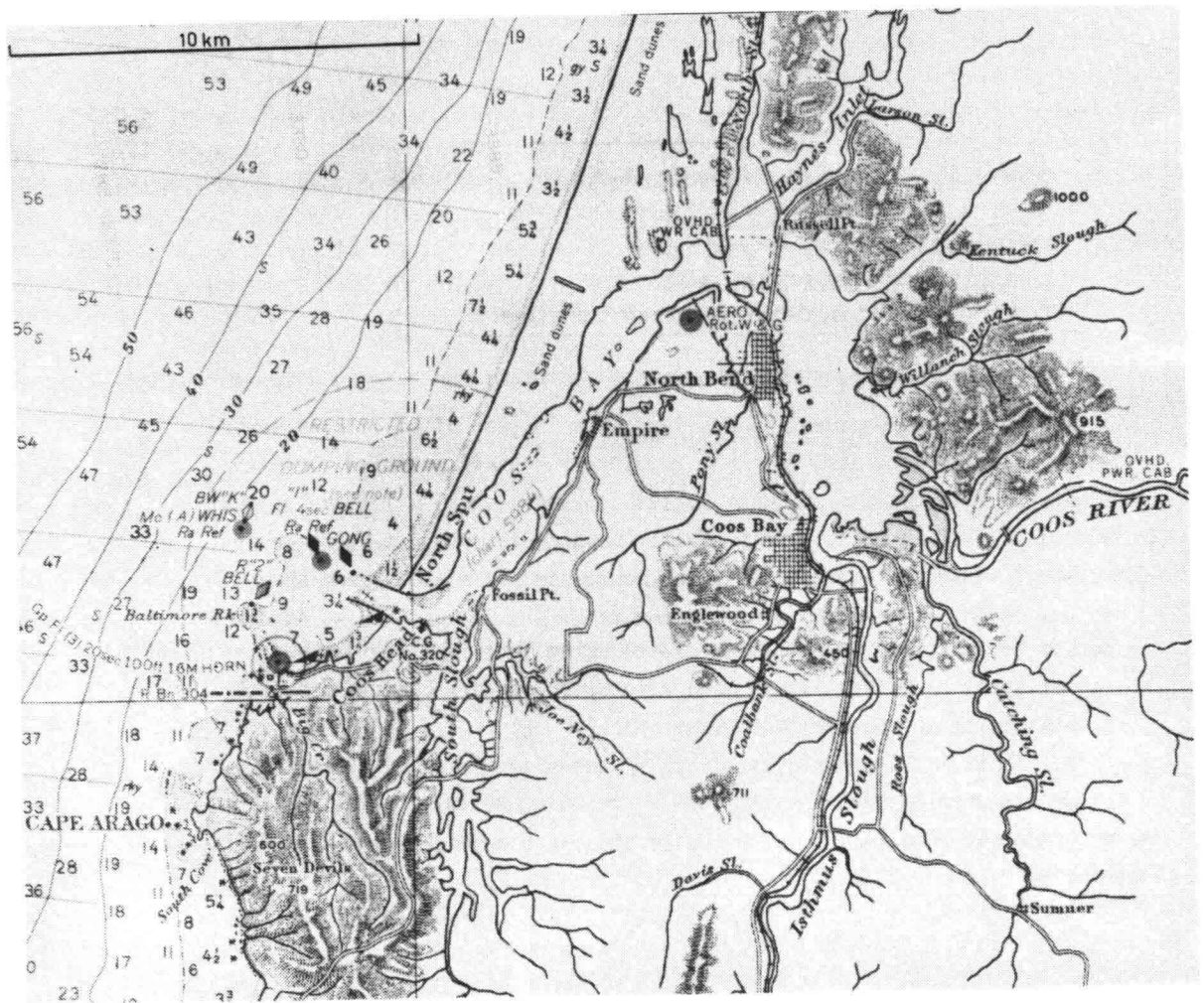
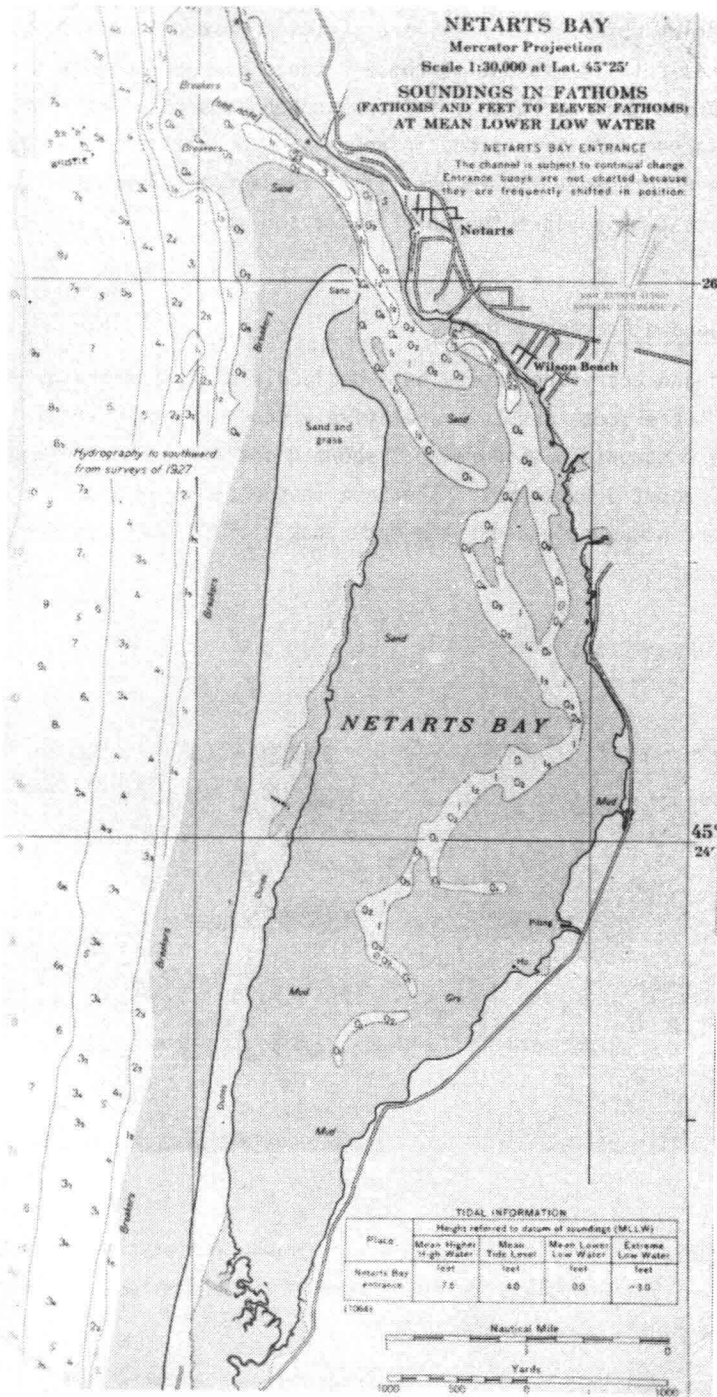


Figure 29.9  
COOS BAY, OREGON, U.S.A  
( scale as shown, depths in fathoms )

A river flow is not necessary for such a spit development. At Netarts Bay, also on the Oregon Coast, the sand transport is from south to north. The tidal prism for this estuary is much smaller than for Coos Bay; a shoal has formed before the entrance and there is even a small chance that a heavy storm will close the entrance completely. This area is shown in figure 29.10.

One last comment about these last figures seems appropriate: both spits are covered with dunes of blowing sand. A photo made along this coast was included earlier - figure 25.4.



**Figure 29.10**  
**NETARTS BAY, OREGON, U.S.A.**  
( scale as shown, depths in fathoms and feet )

30. SHORE PROTECTION

L.E. van Loo

W.W. Massie

30.1 Introduction

We have seen in the two previous chapters how coasts can develop - can erode or accrete. Unfortunately, these processes do not always agree with the wishes of man. A valuable structure may be washed away as a beach erodes, or a channel to a harbor may silt up making the entrance too shallow for shipping.

This chapter will constitute a brief summary of the available shore protection methods. A detailed discussion of the functional use and structural details of most of these methods can be found in the *Shore Protection Manual*. Further information on construction of shore protection structures is provided in courses on hydraulic structures. Some principles presented in volume III of these notes (Breakwater Design) can also be applied to shore protection works.

30.2 Eroding and Accreting Shores

Eroding and accreting shores have decidedly different characteristics. Eroding shores tend to be relatively steep for the material from which they are comprised. Figure 30.1 shows a coast which is eroding at a rate of about 3 m per year. The bank in the photo is about 25 m high. This photo was made along the outer coast of Cape Cod on the U.S. northeast coast.



FIGURE 30.1  
ERODING COAST  
CAPE COD, MASS. U.S.A.

Figure 30.2, on the other hand, shows a beach accretion along the Brouwersdam in South Holland, The Netherlands. This oblique aerial photo shows a very gently sloping beach.

In both cases this long term coastline change results from a longshore sediment transport. It can be handy to review chapters 25 and 26 before studying the various shore protection works in the next sections.



FIGURE 30.2  
BEACH ACCRETION NEAR  
BROUWERSDAM, NETH.

### 30.3 Jetties

When a longshore transport threatens to cause a shallowing of a harbor entrance, for example, this process can be interrupted by constructing a jetty perpendicular to the coast slightly "up-drift" from the harbor entrance. This jetty or breakwater should extend at least through the breaker zone, even during storms, and even after the coast has moved forward from accretion. Material transported along the coast will accumulate against the jetty on the "up-drift" side, opposite the channel.\*

Most breakwaters attached to land can be considered to be jetties. Their design is the topic of volume III of these notes.

### 30.4 Groins

A jetty only prevents accumulation of material in a small area or stimulates accumulation in another rather restricted area; its influence is purely local.

Groins, on the other hand, are a series of smaller jetties spaced at relatively short intervals along a coast. They tend to stabilize the entire coast along which they are built by keeping the coastal sand trapped between adjacent groins. As such, they can be used to defend an eroding coast.

Figure 30.3 shows an oblique aerial photograph of a portion of the coast of New Jersey, U.S.A. The groins on this coast are reducing the transport of sediment in the southerly direction - to the left in the photo. These groins are built much farther apart than is common practice.

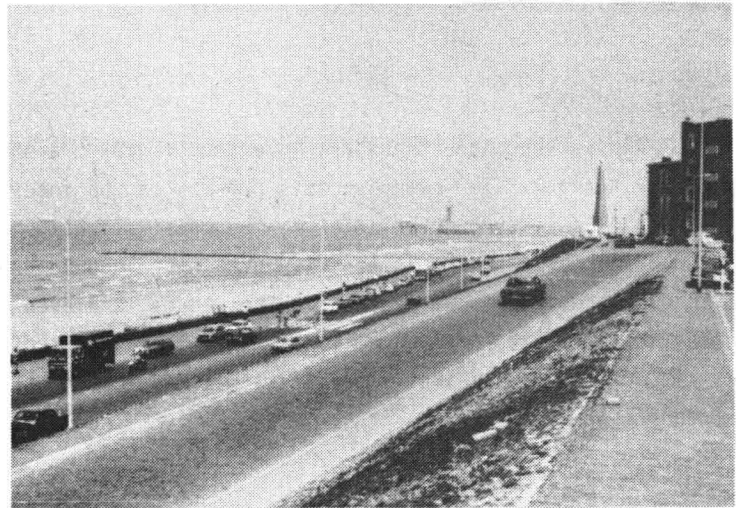
\* A case is known to one of the authors of a jetty being built on the wrong side of the channel; the consequences were not happy!

FIGURE 30.3  
GROINS ALONG NEW JERSEY  
COAST, U.S.A.



A spacing equal to a few times the length of the groins is more common as shown in figure 30.4 along the coast of Scheveningen, The Netherlands.

FIGURE 30.4  
GROIN PROTECTED COAST  
SCHEVENINGEN, NETH.



The purpose of groins is to reduce the longshore sediment transport rate along a coast and, if properly designed, they can be used to achieve sediment transport curve 2 in figure 26.2b, the ideal situation in that case. Proper design implies that the correct choices for groin length, spacing, height and possibly even permeability to sand have been made. Since for solution 2 in figure 26.2b only a small portion of the sand transport is to be stopped, the groins should be short - shorter than the width of the breaker zone. Long groins extending through the breaker zone tend to achieve a sand transport relation more like curve 4 in figure 26.2b.

A special type of groin is a row of piles purposely spaced so as to make a porous barrier thus reducing but not totally blocking the longshore sand transport.

The physics of a groin system is not completely understood making the successful design of a groin system more an art than a science; a groin system can prove to be very effective for influencing longshore transport of sediment, however.



a. DOUBLE PILE ROW FILLED WITH STONE  
VLISSINGEN, NETH.



b. BASSALT STONE GROIN  
SCHEVENINGEN NETH.

FIGURE 30.5  
EXAMPLE OF GROIN  
STRUCTURES.

Figure 30.5 shows two of the many types of groins; more are illustrated in the *Shore Protection Manual*.

### 30.5 Dunes

Unfortunately, neither a jetty nor a set of groins does anything to prevent material transport perpendicular to the coast. This was dramatically demonstrated late in 1973 when several severe northwest storms caused a significant coastal erosion near Scheveningen, The Netherlands. This was an example of the development depicted earlier in figure 25.5. If this offshore transport can result in too severe a (temporary) beach erosion, the beach or dunes can be reinforced. The easiest way to accomplish this is to increase the sand volume in the higher portions of the shore. Making a row of dunes wider rather than higher requires less sand to provide a given degree of protection, however. Even simply moving sand from the foreshore to the higher part of the beach can be effective. The reason for this is that the resulting beach profile is made more like the equilibrium profile under storm conditions so that offshore erosion will take place more slowly.

### 30.6 Detached Breakwaters

We have already seen how a segmented breakwater parallel to the coast can be used to stimulate a tombolo development - figure 28.7. As explained in section 28.4, such breakwaters reduce the longshore transport capacity in their shadow resulting in sediment deposition and the tombolo formation. Obviously, since such a breakwater is rather impermeable, the offshore transport of sand is also restricted.

This has led in the past to proposals by some that continuous breakwaters be built at the outer edge of the breaker zone in order to prevent offshore transport of sand. Unfortunately, proponents failed to realize that such structures also prevent the onshore transport of sand even more effectively. Any sand lost in the offshore direction now never returns; the net effect can be worse than doing nothing! In addition, such dams can suffer from severe foundation problems just as do seawalls. This is described in the following section.

### 30.7 Seawalls

Since offshore breakwaters are expensive (difficult) to build, especially near the breaker line, an alternative might be to construct an impermeable seawall on the beach parallel to the coast. The philosophy behind such a concept is that erosion will be prevented by simply cutting off the local supply of material.

Unfortunately, a rigid massive seawall tends to reflect the incoming waves. The increased turbulence resulting from this reflection stimulates the erosion of a deep trench before the seawall. The presence of this trench endangers the foundation so that a risk exists that the wall will fail by collapsing into the scour trench. This can be prevented, of course, by maintaining a beach in front of the seawall using some other means. If this is to be done, however, the logical question is, "why build a seawall, then?" It can be very effective for keeping people from using the beach!

### 30.8 Sand By-Passing

The "displacement of problems" described in the previous section often has the particular characteristic that our structure (a harbor entrance, for example) generates two complementary problems - an accretion and an erosion. In such a case, both problems can be solved by simply moving sand from the accretion area to the erosion area.

If the distance between the accretion and erosion areas is not too great an artificial by-passing operation may be economical. Sand accumulated by a jetty or single tombolo is moved to the eroding beach using some type of dredge. For very short distances, a pipeline on a suction dredge may be used. Occasionally, such a suction dredge is built on a fixed platform in the accretion area. More about such installations is told in the *Shore Protection Manual*.

31. COASTAL MORPHOLOGISTS' TEN COMMANDMENTS

W.W. Massie

We have just seen in the previous chapter how many shore protection works displace problems to adjacent areas. Knowing this, and with tongue in cheek, Per Bruhn (1972) presented his version of the Ten Commandments as applied to coastal morphology. These are reproduced here with only minor editorial changes in tabel 31.1. Any resemblance to the original version of the Ten Commandments is intentional.

This concludes our discussion of coastal morphology. Coastal morphology is a major topic of volume II of these notes. This present volume continues in the next chapter with an introduction to the problems associated with offshore engineering.

Table 31.1. THE TEN COMMANDMENTS FOR COASTAL PROTECTION

- 1) Thou shalt love thy shore and beach.
- 2) Thou shalt protect it gainst the evils of erosion.
- 3) Thou shalt protect it wisely, yea, verily and work with nature.
- 4) Thou shalt avoid that nature turns its full forte gainst ye.
- 5) Thou shalt plan carefully in thy own interest and in the interest of thine neighbour.
- 6) Thou shalt love thy neighbour's beach as thou lovest thine own beach.
- 7) Thou shalt not steal thy neighbour's property, neither shalt thou cause damage to his property by thine own protection.
- 8) Thou shalt do thy planning in cooperation with thy neighbour and he shalt do it in cooperation with his neighbour and thus forth and thus forth. So be it.
- 9) Thou shalt maintain what thou has built up.
- 10) Thou shalt show forgiveness for the sins of the past and cover them with sand. So help thee God.

32. OFFSHORE ENGINEERING

C.J.P. van Boven

W.W. Massie

32.1 Disciplines Involved

Offshore engineering refers to the engineering work related to all sorts of structures located offshore - see chapter 2 and figure 25.1. This definition includes work done by many other branches of engineering as well as civil engineering. While the major emphasis within this chapter will be on civil engineering aspects of offshore work, the ties to other specialized engineering fields will also at least be indicated.

Since many offshore structures are used by the petroleum industry, a strong relationship to mining and mechanical engineering is obvious. In general, the mining engineers determine what operations need to be carried out and where this must be done. Mechanical and electrical engineers determine what mechanical and electrical equipment is needed and translate this into a necessary work area and loading condition on this area.

Naval architects are concerned with floating structures whether they are real ships or fixed structures which are being towed to its final location. Also they provide valuable information about characteristics of ships which will be used in conjunction with fixed structures.

Oceanographers provide information on waves, sea currents, chemical and biological conditions - related to material properties and marine fouling. Indeed, many disciplines are drawn together with civil engineering to execute offshore engineering works. The specification of the various civil engineering specialities which can contribute to offshore engineering is postponed to a later section of this chapter. First, we discuss some of the various types and uses of offshore structures.

32.2 Types of Offshore Structures

Offshore structures can be grouped by form roughly into three categories: fixed, anchored, and free floating constructions.

Fixed Structures:

Fixed structures are most suited for water depths less than, say, 200 m and uses for which the platform must be stable - radar islands, for example. These fixed structures can again be subdivided into three groups: gravity, jacket and jack-up structures.

Gravity structures are the heaviest of the offshore structures and derive their stability against overturning from their weight combined with their broad base. (The word gravity is used in the same way to describe a type of dam.) Offshore gravity structures are built from concrete at some protected location and then floated and towed to the desired site where they are sunk and placed on the bottom. Figure 32.1 shows a sketch of the ANDOC (Anglo Dutch Offshore Concrete) platform being built near Rotterdam in 1975-76. The base

This chapter has not  
been revised; much of  
the quantitative data  
may be out of date.  
W.W.M. : 1985.

(in prototype) is about 100 m square and 30 m high; the structure has been placed in about 150 m water depth in the northern portion of the North Sea.

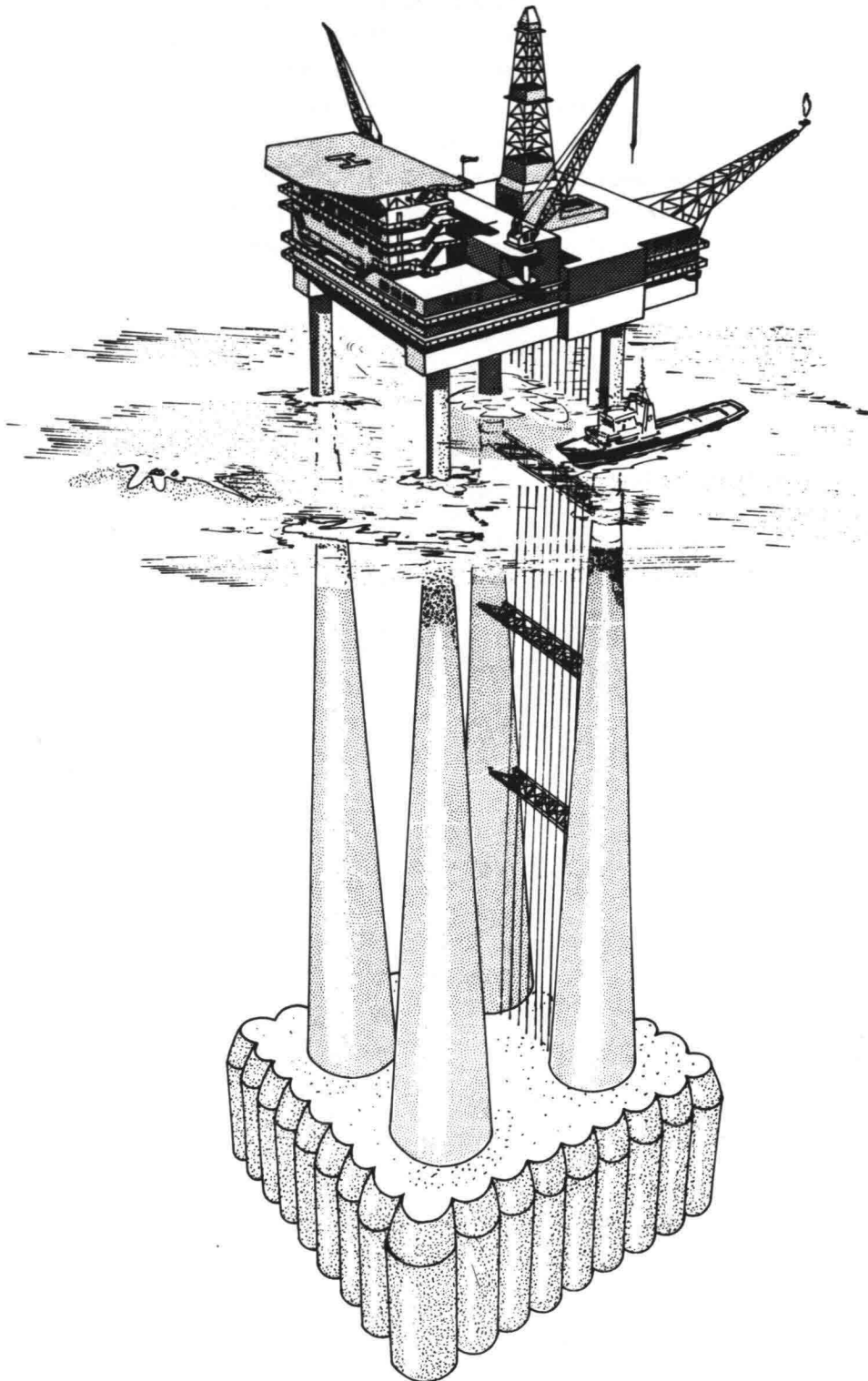


Figure 32.1  
SKETCH OF ANDOC GRAVITY STRUCTURE

A jacket structure is a space frame constructed from hollow tubular elements. In order to appreciate the scale of such structures we must realize that these tubes for a jacket in the northern North Sea can be up to 10 meters in diameter with wall thicknesses of up to 100 mm. Such a structure to be placed in the Thistle Oil Field in a water depth of about 160 m will have a dead weight of about 30 000 tons. Complete and ready for use, the estimated cost of such a structure is about 300 million guilders\*. The largest of the models in figure 32.2 shows such a structure. These are built on land and are either moved to their final location by barge or are floated and towed to position. In contrast to gravity structures, they are dependent upon pile foundations for their stability.

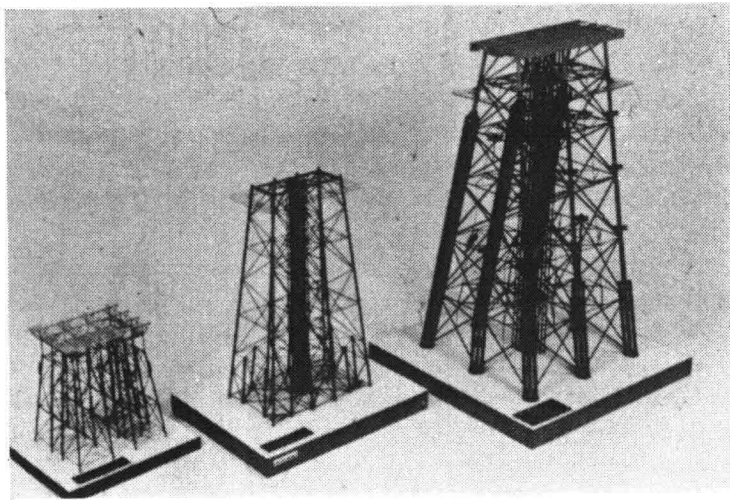
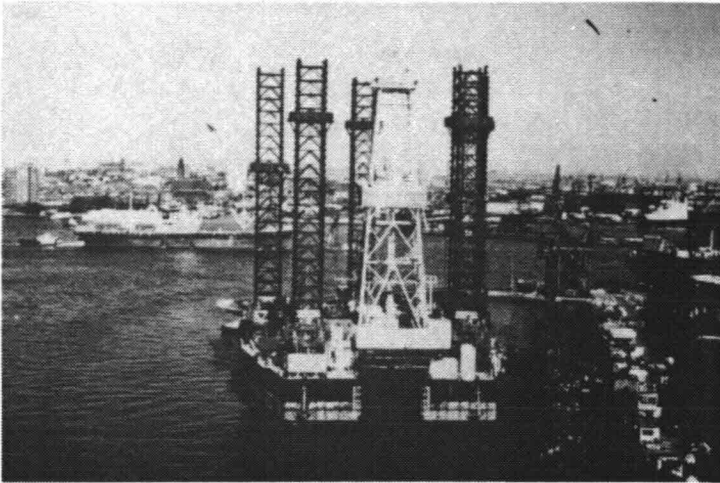


Figure 32.2  
MODELS OF JACKET CONSTRUCTIONS

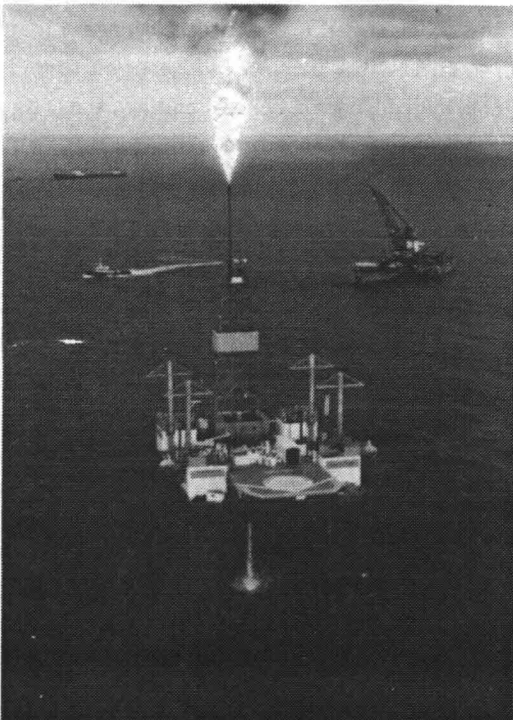
The third type of fixed structure, the jack-up platform, consists of a floating pontoon which raises itself above the sea surface by jacking itself along legs which are lowered to the sea bottom after the structure has been floated into position. Since jack-up platforms can be relatively easily moved from place to place they are best suited for temporary projects. Unfortunately, the raised legs have an adverse effect on the stability (sea-worthiness) during transport so that limitations on size and leg length restrict their normal use to shallow water locations (up to 90 m). The bearing capacity of the sea bottom is obviously important for their optimum use. Figure 32.3 shows a jack-up platform floating with its legs raised and in use as a semi-permanent production platform.

---

\* Such large quantities of steel or money are difficult to visualize. It can be instructive, therefore, to note that this structure is cheaper than beefsteak.



a. FLOATING

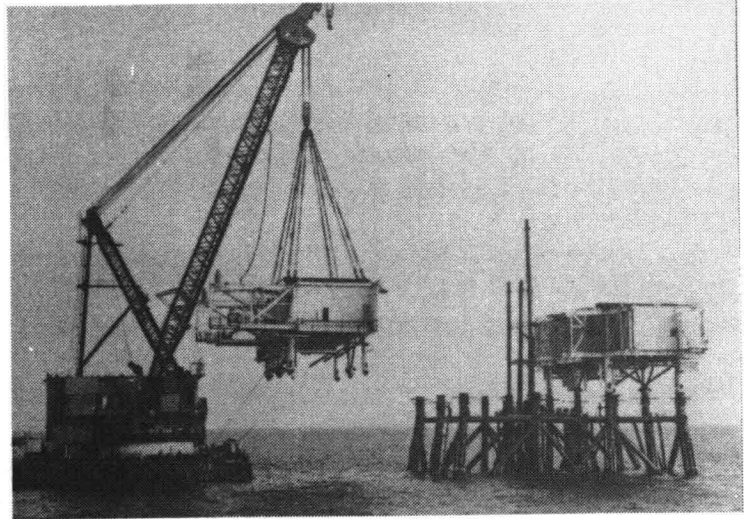
b. IN USE AS PRODUCTION PLATFORM  
EKOFISK FIELD, NORTH SEA.Figure 32.3  
JACK-UP PLATFORM

#### Anchored Structures:

Anchored structures depend upon buoyant forces acting against some form of anchor force to provide their stability and maintain their position on the working site. Several subtypes are available: ships, semi-submersibles, articulated platforms and buoys.

We are all familiar with ships. Figure 32.4 shows one of the larger crane ships at work in the North Sea assembling a jacket structure. The analysis of such ships is primarily the responsibility of the naval architects. Civil engineers become involved with the anchoring, primarily.

Figure 32.4  
CRANE SHIP AT WORK.  
1750 TON LIFT, B.P. FORTIES  
FIELD, NORTH SEA.



Semi-submersibles are floating working platforms consisting of a deck supported above the waves by a group of submerged floatation chambers, as shown in figure 32.5. This particular general form is chosen in order to reduce the hydrodynamic forces and motions in waves. In an attempt to limit the vertical motions of a semi-submersible, it has been suggested that they be connected to heavy anchored with highly tensioned vertical cables. Such a tension leg platform has little vertical motion, but its inverted pendulum sidewise motion can be most unpleasant. This special type of anchored floating structure is however a good candidate for use as a production platform in water depths of more than 200 m - outside the continental shelf.

Figure 32.5  
SKETCH OF A SEMI - SUBMERSIBLE PLATFORM

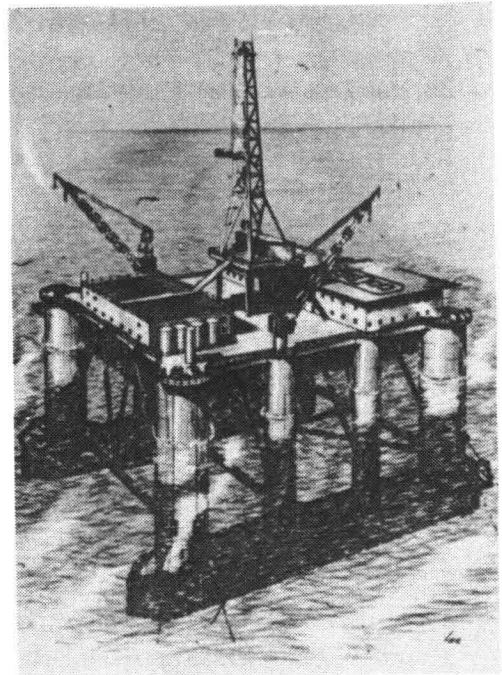
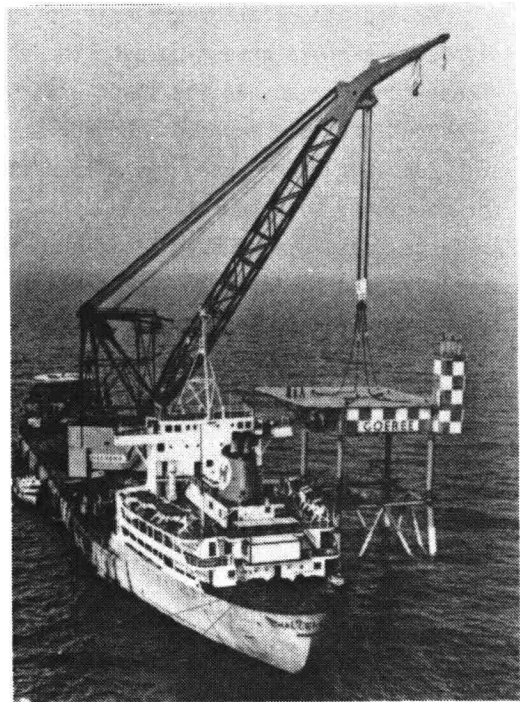




Figure 32.7  
THE LIGHT TOWER GOEREE



As approach channels to harbors have become longer (chapter 15) and ships have become larger, it has become necessary to place more sophisticated navigational aids such as high resolution radar offshore. A special requirement of such a radar platform is that it have a high torsional stiffness so that the reference direction of the radar remains constant.

#### Moorings

Offshore moorings have been developed for use in areas where it is uneconomical to develop conventional harbors of sufficient depth for the larger ships. For the oil industry, such moorings provide for both ship anchoring and connection to a pipeline. Fixed structures are *not* generally used - they suffer too much damage from a collision with the ship and often do not let the ship swing into the on-coming waves. Buoys and articulated platforms are most suited to this work. Ships can even be moored to some large oil storage buoys.

#### Oil Exploration

Initial oil exploration works carried out from the sea surface usually use ships. Later exploratory borings are carried out from anchored or dynamically positioned ships or semi-submersibles. Jack-up platforms can be used in relatively shallow areas. The choice among types depends largely upon water depth. Since exploratory borings usually do not take too long at one site (a few months, perhaps) portability is important for this type of equipment.

#### Oil Production

Once the extent of an oil or gas field has been defined, production platforms can be designed and installed. In contrast to exploration platforms, these have a much longer useful life at a single site (a few decades, hopefully). Fixed jacket or gravity platforms are then usually the most economical.

An idea of the production capacity of a production platform can be obtained by noting that the steel jacket construction described in the previous section is intended for a production of 300 000 barrels of oil per day from 60 wells.

#### Oil Storage

One of the simplest forms of oil storage uses a ship more or less permanently moored at the oil field. Gravity structures and an occasional steel structure are also used. The inclusion of oil storage in a mooring buoy for this purpose has also been effected. Gravity oil production structures usually include a storage reservoir as part of their base. This is true for the ANDOC structure shown in figure 32.1. Figure 32.8, on the other hand, shows a gravity structure designed exclusively for oil storage.

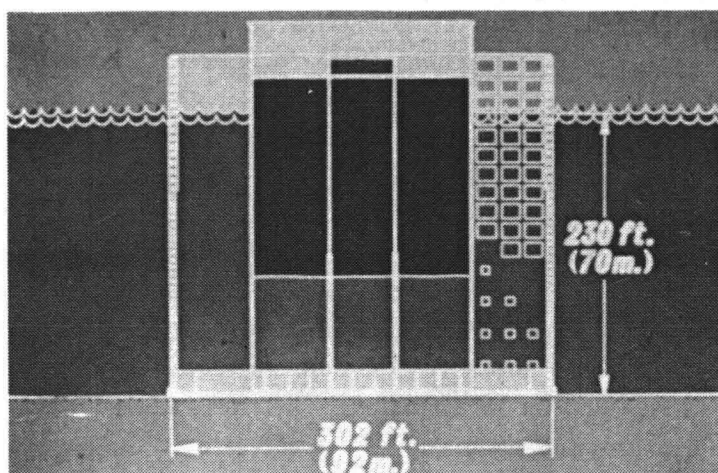


Figure 32.8  
EKOFISK OIL STORAGE TANK

#### Pipelines

While it may seem at first glance that pipelines are rather unimportant, their dependable function is often critical. Submarine pipelines are used not only in the oil industry, they also serve as sewer outfalls, for example. One of the major problems with pipelines is keeping them on the sea bottom. Ideally, they are buried deep enough over their entire length to hold them in position and protect them from ship anchors. Unfortunately, the sea bottom is not smooth; large areas are covered with irregular humps of sand similar to sand dunes, called megaripples. Experts (morphologists) are about equally divided over whether these ripples are stable. There is a good chance that under such conditions a pipeline will be buried in the crests of the megaripples and be hanging free between them. Hydrodynamic forces acting on the exposed pipeline can cause vibrations. If a resonant vibration occurs metal fatigue and failure can result. This is discussed further elsewhere. Living evidence of the fact that problems still exist with pipelines was provided when an oil pipeline in the North Sea unexpectedly floated to the surface late in 1975.

### Construction Equipment

Various types of fixed and floating equipment are needed to install and service offshore facilities. Figure 32.4, for example, shows a very large crane in operation. Jack-up cranes are sometimes used to good advantage in very shallow water for construction of breakwaters, for example. These cranes can be floated into place in calm weather and can elevate themselves above breaking waves.

Ships and semi-submersibles are usually used for laying pipelines. Because they must exert a strong tension on the pipeline during the pipelaying operation (to prevent buckling) these units must be anchored.

### 32.4 Civil Engineering Aspects

Civil engineering aspects of offshore engineering can be subdivided to some extent along the lines of specialization within the civil engineering field. In this section, however, a subdivision involving the problem characteristics will be used.

#### Environmental Loads

The determination of environmental loads on an offshore structure can be subdivided into two sub-problems: the determination of environmental conditions, and the translation of these conditions into loads.

Environmental conditions result from nature. These include wind, waves, currents, ice formation, and earthquakes. A major problem is the determination of the probability with which a given environmental condition - or combination of conditions - will be exceeded within the lifetime of the structure. A bit of the technique of this has been indicated earlier in chapter 11.

Luckily, not all of the environmental conditions listed above are universally found. Ice, either drifting on the water surface or freezing on the superstructure, is only a problem in colder climates. The load resulting from ice frozen on the superstructure is not usually important for the design of the structure as a whole; it can be very important for individual parts of the structure, however. Earthquakes can present design problems for structures to be located in the Pacific Ocean basin and in the eastern parts of the Mediterranean Sea.

The second part of this problem is equally complex. Because the environmental loads on a structure are not, in general, directly proportional to the environmental conditions (such as wave height or current velocity) which cause them, the transformation of conditions into loads is not simple. The common technique of multiplying a conditions spectrum by a response function to determine a loading spectrum is not, in general, adequate.

The determination of the environmental conditions is a task of coastal engineers and oceanographers. The transformation of conditions into loads is a current research topic for coastal engineers as well as fluid mechanics specialists.

The importance of the total of environmental loads should not be underestimated. They form, by far, the most critical loadings, and have even led to failure of offshore structures. Figure 32.9 shows a jacket type production platform during a storm.

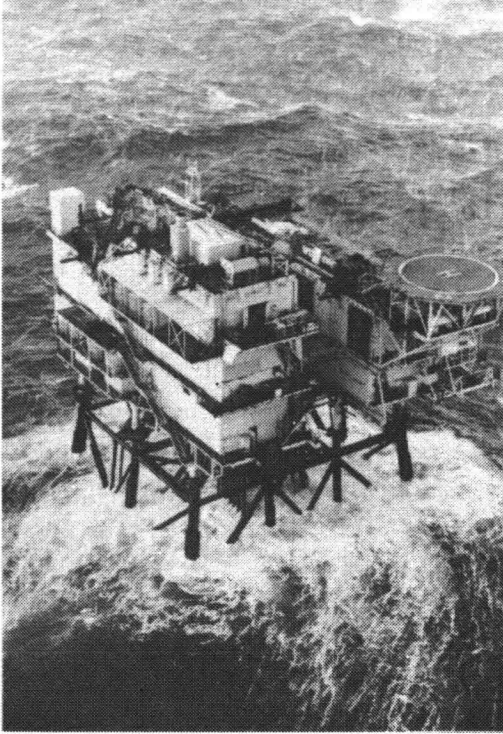


Figure 32.9

PRODUCTION PLATFORM DURING A STORM.  
FORTIES OILFIELD, NORTH SEA WIND FORCE 12

### Structural Design

Once the environmental loads have been estimated, the detailed structural design in steel or concrete can be started. Obviously, since the environmental loads are dependent upon the size and location of construction elements, load determination and structural design are closely related, in practice.

Special structural problems are encountered with offshore structures, however. First, as already indicated in chapter 3, material properties can be affected by the sea water environment. Corrosion of steel is only one of the more obvious problems. However, corrosion combined with large dynamic environmental loads requires the modification of traditional fatigue stress relationships for use offshore.

The physical size of elements and the complexity of connections lead to complex stress concentration problems.

### Foundations

The foundation design is also related to the structural design. One of the first problems of foundation design is the determination of bottom material properties in situ. Recent technical developments provide apparently good data now, however. Even so, foundations for fixed offshore structures must sustain very large static and dynamic loads when compared to land-based foundations. When the struc-

ture is in shallow water, waves can cause additional short period dynamic fluctuations in the soil pore water pressure which complicate the foundation design problem.

The anchoring of moored floating structures provides another specialized facet of offshore foundation engineering. For economic reasons, it is desirable to obtain a maximum anchor force with a minimum anchor weight.

Erosion near footings of structures and near pipelines can complicate foundation design. The foundation engineer and the coastal engineering morphologists should attack this problem cooperatively.

#### Corrosion and Fouling

Corrosion has already been indicated with regard to fatigue in structural design. Materials engineers are, of course, also concerned with the problem as they seek to improve materials used in offshore structures.

Fouling by the accumulation of marine growth on an offshore structure can have significant consequences. Since a fouling layer increases the effective size of a structural element, it increases the environmental load. A layer of marine growth over 20 cm thick has been found on a 100 cm diameter element of an offshore platform after 10 years. This layer has increased the effective diameter of the element by 40%! Such marine growths develop relatively rapidly on offshore structures as compared to coastal structures. Offshore, the marine life has less hinder from pollution and less competition for the available food resources of the ocean.

Obviously, accumulations of marine growth on structures also hinder periodic inspections which are often required by insurance underwriters.

#### Pollution Control

Both domestic and industrial wastes are produced on offshore structures. Sanitary engineers are beginning to attack the problem of disposal of these often relatively small quantities of environmentally damaging wastes.

#### Construction

Construction aspects of the fabrication of an offshore structure on land or in a drydock are not considered here. Problems associated with the placing of a structure on a site at sea are of interest to us, however.

Various problems arise during the transport of a large structure to its operating site. The floating stability and towing problems are handled in cooperation with the naval architects. The mobilization of the necessary number of sea-going tugboats to bring a structure to its location can present a challenging management problem. The precise determination of position of structures - necessary for the installation of connecting pipelines, etc. - provides an interesting geodesy problem.

Once the site has been reached other equipment must be mobilized to complete the construction at the site. The lifting capacity of seaworthy floating cranes can be an important limitation even though this capacity seems high - a few thousand tons. Piles must be driven at sea in order to guarantee the stability of jacket structures. Divers may be needed for a whole variety of underwater operations.

Since operations carried out at sea are so expensive compared to similar operations elsewhere, careful selection of construction techniques and management of equipment can be economically rewarding. Construction limitations and problems are discussed further in volume IV.

### 32.5 Other Problems

Several rather strange seeming problems arise which have special significance for offshore structures. The isolation of personnel on board the structures can lead to sociological problems not unlike those experienced on ships.

Since many offshore structures are located outside the area of the legal territorial waters, legal questions concerning taxes and customs can be expected. The threat of armed take-over of an offshore structure by pirates poses legal as well as strategic defense questions.

SYMBOLS AND NOTATION

W.W. Massie

The symbols used in this book are listed in this table. International standards of notation have been used where available except for occasional uses where a direct conflict of meaning would result. Certain symbols have more than one meaning, however this is only allowed when the context of a symbol's use is sufficient to define its meaning explicitly. For example, T is used to denote both wave period and temperature.

In the table a meaning given in capital letters indicates an international standard. The meaning of symbols used for dimensions and units are also listed toward the end of the table.

Roman Letters

Sym- bol	Definition	Equa- tion	dimensions	Units
A	AREA	20.01	$L^2$	$m^2$
$A_E$	of harbor entrance	23.05	$L^2$	$m^2$
$A_H$	of harbor surface	23.10	$L^2$	$m^2$
a	acceleration		$LT^{-2}$	$m/s^2$
$a_C$	Coriolis acceleration	3.01	$LT^{-2}$	$m/s^2$
$a_j$	Coefficient			
B	distance of river influence in ocean	22.06	L	m
b	distance between wave orthogonals	9.01	L	m
C	Chézy Friction Coefficient	20.02	$L^{1/2}T^{-1}$	$m^{1/2}/s$
c	concentration	25.01	-	$(m^3/m^3)$
c	wave speed	5.05	$LT^{-1}$	m/s
$c_g$	wave group velocity	5.06	$LT^{-1}$	m/s
$c_v$	volume concentration	16.02	-	-
D	depth of frictional influence	3.08	L	m
	apparent diffusion coefficient	23.03	$LT^{-1}$	m/s
$D_0$	diffusion coefficient at $x=0$	22.06	$LT^{-1}$	m/s
d	storm duration	12.03	T	hr

Sym- bol	Definition	Equa- tion	dimensions	Units
E	expected chance	11.04	-	-
	estuary number	22.02	-	-
	Wave Energy per unit surface area	5.09	$MT^{-2}$	N/m
$E_T$	Wave energy per unit width	5.08	$MLT^{-2}$	N
e	BASE OF NATURAL LOGARITHMS		-	-
F	Froude Number	22.20	-	-
	fetch length	12.04	L	m
f( )	function of ( )			
f	frequency	10.09	-	-
f	hydraulic loss coefficient	16.01	-	-
G	coefficient	23.05	$L^{\frac{1}{2}}T^{-1}$	$m^{\frac{1}{2}}/\text{tide}$ period
g	ACCELERATION OF GRAVITY		$LT^{-2}$	
H	wave height	5.01	L	m
H'	wave height neglecting re- fraction, diffraction	table 9.1	L	m
$H_{rms}$	root mean square wave height	10.01	L	m
$\bar{H}$	average wave height	10.04	L	m
h	water depth	5.01	L	m
$\bar{h}$	average water depth	20.03	L	m
i	subscript index			
K	coefficient	3.18	varies	varies
$K_r$	refraction coefficient	9.03	-	-
$K_{Sh}$	shoaling coefficient	7.06	-	-
k	wave number	5.01	$L^{-1}$	1/m
L	harbor length		L	m
$L_w$	length of intrusion wedge	22.18	L	m
$\ell$	life of structure	11.12	T	yr
M	number of storms per year	10.09	-	-
	mixing parameter	22.01	-	-
m	beach slope	8.01	-	-
N	number of terms in series		-	-
	number of waves in record		-	-
N'	number of terms in series		-	-

Sym- bol	Definition	Equa- tion	dimensions	Units
n	normal direction notation	3.02	L	m
	ratio of group velocity to wave velocity	5.07	-	-
P()	probability of exceedence of ( )	10.02	-	-
P	volume of tidal prism	20.01	$L^3$	$m^3$
p	pressure	5.11	$ML^{-1}T^{-2}$	$N/m^2$
p'	absolute pressure	3.18	$ML^{-1}T^{-2}$	$N/m^2$
p*	vacuum head	16.01	L	m
p	wave breaking parameter	ch.8.3	-	-
p()	probability of occurrence of ( )	11.06	-	-
Q	volume flow rate		$L^3T^{-1}$	$m^3/s$
Q <sub>w</sub>	volume flow rate in salt tongue	22.21	$L^3T^{-1}$	$m^3/s$
q	volume flow rate per unit width		$L^2T^{-1}$	$m^3/s\ m$
r	radius of curvature	3.03	L	m
R	recurrence interval	10.11	T	yrs
S	salinity	3.18	-	°/oo
S <sub>s</sub>	salinity at moment of slack water	22.03	-	°/oo
S	sand transport	25.01	$L^3T^{-1}$	$m^3/yr$
s	sedimentation	23.20	$L^3T^{-1}$	$m^3/tide$
T	wave PERIOD	5.01	T	s
T <sub>e</sub>	equivalent wave period	10.15	T	s
T <sub>i</sub>			T	s
T	average wave period	10.14	T	s
T'	tide period	20.04	T	hr
T	TEMPERATURE		degrees	°C
t	TIME		T	s;hr
U	wave power per unit crest length	5.10	$ML^2T^{-3}$	N/s
U <sub>w</sub>	wind speed	12.01	$LT^{-1}$	m/s
u	component velocity in x direc- tion	5.01	$LT^{-1}$	m/s
V	total velocity		$LT^{-1}$	m/s
V <sub>s</sub>	suction pipe velocity	16.01	$LT^{-1}$	m/s
v	component velocity in y direc- tion		$LT^{-1}$	m/s
v	specific volume	3.18	$M^{-1}L^3$	$cm^3/g$
v <sub>∞</sub>	coefficient	3.18	$M^{-1}L^3$	$cm^3/g$
v <sub>v</sub>	volume of voids	23.23	$L^3$	$m^3$

Sym- bol	Definition	Equa- tion	dimensions	Units
w	component velocity in z direction		$LT^{-1}$	m/s
X	COORDINATE DIRECTION		L	m
x	COORDINATE DIRECTION		L	m
Y	COORDINATE DIRECTION		L	m
y	COORDINATE DIRECTION		L	m
Z	VERTICAL COORDINATE DIRECTION		L	m
$Z_p$	depth of submerged dredge pump	16.01	L	m
$Z_s$	depth of dredge suction pipe	16.01	L	m
z	VERTICAL COORDINATE DIRECTION		L	m
$z'$	VERTICAL COORDINATE DIRECTION	3.17	L	m

## GREEK LETTERS

$\alpha$	coefficient	23.07	-	-
$\beta$	water surface slope	3.16	-	-
$\gamma$	wave breaking index	ch.7.5	-	-
$\gamma$	unit weight		$ML^{-2}T^{-2}$	$N/m^3$
$\gamma_g$	unit weight of sand grains	16.02	$ML^{-2}T^{-2}$	$N/m^3$
$\gamma_m$	unit weight of suspension	16.01	$ML^{-2}T^{-2}$	$N/m^3$
$\gamma_w$	unit weight of water	16.01	$ML^{-2}T^{-2}$	$N/m^3$
$\delta$	relative density of water masses	22.15	-	-
$\epsilon$	eddy viscosity	3.05	$ML^{-1}T^{-1}$	Ns/m
$\zeta$	vertical displacement of water particle	5.04	L	m
$\theta$	POLAR COORDINATE	3.13	-	rad.
	layer thickness	22.13	L	m
$\theta$	phase angle	20.04	-	rad.

Sym- bol	Definition	Equa- tion	dimensions	Units
$\Lambda$	coefficient	3.16	-	-
$\lambda$	WAVE LENGTH	5.01	L	m
$\xi$	horizontal displacement of water particle	5.03	L	m
$\Pi$	PRODUCT notation			
$\pi$	3.1415926536		-	-
$\rho$	density of water	3.20	$ML^{-3}$	$kg/m^3$
$\bar{\rho}$	average density of water	23.06	$ML^{-3}$	$kg/m^3$
$\Sigma$	THE SUM OF			
$\sigma$	NORMAL STRESS		$ML^{-1}T^{-2}$	$N/m^2$
$\sigma_H$	STANDARD DEVIATION of wave height	10.05	L	m
$\sigma_t$	$\rho-1000$	3.21	$ML^{-3}$	$kg/m^3$
$\tau$	SHEAR STRESS	22.19	$ML^{-1}T^{-2}$	$N/m^2$
$\Phi$	fetch parameter	12.04	-	-
$\phi$	latitude	3.01	-	deg.
	angle of wave incidence	9.04	-	deg.
$\Omega$	angular velocity of earth	3.01	$T^{-1}$	rad/s
$\omega$	circular frequency	5.01	$T^{-1}$	rad/s

#### Special symbols

—	amplitude of time average of	tab.7.1		
$\Psi$	volume		$L^3$	$m^3$
$\Psi_H$	volume of harbor	23.08	$L^3$	$m^3$
$\infty$	infinity			
$\frac{0}{00}$ } $\%0$ }	parts per thousand by weight	3.18	-	-

Subscripts

Sym- Definition

bol

b bottom; evaluated at  $z = -h$ 

br breaker; evaluated at outer edge of breaker zone

cr critical

D density; caused by density influence

d design

e equivalent

f filling; caused by harbor tide

g group; wave group

I interface

i index counter

m maximum

O evaluated for ocean conditions

o evaluated in deep water

p pump

r river

refraction

s surface

suction

sh shoaling

sig significant

x component in x direction

y component in y direction

z component in z direction

1	} used to distinguish similar values
2	
3	
4	

actual meaning from context.

Functions usedTrigonometric functions

sin ( ) sine of ( )

cos ( ) cosine of ( )

tan ( ) tangent of ( )

arcsin ( ) angle whose sine is ( )

arccos ( ) angle whose cosine is ( )

arctan ( ) angle whose tangent is ( )

hyperbolic functions

$\sinh( )$	hyperbolic sine of ( )
$\cosh( )$	hyperbolic cosine of ( )
$\tanh( )$	hyperbolic tangent of ( )
$\operatorname{arsinh}( )$	argument whose hyperbolic sine is ( )
$\operatorname{arcosh}( )$	argument whose hyperbolic cosine is ( )
$\operatorname{artanh}( )$	argument whose hyperbolic tangent is ( )

logarithmic functions

$\log( )$	logarithm to base 10 of ( )
$\ln( )$	logarithm to base e of ( )
$\exp( )$	e raised to the power ( )
$P( )$	probability of exceedance of ( )
$f( )$	general function of ( )
$\Pi( )$	product of ( )
$\Sigma( )$	sum of ( )

Dimensions and units

Sym-	Definition
bol	
$^{\circ}\text{C}$	degree celsius
cm	centimeter = $10^{-2}$ m
ft	foot
g	GRAM
h	hour
hr	hour
kg	KILOGRAM
km	kilometer = $10^3$ m
kt	knot = nautical miles per hour
L	LENGTH DIMENSION
lb	pound force
M	MASS DIMENSION
m	METER
mg	miligram = $10^{-3}$ g
mm	millimeter = $10^{-3}$ m
$\mu\text{m}$	micrometer = $10^{-6}$ m
N	NEWTON
rad	radians
s	SECOND
T	TIME DIMENSION
yr	year
$^{\circ}$	degree temperature degree angle
$^{\circ}/_{00}$	} parts per thousand
%	

REFERENCES

The following list includes bibliographic data on all of the references used in the previous chapters. Works are listed in alphabetical order by first author and in sequence of publication.

- Anonymous (1880-1895): *Report on the Scientific Results of the Voyage of H.M.S. Challenger During the Years 1873-1876*: 50 volumes Republished in 1972 by Johnson Reprint Corporation, London.
- (1960): *Prediction of Siltation in Europoort*: Report M703, Delft Hydraulics Laboratory, Delft, August. in DUTCH, original title: *Prognose Slibbezwaar Europoort I*.
- (1973): *Shore Protection Manual*: U.S. Army Coastal Engineering Research Center: U.S. Government Printing Office, Washington D.C.
- (1975): *Almanac for Water Tourism*, volume I: Koninklijke Nederlandse Touristenbond ANWB, Den Haag: pp 340-342. In DUTCH, original title: *Almanak voor Watertourisme*.
- Allersma, E; Hoekstra, A.J.; Bijker, E.W. (1967): *Transport Patterns in the Chao Phya Estuary*: Delft Hydraulics Laboratory publication number 47, March.
- Allersma, E. (1968): *Mud on the Oceanic Shelf Off Guiana: Symposium on Investigations and Resources of the Caribbean Sea and Adjacent Regions*, Willemstad, Curacao, 18-26 November: pp 193-203. FAO, UNESCO.
- Allersma, E., Massie, W.W. (1973): *Statistical Description of Ocean Waves*: Coastal Engineering Group, Department of Civil Engineering, Delft University of Technology
- Bailey, Hubert S. jr. (1972) *The Background of the Challenger expedition: American Scientist*, volume 60 number 5, pages 550-560.
- Bakker, W.T. (1968): *The Dynamics of a Coast with a Groyne System: Proceedings, 11<sup>th</sup> Conference on Coastal Engineering*, London: volume 1, chapter 31.
- Bakker, W.T.; Klein Breteler, E.H.J.; Roos, A. (1970): *The Dynamics of a Coast with a Groyne System: Proceedings, 12<sup>th</sup> Conference on Coastal Engineering*, Washington, D.C.: volume II pp. 1001-1020.

- Bascom, Willard (1974-1): The Disposal of Waste in the Ocean:  
*Scientific American*, volume 231, number 2, August: pp 16-25.
- (1974-2): Letter to the Editor:*Scientific American*, volume 231, number 5, November: pp 8-9.
- Bijker, E.W. (1967): *Some Considerations about Scales for Coast [a] Models with Movable Bed*: Doctorate Thesis, Delft University of Technology. also appeared as: Publication number 50, Delft Hydraulics Laboratory, Delft.
- ; Svasek, J.N. (1969): Two Methods for Determination of Morphological Changes Introduced by Coastal Structures: *Proceedings 22<sup>nd</sup> International Navigation Congress*, Paris, subject II-4, pp. 181-202.
- Botstrom, Robert C.; Sherif, Mehmet A. (1972):—————  
: report summary in: *Scientific American*, volume 226 number 2, February: pp. 41-42.
- Bretschneider, C.L. (1952): Revised Wave Forecasting Relationships: *Proceedings of the Second Conference on Coastal Engineering*: American Society of Civil Engineers, Council on Wave Research.
- Cressard, A. (1975): The Effect of Offshore and Gravel Mining on the Marine Environment: *Terra et Aqua*, number 8/9: pp. 24-33.
- Defant, Albert (1961): *Physical Oceanography*, volume I: Pergamon Press, London.
- Dorrestein, R. (1967): *Wind and Wave Data of Netherlands Lightvessels since 1949*: Mededelingen en Verhandelingen K.N.M.I. Number 90: Staatsdrukkerij, The Hague.
- Escoffier, F.F. (1940): The Stability of Tidal Inlets: *Shore and Beach*, volume 8, pp. 114-115, October.
- Fisher, F.H.; Williams, R.B.; Dial jr, O.E. (1970): *Analytic Equation of State for Water and Sea water*: Fifth report of the Joint Panel on Oceanographic Tables and Standards, Kiel, December: UNESCO Technical Papers in Marine Science number 14, Annex II, pp. 10-20.
- Frijlink, H.C. (1959): *River Studies and Recommendations on Improvement of Niger and Benue*: NEDECO, Netherlands Engineering Consultants, The Hague: (out of print).

Führböter, A. (1961): *The Flow of Sand Water Mixtures in Pipelines*:  
Doctorate Thesis, University of Hanover, Germany.

Galvin, Cyril J. (1968): Breaker Type Classification on Three Laboratory Beaches: *Journal of Geophysical Research*, volume 73 number 12, June 15: pp. 3651-3659.

— (1972): A Gross Longshore Transport Rate Formula: *Proceedings of the 13<sup>th</sup> Coastal Engineering Conference*, Vancouver, Canada, volume II: pp. 953-970.

Gould, Charles, L. (1973): Putting Pollution Problems in Perspective: *Civil Engineering*, volume 43 number 8, August: pp. 64-66: American Society of Civil Engineers.

Hansen, W. (—): Theory with Applications for the Computation of Water Level and Currents in Enclosed Seas: *Tellus*, volume 8, number 3: In GERMAN, original title: Theorie zur Errechnung des Wasserstandes der Strömungen in Rand meeren nebst Anwendungen.

Harlemann, Donald R.F.; Abraham, G. (1966): *One Dimensional Analysis of Salinity Intrusion in the Rotterdam Waterway*: Publication number 44, Delft Hydraulics Laboratory, Delft: October.

Harris, D.L. (1963): *Characteristics of The Hurricane Storm Surge*: Technical Paper number 48, Weather Bureau, U.S. Department of Commerce.

Housner, George W.; Hudson, Donald (1959): *Applied Mechanics Dynamics*, 2<sup>nd</sup> edition: D. van Nostrand Company, Inc., Princeton, N.J. U.S.A.

Ippen, Arthur T.; Harleman, Donald R.F. (1961): *One Dimensional Analysis of Salinity Intrusion in Estuaries*: Technical Bulletin number 5, Committee on Tidal Hydraulics, U.S. Army Corps of Engineers, Vicksburg, Mississippi: June.

Ippen, Arther T. - editor (1966): *Estuary and Coastline Hydrodynamics*: Engineering Societies Monographs, Mc Graw Hill Book Company

Jannasch, H.W.; Wirsén, C.O. (1973): \_\_\_\_\_ :  
report summary in: *Scientific American*, volume 228, number 4, April: pp. 45.

Jarrett, J.J. (1976): Tidal Prism - Inlet Area Relationship: CERC - WES *General Investigation of Tidal Inlets*; Report 3, p. 32, February: Department of the Army Corps of Engineers.

- Johnson, J.W. (1973): Characteristics and Behavior of Pacific Coast Tidal Inlets: *Journal of the Waterways, Harbors and Coastal Engineering Division*: volume 99, number WW 3, pp. 325-339, August: American Society of Civil Engineers, New York, U.S.A.
- Kinsman, Blair (1965): *Wind Waves, Their Generation and Propagation on the Ocean Surface*: Prentice-Hall, Inc., Englewood Cliffs, N.J., U.S.A.
- Lamb, H. (1945): *Hydrodynamics*, 6<sup>th</sup> Edition: Dover Publications, Inc., New York.
- Marchay, C.A. (1964): *Sailing Theory and Practice*: Dodd, Mead and Company
- Maury, Matthew F. (1855): *The Physical Geography of the Sea and its Meteorology*: Reprinted 1963 by Harvard University Press, Cambridge Massachusetts, U.S.A.
- de Nekker, J; In't Veld, J.K. (1975): Dredged Rotterdam Harbor Mud: its Qualities and Use as Soil: *Terra et Aqua*, number 8/9: pp. 34-40.
- Newman, Gerhard; Pierson, Williard (1966): *Principles of Physical Oceanography*: Prentice-Hall, Inc., Englewood Cliffs, N.J., U.S.A.
- O'Brien, M.P. (1969): Equilibrium Flow Areas of Inlets on Sandy Coasts: *Journal of the Waterways & Harbors Division*: volume 92, number WW 1, pp. 43-52, February: American Society of Civil Engineers, New York, U.S.A.
- Partheniades, Emmanuel; Dermisis, Vassilios; Mehta, Ashish J. (1980): Graphs for Saline Wedges in Estuaries: *Civil Engineering*: volume 50, number 1, pp. 90-92, January: American Society of Civil Engineers, New York, U.S.A.
- Shepard, Francis P.; Wanless, Harold R. (1971): *Our Changing Coastlines*: McGraw-Hill Book Company, New York.
- Shigemura, Toshiyuki (1980): Tidal Prism - Throat Area Relationships of the Bays in Japan: *Shore and Beach*: volume 48, number 3, pp. 30-35, July.

- Slijkhuis, P. (1974): *Shore Protection of Delfland*: unpublished discussion.
- Starbird, Ethel A. (1972): A River Restored: Oregon's Willamette: *National Geographic*, volume 141, number 6, June: pp. 816-835.
- van Staveren, Jan (1974): *Pollution of Seawater*: unpublished report, Coastal Engineering Group, Department of Civil Engineering, Delft University of Technology: in DUTCH, original title: Vervuiling van Zeewater.
- Stoker, J.J. (1957): *Water Waves*: Interscience Publishers, Inc., New York.
- Sverdrup, H.U.; Johnson; Fleming, R.H. (1942): *The Oceans, Their Physics, Chemistry, and General Biology*: Prentice Hall, Inc., Englewood Cliffs, N.J., U.S.A.
- ; Munk, W.H. (1947): *Wind, Sea, and Swell: Theory of Relations for Forecasting*: Publication number 601, U.S. Naval Hydrographic Office, Washington, D.C., U.S.A.: out of print.
- Swart, D.H. (1974): *Offshore Sediment Transport and Equilibrium Beach Profiles*: Doctorate Thesis, Delft University of Technology: Also appears as: Publication number 131, Delft Hydraulics Laboratory, Delft: and also as: Report M918 part 2, Delft Hydraulics Laboratory, Delft.
- Thomas, J.L. (1974): A Counter-Perspective on Pollution Problems: *Civil Engineering*, volume 44 number 8, August: pp. 80-81: American Society of Civil Engineers.
- Weyle, Peter K. (1968): *Oceanography, an Introduction to the Marine Environment*: John Wiley and Sons, Inc.
- Wiegel, Robert L. (1954): *Gravity Waves, Tables of Functions*: The Engineering Foundation Council on Wave Research, Berkley, California,
- (1964): *Oceanographical Engineering*: Prentice Hall, Inc., Englewood Cliffs, N.J., U.S.A.



